University of Bath

UNIVERSITY OF BATH

PHD

The Pharmacology of the Sigma-1 Receptor

Brimson, James

Award date:
2010

Awarding institution:
University of Bath

Link to publication

The Pharmacology of the Sigma-1 Receptor

James Michael Brimson

A thesis submitted for the Degree of Doctor of Philosophy

University of Bath

Department of Pharmacy and Pharmacology

April 2010

Acknowledgements

Abstract

The sigma-1 receptor, although originally classified as an opioid receptor is now thought of as distinct receptor class, sharing no homology with any other known mammalian protein. The receptor has been implicated with a number of diseases including cancer and depression. Modulation of the receptors activity with agonists has potential antidepressant activity whereas antagonists lead to death of cancer cells.

Using radioligand binding assays, utilizing the cancer cell line MDA-MB-468, which highly expresses the sigma-1 receptor, a series of novel specific, high affinity, sigma-1 receptor ligands have been characterised. These ligands differed from any previous sigma-1 receptor ligand in that they are very simple ammonium salts, containing a single nitrogen atom and either straight or branched carbon chains. The binding studies revealed that the straight-chain ammonium salts gave nH values of 1 whereas the branched-chain ammonium salts had statistically significant lower nH values.

The ammonium salts were tested for sigma-1 receptor activity *in vitro* using ratiometric Fura-2 calcium assays and the MTS cell proliferation assay. Branched-chain ammonium salts appeared to have sigma-1 receptor antagonist like effects on cytoplasmic calcium and cell proliferation, whereas the straight-chain ammonium salts behaved as sigma-1 receptor agonists. Three ammonium salts stood out as potential effective sigma-1 receptor drugs, the straight-chain ammonium salt dipentylammonium, and two branched-chain ammonium salts, bis(2-ethylhexyl)ammonium and triisopentylammonium. The ammonium salts were then tested *in vivo,* dipentylammonium showed significant antidepressant properties when tested in behavioural models for depression and bis(2-ethylhexyl)ammonium and triisopentylammonium were able to significantly inhibit the growth of tumours implanted in mice.

Finally I looked at the coupling of the sigma-1 receptor with G-proteins and show that sigma-1 receptor antagonists dose dependently reduce G-protein activity and inhibition of G-proteins enhanced the sigma-1 antagonists' effects of calcium signalling.

Table of contents

Chapter 1

1 Introduction

1.1 The importance of receptors and receptor theory

Cells need to respond to a vast number of extracellular signals, whether the signal is telling the cell to produce a product, pass on a signal, divide, differentiate or die, the cell needs to be able to detect and distinguish between different signals. The cell does this by making use of receptors, which may be embedded in the membrane or free in the cytoplasm of the cell. There are vast arrays of receptors, which have evolved to sense the thousands of different signals, which a cell may need to respond to. However, the majority of receptors fall in to one of five classes: G-protein-linked; ion channel-linked; containing intrinsic enzymatic activity; tyrosine kinase-linked and intracellular. In order for a receptor to be effective at sensing the signals that are meant for a particular cell in which it is expressed, the receptor must have specificity for a particular ligand (or range of ligands), be able to detect these ligands and be able to transmit the message that the signalling molecule is conveying to the cell.

Receptors, therefore, usually have affinity for their ligand within the range that it is likely to encounter the signalling molecule or molecules, and contain a specifically shaped binding site such that only the specific ligand or ligands for that receptor will bind effectively at the concentrations that the cell is likely to encounter the ligand. Activation of a receptor by a ligand results in a conformational change (Couette *et al.*, 1996, Henchman *et al.*, 2005) that allows the signal to be conveyed in the cell. For example in G-protein coupled receptors this consists of activating a G-protein, which activates a downstream signalling cascade and in ion channel-linked receptors, ligand binding can open the channel allowing ions to flow through the membrane (Jelacic *et al.*, 1999).

A simple receptor model known as the 2 state model suggests a receptor may exist as an equilibrium between 2 states: active or inactive (Black and Leff, 1983, Del Castillo and Katz, 1957) and a ligand known as an agonist has high affinity for and stabilises the active conformation of the receptor shifting the equilibrium to the active state resulting in a physiological response. A ligand known as an inverse agonist has high affinity for and stabilises the inactive state, therefore shifting the equilibrium to the inactive state and removing any constitutive activity, resulting in a negative physiological response (Figure 1.1).
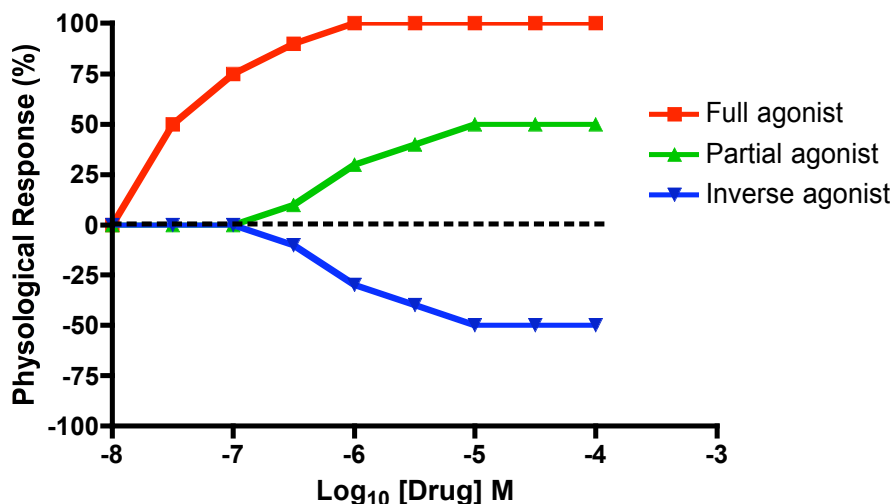
Figure 1.1 Example of a dose response to different types of ligands. The full agonist is able to produce a maximal response, whereas the partial agonist does not, even when occupying the maximum number of receptors. The inverse agonist induces a negative response by reducing any constitutive activity of the receptor.

A receptor agonist may only need to occupy a small fraction of the available receptors in order to produce a maximal response, whereas a ligand known as a partial agonist may need to occupy a greater proportion of receptors in order to elicit a response, and may not be able to elicit a maximal response despite occupying all the available receptors. The relationship between receptor occupancy and receptor activation is known as efficacy. Efficacy can be thought of as a ligand's preference for the active receptor over the inactive receptor, i.e. if the ligand has a higher affinity for the active receptor than the inactive receptor this will result in positive efficacy and therefore, if the ligand has higher affinity for the inactive state of the receptor this results in negative efficacy. A ligand that shows no preference in affinity for the active or inactive receptor has zero efficacy and is known as an antagonist. An antagonist does not activate or inactivate a receptor rather it blocks the binding site preventing the binding of other ligands. For a review on the classification of receptor ligands see Kenakin, 1984.

1.2   History of the σ-1 receptor

The search for understanding of the sigma-1 receptor (σ-1R) has been a long, mysterious and as yet incomplete journey. The receptor has mostly been studied within the central nervous system (CNS). However, more recent work over the past decades has shown the receptor to be abundant in neuronal, and non-neuronal tissues (Vilner *et al.*, 1995b) leading to the study of the σ-1 receptor in cancer biology (Spruce *et al.*, 2004).

The sigma opioid receptor was proposed as a novel fourth opioid receptor in 1976 to account for the effects of N-allylnormetazocine (SKF-10,047) which could not be accounted for by the μ (morphine) receptor, κ (ketocyclazocine) receptor or δ receptor (Martin *et al.*, 1976). Rather than causing analgesia, as with morphine, benzomorphans such as SKF-10,047 and pentazocine cause psychotomimesis. Martin proposed that SKF-10,047 was acting as a sigma opioid receptor agonist, in order to cause the psychological and behavioural effects which were observed (Martin *et al.*, 1976).

SKF-10,047 was defined as an agonist as it raised pulse and respiration rates, as well as body temperature and caused dilation of pupils in Beagles. Interestingly, μ receptor agonists *lowered* pulse and respiration rates, as well as body temperature and produced classic pin-point pupils. Antagonists were defined as agents which were able to prevent these responses (Martin *et al.*, 1976). Later biochemical studies suggest that biochemically agonists do not cause activation of the receptor but can block the effects of antagonists, which do (Hayashi *et al.*, 2000, Katnik *et al.*, 2006, Monnet *et al.*, 2003, Spruce *et al.*, 2004, Tchedre *et al.*, 2008). More recently, data obtained using mice in which the σ-1R has been knocked out further cloud the picture (Cendan *et al.*, 2005, De La Puente *et al.*, 2009, Entrena *et al.*, 2009, Langa *et al.*, 2003, Sabino *et al.*, 2009). Expression of σ-1R acts as a prosurvival signal (Spruce *et al.*, 2004, Wang *et al.*, 2005) and treatment with antagonists causes apoptosis (see below) – perhaps suggesting that antagonists could be acting as inverse agonists at the receptor. Without further understanding the σ-1R, it is premature to redefine the concept of agonist and antagonist at this time. For the purpose of clarity, I will continue to describe agonists as those mimicking the effects of SKF-10,047 although accepting that with hindsight one could argue that SKF-10,047 is really an antagonist. In 1982 Su identified a nanomolar affinity SKF-10,047 binding protein using [^{3}H] SKF-10,047. This SKF-10,047 binding protein appeared to be different from the sigma opioid receptor identified by Martin in 1976 (Su, 1982), as the opioid antagonist

naloxone showed no affinity under the conditions tested. Further study of this protein showed stereoselectivity for the dextrorotary benzomorphans such as (+) SKF-10,047 and (+) pentazocine, rather than the laevorotatory enantiomers. This stereoselectivity is the opposite to that found in the other opioid subtypes in either binding or behavioural studies, further suggesting that the SKF-10,047 binding protein was not an opioid receptor. Su proposed that the receptor was a novel system distinct from the opioid subclasses and may not represent a single homogeneous receptor population. The receptor was later termed "sigma receptor" distinguishing it from the opioid receptors (Su, 1982). Su also noted that none of the endogenous opioid ligands potently inhibited sigma receptor binding and speculated on a potential endogenous sigma ligand. However an endogenous ligand for the sigma receptor has yet to be conclusively identified.

The sigma receptor then became confused with the 1-(1-phenylcyclohexyl)piperidine (PCP) site of the N-methyl-D-aspartic acid (NMDA) receptor, since SKF-10,047 binds the PCP site well, and PCP also happens to bind the sigma receptor with a notable affinity (Vaupel, 1983). Further binding studies using the more specific ligands for both the sigma receptor and the NMDA receptor revealed them to be distinct from each other (Quirion *et al.*, 1987, Tam, 1985). This distinction was furthered when using autoradiographic techniques identified the locations of the PCP and the SKF-10,047 sites and found them to be distributed differently (Gundlach *et al.*, 1986, Largent *et al.*, 1986). Since then the radioligand of choice for sigma receptor studies has been [³H] (+) pentazocine in place of [³H] (+) SKF-10,047.

Further studies of the sigma receptor using (+) pentazocine found a second sigma-like binding site, which has a similar binding profile to that of the receptor previously described by Su (Su, 1982). However the affinities for the (+) benzomorphans were lower, and moreover in some instances there appeared to be a greater selectivity for the (-) isoforms (Bowen *et al.*, 1990, Hellewell and Bowen, 1990). This led to the classification of the two subclasses of the sigma receptor, the sigma-1 receptor (σ-1R) and the sigma 2 receptor (σ-2R). Following the identification of the 2 subtypes there was an attempt to clear up the confusion in the literature caused by studies using non specific sigma ligands (Quirion *et al.*, 1992). A proposal was laid out specifying the binding properties of the σ-1R and σ-2R, concluding amongst other things that the preferred radioligands should be [³H] (+) pentazocine for the σ-1R and [³H] (+) 1,3-di-o-tolylguanidine (DTG) in the presence of σ-1R blockers for the σ-2R (Quirion *et al.*, 1992).

1.3 σ-1 receptor ligands

The σ-1R was identified for its affinity for dextrorotary benzomorphans such as (+) pentazocine or (+) SKF-10,047 (Martin *et al.*, 1976). However since its discovery the σ-1R has become known for its ability to bind a wide range of ligands including antipsychotics such as haloperidol (Su, 1982), antidepressants such as imipramine and fluoxetine (Bermack and Debonnel, 2005), and neurosteroids including progesterone (Su *et al.*, 1988, Waterhouse *et al.*, 2007). A vast number of synthetic compounds have been synthesised, with high σ-1R affinities including 1-(4-iodophenyl)-3-(2-adamantyl)guanidine (IPAG) and DTG. For a list of σ-1R ligands, structures and affinities see table 1.1.
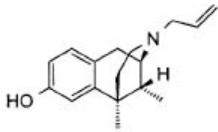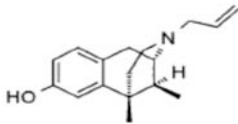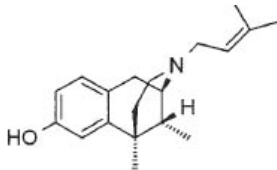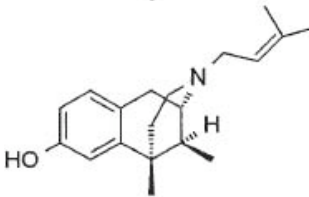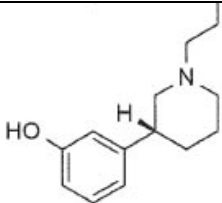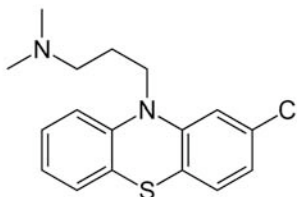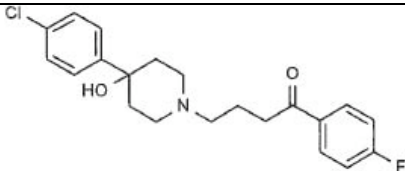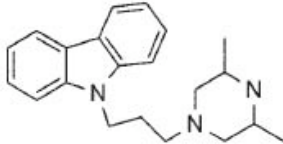
Table 1.1

σ-1 Ligand	Affinity (μM)	Function	Structure
Benzomorphans			
(+) SKF-10,047	0.060[b]	Agonist	
(-) SKF-10,047	5.2[b]	Agonist	
(+) Pentazocine	0.003[b]	Agonist	
(-) Pentazocine	0.083[b]	Agonist	
(+) 3-PPP	0.03[b]	Agonist	
Antipsychotics			
Chlorpromazine	0.685[1]	Antagonist	
Haloperidol	0.0037[b]	Antagonist	
Rimcazole	0.9[c]	Antagonist	

Table 1.1 continued

Antidepressants
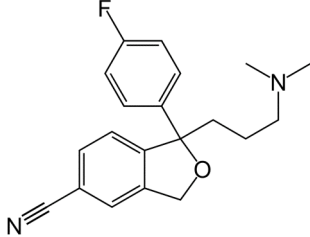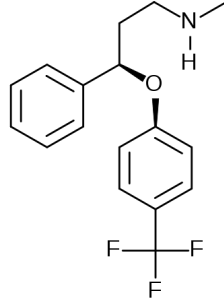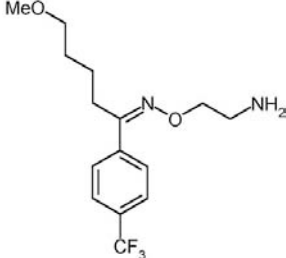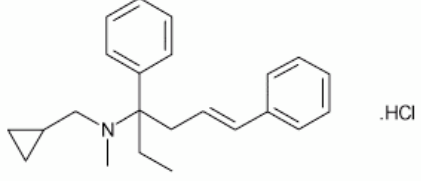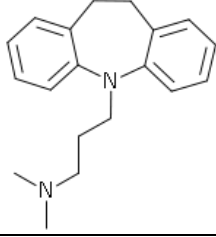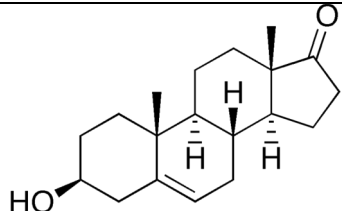
Citalopram	0.292[a]	Agonist	
Fluoxetine	0.240 [a]	Agonist	
Fluvoxamine	0.036 [a]	Agonist	
Igmesine	0.039[g]	Agonist	
Imipramine	0.343[a]	Agonist	
Neurosteroids			
Dehydroepiandrosterone	1.000[h]	Agonist	

Table 1.1 continued
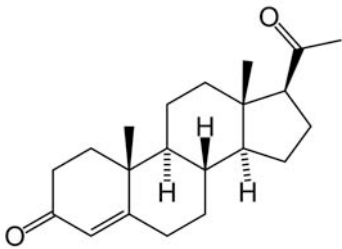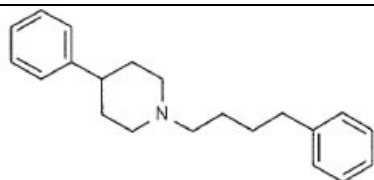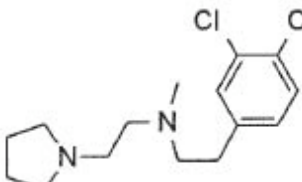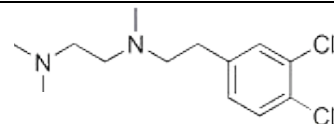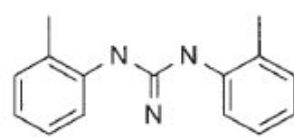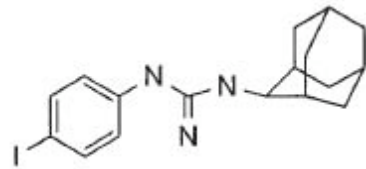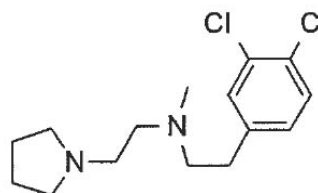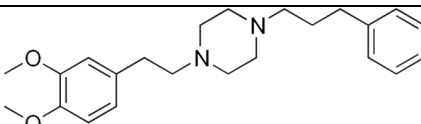
Other Synthetic Compounds			
Progesterone	0.061^b	Antagonist	
4-PPBP	0.0008^e	Antagonist	
BD 1008	0.0022^b	Antagonist	
BD1047	0.036^j	Antagonist	
DTG	0.028^b	Agonist	
IPAG	0.0028^d	Antagonist	
NE 100	0.0046^b	Antagonist	
SA4503	0.017^f	Agonist	

Table 1.1

Sigma-1 receptor ligands, their affinities (µM), σ-1 agonist/antagonist and structure.

[a]Narita *et al*., 1996	[e]Glennon *et al*., 1991	[i]Itzhak *et al*., 1990
[b]Whittemore *et al*., 1997	[f]Matsuno *et al*., 1997	[j]Matsumoto *et al*., 1995
[c]Gilmore *et al*., 2004	[g]Roman *et al*., 1990	
[d]Wilson *et al*., 1991	[h]Su *et al*., 1988	

The endogenous ligand for the σ-1R has yet to be identified. Neurosteroids, in particular progesterone, are the main candidates for the endogenous ligand (Ramamoorthy *et al.*, 1995, Su *et al.*, 1988). However their affinities for the σ-1R (Figure 1.2 and Table 1.2) appear to be too low for them to be endogenous ligands. The physiological levels of progesterone during pregnancy can reach up to 400nM, however only 2% of this is free to pass the blood brain barrier (Pardridge, 1988, Schwarz *et al.*, 1989), resulting in only approximately 8nM free progesterone that is able to interact with σ-1Rs in the CNS (Schwarz *et al.*, 1989).
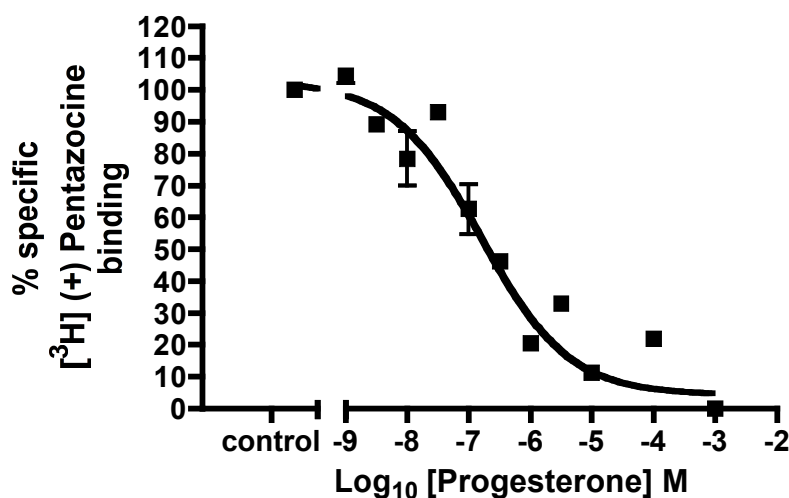
Figure 1.2: Progesterone competition with [³H] (+) pentazocine in permeabilised MDA-MB-468 cells. The K_{50} (concentration of ligand occupying 50% of available receptors) for progesterone binding to the σ-1R in MDA-MB-468 cells is 64nM (nH - 0.61). Error bars indicate SEM from 3 independent competition binding assays.

Tissue	σ-1R K_{50}	Radiolabelled ligand
MDA-MB-468	64 nM[a]	[³H] (+) pentazocine
Brain membranes	268 nM[b]	[³H] (+) SKF-10,047
Spleenocytes	376 nM[b]	[³H] (+) SKF-10,047

Table 1.2: Affinity of Progesterone for the σ-1 R. [a] data obtained form 3 independent [³H] (+) pentazocine competition binding assays. [b] data obtained from Su *et al.*, 1988.

Progesterone however, along with other steroids still remain strong candidates for the endogenous ligand for the σ-1R (Bergeron *et al.*, 1999), since progesterone binding shows as low nH value (Figure 1.2) there could be a multiple affinity site binding. Furthermore, the gonads express high levels of the σ-1R (Su, 1993). Other endogenous ligands have been suggested including the hallucinogen N,N-dimethyltryptamine. However, despite showing agonist activity at the σ-1R, its affinity is far lower than that of progesterone at

15µM, and in order to see an effect at voltage-gated sodium channels a dose of 100µM N,N-dimethyltryptamine is required (Su *et al.*, 2009). Moreover no conclusive study has been conducted to quantify the amount of N,N-dimethyltryptamine found in blood or cerebrospinal fluid (Burchett and Hicks, 2006). N,N-Dimethyltryptamine also interacts with the 5-HT$_{2A}$ receptor (Gouzoulis-Mayfrank *et al.*, 2005) at a concentration over 10 times lower than required to interact with the σ-1R (K_i 4µM) (Cozzi *et al.*, 2009) and therefore its is still unclear whether the effects are mediated through the σ-1R or the 5-HT$_{2A}$ receptor.

As more and more σ-1R ligands have been identified, and the study of the σ-1R furthered, some confusion in the classification of σ-1R ligands has emerged. As described above, the original behavioural experiments by Martin *et al.* (1976) using ligands such as (+) SKF-10,047 and (+) pentazocine resulted in psychotomimesis (along with the effects previously described), and these ligands were classified as σ-1R agonists since they produced a response in the animals. It was only later when the σ-1R ligands were investigate more closely that it was discovered that the σ-1R antagonists modulate cytoplasmic calcium levels (Brent *et al.*, 1996a, Brent *et al.*, 1996b), block voltage-gated potassium channels (Aydar *et al.*, 2002, Soriani *et al.*, 1998), control plasma membrane cholesterol content (Hayashi and Su, 2003b, Hayashi and Su, 2004, Hayashi and Su, 2005b, Palmer *et al.*, 2007, Schwarz *et al.*, 1989, Su *et al.*, 1988) and induce apoptosis (Aydar *et al.*, 2006, Aydar *et al.*, 2004, Bem *et al.*, 1991, Brent and Pang, 1995, Palmer *et al.*, 2007, Spruce *et al.*, 2004, Vilner *et al.*, 1995b), whereas the σ-1R agonists block these effects. This is of course the reverse of the way in which receptor ligands are classified, however, this nomenclature is set in the literature such that ligands such as (+) pentazocine and (+) SKF-10,047 are σ-1R agonists and ligands such as IPAG and rimcazole are σ-1R antagonists.

1.4 σ-1 receptor structure and function

The σ-1R has been cloned, originally from guinea pig (Hanner *et al.*, 1996), and has now been cloned from a number of other species including humans, rats and mice (Kekuda *et al.*, 1996, Mei and Pasternak, 2001, Pan *et al.*, 1998). Currently there is still no crystal structure available; consequently the σ-1R structure has been predicted using sequence homology and hydrophobicity analysis. The original analyses have predicted at least one transmembrane region (Hanner *et al.*, 1996, Kekuda *et al.*, 1996, Seth *et al.*, 1997) (Figure 1.3A). More recently, however, Aydar *et al.* (2002) have provided evidence that the σ-1R

is found in the plasma membrane with both the N and C termini in the cytoplasm (Figure 1.3B). They showed this by green fluorescent protein (GFP) tagging either the N or C terminal, followed by expression in a human cell line. Subsequently they were only able to see anti-GFP antibody binding having permeabilised the cell membranes (Aydar *et al.*, 2002). Therefore, both the N and C termini must reside inside the cell otherwise GFP antibody binding would have been observed in intact cells. It should be noted, however, that adding the bulky GFP tag to the relatively small σ-1R and expressing it in cells that otherwise do not express this receptor could have potentially altered its membrane topology.

A
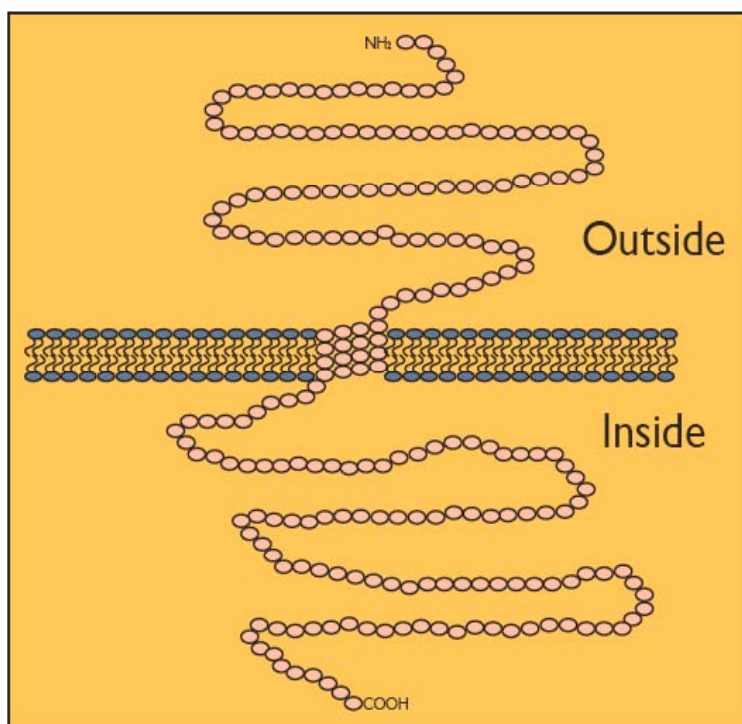
B
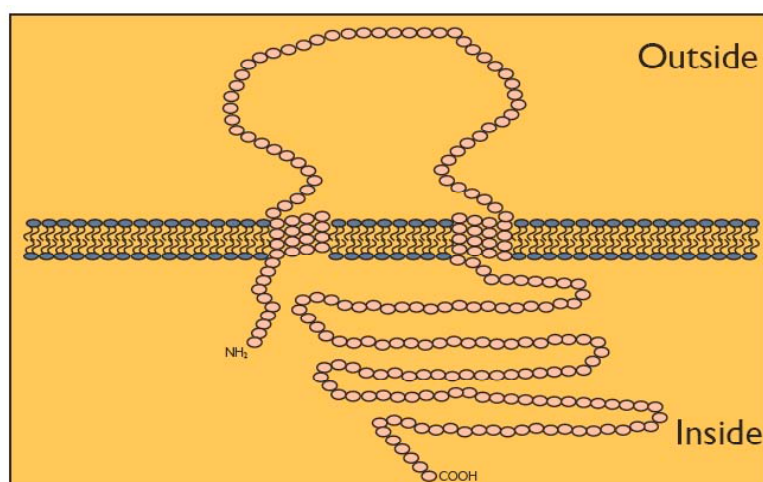
Figure 1.3: Predicted σ-1R structures. A: σ-1R with single transmembrane region, with the N terminus on the outside. **B:** σ-1R with two transmembrane regions with both the N and C termini on the inside. Figures adapted from Aydar *et al*., 2004.

Analysis of the σ-1R gene sequence has shown it to be a unique class of receptor, distinct from the opioid receptors and the NMDA receptor (Hanner *et al*., 1996, Seth *et al*., 1997). The σ-1R consists of a 223 amino acid long protein, which shares no homology with any other known mammalian protein.

In the N-terminus of the σ-1R protein sequence there is an arginine-arginine endoplasmic localisation signal (see appendix for sequence). The σ-1R is located at both endoplasmic reticulum and the cell membrane (Aydar *et al.*, 2002), particularly lipid-rich areas (Aydar *et al.*, 2006, Hayashi and Su, 2003b). It has been reported that σ-1R translocates from the endoplasmic reticulum to the plasma membrane on stimulation with σ-1R agonists such as (+) pentazocine (Hayashi and Su, 2001, Mavlyutov and Ruoho, 2007, Morin-Surun *et al.*, 1999) where they have been shown to block voltage-gated ion channels (Monnet *et al.*, 2003).

Experiments using Ca^{2+}-free buffers indicate that the σ-1R favours calcium influx mediated at the plasma membrane rather than Ca^{2+} release from intracellular stores (Mavlyutov and Ruoho, 2007, Morin-Surun *et al.*, 1999, Novakova *et al.*, 1998, Spruce *et al.*, 2004). σ-1R agonists alone do not induce calcium influx into the cell, rather they are able to potentiate glutamate-induced Ca^{2+} increases (Monnet *et al.*, 2003). σ-1R antagonists, including rimcazole and IPAG induce a rapid increase in cytoplasmic $[Ca^{2+}]$, which can be inhibited by σ-1R agonists such as (+) pentazocine and SKF-10,047, although a 30 minute pre-incubation is required (Spruce *et al.*, 2004). The spike in intracellular $[Ca^{2+}]$ caused by σ-1R antagonists leads to caspase-dependent apoptosis, which suggests that the presence of the σ-1R acts as a survival signal to the cell (Spruce *et al.*, 2004).

1.5 σ-1 receptors, G-proteins and ion channels

The debate as to whether σ-1Rs are G-protein coupled or not has been going back and forth and is yet to be satisfactorily concluded. Early σ-1R binding studies showed that the binding of σ-1R ligands could be altered by the addition of GTP and its analogues. Using rat brain membranes Itzhak (1989) showed that the σ-1R ligands (+) 3-PPP, (+) pentazocine and (+) SKF-10,047 bind the σ-1R at a high and a low affinity site in the presence and absence of GTP or its analogues. Other similar data showed that GTP and its analogues are able to modify the binding characteristics of σ-1R ligands (Beart *et al.*, 1989, Connick *et al.*, 1992). It has also been shown that σ-1R ligands can activate GTPase activity (Tokuyama *et al.*, 1997). Furthermore, these studies have also shown that treatment with G-protein inhibitors such as pertussis toxin inhibits high-affinity (+)-3-PPP

binding, and removes the effect of GTP analogues on ligand binding (Itzhak, 1989). These data suggest that the σ-1R is G_i-protein coupled. However, cloning the σ-1R has revealed a 223 amino acid protein that in no way resembles the classical 7 transmembrane G-protein coupled receptor. Other studies using GTPγS were unable to affect ligand binding at the σ-1R (Hong and Werling, 2000). There has also been no evidence of σ-1R activating cyclic adenosine monophosphate (cAMP) production, suggesting it does not couple through Gs proteins (Odagaki *et al.*, 2005). In order to explain this contradiction of results it has been proposed that the σ-1R could fall into further subtypes with one subtype acting though G-proteins and another G-protein independent (Bermack and Debonnel, 2005).

All the studies on the σ-1R's link to G-proteins have used σ-1R agonists (Table 1.3), which with regard to the σ-1R do not behave biochemically in the same way true receptor agonists do. They appear to behave more like typical antagonists, not having any effect at the σ-1R themselves other than possibly causing the translocation from the endoplasmic reticulum to the plasma membrane (Hayashi and Su, 2001, Mavlyutov and Ruoho, 2007, Morin-Surun *et al.*, 1999) where the σ-1R can block ion channels (Monnet *et al.*, 2003) or potentiate the response from other receptors (Monnet *et al.*, 2003). The σ-1R antagonists on the other hand appear to have activity at the σ-1R, with rimcazole and IPAG causing an increase in cytoplasmic $[Ca^{2+}]$ which subsequently activates phospholipase C (PLC), and calcium dependent protein kinase B (PKB) inhibition, leading to caspase dependent apoptosis which could be inhibited with a 30min preincubation with σ-1R agonists (+) SKF-10,047 or (+) pentazocine (Spruce *et al.*, 2004).

Spruce *et al.* (2004) also showed that expressing the σ-1R alone was not enough to indicate sensitivity to σ-1R antagonists, as cerebellar granule neurons and human prostate epithelial cells showed no $[Ca^{2+}]$ increase in response to the σ-1R antagonists despite having high σ-1R expression. This therefore suggests that the receptor can couple in different ways depending on the cell type, which could be a possible explanation for the discrepancy in the results seen in Table 1.3

Author	Drug	Agonist/ Antagonist	Experimental output	G-Protein?	Affect
Hong and Werling, 2000	BD737	Agonist	[^{35}S]GTPγS	No	
Hong and Werling, 2001	Neuropeptide Y	Agonist	[^{35}S]GTPγS	No	
Lupardus et al., 2000	(+) SKF-10,047	Agonist	[K$^+$] Current + GTPγS or GDPβS	No	
Lupardus et al., 2000	(+) Pentazocine	Agonist	[K$^+$] Current + GTPγS or GDPβS	No	
Odagaki et al., 2005	(+) 3PPP	Agonist	[^{35}S]GTPγS	No	
Connick et al., 1992	DTG	Agonist	Gpp(NH)p effect competition binding	Yes	↑ nH of binding curve
Itzhak, 1989	(+) 3PPP	Agonist	Gpp(NH)p effect competition binding	Yes	↑ nH of binding curve
Itzhak, 1989	(+) Pentazocine	Agonist	Gpp(NH)p effect competition binding	Yes	↑ nH of binding curve
Itzhak, 1989	(+) SKF-10,047	Agonist	Gpp(NH)p effect competition binding	Yes	↑ nH of binding curve
Schiess and Partridge, 2005	Pregnenolone Sulphate	Agonist	Membrane potentials + pertussis toxin	Yes	↓ Neuron firing
Ueda et al., 2001	DHEAS	Agonist	[^{35}S]GTPγS + pertussis toxin	Yes	↑ GTPγS binding
Ueda et al., 2001	Pregnenolone sulphate	Agonist	[^{35}S]GTPγS + pertussis toxin	Yes	↑ GTPγS binding

Table 1.3: σ-1R coupling to G-proteins in response to σ-1R agonists.

The σ-1Rs interaction with Ca^{2+} channels was demonstrated by the ability of (+) pentazocine to inhibit depolarization in rat forebrain synaptosomes (Brent *et al.*, 1996b). It has been proposed that the modulation of calcium signalling by the σ-1R involves direct coupling in multi-protein complexes. σ-1Rs have been shown to anchor the cytoskeleton adaptor protein ankyrin to the endoplasmic reticulum membrane and modulate the function of ankyrin and the inositol 1,4,5-trisphosphate (IP_3) receptor (Hayashi and Su, 2001). In the presence of the σ-1R agonist (+) pentazocine the σ-1R ankyrin complex dissociates from the IP_3 receptor, leading to increased IP_3 binding which in turn leads to increased Ca^{2+} efflux from the endoplasmic reticulum into the cytoplasm, whilst in the presence of the σ-1R antagonist NE-100 the σ-1R dissociates alone leaving the ankyrin associated to the IP_3 receptor (Figure 1.4). These modulations of calcium currents implicates the σ-1R in various cell functions including neurotransmitter release (Hayashi and Su, 2001).
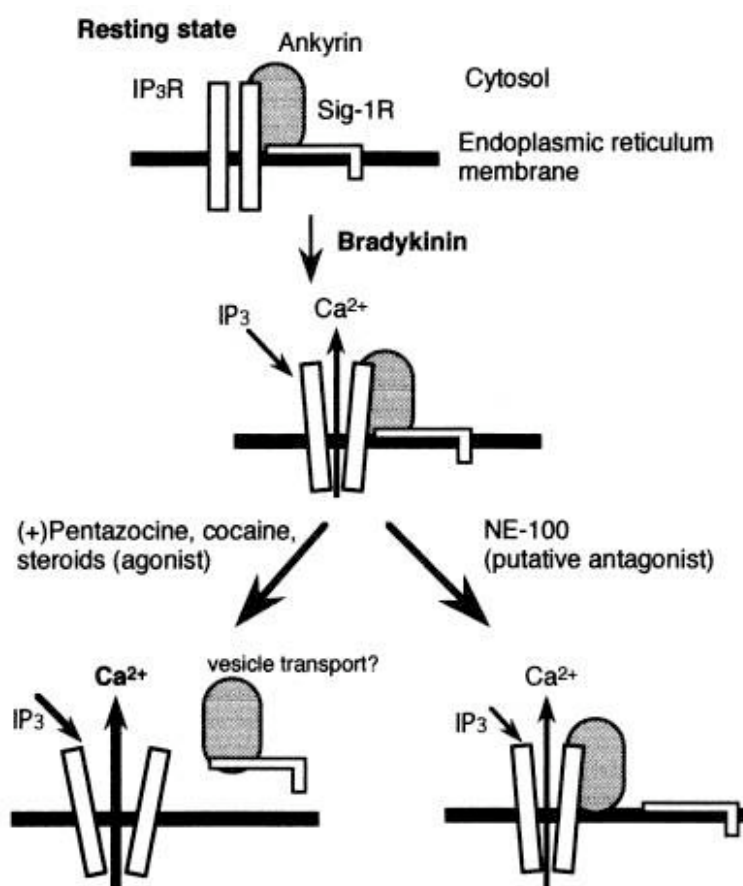
Figure 1.4: Possible σ-1R regulation of the IP_3 receptor and ankyrin (Hayashi and Su, 2001). σ-1R agonists such as (+) pentazocine lead to σ-1R and ankyrin dissociation from the IP_3 receptor leading to increased Ca^{2+} release whereas σ-1R antagonists such as NE-100 lead to σ-1R dissociation alone, leaving ankyrin associated with the IP_3 receptor reducing the Ca^{2+} release.

σ-1R ligands have been shown to inhibit numerous types of K^+ channel including voltage-gated K^+ channels and Ca^{2+}-activated K^+ channels; these inhibitions are not sensitive to the G-protein inhibitor GDPβS or the G-protein activator GTPγS and in the absence of the σ-1R the inhibition by σ-1R ligands did not occur (Lupardus *et al.*, 2000). σ-1R agonists also cause the inhibition of Na^+ channels, and again knocking down the σ-1R reduced the effect of the σ-1R agonists (Johannessen *et al.*, 2009). However it should be noted that these experiments were looking at σ-1R agonists, not antagonists.

1.6 σ-1 receptor distribution and knock-out.

The σ-1R is expressed in many parts of the brain and central nervous system, and may also be found in many non-neuronal cells including the heart, liver, placenta, immune cells, kidney, gonads and pancreas (Ola *et al.*, 2001, Seth *et al.*, 1997, Zamanillo *et al.*, 2000). The σ-1R has also been found to be expressed at high levels in embryonic stem cells, at all stages of embryogenesis, found at high levels in the CNS, developing spinal cord, developing limbs, and inside the thoracic and abdominal cavities (Langa *et al.*, 2003). This is a period of rapid growth and cell division, the presence of σ-1Rs at this time reiterates the proposal that these receptors are part of a survival signal.

σ-1R knock-down using σ-1R specific siRNAs in human lens cells resulted in cell death, compared to cells treated with the non-targeting control siRNA (Wang and Duncan, 2006). A similar study using σ-1R antagonists with the human lens cells resulted in cell pigmentation and death (Wang *et al.*, 2005). These two studies and the study by Spruce *et al.* (2004) using σ-1R antagonists to selectively kill cancer cells, suggest that the σ-1R acts as a survival signal to the cells, and that switching it off either by stopping expression with siRNAs or by using σ-1R antagonists leads to death of the cell.

A σ-1R knock-out mouse has been created (Langa *et al.*, 2003). Despite the wide distribution of the σ-1R, the homozygous σ-1R knock-out mice were viable and fertile. Moreover, they do not appear to show any obvious phenotype when compared to wild-type mice (Langa *et al.*, 2003). Acute knock-down of the σ-1R does have detrimental effects on a number of cell lines including cell death (Wang and Duncan, 2006, Wang *et al.*, 2005) which suggests that there are some compensatory mechanisms which take over in the σ-1R knock-out mouse (Hayashi and Su, 2005). When the σ-1R knock-out mice were treated with σ-1R agonist SKF-10,047 it did not induce an increase in motility as seen in the wild

type mice, supporting the hypothesis that the σ-1R is involved in psycho-stimulant actions (Langa *et al.*, 2003).

There have been a number of studies looking at the involvement of σ-1Rs in pain and analgesia, including a number using the knock-out mice. It has been shown that formalin-induced pain is reduced in σ-1R homozygous knock-out mice (Cendan *et al.*, 2005), capsaicin-induced mechanical allodynia was abolished in the σ-1R knock-out mice (Entrena *et al.*, 2009) and cold or mechanical allodynia does not develop in σ-1R knock-out mice that have been exposed to partial sciatic nerve injury (De La Puente *et al.*, 2009). The underlying mechanism through which the σ-1R modulates pain responses appears to be through the regulation of cytoplasmic calcium, and calcium dependent processes (Figure 1.5).
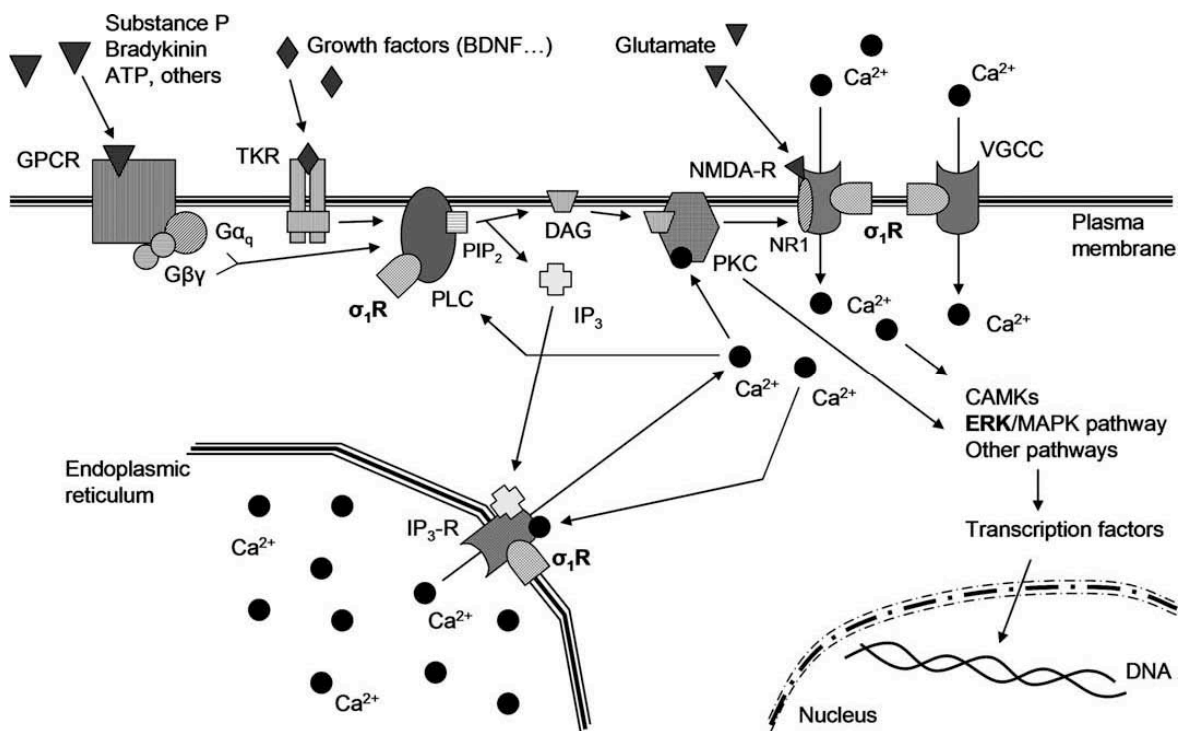
Figure 1.5 Activation of the σ-1R increases intracellular calcium (De La Puente *et al.*, 2009). σ-1R activation leads to increased cytosolic calcium through the potentiation of calcium entry at the plasma membrane through the N-methyl D-aspartate (NMDA) receptor and voltage-gated calcium channels (VGCC), as well as through calcium mobilisation from intracellular stores through phospholipase C (PLC) activation and the inositol trisphosphate (IP_3) receptor. This is followed by kinase sensitization and rapid transcriptional activation of key gene products involved in pain hypersensitivity. Blocking σ-1R activation or the absence of the σ-1 receptor prevent the up regulation of calcium dependent signalling. GPCR - G-protein coupled receptor; TKR - tyrosine kinase receptor; DAG - diacylglycerol; BDNF - brain derived neurotrophic factor; PKC - protein kinase C; NR1 - NMDA receptor subunit 1; PIP_2 - phosphatidylinositol 4,5-bisphosphate.

1.7 σ-1 receptors and cholesterol.

Despite sharing no homology with any known mammalian protein, the C terminus of the σ-1R does share homology with a fungal C7-C8 sterol isomerase, a product of the *ERG2* gene, which shares a 30% identity with the σ-1R (Hanner *et al.*, 1996). The ERG2 protein has high affinities for σ-1R ligands such as ifenprodil (also an NMDA receptor antagonist), haloperidol and pentazocine (Moebius *et al.*, 1997). The isomerase catalyses the shift of the C8(9) double bond on the B ring of sterols to the C7(8) position in the ergosterol biosynthetic pathway (Figure 1.6). Yeast lacking or containing a mutation in the *ERG2* gene require exogenous ergosterol, as its precursors are not a substitute without other mutations (Silve *et al.*, 1996). σ-1R ligands such as ifenprodil and haloperidol are able to inhibit the growth of yeast by interfering with the C7-C8 isomerase catalytic activity (Moebius *et al.*, 1996, Silve *et al.*, 1996). The *ERG2* has therefore be suggested to be an ancestor of the σ-1R (Moebius *et al.*, 1996). However the σ-1R is unable to rescue *ERG2* negative strains of yeast (Hanner *et al.*, 1996), which suggests that the σ-1R has by itself no isomerase activity.

The mammalian protein, emopamil binding protein (EBP) shares pharmacological similarities with the σ1R, having moderate to high affinities for σ-1R ligands such as pentazocine, haloperidol and ifenprodil (Moebius *et al.*, 1997) and has C7-C8 isomerase activity and therefore is considered to be the mammalian homologue of the yeast *ERG2* gene (Moebius *et al.*, 2003). Interestingly despite sharing many pharmacological similarities with the σ-1 R, EPB shares no homology with the σ-1 R, and the transmembrane topology is different, with EPB having 4 transmembrane regions, and the σ-1R only 2 (Moebius *et al.*, 1997a, Moebius *et al.*, 1997b, Silve *et al.*, 1996).
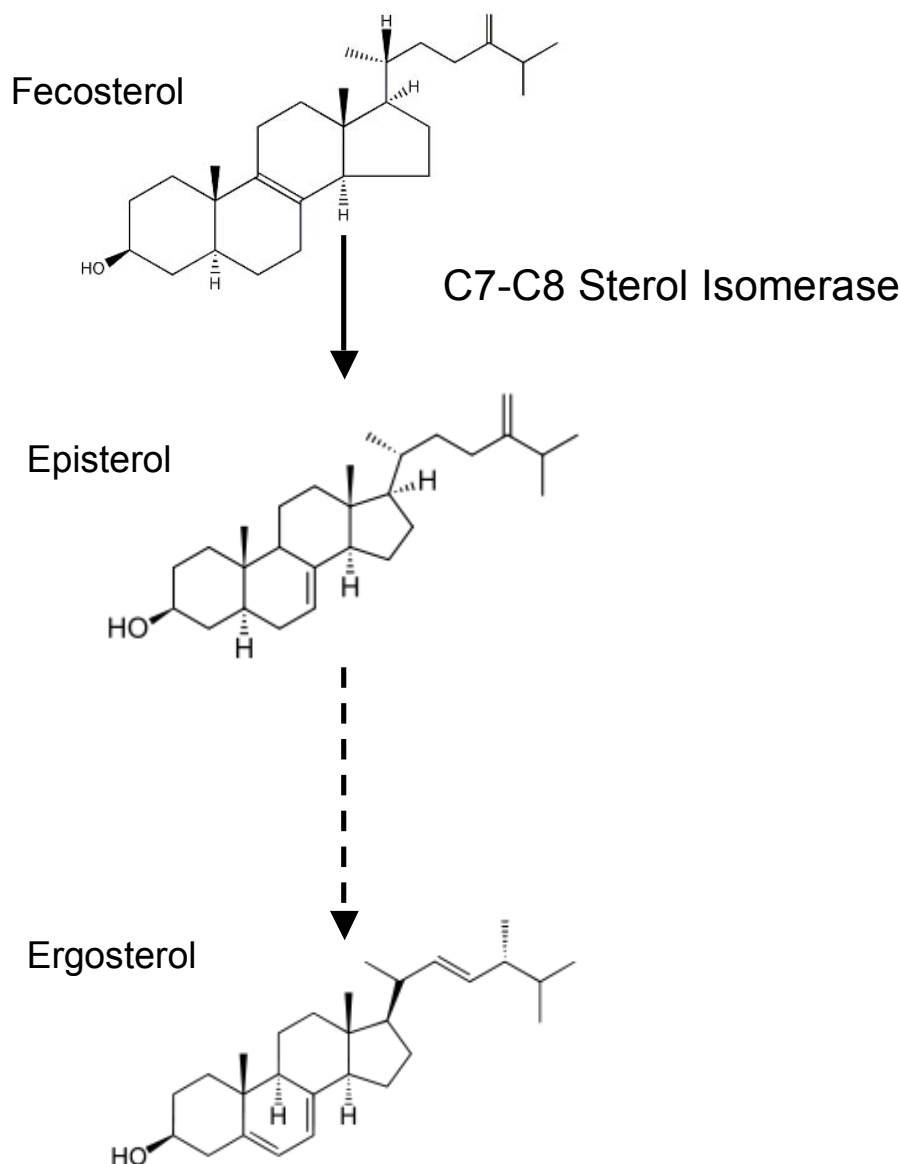
Figure 1.6: Fungal sterol biosynthesis pathway highlighting the C7-C8 Sterol isomerase step. Ergosterol plays a similar role in the membrane of yeast as cholesterol plays for mammals, The C7-C8 sterol isomerase is an important enzyme in ergosterol biosynthesis in yeast as yeast lacking the enzyme do not survive.

The pharmacological similarity between the σ-1R and these other cholesterol binding proteins led to further research into cholesterol binding to the σ-1R (Figure 1.7) (Palmer *et al.*, 2007). Two cholesterol binding domains were identified in the σ1R, located such that cholesterol docking takes place within the plasma membrane and sharing a number of amino acids which appear to be obligatory for other σ-1R ligand binding (Palmer *et al.*, 2007). It has been hypothesised that the σ-1R is capable of inserting cholesterol into the plasma membrane (Hayashi and Su, 2003b, Palmer *et al.*, 2007), modulating lipid raft formation (Hayashi and Su, 2005a, Hayashi and Su, 2003b, Hayashi and Su, 2004, Hayashi and Su, 2005b, Mavlyutov and Ruoho, 2007, Palmer *et al.*, 2007, Takebayashi *et al.*, 2004)
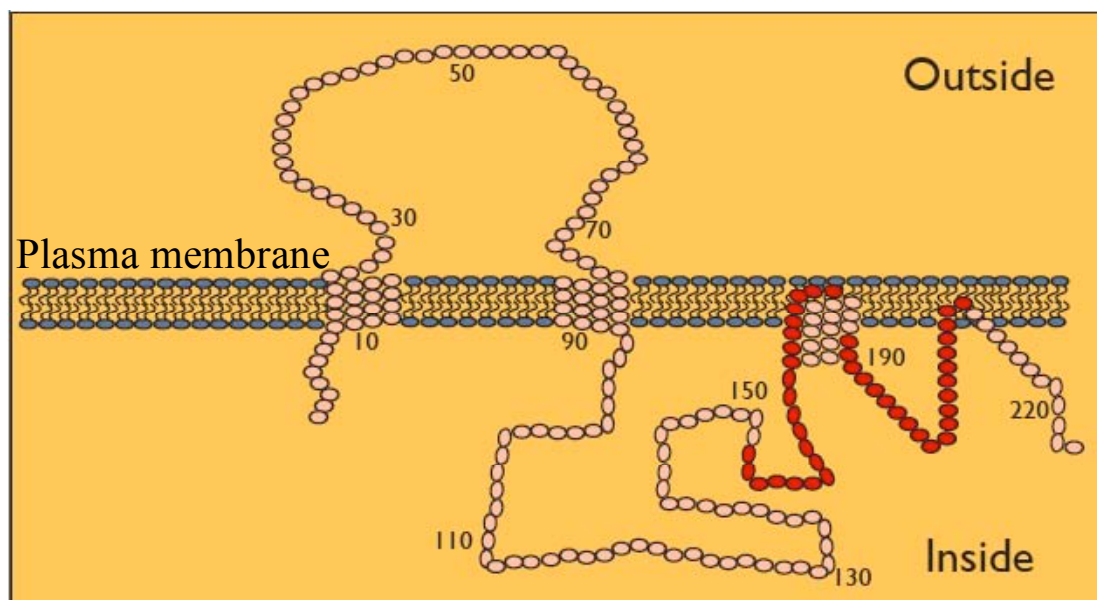
Figure 1.7: Predicted σ-1R structure highlighting the amino acids involved in cholesterol binding. Adapted from Palmer *et al*., 2007. The σ-1R with 2 transmembrane regions and a 3rd membrane-associated region containing the amino acids essential for cholesterol binding.

1.8 σ-1 receptors and lipid rafts

It was once thought that the main function of phospholipid bilayers was as a solvent for membrane proteins which were free to move about randomly (Singer and Nicolson, 1972). It is now widely accepted that the plasma membrane plays a more functional role in cellular function. Free-moving, stable, lateral assemblies of sphingolipids and cholesterol form what are known as lipid rafts (Figure 1.8) (Edidin, 2003, Simons and Ikonen, 1997). Amongst other functions lipid rafts bring together and appear to be able to control a number of signalling proteins, including glycosylphosphatidylinositol (GPI)-anchored proteins (Hooper, 1999), double acetylated proteins such as the src-family kinases or the α-subunit of the heterotrimeric G-proteins (Resh, 1999) and transmembrane proteins. Lipid rafts are involved in a number of cellular functions including cellular differentiation and programmed cell death (apoptosis) (Galbiati *et al.*, 2001, Zhang *et al.*, 2009). The distribution of lipid rafts over the cell membrane differs depending on the cell type. In neurons lipid rafts are more abundant on somal and axonal membranes than on dendritic membranes. Lipid rafts are also found on post-synaptic sites of neurones (Suzuki, 2002). Neuronal lipid rafts appear to play a role in cell adhesion, modulation of ion channels and neurotransmitter release (Chamberlain *et al.*, 2001).

Cholesterol plays an important part in lipid raft formation, maintaining membrane integrity and fluidity (Silvius, 2003), whilst also acting as a spacer between the hydrocarbon chains of the sphingolipids (London and Brown, 2000, Simons and Toomre, 2000). There is evidence to suggest that the σ-1R binds to cholesterol, as described above in (Figure 1.7) (Palmer *et al.*, 2007), and that it associates with lipid rafts, modulating their cholesterol content changing their formation and therefore potentially affecting the signalling molecules that are associated with these lipid rafts (Hayashi and Su, 2003b, Hayashi and Su, 2003a, Hayashi and Su, 2004, Hayashi and Su, 2005b, Palmer *et al.*, 2007, Takebayashi *et al.*, 2004).
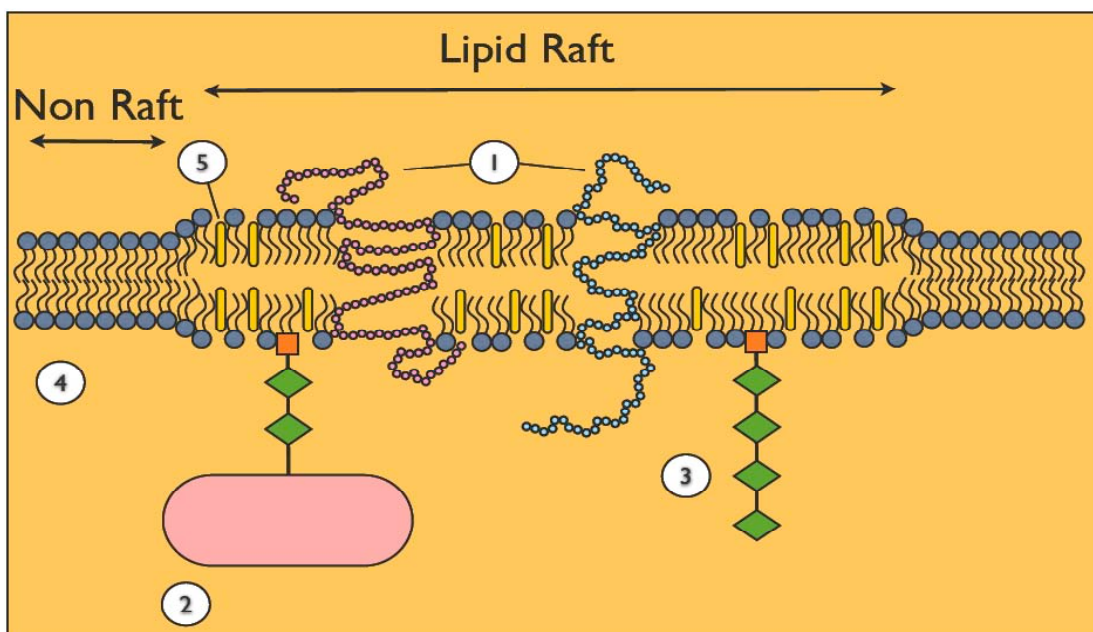
Figure 1.8: Lipid raft formation. The lipid raft forms a stable domain separating it from the rest of the membrane, recruiting specific receptors and proteins to form scaffolds for signalling processes. **1:** Raft associated membrane receptors **2:** GPI-anchored protein **3:** Glycolipid **4:** Non-raft membrane **5:** Cholesterol. Adapted from Edidin (2001).

The cholesterol content of the plasma membrane is tightly regulated, involving the uptake of cholesterol rich low-density lipoproteins from the plasma and from synthetic pathways. Cholesterol accumulation has been shown to occur in a number of solid tumours including prostate (Freeman *et al.*, 2005, Freeman and Solomon, 2004, Hager *et al.*, 2006, Zhuang *et al.*, 2002) and oral cancers (Kolanjiappan *et al.*, 2003). Furthermore, cholesterol dysregulation has been identified in other malignancies including lung and breast cancers (Duncan *et al.*, 2004). Given that cholesterol is an important component of lipid rafts, it is not surprising that lipid rafts appear to be up-regulated in a number of cancer cell lines, moreover disrupting lipid rafts by depleting cholesterol leads to apoptosis in certain breast cancer cell lines including MCF-7 and MDA-MB-231 cell lines and prostate cancer cell lines including PC-3 (Li *et al.*, 2006).

The σ-1R has been implicated in lipid and cholesterol transport from the endoplasmic reticulum to the plasma membrane. When functionally dominant negative σ-1Rs that are unable to interact with endoplasmic lipids or cholesterol, were transfected into NG108 cells (a neuroblastoma cell line) there was a build up of lipid and cholesterol at the endoplasmic reticulum and a decrease cholesterol at the plasma membrane (Hayashi and Su, 2003). This, along with the evidence that the σ-1R can translocate from the endoplasmic reticulum to the plasma membrane (Hayashi and Su, 2001, Mavlyutov and Ruoho, 2007, Morin-Surun *et al.*, 1999), suggests strongly that the σ-1R can modulate the cholesterol content of the plasma membrane, controlling the formation of lipid rafts and signalling domains.

1.9 σ-1 receptors and cancer

In normal healthy cells at any one time there are specific signals that prevent programmed cell death (apoptosis) and are likely to have evolved to maintain correct spatiotemporal patterning during development (Kerr *et al.*, 1972, Raff, 1992). There are also signals that lead to apoptosis for example when a cell is damaged or has reached the end of its lifespan.

Cancer is caused by abnormalities in the genetic material of cells, which can be caused by carcinogens such as tobacco smoke, radiation, chemicals, or infectious agents (e.g. viruses). Other cancer abnormalities can be caused by random mutations and errors during DNA replication, or can be inherited from a parent, therefore the abnormal gene will be found in every cell of the offspring. There are two classes of genes which are affected that go on to cause cancers. Oncogenes (under normal circumstances are called proto-oncogenes) have roles in the promotion of cell division, if a mutation takes place in the proto-oncogene such that its expression is up regulated or its product is constantly active, driving cell division and growth, it becomes a tumour producing agent (Vogt, 1993). Examples of oncogenes include the GTPase Ras (Bracquart *et al.*, 2009), tyrosine kinase receptors such as epidermal growth factor receptor (Lurje and Lenz, 2009) and transcription factors such as the Myc gene (Ruggero, 2009). The other class of genes that are affected that lead to cancers are known as tumour suppressor genes, these genes produce products that are responsible for preventing the cell from dividing. Examples include p53, which is mutated in 50% of human tumours (Hollstein *et al.*, 1991) and acts to hold the cell in the G_1 phase of the cell cycle such that damaged DNA can be repaired, and

is able to initiate apoptosis if the DNA damage is beyond repair (Zilfou and Lowe, 2009). Other examples include adenomatosis polyposis coli (APC), which when mutated leads to colorectal cancer (Markowitz and Bertagnolli, 2009), PTEN which works to negatively regulate the levels of phosphatidylinositol 3,4,5-trisphosphate preventing cells dividing too rapidly (Chu and Tarnawski, 2004) and CD95 (the Fas Receptor) which, on activation, leads to the formation of the death inducing signalling complex (DISC). Tumour suppressor genes usually require a mutation in both alleles in order to lead to a tumour-forming mutation as usually the remaining allele is sufficient to protect the cell from tumourogenesis, whereas a single allele mutation of an oncogene is enough to allow the cell to avoid apoptosis (Knudson, 1971).

Apoptosis can be triggered by an number of stimuli, including activation of death receptors (by cytokines such as tumour necrosis factor or Fas Ligand) and the formation of the DISC, oxidative stress, growth factor insufficiencies or calcium influx into the cytoplasm through channels in the plasma membrane or released from the endoplasmic reticulum (Mattson and Chan, 2003). The σ-1R has been shown to be involved in the influx of calcium into the cytoplasm (Spruce *et al*., 2004), and it is possible that the σ-1R can modulate lipid rafts, which have been linked with Fas receptor and DISC (Legembre *et al.*, 2006). The role of calcium in apoptosis is outlined in Figure 1.9, which shows an extracellular stimulus leading to cytoplasmic increases in calcium. With respect to σ-1R antagonist-induced apoptosis, this is likely to take place through the modulation of ion channels in the plasma membrane (Mavlyutov and Ruoho, 2007, Morin-Surun *et al*., 1999, Novakova *et al*., 1998, Spruce *et al*., 2004). The increase in cytoplasmic calcium leads to an uptake of calcium into the mitochondria, which in turn leads to the release of cytochrome C into the cytoplasm, which activates caspase and nuclease enzymes.
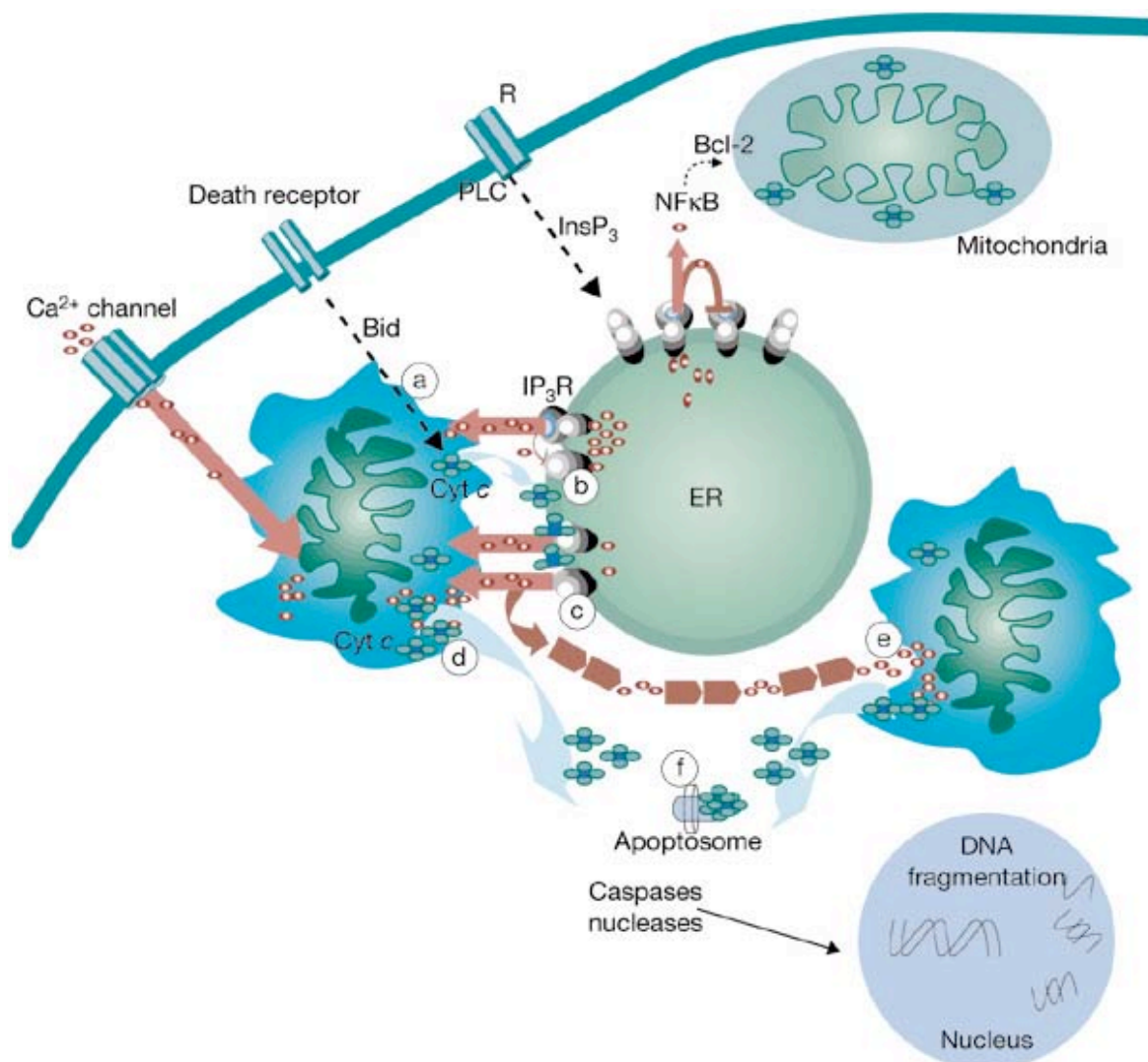
Figure 1.9: The role of calcium and cytochrome C in cellular apoptosis (Mattson and Chan, 2003). Rapid increase in cytosolic calcium via calcium channels at the plasma membrane or via release from stores by phospholipase C activation and IP_3 receptor activation, leads to calcium entry into the mitochondria, inducing the release of cytochrome C. Cytochrome C can cause further release of calcium causing more cytochrome C release from the mitochondria, forming apoptosomes and activating caspase cascades leading to DNA fragmentation. ER - Endoplasmic reticulum.

Cells with limited access to nutrients and survival factors may have evolved by expressing σ-1Rs to prevent them from undergoing premature apoptosis (Goyagi *et al.*, 2003, Maurice and Lockhart, 1997, Ola *et al.*, 2001, Wang and Duncan, 2006, Wang *et al.*, 2005). Avoiding apoptosis is also important to tumour cell survival, and one could suggest that tumours have hijacked the σ-1R as a potential driving force in cell survival (Wang and Duncan, 2006, Wang *et al.*, 2005). Antagonising with σ-1R antagonists provides a potential way of releasing cells from an antiapoptotic drive (Spruce *et al.*, 2004). Conversely, PRE-084, an agonist at the σ-1R, has been shown to prevent amyloid beta-mediated toxicity in the rat retina. In this case, σ-1R agonists are preventing an apoptotic signal (Cantarella *et al.*, 2007).

Cancer can affect people of all ages, and according to the World Health Organisation accounted for 13% (7.4 million) of deaths world wide in 2004, and this figure is expected to rise to 12 million by 2030. Based on risk factors it is thought that 30% of cancers are preventable (Danaei *et al.*, 2005), leaving 70% of cancers that require treatment. The principal treatment methods are a combination of surgery, chemotherapy and radiotherapy. Fundamental to adequate treatment is cancer imaging using ultrasound, endoscopy or radiography. σ-1Rs are highly expressed in a number of cancers and tumours, and have previously been shown to be useful in tumour imaging, using labelled σ-1R ligands in positron emission tomography (PET) scans (Kawamura *et al.*, 2005). A number of studies have shown, using radioligand binding, real time PCR, western blotting and immunohistochemistry techniques, that a wide range of human and mouse tumour cell lines express high levels of σ-1Rs (Aydar *et al.*, 2004, Bem *et al.*, 1991, Vilner *et al.*, 1995b). Using a range of cell lines Spruce *et al.* (2004) showed that the σ-1R antagonists such as rimcazole, haloperidol, BD1047, BD1067, *cis*-U50488 and IPAG were able to reduce tumour cell viability, moreover rimcazole and *cis*-U50488 were able to inhibit or reduce xenograft tumour growth. Wang *et al.* (2004) showed in a similar study that neoplastic breast epithelial cells expressed the σ-1R, and that haloperidol and progesterone inhibited tumour growth in a dose-dependent fashion at high concentrations. Aydar *et al.* (2006) also showed that silencing the expression of the σ-1R using an RNAi vector resulted in reduction of cell adhesion to the culture dish. This evidence appears to suggest that the σ-1R plays a role in cell survival and that the σ-1R is a potential target for cancer treatments.

Interestingly, it has also been shown that σ-1R agonists can cause increases in tumour growth (Gardner *et al.*, 2004, Zhu *et al.*, 2003). Both studies showed that σ-1R agonists such as cocaine and PRE-048 dose-dependently increased tumour growth. The growth was also dependent on IL-10, and could be blocked using either σ-1R antagonists or an IL-10 antibody. However a immunohistochemical study of 95 patients with breast cancer showed no statistical correlation between σ-1Rs and tumour size or shape (Simony-Lafontaine *et al.*, 2000). This study did however show that patients with a high σ-1R-expressing tumour lived longer in a disease-free state (81% showed no recurrence of the cancer within 5 years) than those without σ-1R expression (Simony-Lafontaine *et al.*, 2000). These results appear slightly paradoxical as it goes against the notion that the σ-1R is in some way promoting tumour growth and as yet these findings have yet to be explained.

1.10 σ-1 receptors and depression

Depression is a seriously debilitating medical disorder, which can occur in early life and run a chronic course, adversely affecting the prognosis of a number of other medical conditions including diabetes (Charney and Manji, 2004), coronary vascular disease (Lett *et al.*, 2004) and osteoporosis (Cizza *et al.*, 2001). Common symptoms include long-lasting depressed mood, feelings of guilt, anxiety and it is not uncommon for patients with severe depression to commit suicide (Kessler *et al.*, 2005); in 1999 the number of suicides in the USA was 30,000 and is the 3rd leading cause of death between 15 and 24 year olds (Charney and Manji, 2004).

The main theory behind depression is the monoamine hypothesis (Schildkraut *et al.*, 1965), which states that depression is caused by a functional lack of monoamine neurotransmitters such as serotonin (5-HT), dopamine and noradrenaline in specific parts of the brain. The hypothesis was borne out of clinical observations of various drugs that appeared to alleviate depression and were known to have effects on monoaminic neurotransmission in the brain. Early versions of antidepressants were monoamine oxidase inhibitors, such as phenelzine, which acutely increase monoamine function by preventing their metabolism (Manji *et al.*, 2001, Morilak and Frazer, 2004) resulting in an increase in the cytosolic stores of 5-HT, noradrenaline and dopamine (Figure 1.10). Another early form of antidepressants were the tricyclics such as imipramine and clomipramine, these work by blocking the monoamine transporters, again resulting in an increase in available noradrenaline or 5-HT in the synaptic cleft. The tricyclic and the monoamine oxidase antidepressants have a number of undesirable side-effects, are incompatible with many other drugs, in the case of the monoamine oxidases foods ("The cheese effect" - monoamine oxidase inhibition in the gut results in the prevention of the breakdown of normally innocuous amines) and interactions with other neurotransmitter receptors result in toxicity in overdose (Stahl, 2005). Recent development of selective re-uptake inhibitors such as the selective 5-HT re-uptake inhibitors (SSRIs) have strengthened the monoamine hypothesis (Renard *et al.*, 2001, Ressler and Nemeroff, 2000), and largely superseded the tricyclics and monoamine oxidase inhibitors (Stahl, 2005). SSRIs include fluoxetine, fluvoxamine, citalopram and sertraline; they act to selectively block 5-HT re-uptake over noradrenaline re-uptake and are less likely than the tricyclics to cause dangerous side effects, and do not cause "the cheese effect."
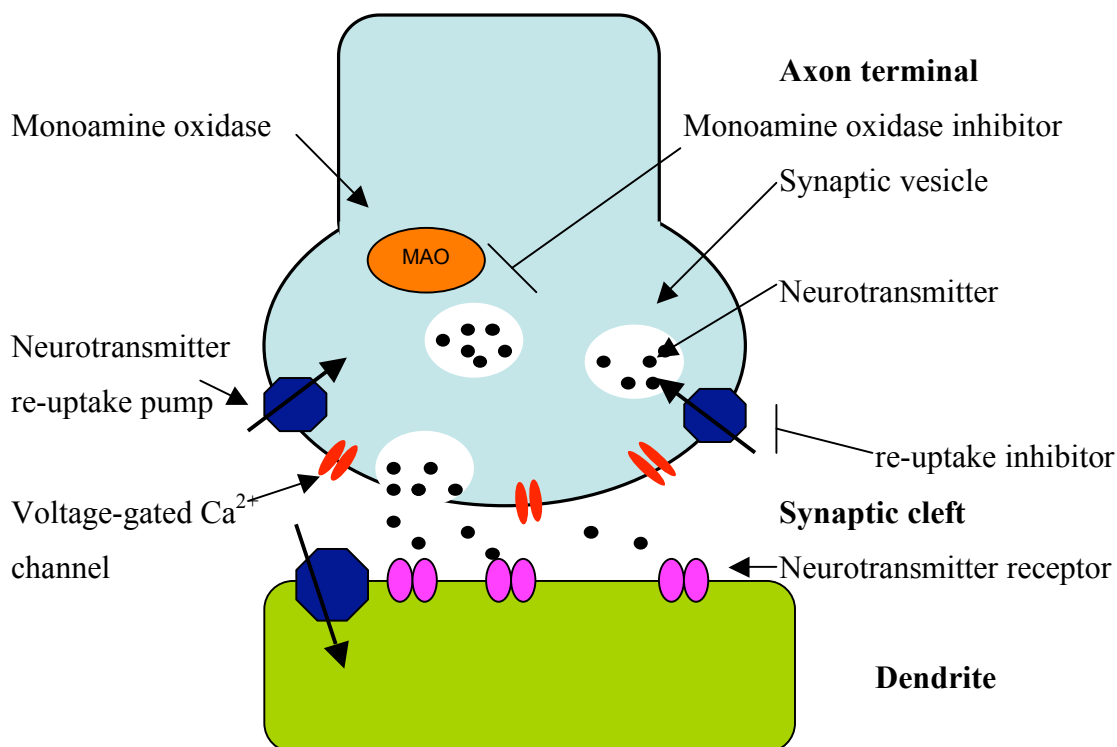
Figure 1.10 The synapse. Neurotransmitter release from the axon in response to depolarisation passing the signal onto the adjacent cell. Monoamine oxidase (MAO) inhibitors act to prevent neurotransmitter breakdown resulting in an increased stock of transmitter waiting to be released. Tricyclic antidepressants nonspecifically block neurotransmitter re-uptake pumps. Selective re-uptake inhibitors prevent the specific uptake of a specific neurotransmitter.

Despite the evidence for the monoamine hypothesis, such as the fact that nearly all effective antidepressant drugs result in noradrenaline or 5-HT increase in the synapse, either through blocking re-uptake or preventing breakdown of the neurotransmitters (Stahl, 2005), there are problems with the monoamine hypothesis. The current antidepressant drugs are effective in less than 50% of patients (Nestler *et al.*, 2002). Furthermore, chronic treatment with antidepressant drugs is required in order to see clinical effects, the reason for this is still unknown (Hyman and Nestler, 1996).

A major problem in antidepressant activity is the lack of validated animal models as the symptoms of depression, such as depressed mood, feelings of worthlessness and suicidality are difficult to measure and quantify in laboratory animals (Nestler *et al.*, 2002). The current animal models therefore measure one of two things, the effect of known antidepressants, or the response to stress. Despite this the available models such as the forced swim test, where a mouse or rat is made to swim in a container and lack of

struggling is thought to represent a state of despair (Porsolt *et al.*, 1977), have had some success in predicting the antidepressant efficacy of new drugs in humans. However, no novel (non-monoamine-based) antidepressants have been identified (Nestler *et al.*, 2002). Another problem with the available animal models is that acute treatment with the current available antidepressants results in apparent antidepressant activity despite in a clinical setting chronic treatment is required to see a antidepressant effect (Hyman and Nestler, 1996). It should also be noted that the animals used in these studies of depression are "normal" animals without a genetic or underlying depressive condition. As yet no animal model for depression has been produced, and until the genes that make a subject susceptible to depression are identified a model is unlikely to be produced (Nestler *et al.*, 2002).

The interest in the σ-1R and its involvement in depression began when it was noted that the antidepressants fluvoxamine, fluoxetine, citalopram, sertraline, clorgyline, and imipramine all had nanomolar affinity for the σ-1R (Itzhak and Kassim, 1990, Narita *et al.*, 1996). It has since been shown that these antidepressants can behave as σ-1R agonists. The SSRI sertraline and the monoamine oxidase inhibitor clorgyline selectively, in a haloperidol sensitive fashion, potentiated NMDA neurotransmissions. Further evidence for the σ-1Rs involvement in depression comes from a study showing that the SSRI imipramine reduced the number of σ-1Rs without affecting their affinity for [3H] DTG (Shirayama *et al.*, 1993). It has been reported that the σ-1R specific drug NE-100 may regulate the 5-HT$_{2A}$ receptor (Narita *et al.*, 1995), suggesting that the σ-1R interacts with serotonergic neurons. Furthermore, direct evidence from behavioral studies demonstrated that the σ-1R agonists tested, including (+) pentazocine, DTG, SKF-10,047 dose-dependently decreased the immobility time in the forced swim test, and the effects were antagonized by the σ-1R antagonists NE-100 or BD1047 (Urani *et al.*, 2004). Other σ-1R agonists have been shown to have antidepressant properties using the tail suspension test, including SA4503 (Matsuno *et al.*, 1996b, Matsuno *et al.*, 1997, Ukai *et al.*, 1998). Igmesine has been shown to have antidepressant properties in the forced swim test (Urani *et al.*, 2001) tail suspension test (Ukai *et al.*, 1998) and the conditioned fear stress test (Urani *et al.*, 2004). Igmesine has been used in a clinical study, where patients were given either the placebo, igmesine (25mg or 100mg/day) or as a positive control, 20mg/day fluoxetine. Igmesine and fluoxetine both showed statistically significant effects superior to the placebo (Volz and Stoll, 2004), suggesting that igmesine is potentially a clinically active antidepressant. However, igmesine has not been developed further as an antidepressant. Interestingly

Urani *et al.* (2002, 2004) showed that the σ-1R agonists SKF-10,047, PRE-084, igmesine, and DHEA sulphate, were more effective than SSRI or tricyclic antidepressants. Venlafaxine is an inhibitor of both 5-HT and noradrenaline reuptake, has affinity for the σ-1R (Dhir and Kulkarni, 2007), and chronic treatment with venlafaxine has a shorter delay before antidepressant effects can be seen compared to other antidepressants (Mitchell and Redfern, 2005), which could potentially be attributed to the σ-1R activity.

A study utilizing σ-1R knock-out mice to investigate the involvement of σ-1Rs in depressive behaviour showed that σ-1R negative mice had an increased immobility time in the forced swim test, therefore indicating a potential increase in depressive like behaviour (Sabino *et al.*, 2009). This is consistent with the studies showing σ-1R agonists reduce immobility time in the forced swim test, (Akunne *et al.*, 2001, Dhir and Kulkarni, 2007, Dhir and Kulkarni, 2008, Matsuno *et al.*, 1996a, Reddy *et al.*, 1998, Ukai *et al.*, 1998, Urani *et al.*, 2001, Wang *et al.*, 2007) and the binding studies that show currently clinically used antidepressants having σ-1R affinity (Dhir and Kulkarni, 2007, Dhir and Kulkarni, 2008, Itzhak and Kassim, 1990, Narita *et al.*, 1996, Wang *et al.*, 2007). Sabino *et al.* (2009) suggest that the antidepressant effects seen though agonising the σ-1R (or depressant effects seen by knocking it out) are linked to serotonergic neurotransmission, since σ-1R agonists such as (+) pentazocine an DTG have been shown to increase serotonergic neurone firing (Bermack and Debonnel, 2001). This study further highlights the discrepancy in the nomenclature of σ-1R ligands, since knocking out the σ-1R has the same effect as using the σ-1R agonists such as SKF-10,047 begging the question are the σ-1R agonists actually switching off the σ-1R?

Another mechanism has been put forward to explain the antidepressant effects of σ-1R agonists, which involves the endoplasmic reticulum stress response (Sabino *et al.*, 2009). Proteins synthesised at the endoplasmic reticulum are folded with the aid of chaperone proteins. Misfolded, malformed proteins are disposed of by endoplasmic reticulum-associated protein degradation. When the amount of unfolded protein exceeds the endoplasmic reticulum's capacity, cells can activate a defence mechanism known as the endoplasmic reticulum stress response (Yoshida, 2007). It is thought that deregulation of this stress response leads to a number of neurodegenerative and mood disorders including Alzheimer's disease (Hoozemans *et al.*, 2005, Katayama *et al.*, 1999, Unterberger *et al.*, 2006) and bipolar disorder (Kakiuchi *et al.*, 2005, Kakiuchi *et al.*, 2004). Since the σ-1R, as described previously in relation to tumour formation, is cytoprotective it has been

hypothesised that the σ-1R is an endoplasmic reticulum chaperone protein that can counteract endoplasmic reticulum stress (Hayashi and Su, 2007) (e.g. controlling calcium signalling and possibly membrane cholesterol content). With respect to the Sabino *et al.* (2009) knock-out study, it could be the case that loss of the σ-1R results in a decreased ability to deal with endoplasmic reticulum stress, leading to cell death and impairment of neurotransmission, which results in the depressive like behaviour of the mice.

1.11 Other aspects of the σ-1 receptor

Addiction

The σ-1 receptor has been known to have actions in addictive processes, despite the confusion with the NDMA and PCP receptors, selective σ-1 receptor drugs have been shown to modulate dopaminergic and serotoninergic systems. A number of recent studies have shown that σ-1R activation plays a role in the plasticity underlying reinforcement, and addictive processes (Maurice and Su, 2009).

Cocaine

Cocaine binds to the σ-1R with an affinity, depending on the enantiomer used, (+) 25.9μM (-) 6.7μM (Sharkey *et al.*, 1988) and is able to activate the σ-1R producing its stimulant properties. Furthermore, pre-treatment with σ-1R antagonists blocks these stimulant effects. Also targeting the σ-1R with an antisense probe was able to inhibit the stimulant effects in the animals of cocaine (Matsumoto *et al.*, 2002, Romieu *et al.*, 2002).

A second interesting connection between cocaine and the σ-1R is the link between cocaine, the σ-1R, HIV and immunity. Because cocaine binds the σ-1R and cocaine leads to enhanced HIV replication, the role of the σ-1 receptor in immune alteration has been investigated. Treatment of microglial cells with cocaine resulted in a dose-dependent increase in HIV expression, this increase was blocked by the σ-1R antagonist BD1047 (Gekker *et al.*, 2006).

Amnesia

The σ-1R has been studied extensively with respect to learning and memory, selective σ-1R agonists when injected alone failed to improve learning, consolidation or retention phases of mnemonic processes but markedly improved the mnemonic process in animal

models of amnesia (Maurice and Su, 2009). In amnesia models induced by blocking cholinergic or glutamateric neurotransmissions the σ-1R agonists lowered the mnemonic deficits measured by behavioral processes assessing long term, short term and contextual or spatial memory (Maurice and Lockhart, 1997). A number of σ-1R ligands have been investigated mnemonic models including (+) pentazocine and (+) SKF-10,047, as well as more selective σ-1 receptor ligands such as PRE-084 and igmesine. In the water-maze test the impairment of spatial memory measured in aged rats could be reduced by σ-1R agonist treatment (Maurice et al., 1994).

Alzheimer's disease

As described above, σ-1R expression and σ-1R agonists protect cells from apoptosis and there has been a number of studies that have looked into the use of σ-1R ligands for the protection of brain tissue in Alzheimer's disease. The acetylcholinesterase inhibitor, donepezil, is used to treat Alzheimer's disease and has been found to have high σ-1R affinity (15 nM) (Kato et al., 1999). Donepezil acts as a σ-1R agonist and has anti-amnesic effects against dizocilpine-, β-amyloid 25–35 peptide, or carbon monoxide-induced mnemonic impairment (Maurice et al., 2006). The σ-1R has been shown in vitro to be important in Alzheimer's disease, β_{25-35} peptide-induced cell death in cultured cortical neurons could be inhibited by the σ-1R agonist PRE-084, and the agonist effects could be reversed by the σ-1R antagonist NE-100 (Marrazzo et al., 2005). Furthermore, when the σ-1R agonists were injected into mice along with β_{25-35} peptide, the σ-1R ligands reduced β_{25-35} peptide damage to the hippocampus and reduced the learning and attention deficits in the mice (Goyagi et al., 2001).

Schizophrenia

Schizophrenia is characterised by positive symptoms (*positive symptoms* refers to symptoms that most individuals do not normally experience but are present in schizophrenia) that include delusions, hallucinations, paranoia and loss of touch with reality and negative symptoms (*negative symptoms* refer to the loss of traits found in normal/healthy individuals), which consist of loss of memory, lack of attention span and loss of motivation. The traditional antipsychotic, haloperidol, binds σ-1R with high affinity (Su et al., 1988), however, the link between schizophrenia and the σ-1R has yet to be satisfactorily demonstrated (Maurice and Su, 2009). Studies of polymorphisms in the σ-1R gene with relation to schizophrenia have yielded conflicting results. One study using 46 randomly selected schizophrenic patients showed that the TT haplotype in the GC-241-

240TT polymorphism and a substitution of A to C producing the substitution of a glutamine for a proline in the human σ-1R were significantly associated schizophrenia (Ishiguro *et al.*, 1998). However, whilst other studies have identified these polymorphisms, they have not shown a significant correlation between these polymorphisms and an increased risk of schizophrenia (Ohmori *et al.*, 2000, Uchida *et al.*, 2003).

Rimcazole was developed as a σ-1R targeting antipsychotic by the Wellcome Research Laboratories. Rimcazole was hypothesised as a novel antipsychotic which lacked the common side effects of other antipsychotics such as chronic blockade of dopamine receptors (Ferris *et al.*, 1982). Clinical trials (in the 1980s) ended when at low doses limited efficacy was observed and higher doses resulted in grand mal seizures (Borison *et al.*, 1991, Chouinard and Annable, 1984).

1.12 Aims of this thesis

The original pharmacophore of the σ-1R has been based on the original opioid receptor ligands, which often contain more than 1 nitrogen and have complex aromatic ring structures. A number of studies looking for a structure-activity-relationship between ligands and the σ-1R have been carried out before (Ablordeppey *et al.*, 1998, Ablordeppey *et al.*, 2000, Glennon *et al.*, 1994). However all these studies have started with complex structures and not provided a simple new σ-1 ligand. In this thesis I set out to reduce the complexity and identify a simple structure with σ-1R affinity and activity, without the minimum 7 synthetic steps required to make a new chemical entity (Baxendale *et al.*, 2007, Ley and Baxendale, 2002). Furthermore, I sought to determine whether such a simple pharmacophore can be used as a basis for selective agonists and antagonists.

Chapter 2

2 Materials and Methods.

2.1 General materials

General laboratory chemicals were purchased from Sigma-Aldrich Company Ltd (Dorset, UK). Tissue culture media, antibiotics, trypsin and serum were purchased from Invitrogen (Paisley, UK). Nunc tissue culture flasks and Nunc multiple well plates were purchased from Fisher Scientific (Loughborough, Leicestershire, UK).

2.2 Tissue culture

MDA-MB-468 (ATCC LGC Promotech, Middlesex, UK) and HEK 293 (ECACC) cells were grown in Dulbecco Modified Eagle's minimum essential media (DMEM), supplemented with 4mM L-glutamine, 10% foetal calf serum (FCS), Fungizone (amphotericin B, 2.5µg/ml), penicillin (100 units/ml) and streptomycin (100µg/ml). MAC 13 and MAC 16 cells were grown in RPMI media supplemented with L-glutamine, 10% FCS, Fungizone (amphotericin B, 2.5µg/ml) and penicillin (100 units/ml) /streptomycin (100µg/ml). The cells were incubated at 37 °C in a humidified air / 5% CO_2 atmosphere.

Figure 2.1: Phase contrast micrograph showing MDA-MB-468 cells growing in DMEM supplemented with FCS, L-glutamine, penicillin/streptomycin and Fungizone.
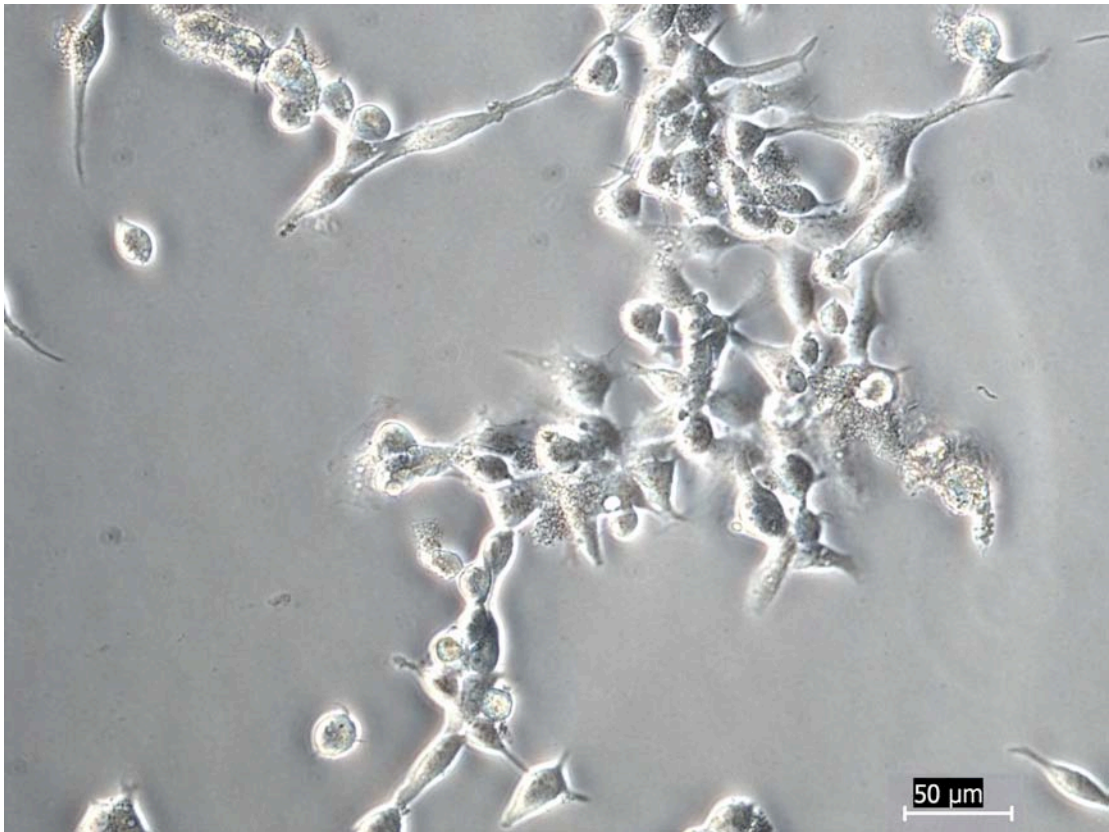
Figure 2.2: Phase contrast micrograph showing HEK 293 cells growing in DMEM supplemented with FCS, L- glutamine, penicillin/streptomycin and Fungizone.

2.3 MDA-MB-468 propagation and storage

MDA-MB-468 cells are human breast adenocarcinoma cells isolated from a 51-year-old black female. They were chosen for their high expression of the σ-1R (Spruce *et al.,* 2004). MDA-MB-468 cells are adherent to tissue culture plastic. Cells were split having reached 80% confluency, using 0.25% w/v trypsin 0.5mM ethylenediaminetetraacetic acid (EDTA), and incubated at 37°C until the cells had detached from the flask. An equal volume of DMEM 10% FCS was added to the cells before they were transferred to a sterile centrifuge tube and spun down at 240*g*. The pellet was resuspended in the required volume of DMEM 10% FCS, and transferred into tissue culture flasks.

When freezing cells down for storage, the pellet would be resuspended in DMEM 10% FCS supplemented with 5% v/v DMSO, placed in to cryovials and the cells chilled down slowly to 4°C before being place at -20°C over night. The following day the vials were transferred to -80°C where they were stored until required.

When thawing cells, vials were taken straight from the -80°C freezer, and placed into a

pre-warmed 37°C water bath to thaw. Once thawed the contents of the vial were transferred to a tissue culture flask containing DMEM 10% FCS that had been pre-warmed to 37°C in the humidified air incubator with 5% CO_2. The flasks were incubated at 37°C overnight. The following day the media would be changed removing all cells that failed to adhere to the tissue culture plastic.

2.4 General ligand preparation

The simple amines were purchased from Sigma-Aldrich (Dorset, UK), Fluka (Sigma-Aldrich, Dorset, UK) or Acros Organics (Fisher Scientific, Loughborourgh, UK) as either hydrochloride salts (HCl•) or as a free base (see Table 2.1).

Name	Salt/Base	Vender	Chemical formula	Structure
Primary amines				
Propylammonium	**Free base**	**Fluka**	C_3H_9N	
Butylammonium	**Free base**	**Fluka**	$C_4H_{11}N$	
Pentylammonium	**Free base**	**Fluka**	$C_5H_{13}N$	
Hexylammonium	**Free base**	**Fluka**	$C_6H_{15}N$	
Branched-chain Primary amines				
1-Adamantlyammonium	**Free base**	**Sigma Aldrich**	$C_{10}H_{17}N$	
2-Adamantlyammonium	**HCl•**	**Sigma Aldrich**	$C_{10}H_{17}N$	
Secondary amines				
Dimethylammonium	**HCl•**	**Sigma Aldrich**	C_2H_7N	
Diethylammonium	**HCl•**	**Sigma Aldrich**	$C_4H_{11}N$	
Dipropylammonium	**HCl•**	**Sigma Aldrich**	$C_6H_{15}N$	
Dibutylammonium	**Free base**	**Sigma Aldrich**	$C_8H_{19}N$	
Dipentylammonium	**Free base**	**Sigma Aldrich**	$C_{10}H_{23}N$	
Dihexylammonium	**Free base**	**Sigma Aldrich**	$C_{12}H_{27}N$	
Secondary branched				
Diisopropylammonium	**Free base**	**Sigma Aldrich**	$C_6H_{15}N$	
Diisobutylammonium	**HCl•**	**Sigma Aldrich**	$C_8H_{19}N$	
Bis(2-ethylhexyl)ammonium	**Free base**	**Sigma Aldrich**	$C_{16}H_{35}N$	
Di-sec-butylammonium	**Free base**	**Sigma Aldrich**	$C_8H_{19}N$	
di-tert-amylammonium	**Free base**	**Sigma Aldrich**	$C_{10}H_{23}N$	
Tertiary amines				
Trimethylammonium	**HCl•**	**Fluka**	C_3H_9N	
Triethylammonium	**HCl•**	**Fluka**	$C_6H_{15}N$	
Tripropylammonium	**HCl•**	**Sigma Aldrich**	$C_9H_{21}N$	

Table 2.1 continued
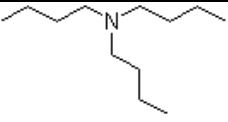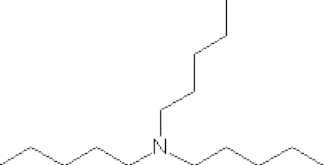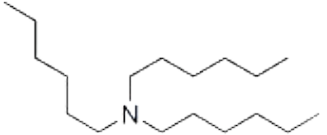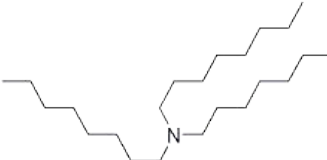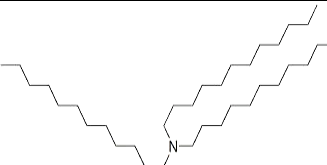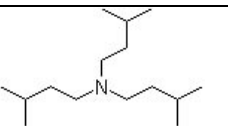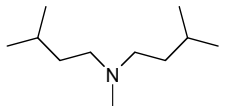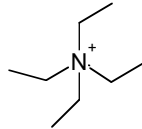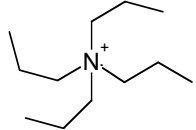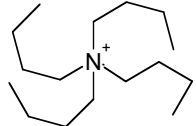
Tributylammonium	**HCl•**	**Fluka**	$C_{12}H_{27}N$	
Tripentylammonium	**Free base**	**Sigma Aldrich**	$C_{15}H_{33}N$	
Trihexylammonium	**Free base**	**Sigma Aldrich**	$C_{18}H_{39}H$	
Trioctylammonium	**Free base**	**Sigma Aldrich**	$C_{24}H_{51}N$	
Tridodecylammonium	**Free base**	**Sigma Aldrich**	$C_{36}H_{75}N$	
Branched-chain tertiary amines				
Triisopentylammonium	**Free base**	**Fluka**	$C_{15}H_{33}N$	
NN-diiso butylmethylammonium	**Free base**	**Sigma Aldrich**	$C_9H_{21}N$	
Quaternary amines				
Tetramethylammonium	**HCl•**	**Acros Organics**	$C_4H_{12}N$	
Tetraethylammonium	**HCl•**	**Sigma Aldrich**	$C_8H_{20}N$	
Tetrapropylammonium	**HCl•**	**Acros Organics**	$C_{12}H_{28}N$	
Tetrabutylammonium	**HCl•**	**Sigma Aldrich**	$C_{16}H_{36}N$	

Table 2.1: Simple ammonium salt structure, salt, and where it was purchased from.

The free base amines were made soluble in water by making the HCl salt. 5 ml of free base amine was dissolved in 15ml of ether, and hydrochloric acid (HCl) was added slowly until the mixture turned acidic, measured using universal indicator paper (Sigma-Aldrich, Dorset, UK). The resulting solid was filtered and any remaining solvent was removed under vacuum. If the solid did not come out of solution the solvents were removed under vacuum. 9-(3-((3R,5S)-3,5-dimethylpiperazin-1-yl)propyl)-9H-carbazole (rimcazole) (purchased from Sigma-Aldrich, Dorset, UK) was dissolved in DMSO, or methanol. 1-(4-iodophenyl)-3-(2-adamantyl)guanidine (IPAG) (purchased form Tocris Bioscience, Bristol, UK) was dissolved in DMSO. [³H] (1S,9S,13S)-1,13-dimethyl-10-(3-methylbut-2-en-1-yl)-10-azatricyclotrideca-2,4,6-trien-4-ol ((+)-pentazocine) (specific activity 32.2 Ci/mmol) was purchased from Perkin-Elmer (Beaconsfield, UK).

Rimcazole **(+) Pentazocine**
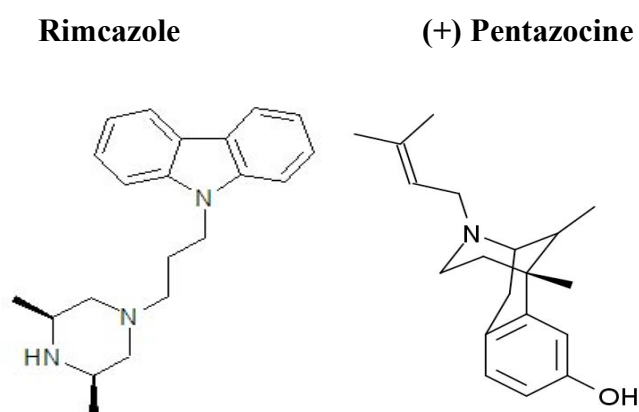
Figure 2.3: Structures of rimcazole and (+) pentazocine.

2.5   General radioligand binding

Cells were harvested prior to the experiments using 0.25% trypsin 1mM EDTA and stored at -20°C before use. On the day of the experiment cells were thawed and resuspended in 10mM tris(hydroxymethyl)aminomethane (Tris) buffered saline (TBS) (10mM Tris 0.9% NaCl pH 7.4). The cells were permeabilised (5 pulses at 3.74KV/cm) and put on ice before use in the assay. Assays were set up in sets of 24 10ml tubes.

2.6   Saturation binding

The assay was set out as with the competition binding, other than the [³H] (+) pentazocine was made up 3000nM, 1000nM, 300nM, 100nM, 30nM, and 10nM, and 10 µl was added and to the 100µl final volume. The assays were carried out in duplicate and specific

binding calculated by subtracting the non-specific binding [^{3}H] (+) pentazocine (determined with 0.1mM rimcazole in the assay) from the total [^{3}H] (+) pentazocine binding.

2.7   Competition assays

 [^{3}H] (+) Pentazocine was diluted in TBS to 300nM and 10μl were added to the tube giving a final assay concentration of 30nM. The competing ligand was prepared at 10 times the required concentration, and 10μl added to the tube. The volume was then made up to 50μl TBS, before adding 50 μl of the permeabilised cells to give a final volume of 100μl. The assay was then allowed to equilibrate for at least two hours at room temperature. After equilibration the cells were harvested using a Brandel M-24R cell harvester through untreated GF/B fired glass fibre filters (Semat International, St Albans. UK), washing with 3 times 10ml room temperature TBS. The glass fibre filters containing the cells with bound [^{3}H] (+) pentazocine were placed into scintillation vial with 2ml of scintillant. The scintillant was allowed to soak into the filters overnight before counting in a Perkin Elmer Liquid scintillation analyzer Tricarb 2800TR (5min counts). Non-specific [^{3}H] (+) pentazocine binding was determined using 0.1mM rimcazole.   Under   these   conditions less than 10% of the [^{3}H] (+) pentazocine was bound.

Muscarinic receptor binding assays

Rat brain membranes were prepared from freshly killed rats. The brain was immediately removed and placed on ice with TBS pH of 7.4. The brain was homogenised in 10ml of ice cold TBS by a Teflon-in-glass homogeniser for two 30s periods, the homogenates were weighed and then centrifuged at 40000g for 30 minutes at 4°C. The resultant supernatant was discarded and the pellets resuspended by homogenisation in fresh TBS. Protein concentrations were determined using the Bradford protein assay (Section 2.9). 1.35nM [^{3}H] QNB (L-quinuclidinyl [phenyl-4-^{3}H] benzilate; 48.0 Ci/mmol) (GE Healthcare), was incubated with rat brain membranes (0.5mg/ml) to which varying concentrations of ammonium salt compounds were added as with the σ-1R competition assays. The membranes were incubated and harvested as with the [^{3}H] (+) pentazocine binding assays.

Competition binding with antagonists

The assay was set as except that incubations were carried out for 6 hours to allow time for equilibration, since competing ligands with lower affinities require more time to reach equilibrium. The assay was also carried out on ice to prevent receptor internalization and preserve the 2 state nature of the receptor. The cells were also washed 3 times in 10ml of TBS after permeabilisation to remove any native GTP. Cellular GTP concentration was checked using high performance liquid chromatography (HPLC).

2.8 Cyclic AMP measurements

MDA-MB-468 cells were cultured until confluent in a 175cm Nunc tissue culture flask before being harvested with 0.25% trypsin, EDTA 0.5mM. Cells were plated into 24-well multiplates at a confluency of 50%. The following day, DMEM was replaced with Tris-buffer Krebs solution and cells were allowed to equilibrate for 30 minutes. Drugs were added for 30 minutes and the supernatant was removed before samples were quenched by the addition of 100μl 0.6M PCA. The supernatant was removed and neutralised with 18μl 2M K_2CO_3. Further centrifugation allowed for the removal of potassium perchlorate precipitate. The supernatant was assayed for cAMP content using a commercially available kit (TRK432, GE Healthcare, Little Chalfont, UK). Assays were routinely performed at 4^oC in a total volume of 100μl. A 25μl portion of K_2CO_3-neutralised PCA containing standard amounts of cAMP (0.00625 to 4 pmoles) was added to 25μl buffer (Tris HCl 50mM, EDTA 4mM, pH 7.5) containing trace levels of [^{3}H] cAMP (approximately 450fmol, 12.5nCi, 27,500 disintegrations per minute (DPM)). A soluble preparation of cAMP binding protein (50μl) was then added and assays were allowed to equilibrate. After 2 hours at 4^oC a 50μl aliquot of activated charcoal suspension was added and after 3 minutes, samples were centrifuged at 15,000g for 3 minutes. Activated charcoal bound rapidly to the unbound cAMP thus separating it from that bound which remained in the supernatant The supernatant (100μl) was carefully removed and transferred into a scintillation vial, to which was added 2ml scintillation cocktail. Radioactivity was assessed using a liquid scintillation counter.

In parallel, 25μl aliquots of cell extracts were treated in the same fashion. The amount of cAMP in each sample was calculated using GraphPad Prism by reading off the standard curve, fitted with linear regression.

2.9   Protein measurements

Protein amounts were determined using BioRad Protein Dye Reagent, based on Coomassie Brilliant Blue G250. Bovine serum albumin (BSA) was dissolved in 0.1M sodium hydroxide. 10 µl were placed in a well of a 96-well plate at a concentration of 0-400µg/ml, followed by 200µl of the protein dye reagent (1:5 dilution). Following an incubation of 10 minutes absorbance was measured at 595nm.

2.10 MTS cell proliferation assay

Cells were harvested with 0.25% trypsin and 1mM EDTA and spun down at 240g. The pellet was washed in fresh DMEM containing 10% FCS, before the cells were seeded onto a 96 well plate and allowed to adhere overnight. If cells were to be transfected, this took place on day 2 so they were left a further 24 hours before the addition of drugs, however if not then the drugs were added on day 2 and the cells incubated overnight (10X concentration and 10µl into 90µl of DMEM to give 1 X in the well).

The day after drug addition the metabolic activity was measured using the CellTiter 96® AQ$_{ueous}$ Non-Radioactive Cell Proliferation Assay (MTS assay) (Promega, Southampton, UK). Metabolically active cells will convert 3-(4,5-dimethylthiazol-2-yl)-5-(3-carboxymethoxyphenyl)-2-(4-sulfophenyl)-2H-tetrazolium (MTS) into media-soluble formazan, the absorbance of which can be measured at 490nm. The amount of formazan produced is directly proportional to the number of living cells in the well.
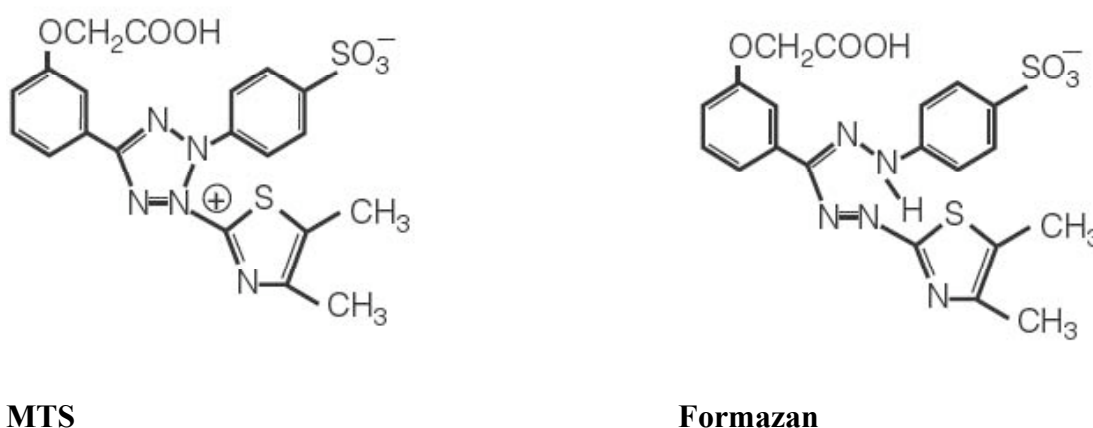
MTS   **Formazan**

Figure 2.4: Structures of MTS and formazan
MTS from Promega and formazan which is produced by metabolically active cells from the MTS, images obtained from Promega MTS assay manual.

On the day of metabolic activity measurement, phenazine methosulfate (PMS) (an electron coupling reagent) was mixed with the MTS in a 1:20 ratio before 10μl of the MTS/PMS mix was added to the well of the 96 well plate containing 100μl of tissue culture media. Readings at 490nm were taken every 15 minutes for up to 2 hours until the readings levelled off. In between readings the 96 well plate was kept in the 37°C, 5% CO_2 humidified air incubator. Rates of cell metabolism were compared by taking the absorbance at the final time point at which the increase in absorbance is still linear (if the absorbance had reached a plateau by 2 hours then an earlier time point was used), minus the blank (well with media MTS/PMS but no cells) and taking away the absorbance at time 0 minus the blank. The absorbance measured in untreated cells was designated as 100% and the absorbance in the blanks designated 0%.

2.11 Fura-2 calcium measurements

On the day of the experiment cells were harvested with 0.25% trypsin 1mM EDTA and spun down at 240g, the cell pellet was resuspended in a buffer containing 115mM NaCl, 5mM KCl, 1mM NaH_2PO_4, 0.5mM $MgSO_4$, 11mM glucose, 1.36mM $CaCl_2$, 0.1% BSA, 50mM Tris (note that Tris and not 4-(2-hydroxyethyl)-1-piperazineethanesulfonic acid (HEPES) was used to buffer the cells as HEPES has σ-1R affinity (Figure 2.5), with an affinity of approximately 10mM) pH 7.4. Approximately 20 million cells were resuspended in 2 ml of buffer. The cells were loaded with cell permeable Fura-2-acetoxymethyl ester (Fura-2-AM) (5μM) (Invitrogen, UK) (a modified version of the calcium indicator developed in 1985 (Grynkiewicz *et al.*, 1985), dissolved in DMSO and diluted 1/1000 in TBS) and incubated at room temperature for 45 minutes. Loading at room temperature rather than 37°C for 45 minutes reduced the cellular compartmentalization of the Fura-2 resulting in better loading of the cells (Roe *et al.*, 1990).
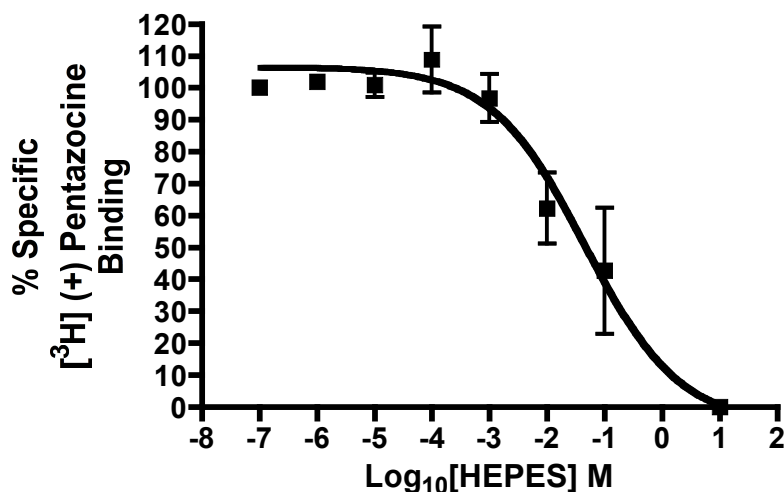
Figure 2.5: HEPES competition with [³H] (+) pentazocine. Error bars represent SEM from 3 independent radioligand competition experiments, using permeabilised MDA-MB-468 cells. HEPES affinity for the σ-1R was determined as (pKi + SEM) 1.9 ± 0.5.

The cells were then spun down and washed in the warmed calcium buffer three times before being made up to 1 million cells per ml and incubated at room temperature for a further 30 minute to allow the acetoxymethyl groups to be removed by cellular esterases resulting in free Fura-2 in the cells. The cells were then kept in suspension in the dark at room temperature before use in calcium measurements. 2 ml of Fura-2 loaded cells were placed in a cuvette with a magnetic stirring bar and placed into the fluorometer, (Perkin Elmer luminescence spectrometer LS-50B) and were maintained at 37°C. The cells were excited at 340nm and 380nm and emissions were recorded at 510nm. When bound to Ca^{2+} Fura-2 undergoes an excitation shift between 335nm (calcium free) and 363nm (calcium saturated) whilst the emission wavelength remains unchanged. This can be visualized by scanning the excitation wavelength between 300nm and 400nm and recording the emission at 510nm Figure 2.6.
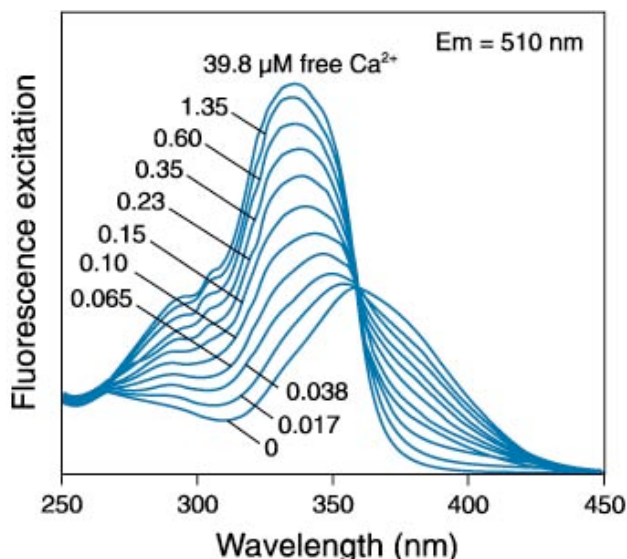
Figure 2.6: Fluorescence excitation spectra of Fura-2. Multiple solutions containing between 0 and 39.8 μM free $[Ca^{2+}]$, scanned between 250nm and 450nm and emission (Em) read at 510 nm. Data obtained from Invitrogen.

The largest dynamic range for $[Ca^{2+}]$ dependent fluorescent signals is obtained by using the ratio of fluorescence emitted at 510 after excitation at 340nm and 380nm. At low concentrations of dye, taking 340/380 ratios allows accurate measurements of intracellular calcium and allows for differences in dye loading, cell thickness and other problems that can effect calcium measurements.

Drugs were made up at 100 times concentration and pH balanced to 7.4 before 20μl was injected into the cuvette resulting in 1 x concentration in the cuvette. At the end of each individual experiment 20μl of 1mg/ml digitonin was added to the cuvette to permeabilise the cells allowing calcium to flood the dye giving a maximum fluorescence, followed by 60μl of 0.5M EDTA pH 8.5 to chelate the calcium giving a minimum fluorescence. These values were then used to calculate the cytosolic calcium concentration of the cells, using the Grynkiewicz *et al.* (1985) equation.

$[Ca^{2+}]_i = K_d (R-R_{min}) / (R-R_{max})$.

Where the K_d for Fura-2 is 225nM, R is the ratio of emissions recorded at 340nm and 380nm, R_{min} is the minimum ratio of emissions recorded at 340nm and 380nm after the addition of EDTA chelating the calcium, and R_{max} is the maximum ratio emissions recorded at 340nm and 380nm after the addition of digitonin causing the Fura-2 to be saturated with calcium. Unloaded cells were used to check autofluorescence and drug fluorescence.

2.12 High Performance Liquid Chromatography

MDA-MB-468 cells were cultured until confluent in a 175cm Nunc tissue culture flask before being harvested with 0.25% trypsin, EDTA 0.5mM. Cells were spun down and washed in TBS containing 2mM $MgCl_2$ before being permeabilised with 5 pulses of 3.74KV/cm. The permeabilised cells were treated with drugs at 37ºC for 30 mins, in a 200μl assay volume. The samples were quenched with 100μl 2M PCA and neutralized with 58μl K_2CO_3. 250μl samples were loaded on the following HPLC gradient through a Partisphere SAX 5μm column (Whatman, UK), dimensions 4.6mm x 125mm, with buffer A consisting of H_2O, and Buffer B consisting of 1.3M $(NH_4)_2HPO_4$, pH 4.8 with H_3PO_4.

Time	Buffer and gradient
0-2 min	0% B, 1 ml/min
2-15 min	linear gradient up to 39% B (3%/min)
15.1 min	0% B
16 min	1ml/min
16-21 min	ramp volume from 1-1.5ml/min
21.0 min	0.02ml/min

Table 2.2: HPLC conditions.

The absorbance at 260nm was measured throughout. The GTP control ran at 19.8 minutes and GDP at 14.2 minutes. Area under the curve was measured using Gilson Unipoint software (Anachem, Luton, UK).

2.13 σ-1 GFP expression

The pCMV6-AC-Sigma-1 GFP vector was purchased from Origene (Cambridge Biosciences, Cambridge, UK). The vector contains the CMV promoter driving heterologous expression of the σ-1R. The receptor is in frame with turbo Green fluorescent protein (tGFP) at the C-terminus. The tGFP allows positive identification of mammalian cells transfected with the plasmid. Mammalian cells were transfected with the σ-1 GFP vector using the transfection reagent, Jet PEI (Autogen Bioclear, Calne, UK).
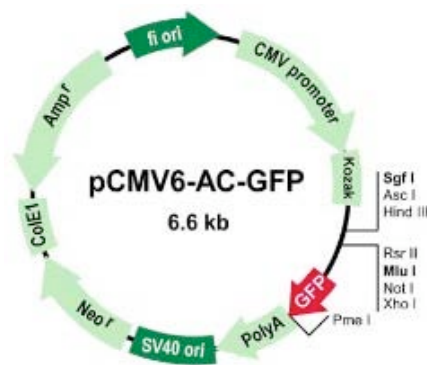
Figure 2.7: Map of vector pCMV6-AC-GFP Origene TrueClone hand Book (Cambridge Biosciences, Cambridge, UK)**.** The σ-1 cDNA was cloned into sites SGF I and Mlu I.

2.14 Mammalian cell transfection

The following transient transfection protocol, modified from the Jet PEI handbook (Autogen Bioclear, Calne, UK), is for 24 well plates, if larger or smaller volumes of cells were required then the volumes of reagents were adjusted accordingly. Prior to transfection the HEK 293 cells were seeded at 50,000 cells/ well in 1ml of DMEM containing 10% FCS. The cells were allowed to adhere to the plate before being transfected. The transfection complexes were prepared as follows. Per well: 1μg of DNA was diluted in 150mM NaCl to a final volume of 50μl, in a separate tube 2μl of Jet PEI was diluted in 150mM NaCl to a final volume of 50μl. The Jet PEI was added to the DNA solution, mixed then incubated at room temperature for 30 mins. Jet PEI/DNA mixture (100μl per well) was added drop wise whilst swirling the plate. The plates were then returned to the humidified incubator at 37°C and 5% CO_2 where they were left for 24 to 48 hours before transfection was assessed.

2.15 Cloning and sub-cloning

On receiving vectors containing σ-1Rs or siRNAs they were grown up by transforming chemically competent DH5α *Escherichia coli* using a heat shock method modified from Froger and Hall, 2007. DH5α *E. coli* were thawed slowly on ice and then transferred in to microcentrifuge tubes containing 50μl aliquots before the DNA that was to be transformed was added, the cells were then incubated on ice for up to 30 minutes, before being transferred to a 42°C water bath for 30 seconds then returned to the ice. 250μl of room temperature Super Optimal Broth with Catabolite repression (SOC) (consisting of 2% w/v bacto tryptone, 0.5% w/v yeast extract, 10mM NaCl, 2.5mM KCl, 10mM $MgCl_2$, and

20mM glucose and sterilized by autoclaving at 121°C for 15 minutes) was added and the cells incubated for 1 hour (2 hours for kanamycin resistant vectors) at 37°C with shaking. The transformed *E. coli* were then plated onto Lysogeny Broth (LB) (10g/l tryptone, 5g/l yeast extract, 10g/l NaCl pH 7.5 and sterilized by autoclaving at 121°C) agar (1.5% w/v) plates containing the appropriate antibiotic, and incubated at 37°C overnight. The next day colonies were picked and grown in LB media containing the appropriate antibiotic (ampicillin 1μg/ml final concentration) at 37°C with shaking overnight. The following day the *E. coli* were pelletted by centrifugation and the plasmid extracted using a Qiagen (Crawley, UK) plasmid isolation kit.

2.16 σ-1 knock-down

The σ-1RNAi pSilencer vector and the non targeting RNAi control were obtained from Dr Christopher Palmer, Imperial College London described in Aydar *et al*., 2006. MDA-MB-468 cells were transfected with the σ-1RNAi pSilencer vector or the non-targeting RNAi control using the Jet PEI DNA transfection reagent, using the protocol described above. σ-1R activity was assessed 24 to 48 hours later using radioligand binding, MTS cell proliferation assay, or by measuring calcium influx.

2.17 σ-1 GFP mutagenesis

Site directed mutagenesis is the addition, removal or substitution of a specific amino acid/s the method for which was modified from (Hutchison *et al.*, 1978). Forward and reverse oligonucleotides (Sigma Genosys, Cambridge, UK) of approximately 30 base pairs were designed with a mutation in the middle as detailed in table 2.2 below. The oligonucleotides were used in a polymerase chain reaction (PCR) mutagenesis protocol using a high fidelity polymerase enzyme. The σ-1 GFP (approximately 15μl at 2ng/μl) construct was mixed with the oligonucleotides, dATP, dGTP, dCTP, dTTP (5μl at 2mM each), 5 times phusion polymerase buffer (10μl) and 1μl of phusion polymerase (NEB, Hitchin, UK). The PCR mix was then heated to 98°C for 5 minutes, followed by 18 cycles of 98°C for 30 seconds, 60°C for 30 seconds and 68°C for 4.5 minutes. A final extension step at the end for 5 minutes at 68°C was added to the protocol. After the PCR cycle was finished 5μl of Dpn1 buffer and 1μl of the restriction enzyme Dpn1 was added to the tube and incubated at 37°C for 1 hour. Dpn1 will only cut were the recognition site (5'-GA*TC-3') is methylated. The

σ-1 GFP construct grown up in *E. coli* is methylated, whilst the PCR product is not, therefore the Dpn1 treatment should remove any "parent" DNA leaving only the PCR product containing the desired mutation. After Dpn1 digestion 5µl of the resulting mixture was used to transform competent *E. coli*, which were then grown overnight at 37°C on LB agar plates containing ampicillin as the selection agent. The next day colonies were picked and grown up overnight in 10ml of LB media containing ampicillin at 37°C with shaking. The construct was then isolated using a Qiagen mini-prep kit before being sent for sequencing (Geneservice, Source Bioscience Cambridge, UK) to check the mutation had taken place and to make sure no PCR errors had occurred.

Mutation	Forward primer
D126G	5'-GGCTGAGATCTCGGGTACCATCATCTCTGG-3'
DEE76-78GGG	5'- CCACGTGCTGCCCGGCGGGGGGCTGCAGTGGGTG-3'
DHE53-55GHG	5'-GGGCTGGGCCACGGGCTGGCCTTCTCTCGTC -3'
E102G	5'- CGCCTCGCTGTCCGGGTATGTGCTGCTCTTCGG-3'
E172G	5'-CCAAACACATGGATGGTGGGGTACGGCCGGGG-3'
E64G	5'-CGTCTGATCGTGGGGCTGCGGCGGCTGCACC -3'
EE41/42GG	5'-CGTCTTCCAGCGCGGAGGGATAGCGCAGTTGG-3'
Mutation	Reverse primer
D126G	5'-CCAGAGATGATGGTACCCGAGATCTCAGCC-3'
DEE76-78GGG	5'-CACCCACTGCAGCCCCCCGCCGGGCAGCACGTGG-3'
DHE53-55GHG	5'- GACGAGAGAAGGCCAGCCCGTGGCCCAGCCC-3'
E102G	5'-CCGAAGAGCAGCACATACCCGGACAGCGAGGCG-3'
E172G	5'- CCCCGGCCGTACCCCACCATCCATGTGTTTGG -3'
E64G	5'-GGTGCAGCCGCCGCAGCCCCACGATCAGACG-3'
EE41/42GG	5'- CCAACTGCGCTATCCCTCCGCGCTGGAAGACG -3'

Table 2.3: Table of forward and reverse primers
Primers designed to induce specific mutations in the σ-1R. Mutated amino acids indicated in the first column, and the bases mutated to achieve these changes are highlighted in red in the next 2 columns with in the sequences of the PCR primers.

Once the sequence was verified and the desired mutation in place, the vector was grown up in *E. coli*, and isolated using a Qiagen midi prep kit. The vector was then transfected into HEK 293 cells using the Jet PEI transfection reagent. Expression was visualized using fluorescence microscopy, and quantified using flow cytometry, or western blotting. Affinity of the mutated receptor was measured using radioligand binding saturation experiments.

2.18 Fluorescence microscopy of cholera toxin B treated cells

The B subunit of the cholera protein complex is non toxic, and functions by binding to cellular surface via the polysaccharide chain of ganglioside G_{M1} (Merritt *et al.*, 1994). The ganglioside G_{M1} is found in membrane microdomains enriched with cholesterol and sphingolipids called lipid rafts. Therefore, fluorescently labelled cholera toxin B is able to highlight lipid raft formation.

MDA-MB-468 cells were plated out into 24 well plates and allowed to adhere to the tissue culture plastic overnight. On the day of the experiment cells were treated with the drug for 30 minutes, control cells were treated with an equal volume of PBS or DMSO depending on which the drug was dissolved. After treatment the cells were washed with PBS and fixed using 4% paraformaldehyde for 15 minutes. The paraformaldehyde was washed off with PBS. The wells were then blocked with 1% bovine serum albumin for 15 minutes to prevent nonspecific binding of the cholera toxin to the well. The cells were again washed with PBS. 200 µl of PBS was then added to each well, and 2 µl of 1mg/ml Alexa Fluor 594 cholera toxin subunit B conjugate (Invitrogen) was added to give a final concentration of 10µg/µl. The cells were then incubated for 2 hours at 37°C. The excess cholera toxin B was then washed off using PBS and then kept in the dark until images were taken on the fluorescence microscope.

2.19 Mouse cancer model

Testing for anti cancer activity *in vivo* was carried out on my behalf by Dr Steve Russell at Aston University Under Home Office Licence.

Animals

Naval Medical Research Institute (NMRI) mice weighing 25g were used for tumour transplantation, they were kept on a 12 hour day: night light cycle, at ambient temperature 22 ± 2 °C and had free access to food (standard chow diet, Special Diet Services, Lillico, Wonham Mill, Bletchworth Surrey, UK) and water, the consumption of which was monitored throughout the experiments.

Mac 13 transplant and treatment

For each drug and the control 3 NMRI mice where transplanted with a fragment of mouse adenocarcinoma (MAC13) in the flank, by means of a trocar (Bibby *et al.*, 1987). Twelve days after the tumour was implanted, animals were treated, on a daily basis, with either ammonium salt (10mg/kg *i.v.*, via the tail vein) or control (100ul PBS *i.v.* via the tail vein). Animals were terminated before the tumour exceeded 1cm^3.

Analysis

The tumour diameters were measured daily from day 12 using a micrometer. Statistical significance in tumour growth between control and treated mice was determined using GraphPad Prism (version4.0 for Macintosh).

2.20 Test for antidepressant activity

Testing for antidepressant activity was carried out in the Pharmacology Division, University Institute of Pharmaceutical Science, Panjab University, Chandigarh, India, by Mr. Kiran Kumar Akula, under the direction of Professor Kulkarni.

Animals

Male albino (laca strain) mice weighing between 22 and 30g (bred in the central animal house facility of the Panjab University) were housed under standard laboratory conditions with free access to food and water, and with a natural light dark cycle. The animals were acclimatised to the laboratory conditions before experiments, which were carried out between the hours of 09:00 and 15:00. Each animal was used only once. The experimental

protocols were approved by the Institutional Animal Ethics Committee (IAEC) and conducted according to the Indian National Science Academy Guidelines (INSA) for the use and care of experimental animals.

Forced swim test

Mice were individually forced to swim inside a rectangular glass jar ($25 \times 12 \times 25$ cm^3) containing 15 cm of water maintained at $24\pm1°$C. An animal is considered to be immobile whenever it remained floating passively in the water in a slightly hunched but upright position, its nose above the water surface. The total immobility period for a total period of 6 min was recorded with the help of stop-watch and percentage decrease in immobility period was calculated with respect to vehicle control group.

Tail suspension test

Mice were suspended on the edge of a lever above the table top (58 cm) by using adhesive tape placed approximately 1 cm from the tip of the tail. The other side of the lever had a writing pen to record the activity on the moving drum. The duration of immobility period was recorded on a moving drum (speed previously standardized) rotating at a speed of 15 cm/minute. A mouse was considered to be immobile when it was suspended passively and completely motionless. The recordings were done for a total period of 6 min. The percent immobility period was calculated from the tracings.

Drugs

Dipentylammonium was made up at 1, 2.5, 5, and 10 mg/kg and tripentylammonium was made up at 2.5, 5 and 10 mg/kg, fluoxetine (a standard antidepressant for comparison) at 10 mg/kg and BD1047 (N-[2-(3,4-dichlorophenyl)ethyl]-N-methyl-2-(dimethylamino)ethylamine) (σ-1R antagonist) at 2 and 4 mg/kg. The drugs were dissolved in normal saline and different doses were administered intraperitoneally in a fixed volume of 1 ml/100g body weight 30 minutes before the animals were subjected to the test.

Locomotive activity

The total number of ambulations and rearing in 15 minutes was measured using a computerised actophotometer, as described in Dhir *et al.* (2005). The actophotometer consists of a chamber divided up into quadrants with light beams, when the mouse breaks a light beam that movement is recorded.

2.21 Data analysis

Saturation data analysis were analysed using GraphPad Prism (version4.0 for Macintosh) non-linear regression analysis to fit saturation curves and calculate maximal radioligand binding and dissociation constants.

Equation: $S = B_{max} \cdot [L] / K_d + [L]$

Where S is the specific binding, [L] is the concentration of free radioligand, B_{max} is the total number of receptors expressed in the same units as S (i.e sites/cell, cpm or fmol/mg protein) and K_d is the equilibrium dissociation constant expressed in the same units as [L] (usually nM).

Scatchard plots were used only as a visual tool for comparing data, rather than for calculating maximal binding and equilibrium dissociation constants. Due to the fact that transforming the data to a linear form distorts the experimental error, whilst linear regression assumes that the scatter around the line follows the Gaussian distribution and that the standard error around X is the same for every point, this is not true for the transformed data, and there are much larger errors associated at the low concentrations of bound ligand, and therefore they have undue influence over the slope of the regression line resulting in a K_d and B_{max} further from the true value than using non linear regression.

Competitive binding data were analysed using GraphPad Prism non-linear curve fitting software. The equation used to fit competition binding data were the sigmoidal dose response (variable slope) model.

Equation: $Y = Bottom + (Top-Bottom) / 1 + (10^{(LogIC50-X)Hillslope})$

Where X is the logarithm of the concentration of competing ligand, Y is the response (i.e counts per minute or % specific radioligand binding) and the Hillslope is the slope factor, a number that describes the steepness of the curve. A one site competitive binding curve that follows the law of mass action will have a slope of -1 (negative as the slope goes down). The IC_{50} is dependent on the K_i of the ligand for the receptor, but also dependent on the concentration of radiolabelled drug used in the assay (i.e increasing the radiolabelled drug concentration will change the IC_{50} whilst the K_i remains the same). In order to give a more

true representation of the drugs affinity for the receptor, the IC_{50} was converted to a K_i value using the Cheng Prusoff equation (Cheng and Prusoff, 1973).

Equation: $K_i = IC_{50}/(1 + ([Radioligand]/K_d))$

The K_i value is derived from the IC_{50} which is on a log scale, therefore it does not make sense to present mean K_i values ± standard error of the mean (SEM) as the error is not symmetrical around the mean. Instead the mean K_i is displayed along with the 95% confidence interval (CI). The K_i was also converted into a pK_i ($-logK_i$), which is on a log scale, therefore the SEM is symmetrical about the mean pK_i.

When comparing two binding models to see which fits the data better the F test was employed to compare the models. The F test compares the increase in the sum of squares with the increase in degrees of freedom between the two models generating a ratio between the two. If the ratio (F value) is much greater than 1 you accept the more complicated model, a *P* value is also given showing the chance of this F value being a coincidence (Box, 1953).

Fura-2 fluorescence data were collected using FL WinLab software (PerkinElmer, USA). The data were collected using the Ratio Data Application, and then converted to intracellular calcium ion concentrations using the ICBC Calibration Application, which uses the Grynkiewicz equation described earlier. The data were then transferred into GraphPad Prism for representation.

MTS and protein assays were read using a Versamax plate reader, and the data collected using Softmax Pro software.

Chapter 3

3 Simple straight-chain ammonium salts - high affinity agonists at the σ-1 receptor

3.1 Background

The σ-1R antagonists have been shown to induce apoptosis in mammary and colon adenocarcinoma cell lines (Brent *et al.*, 1996a), whilst inhibiting the proliferation of colon and mammary carcinoma and melanoma cell lines (Vilner *et al.*, 1995a). In 2004 Spruce *et al.* (2004) showed that σ-1R antagonists such as rimcazole could inhibit tumour growth (Figure 3.1).
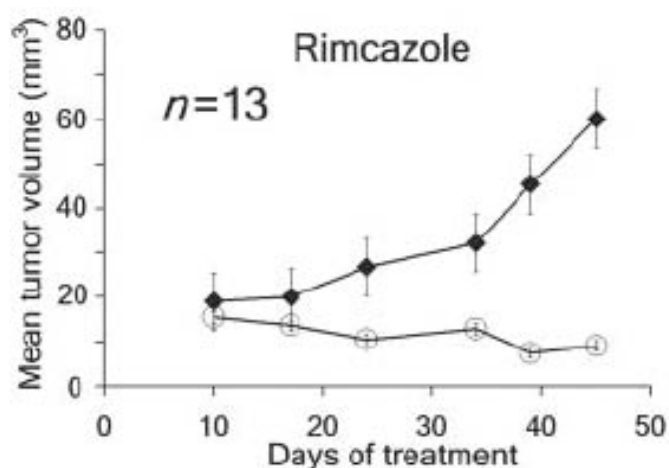
Figure 3.1: Effect of σ-1R antagonist rimcazole on tumour growth. MDA-MB-468 xenographted immunocompromised mice treated with rimcazole showed a reduction in tumour growth compared to the control mice (Spruce *et al.*, 2004).

Around the same time Maffucci *et al.* (2005) published data showing similar effects with inositol 1,3,4,5,6 pentakisphosphate (IP_5) (Figure 3.2) leading to the hypothesis that IP_5 could be a potential σ-1R ligand.
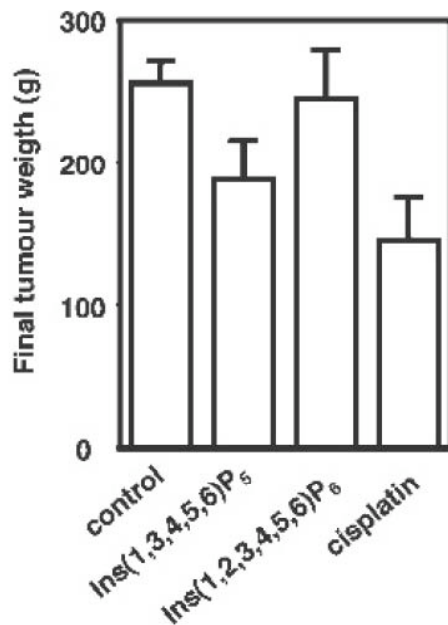
Figure 3.2: Effect of IP$_5$ on tumour growth. Nude mice were implanted with SKOV-3 tumour cells and treated with IP$_5$, IP$_6$ or cisplatin. IP$_5$ reduces final tumour volume after 58 days compared to the control, with a statistically significant P value < 0.05 as does the chemotherapy drug cisplatin used as a positive control P value < 0.01 (Maffucci *et al.*, 2005).

The hypothesis that IP$_5$ could be causing apoptosis in cancer cells through a σ-1R mediated pathway was tested using a radioligand binding assay. The assays were carried out with two different samples of IP$_5$ containing different counterions. When the IP$_5$ with the triethylammonium counterion was put into the radioligand binding assay (Figure 3.3) it appeared that the IP$_5$ had σ-1R affinity. However when the binding assay was repeated with a sample of IP$_5$ with a potassium counterion the affinity for the σ-1R disappeared. When triethylammonium was put into the assay alone it became clear that it was the triethylammonium with the σ-1R affinity and not the IP$_5$.
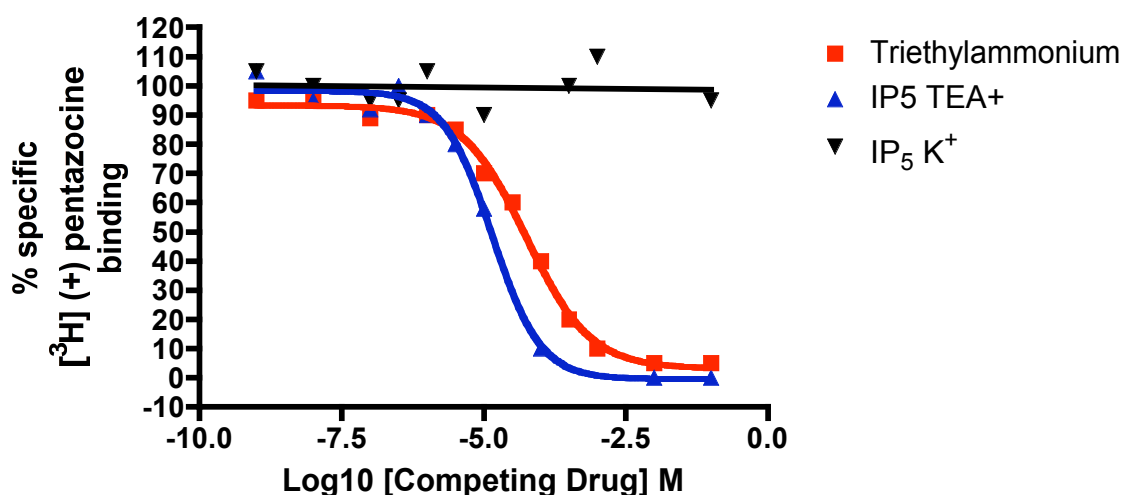
Figure 3.3: IP$_5$ Binding to the σ-1 Receptor. Binding of IP$_5$ with different counterions to the σ-1R, reveals that it is in fact triethylammonium with σ-1R affinity and not IP$_5$. IP$_5$ TEA$^+$ appears to have a higher affinity for the σ-1R that triethylammonium alone, however there are 3 molecules of TEA for each IP$_5$ accounting for this increase.

These preliminary data led to the hypothesis that simple ammonium salts are σ-1R ligands. The purpose of this section of my thesis was to investigate the structure activity relationship of these simple ammonium salts and the σ-1R. The simple ammonium salts differ from commonly used σ-1R ligands, which often contain more than one nitrogen and have complex aromatic ring structures; the simple ammonium salts contain only one nitrogen, and have simple straight carbon chains. There have been a number of previous studies looking for a structural relationship between sigma receptor ligands and their affinity for the σ-1R (Ablordeppey *et al.*, 1998, Ablordeppey *et al.*, 2000, Glennon *et al.*, 1994). The importance of the nitrogen atom has been shown for the phenylalkylpiperidines and phenylalkylpiperazines (Ablordeppey *et al.*, 2000) however no one has looked at such simple molecules as the simple ammonium salts discussed in this chapter.

3.2 Saturation [³H] (+) pentazocine binding in MDA-MB-468 cells

In order to calculate the number of σ-1Rs expressed on the MDA-MB-468 cells (B_{max}) and equilibrium dissociation constant (K_d) of [³H] (+) pentazocine in MDA-MB-468 cells, saturation binding experiments were carried out. Below (Figure 3.4) an example of a saturation binding curve for [³H] (+) pentazocine in permeabilised MDA-MB-468 cells can be seen with inset Scatchard plot for visualisation purposes only as the B_{max} and K_d were calculated using nonlinear regression software (GraphPad Prism, California).
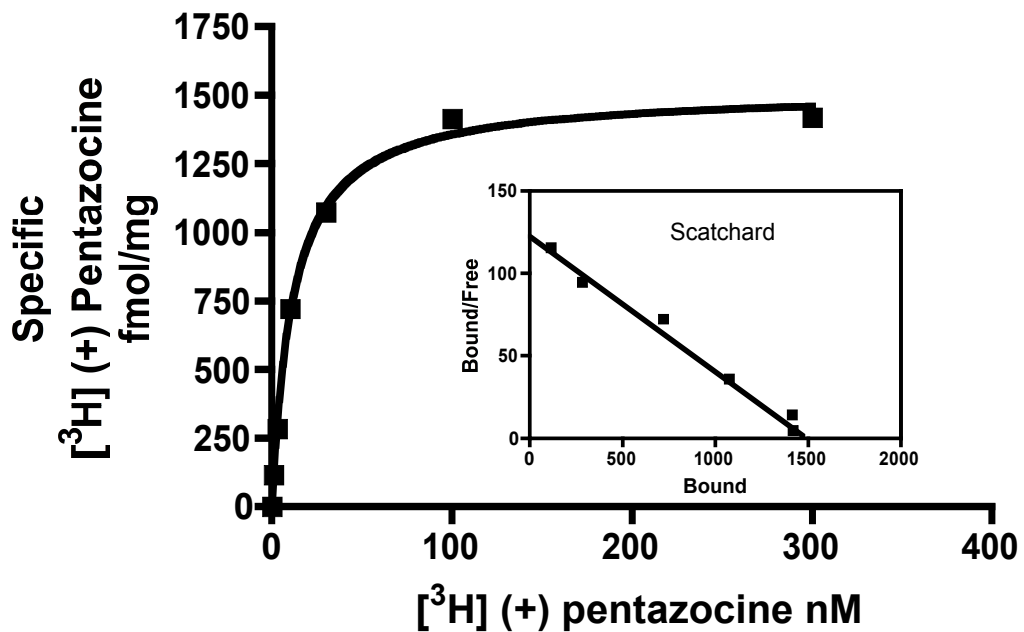
Figure 3.4: Saturation binding of [³H] (+) pentazocine in MDA-MB-468 cells Saturation binding curve for [³H] (+) pentazocine in MDA-MB-468 cells. Non specific binding was determined in the presence of 0.1mM rimcazole. This is a representative figure of 3 independent saturation experiments.

The mean $pK_d \pm$ SEM of [³H] (+) pentazocine from the σ-1R expressed on the MDA-MB-468 cells was determined as 7.77 ± 0.56, K_d 16.97 nM and the B_{max} as 2300 ± 200 fmol/mg protein (*n*=3).

3.3   Primary ammonium salt affinity for the σ-1 receptor

The primary ammonium salts consist of a single nitrogen and a single carbon chain. Primary ammonium salts have previously been shown to be able to selectively cause the release of 5-HT and histamine from rabbit platelets (May *et al.*, 1967). Also pentylammonium and hexylammonium have been shown to have behavioural effects in mice, with lower doses (3mg/kg) resulting in motor stimulation, and higher doses (100mg/kg) giving a motor depressing action (Widy-Tyszkiewicz and Czlonkowski, 1983, Widy-Tyszkiewicz and Sourkes, 1980). Due to the σ-1R's proposed link to 5-HT signalling in depression models, the affinity of primary ammonium salts for the σ-1R was investigated using radioligand binding (Figure 3.5). The data have been normalized to % specific [^{3}H] (+) pentazocine binding. Each curve represents the average of four independent binding experiments.
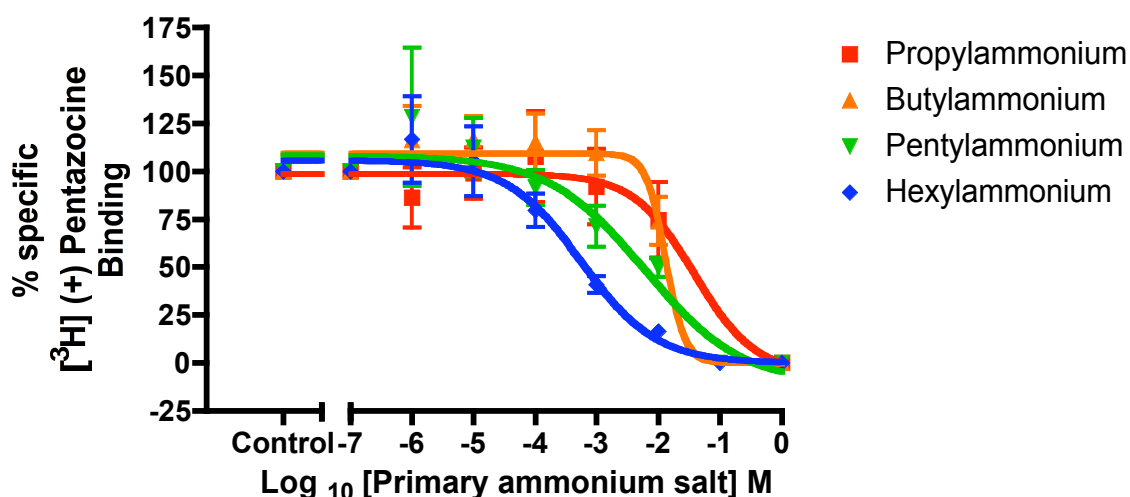
Figure 3.5: Binding of primary ammonium salts to the σ-1R in MDA-MB-468 cells. Competition assays using 30nM [^{3}H] (+) pentazocine and increasing doses of amine. Data are represented as percentage specific binding of [^{3}H] (+) pentazocine; error bars represent SEM from 4 independent competition binding assays.

The K$_i$ values for the binding of the primary ammonium salts ranged from 6mM (0.01mM – 1000mM) (propylammonium) to 0.3mM (0.05mM – 2mM) (hexylammonium). In order to visualise the affinities for the σ-1R more clearly with symmetrical errors, the K$_i$ values obtained from the above competition binding curves were converted into pK$_i$ values (-log$_{10}$K$_i$) shown in Figure 3.6 below.
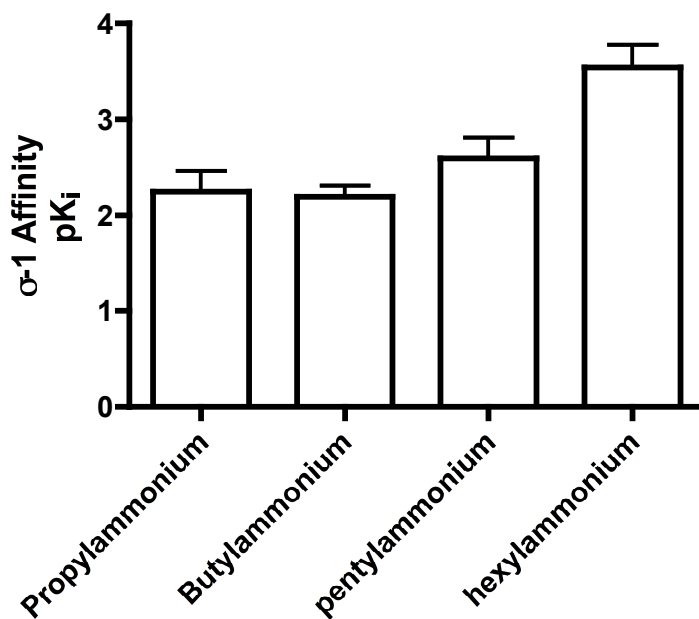
Figure 3.6: Summary of primary ammonium salt binding to the σ-1R. The affinities of the primary ammonium salts for the σ-1R (pK_i ± SEM) n=4 were: propylammonium 2.25 ± 0.22, butylammonium 2.19 ± 0.11, pentylammonium 2.59 ± 0.43, and hexylammonium 3.54 ± 0.23.

There is a slight increase in affinity for the σ-1R in the primary ammonium salts as the carbon chain length increases from 3 to 6; however the increase was not large enough to warrant continuing investigating longer chain lengths in this series of ammonium salts.

3.4 Secondary ammonium salt affinity for the σ-1 receptor

The secondary ammonium salts described in this chapter consist of a single nitrogen and two carbon chains. Dimethylammonium is a normal component of human urine (Asatoor and Simenhoff, 1965, Zhang *et al.*, 1995) and has been shown to interfere with cell growth, causing a decrease in cell size, and have a toxic effect on tumour cells (Guest and Varma, 1991). The mechanism by which dimethylammonium causes these effects has never been investigated, with this in mind, and knowing from the preliminary data that triethylammonium has σ-1R affinity, the secondary ammonium salts affinity for the σ-1R was investigated using radioligand competition assays (Figure 3.7). The data are normalised to % specific [^{3}H] (+) pentazocine binding, and each curve is the average of six independent competition binding assays.
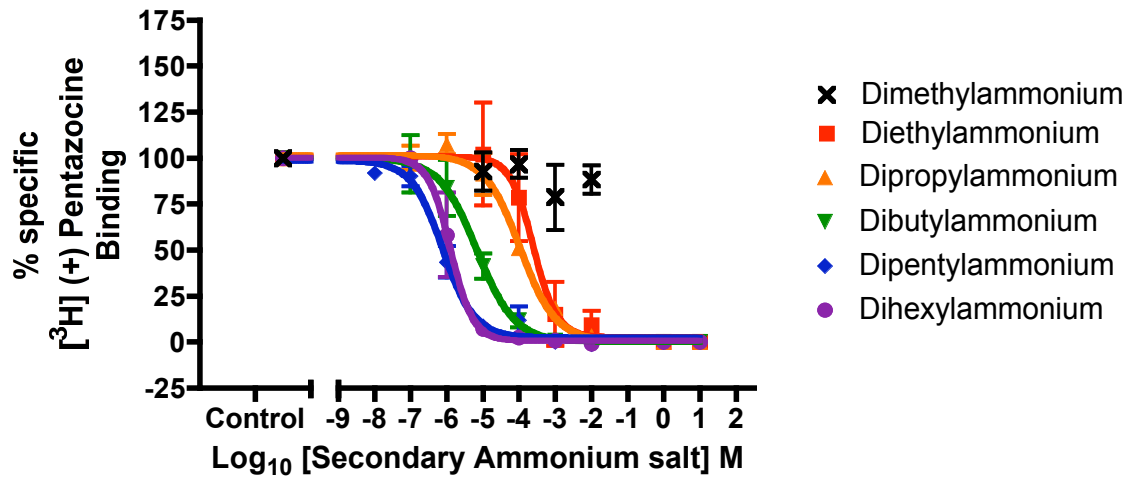
Figure 3.7: Secondary ammonium salt binding to the σ-1R in MDA-MB-468 cells.
Competition assays using 30nM [^{3}H] (+) pentazocine and increasing doses of ammonium salt. Data are represented as percentage specific binding of [^{3}H] (+) pentazocine. Error bars represent SEM from 6 independent competition binding assays.

Dimethylammonium had no affinity for the σ-1R within the range tested (highest dose 10mM). The mean K_i (95% CI) values ranged from diethylammonium 98 µM (30 µM – 320µM) to dipentylammonium 0.3µM (0.2µM - 0.5µM). In order to visualise the affinities for the σ-1R more clearly, K_i values obtained from the above competition binding curves were converted into pK_i values. The pK_i values (±SEM) are shown below in Figure 3.8.
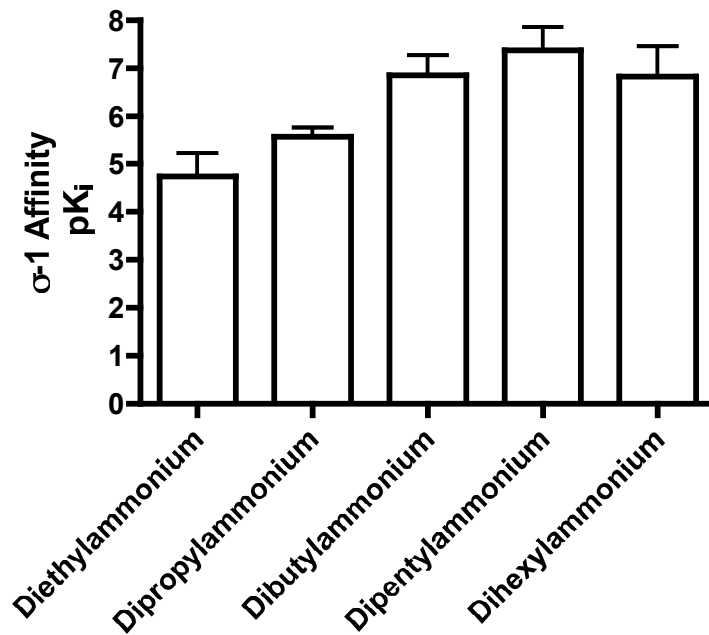
Figure 3.8: Summary of secondary ammonium salt binding to the σ-1R
pK_i values for secondary ammonium salts (*n*=4). The mean pK_i values ± SEM are diethylamine 4.73 ± 0.49, dipropylammonium 5.58 ±0.19, dibutylammonium 6.86 ± 0.40, dipentylammonium 7.37 ± 0.48, dihexylammonium 6.84 ± 0.63.

The dimethylammonium had no affinity in the range tested (highest dose 10mM). There is an increase in affinity for the σ-1R from the two carbon long chain length (diethylammonium pK_i 4.73 ± 0.49) to the five carbon long chain length (dipentylammonium). At the six carbon long chain length (dihexylammonium pK_i 7.37 ± 0.48) the affinity began to decrease and therefore this series was not investigated further.

3.5 Tertiary ammonium salt affinity for the σ-1 receptor

The tertiary ammonium salts discussed in this chapter consist of a single central nitrogen and three straight carbon chains. The preliminary data showed that triethylammonium has σ-1R affinity, therefore, the tertiary ammonium salt series from trimethylammonium with three single carbons to tridodecylammonium with three twelve carbon chains. The affinity of the tertiary ammonium salts were investigated using radioligand binding competition assays (Figure 3.9), the data are normalised to % specific [3H] (+) pentazocine binding. Each curve is made up of six or more independent competition binding assays.
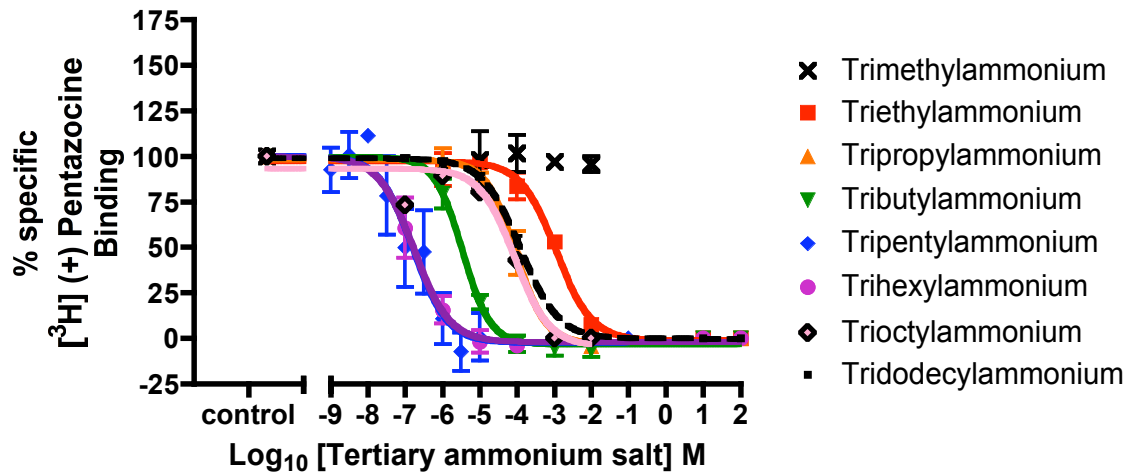
Figure 3.9: Tertiary ammonium salt binding to the σ-1R in MDA-MB-468 cells. Competition assays using 30nM $[^3H]$ (+) pentazocine and increasing doses of ammonium salt, represented as percentage specific binding of $[^3H]$ (+) pentazocine. Error bars represent SEM from 6 independent competition binding assays.

Trimethylammonium had no affinity for the σ-1R within the range tested (highest dose 10mM). The mean K_i (95% CI) values ranged from triethylammonium 420μM (313μM - 620μM) to trihexylammonium 6.4nM (0.4nM-94.4nM).

In order to visualise the affinities for the σ-1R more clearly, K_i values obtained from the above competition binding curves were converted into pK_i values (-$log_{10}K_i$). The pK_i (±SEM) values are represented in Figure 3.10 below.
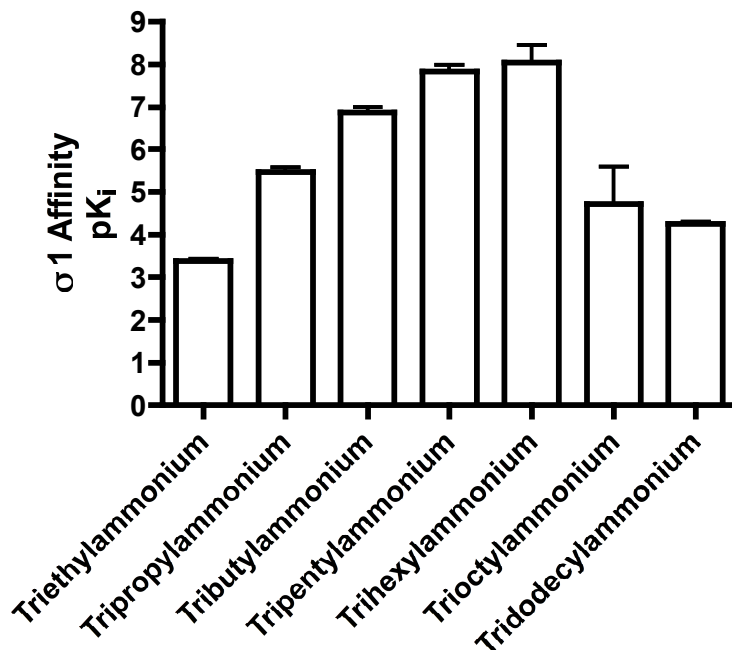
Figure 3.10: Summary of tertiary ammonium salts binding to the σ-1R. The mean pK_i values for tertiary ammonium salts (*n*=6) are triethylammonium 3.38 ± 0.05, tripropylammonium 5.46 ± 0.11, tributylammonium 6.88 ± 0.11, tripentylammonium 7.83 ± 0.16, trihexylammonium 8.05 ± 0.41, trioctylammonium 4.72 ± 0.87, and tridodecylammonium 4.26 ± 0.04.

Trimethylammonium had no affinity in the range tested (highest dose 10mM). There was an increase in affinity from the two carbon long chain (triethylammonium pK_i 3.38 ± 0.05) to the six carbon long chain (trihexylammonium pK_i 8.05 ±0.41). There was a decrease in affinity from the six to the twelve carbon long chain (tridodecylammonium pK_i 4.26 ± 0.04) therefore no ammonium salts were tested with carbon chains longer than twelve.

3.6 Quaternary ammonium salt affinity for the σ-1 receptor

The quaternary ammonium salts discussed in this section consist of a single positive nitrogen and 4 straight carbon chains. Tetraethylammonium is a well known voltage-activated potassium channel blocker (Fukushima *et al.*, 1996). With this in mind the series of quaternary ammonium salts from one carbon to four carbons in chain length were tested for σ-1R affinity using radioligand competition assays (Figure 3.11). The data are represented as % specific [^{3}H] (+) pentazocine binding, and each curve is the average of three independent competition assays.
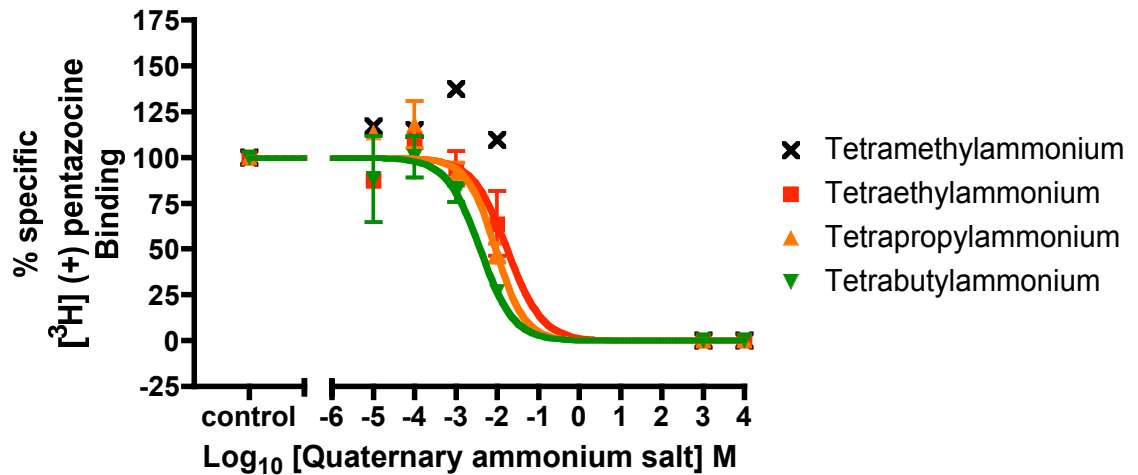
Figure 3.11: Quaternary ammonium salt binding to the σ-1R. Binding of simple straight-chain quaternary ammonium salts, the data are represented as % specific (+) pentazocine binding. Error bars represent SEM from 3 independent competition binding assays.

Tetramethylammonium had no affinity with in the range tested (highest dose 10mM). The mean K_i values for the quaternary ammonium salts ranged from tetraethylammonium 7mM (2 mM – 19 mM) to tetrabutylammonium 2mM (0.8mM – 28mM). In order to visualise the affinities for the σ-1R more clearly, K_i values obtained from the above competition binding curves were converted into pK_i values (-$\log_{10}K_i$) shown in Figure 3.12 below.
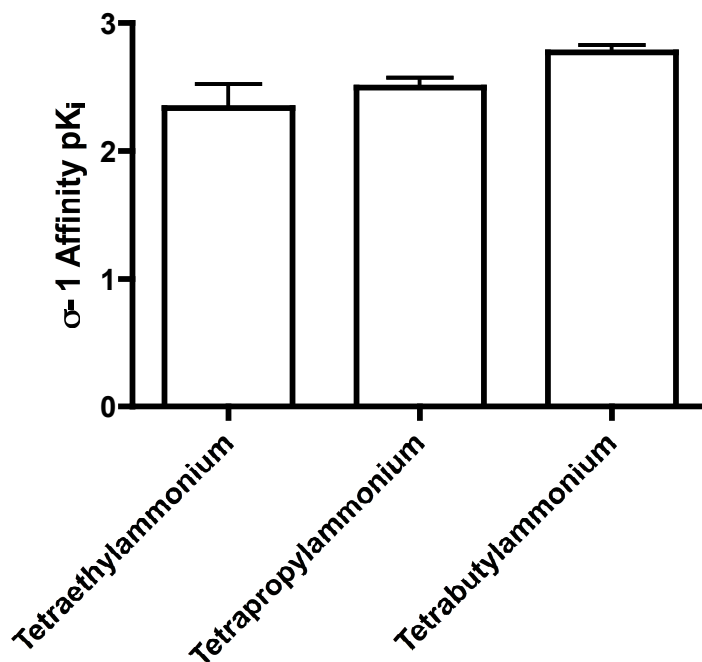
Figure 3.12: Summary of quaternary ammonium salt binding to the σ-1R. The mean pK_i values for the quaternary ammonium salts (*n*=3) are tetraethylammonium 2.34 ± 0.18, tetrapropylammonium 2.49 ± 0.07, and tetrabutylammonium 2.77 ± 0.05.

The quaternary ammonium salts showed only little affinity for the σ-1R, and there was little increase in affinity as the carbon chain length increased, therefore no larger quaternary amines were tested for σ-1R affinity.

3.7 Calcium response to simple straight-chain ammonium salts

σ-1R antagonists have been shown to induce a rapid influx of calcium into the cytoplasm in cancer cell lines (Spruce *et al.*, 2004). Using this as a selection criterion for a σ-1R antagonist the simple straight-chain amines were tested to see if they induced a σ-1R mediated calcium influx into the cells. All the straight-chain amines were put into this assay, and below are some examples from the amines with the highest affinity for the σ-1R.
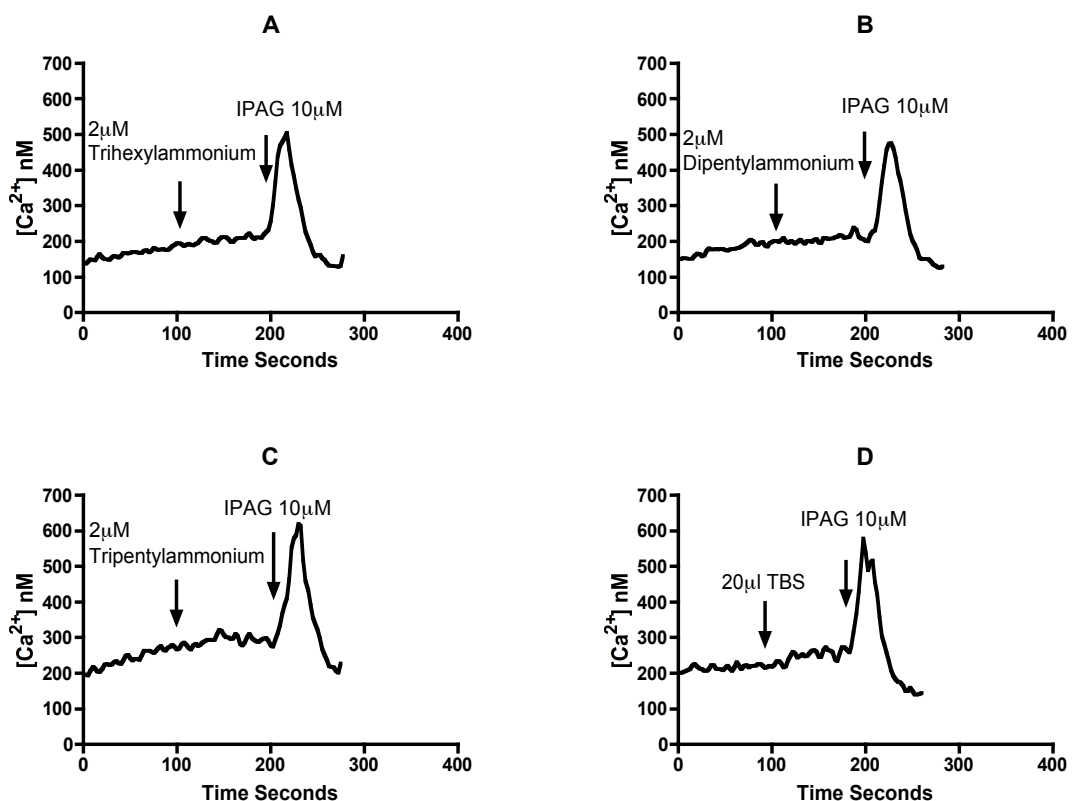
Figure 3.13: Calcium influx in response to simple straight-chain ammonium salts
A: 2μM trihexylammonium followed by a dose of the known σ-1R antagonist IPAG as a positive control, in a stirred suspension of Fura-2 loaded MDA-MB-468 cells. **B:** 2μM dipentylammonium followed by a dose of 10 μM IPAG, in a stirred suspension of Fura-2 loaded MDA-MB-468 cells. **C:** 2μM tripentylammonium followed by a dose of 10μM IPAG, in a stirred suspension of Fura-2 loaded MDA-MB-468 cells. **D:** 20μl of TBS followed by 10μM IPAG in a stirred suspension of Fura-2-AM loaded MDA-MB-468 cells.

Of all the simple straight-chain ammonium salts put into the calcium influx assay, not one induced an influx of calcium into the cells, even when a concentration 100 times the affinity of the amine for the σ-1R was added to the assay.

3.8 Simple straight-chain ammonium salt effect on cellular metabolic activity

It has been shown previously that σ-1R antagonists induce cell death in cancer cell lines (Brent *et al*., 1996a, Spruce *et al*., 2004, Vilner *et al*., 1995a). The MTS assay was used to measure cellular metabolic acitivity induced by σ-1R ligands. IPAG, a well-known σ-1R antagonist was used as a positive control as all the simple straight-chain ammonium salts were tested. Below is an example of an ammonium salt with high σ-1R affinity, tripentylammonium.
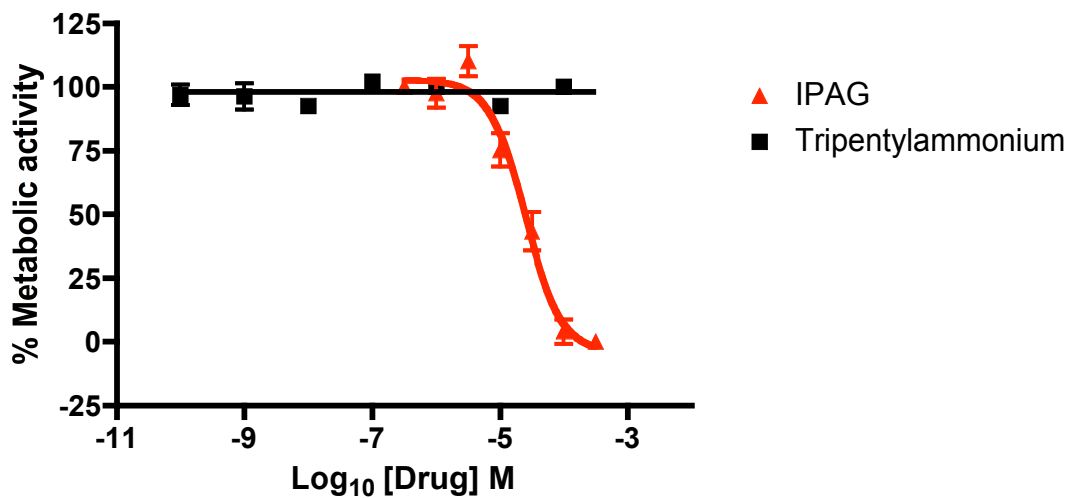
Figure 3.14: Tripentylammonium in MTS assay dose response. The effect of the simple straight-chain ammonium salt, tripentylammonium, on MDA-MB-468 metabolic activity Error bars represent SEM from 4 independent MTS assays.

Of all the simple straight-chain ammonium salts put into the MTS assay not one reduced cell metabolism of the MDA-MB-468 cancer cell line with in the range of concentrations tested (up to 100µM).

In order to assess they toxicity of ammonium salts with the highest affinity for the σ-1R, σ-1R negative HEK 293 cells (Figure 3.15a) were used in the MTS assay. Below are examples of the highest affinity simple straight-chain ammonium salts effect on σ-1R negative cell metabolism (Figure 3.15).
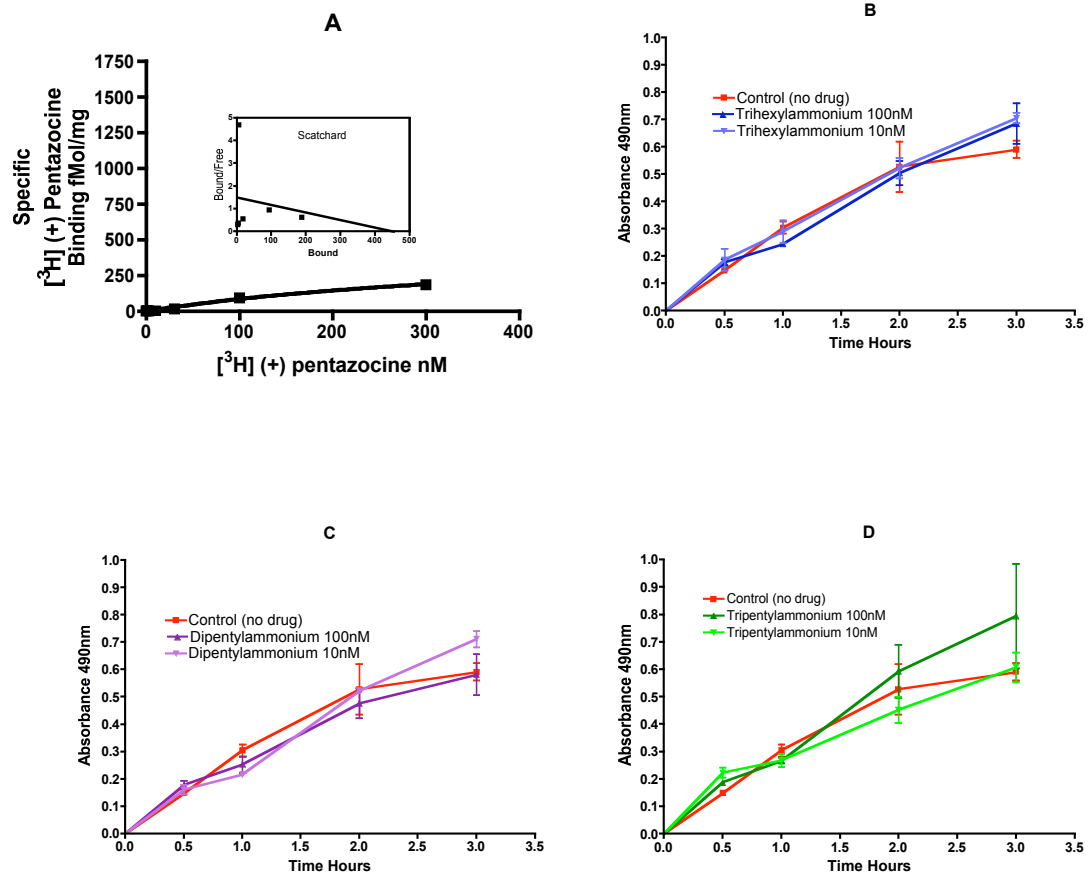
Figure 3.15: Effect of high σ-1R affinity ammonium salts on HEK 293 cell metabolism. A: Saturation binding of [^{3}H] (+) pentazocine in permeabilised HEK 293 cells, K_d 453nM B_{max} 475 fmol/mg (*n*=3). **B:** MTS assay showing the metabolic activity of HEK-293 cells after treatment with 10nM and 100nM trihexylammonium compared to the control treated with TBS. (*n*=3) **C:** MTS assay showing the metabolic activity of HEK-293 cells after treatment with 10nM and 100nM tripentylammonium. (*n*=3) **D:** MTS assay showing the metabolic activity of HEK-293 cells after treatment with 10nM and 100nM tripentylammonium (*n*=3).

The metabolism of the HEK 293 cells treated with the 10nM and 100nM doses of tripentylammonium, dipentylammonium and trihexylammonium, showed no difference compared to the cell metabolism of the untreated HEK 293 cells.

3.9 Straight-chain ammonium salt specificity for the σ-1 receptor: histamine receptors

Histamine receptors, H_1 receptor, H_2 receptor, H_3 receptor and H_4 receptor have all been shown to express in breast cancer cell lines (Medina *et al.*, 2008). Histamine exerts its function by binding to G-protein coupled histamine receptors. The H_2R is coupled to adenylyl cyclase via the G_s G-protein. The H_1 receptor is coupled to phospholipase C via the G_q G-protein. Activation of the H_1 receptor and H_2 receptor results in an increase in cytosolic calcium and therefore the MDA-MB-468 cell line was used to measure the effects of the simple ammonium salts on the histamine receptors. The ammonium salts with the highest affinity for the σ-1R were tested in the calcium assay, including dipentylammonium, tripentylammonium and trihexylammonium. A dose response to histamine in the calcium response assay was carried out and some examples of the calcium peaks a represented below.
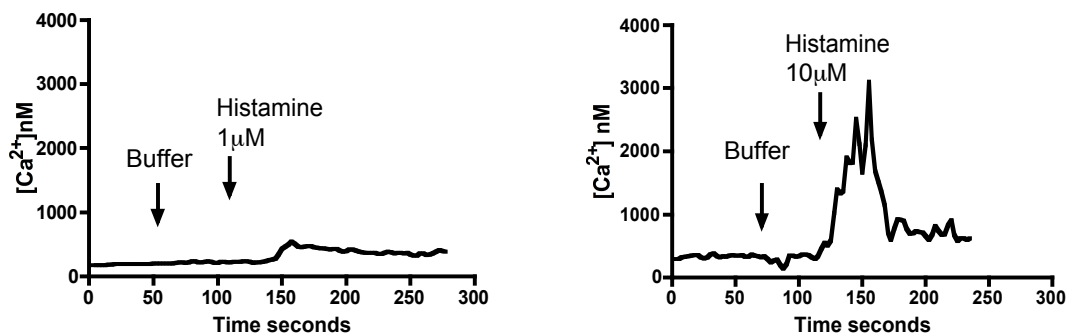
Figure 3.16: Increase in cytosolic $[Ca^{2+}]$ in Fura-2-AM loaded MDA-MB-468 cells in response to histamine. Calcium response in stirred MDA-MB-468 cells loaded with Fura-2-AM, to 1μM and 10μM histamine, having been pre-treated with 20 μl of buffer. This is a representative figure of 3 independent experiments, the mean increase in $[Ca^{2+}]_i$ in response to 1μM histamine was 0.55 ± 0.08 μM and for 10μM histamine was 4 ± 1μM.

Histamine (1μM) induced a peak calcium response of 0.55 ± 0.08 μM and 10μM histamine induced a peak calcium response of 4 ± 1.1 μM. Pyrilamine maleate (Figure 3.17) is a histamine receptor antagonist acting on the H_1 R. Pyrilamine maleate was used as a positive control in the calcium assay (Figure 3.18).
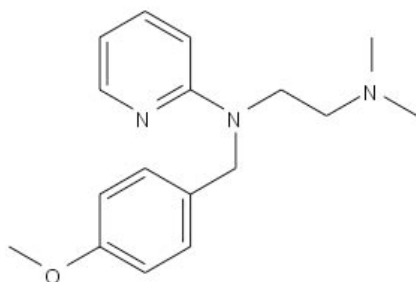
Figure 3.17: Structure of pyrilamine maleate, H₁ receptor antagonist.
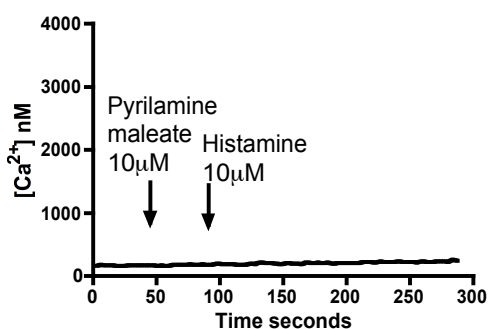
Figure 3.18: Increase in cytosolic free [Ca^{2+}] in Fura-2-AM loaded MDA-MB-468 cells. Calcium response in stirred MDA-MB-468 cells to 10μM histamine after a pre-treatment with 10μM pyrilamine maleate. This is a representative figure of 3 independent experiments. No calcium peak was observed in response to histamine after pre-treatment with pyrilamine maleate.

A 10μM dose of pyrilamine maleate was enough to completely wipe out the calcium response in the MDA-MB-468 cells in response to 10μM histamine. Once the agonist antagonist relationship for histamine and pyrilamine maleate was established in the MDA-MB-468 cell line, the simple straight-chain ammonium salts were tested to see if they could antagonise the histamine-induced calcium influx into the cells (Figure 3.19). A histamine dose response was carried out in the presence of a high dose of simple straight-chained ammonium salt.
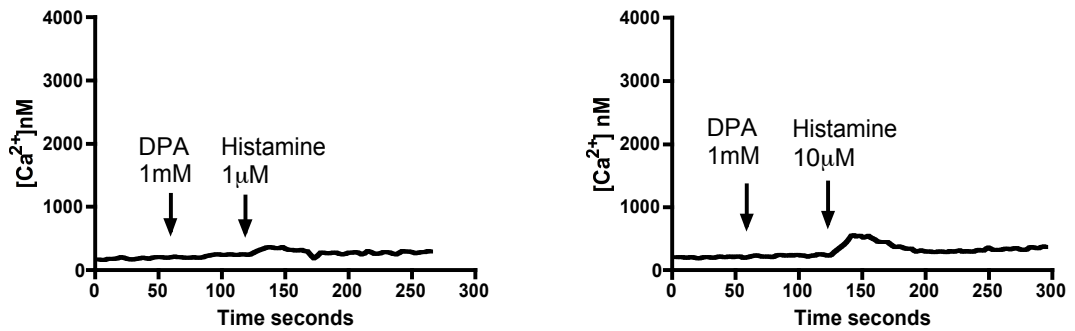
Figure 3.19: Effect of dipentylammonium on the increase of cytosolic $[Ca^{2+}]$ in response to histamine. Calcium response in stirred MDA-MB-468 cells loaded with Fura-2-AM in response to 1μM and 10μM histamine after pre-treatment with 1mM dipentylammonium (DPA). This is a representative figure of 3 independent experiments, the mean calcium influx in response to 1μM histamine was 0.36 ± 0.04μM 10μM histamine in the presence of 1mM dipentylammonium was 0.9± 0.6μM.

1mM dipentylammonium caused approximately a 50% reduction in the calcium response to 1μM histamine, dropping from 0.55 ± 0.08μM to 0.36 ± 0.04μM calcium and in response to 10μM histamine in the presence of 1mM dipentylammonium there was approximately an 80% drop in calcium influx, dropping from 4 ± 1μM to 0.9 ± 0.6μM calcium. The full dose response curve for calcium influx in response to histamine in MDA-MB-468 cells in the presence and absence of 1mM dipentylammonium is shown below (Figure 3.20).
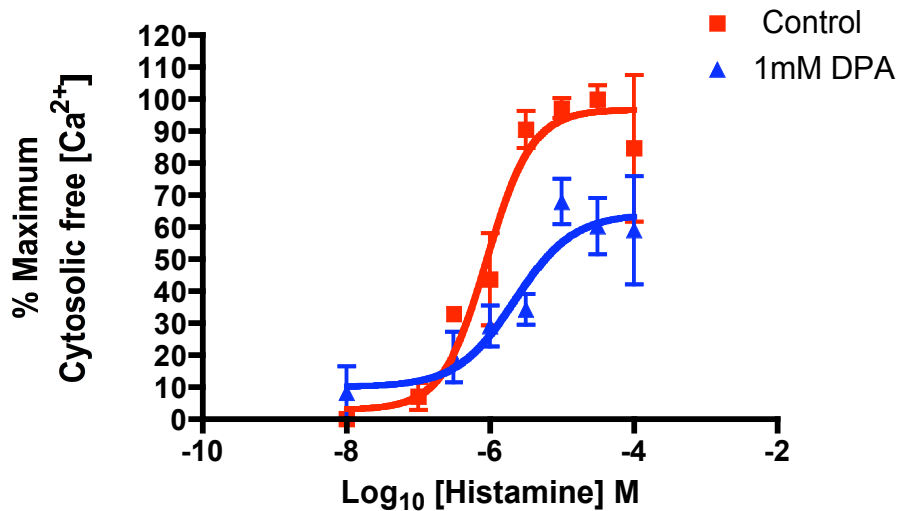
Figure 3.20: Histamine dose response in Fura-2-AM loaded MDA-MB-468 cells with and without 1mM dipentylammonium (DPA). Histamine dose response in the presence and absence of 1mM dipentylammonium. Data from 3 independent experiments are normalised to percentage maximal response to histamine. The pEC_{50} values for histamine in presence and absence of 1mM dipentylammonium were 6.0 ± 0.2 and 5.5 ± 0.7 respectively. The maximum response for the cells treated with 1mM dipentylammonium was 62 ± 8 % of the untreated cells.

Dipentylammonium (1mM) had no effect on the EC_{50} of the calcium response in response to histamine (t test *P* value 0.33). However, it did decrease the maximal response by approximately 40% (t test *P* value 0.015). Of the other ammonium salts tested none had any effect on the calcium response to histamine, below is an example of 100μM tripentylammonium and 100μM trihexylammonium pre-treatment before 1μM histamine was added to the assay.
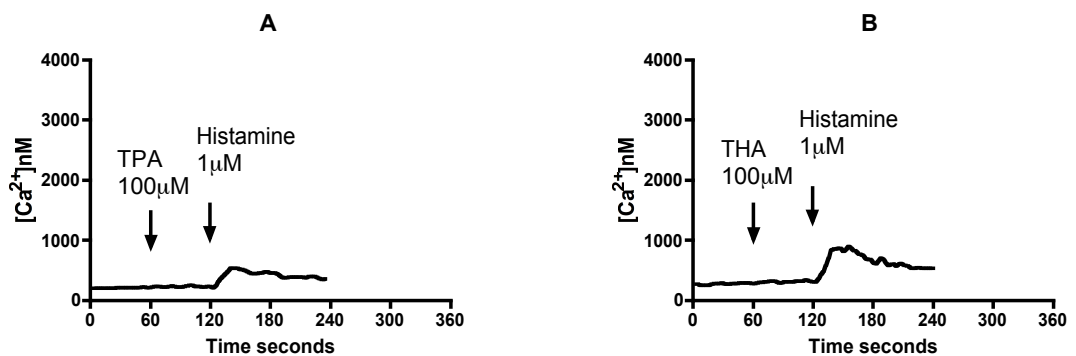
Figure 3.21: Effect of A: Tripentylammonium and B: trihexylammonium on histamine-induced cytosolic [Ca^{2+}] increase. Calcium response in stirred MDA-MB-468 cells loaded with Fura-2-AM in response to 1μM histamine after pre-treatment with 100 μM tripentylammonium (TPA) or 100μM trihexylammonium (THA). This is a representative figure of 3 independent experiments.

The mean peak calcium response to 1µM histamine after pre-treatment with 100µM tripentylammonium was 532 ± 3 nM and for trihexylammonium 0.69 ± 0.07 µM, these values were not significantly different from the control (t test *P* values 0.73 and 0.26 respectively) and were not investigated further.

3.10 Straight-chain ammonium salt specificity for the σ-1 receptor: Muscarinic receptors

It has been shown previously that σ-1R ligands such as (+) pentazocine and 1S,2R-cis-N-[2-(3,4-dichlorophenyl)ethyl]-N-methyl-2-(1-pyrrolidinyl)- cyclohexylamine (BD737) are capable of affecting muscarine-induced intracellular calcium changes in SH-SY5Y neuroblastoma cells which have been shown to express the M_1 and M_3 subtypes of the muscarinic acetylcholine receptor (mACh) (Hong and Werling, 2002). These changes however could not be reversed by σ-1R antagonist haloperidol, therefore it was deduced that (+) pentazocine and BD737 had affinity for the mACh. This was confirmed with radioligand binding using the muscarinic specific radioligand [³H]-QNB (pK_d of 9.5 ± 0.1). The affinities of pentazocine, haloperidol and BD737 for the muscarinic receptor were identified as ($pK_i \pm$ SEM) 6.29 ± 0.06, 6.4 ± 0.07, 5.35 ± 2.3, respectively (Hong and Werling, 2002). With this in mind the simple ammonium salts were assessed for muscarinic receptor affinity using rat brain membranes.
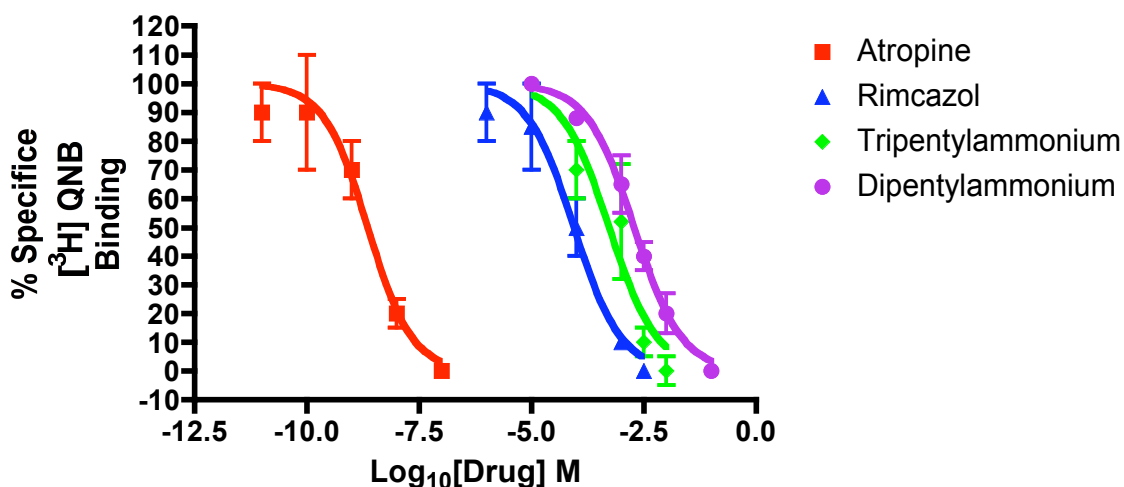
Figure 3.22: σ-1 Ligand binding to the mACh receptor. Binding of σ-1 ligands and simple amines compared to atropine. Example selection of data represented as % specific binding of QNB from between 4 and 7 binding assays.

The full list of compounds tested for muscarinic receptor affinity can be seen in table 3.1 below.

Compound name	Type of compound	σ-1R affinity pK$_i$ ± SEM (MDA-MB-468 cells)	mAChR Affinity pK$_i$ ± SEM (Rat Brain)	mACh K$_i$/σ-1K$_i$	Number of assays (*n*)
Atropine	Muscarinic antagonist	4.51±0.42	9.40±0.34	0.000012	4
Rimcazole	σ-1R ligand	6.22±0.23	4.49±0.10	53	7
IPAG*	σ-1R ligand	8.62±0.67	4.3	20000	1
Tripentylammonium	Straight-chained, tertiary amine	7.83±0.10	4.33±0.38	2000	4
Dipentylammonium	Straight-chained, secondary amine	8.03±0.48	3.42±0.24	7940	5
Pentazocine	σ-1R agonist	8.50[a]	6.29 ± 0.06[b]	162	**
BD737	σ-1R agonist	8.54[b]	5.35 ± 2.30[b]	1550	**
Haloperidol	σ-1R Antagonist and antipsychotic	8.43[a]	6.40 ± 0.07[b]	107	**

Table 3.1: The affinity of ligands for the σ-1R and the mAChR
(pK$_i$ ± SEM), number of assays refers to the QNB binding assays. *IPAG was only assayed on one occasion with QNB, and the affinity for the σ-1R is represented as pK$_{50}$ ± SEM as the nH differs significantly from -1. [a]Whittemore *et al.*, 1997, [b]Hong and Werling, 2002 ** data obtained from Hong and Werling, 2002.

Dipentylammonium and tripentylammonium (pK$_i$ ± SEM, 8.03 ± 0.48 and 7.83 ± 0.10 respectively) both have higher affinities for the σ-1R than the well known σ-1R antagonist rimcazole (pK$_i$ ± SEM, 6.22 ± 0.23). Moreover rimcazole has a higher affinity for the mAChR. The pK$_i$ data for rimcazole compared to dipentylammonium and tripentylammonium for the σ-1R is represented below in Figure 3.23.
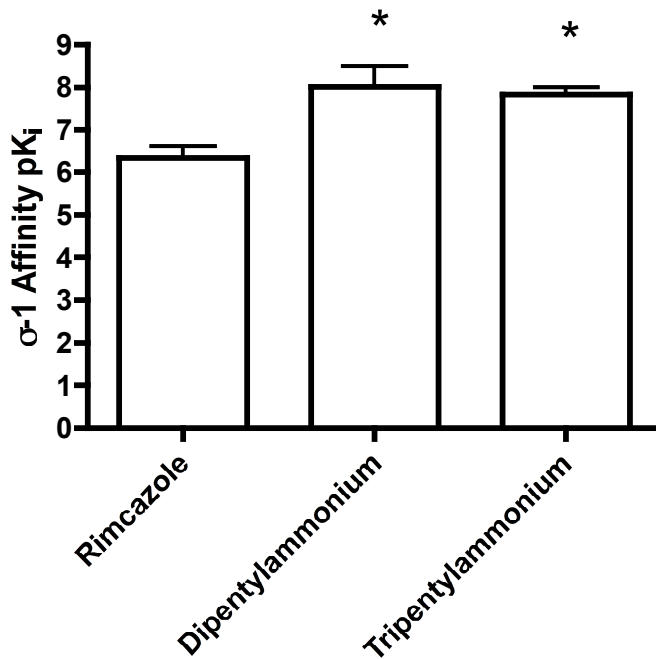
Figure 3.24: Ligand Affinity for the σ-1R. Affinity of rimcazole, tripentylammonium and dipentylammonium for the σ-1R ANOVA *P* value 0.0238 (*n*=3). * Dunnett's post test < 0.05.

Both dipentylammonium and tripentylammonium have statistically significant higher affinities for the σ-1R than the well-characterised σ-1 ligand rimcazole, with ANOVA Dunnett's post test *P* values < 0.05. The affinities of the simple straight-chain ammonium salts with a high affinity for the σ-1R, tripentylammonium and dipentylammonium, for the mAChR compared to the affinity of rimcazole for the mACh are represented in figure 3.25.
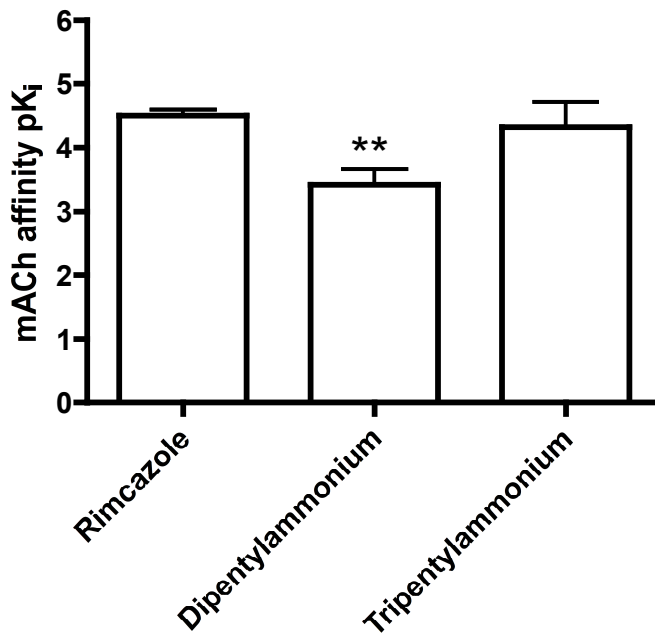
Figure 3.25: Affinity of σ-1R ligands for the mAChR. Affinity of rimcazole, dipentylammonium and tripentylammonium for the mAChR (*n*=4). ANOVA *P* value 0.008. ** Dunnett's post test rimcazole vs dipentylammonium *P* < 0.01.

Dipentylammonium has a statistically significant lower affinity for the mAChR than the well known σ-1R antagonist rimcazole (*P*<0.01). Tripentylammonium shows no significant difference from rimcazole in affinity for the mAChR (ANOVA Dunnett's post test rimcazole vs tripentylammonium *P* >0.05).

3.11 Straight-chain ammonium salt specificity for the σ-1 receptor: dopaminergic and adrenergic receptors.

Since their original description the σ-1R has been linked with dopaminergic neurotransmission (Martin *et al.*, 1976), although in the original studies the ligands used had affinities for the dopamine receptor besides the σ receptor. In electrophysiological models (+) pentazocine and (+) SKF-10,047 increases the firing of dopaminergic neurons whilst DTG and (+) 3 PPP reduce it (Clark *et al.*, 1985, French and Ceci, 1990, Steinfels and Tam, 1989, Zhang *et al.*, 1992). Biochemical tests show that high doses of (+) pentazocine and DTG cause dopamine release (Ebert *et al.*, 1991, Kanzaki *et al.*, 1992) and direct interaction of σ-1R ligands with dopaminergic neurons has been shown using radioligand binding studies (Gundlach *et al.*, 1986, Quirion *et al.*, 1987).

The dopamine receptor can be split into 5 subtypes D_1-D_5, D_1 (Dearry *et al.*, 1990, Monsma *et al.*, 1990, Zhou *et al.*, 1990) and D_5 (Grandy *et al.*, 1989, Sunahara *et al.*, 1991, Tiberi *et al.*, 1991, Weinshank *et al.*, 1991) couple through G_s G-protein to activate adenylyl cyclase (AC), which causes an increase in cellular cAMP. The D_2 receptor can inhibit cAMP production through G_i G-protein inhibition of AC (De Camilli *et al.*, 1979, Enjalbert and Bockaert, 1983, Mcdonald *et al.*, 1984, Onali *et al.*, 1985, Onali *et al.*, 1981), D_3 (Chio *et al.*, 1994b, Mcallister *et al.*, 1995, Potenza *et al.*, 1994, Robinson and Caron, 1996, Tang *et al.*, 1994) and D_4 (Chio *et al.*, 1994a, McAllister *et al.*, 1995, Tang *et al.*, 1994) receptors also have been shown to reduce cAMP production.

The β adrenergic receptor is also coupled through G_s G-protein stimulation of AC causing an increase in cAMP (Skeberdis *et al.*, 1997). MDA-MB-468 cells have been shown to express both dopaminergic and adrenergic receptors (Drell *et al.*, 2003, Lang *et al.*, 2004), therefore the MDA-MB-468 were used to assess the ammonium salts for dopaminergic or adrenergic receptor affinity. Lang *et al.* (2004) show the presence of D_2 receptors on the MDA-MB-468 cells, however they do not rule out the presence of D_1 or D_5 receptors. They show that dopamine treatment of MDA-MB-468 cells leads to the activation of cAMP response element binding (CREB) protein. This is unlikely to be due to the D_2 receptor as it is coupled through G_i, which would reduce cAMP, rather it is more likely to be due to D_1 or D_5 but with the D_2 present the signal will be reduced.

Isoprenaline (Figure 3.26) is an adrenergic β1 and β2 agonist, and on addition to MDA-MB-468 cells dose dependently causes an increase in cAMP production (Figure 3.27).

A   **B**
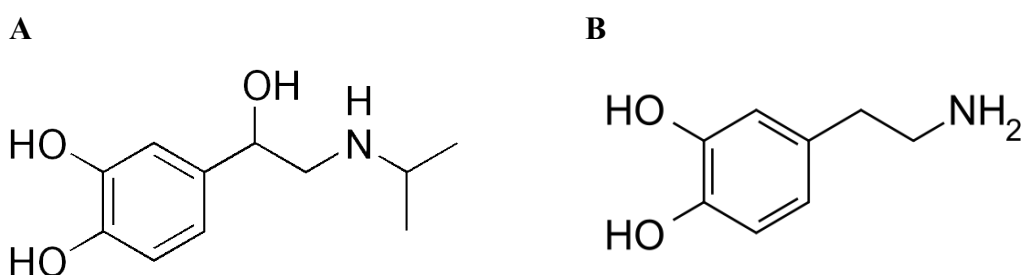
Figure 3.26: Structure of A: isoprenaline and B: dopamine.
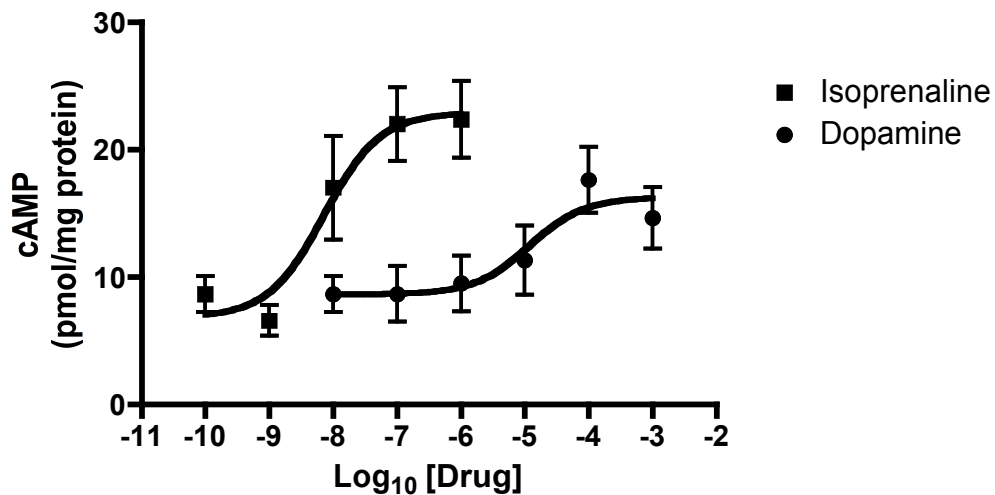
Figure 3.27: cAMP production in response to dopamine and isoprenaline in MDA-MB-468 cells. Measured using commercially available cAMP assay kit. Error bars represent SEM from 8 independent cAMP assays.

MBA-MD-468 cells were treated with the range of amines along with IPAG and pentazocine. Control level of cAMP was 9 ± 1 pmol/mg protein. None of the agents tested (at 100μM) caused a significant change in cAMP levels (one-way ANOVA P value 0.37 (table 3.2)). Isoprenaline raised cAMP levels in MDA-MB-468 cells in a dose-dependent fashion, with EC_{50} of 5.8nM (pEC_{50} 8.2 ± 0.3, mean $\pm$ SEM, n=5). None of the agents tested (at 100μM) affected the response to isoprenaline (100nM) (table 3.2). Dopamine also raised cAMP levels in MDA-MB-468 cells in a dose-dependent fashion (Figure 3.27), with EC_{50} of 14μM (pEC_{50} 4.8 ± 0.2, mean $\pm$ SEM, n=5). None of the agents tested (IPAG, (+) pentazocine, dipentylammonium or tripentylammonium at 100μM) affected the response to dopamine (100μM) (table 3.2), one-way ANOVA P value 0.95.

Drug	cAMP (pmol/mg)	Number of assays
Control (no drug)	8.7 ± 1.4	8
Dopamine (100μM)	17.63 ± 2.5	8
Isoprenaline (100nM)	22 ± 2.9	8
IPAG	8.9 ± 1.9	7
(+) Pentazocine	11.7 ± 2.0	3
Tripentylammonium	8.5 ± 1.5	4
Dipentylammonium	7.8 ± 1.9	4
Dopamine + IPAG	13.2 ± 1.4	6
Dopamine + tripentylammonium	15.5 ± 4.8	4
Dopamine + dipentylammonium	17.3 ± 3.1	6
Isoprenaline + IPAG	20.4 ± 4	5
Isoprenaline + tripentylammonium	30.8 ± 6.3	5
Isoprenaline + dipentylammonium	19.5 ± 4.6	6

Table 3.2: cAMP production in response to dopaminergic, adrenergic and σ-1R ligands.

3.12 Straight-chain ammonium salts as σ-1 receptor agonists and antidepressants

There has been much published evidence that σ-1R agonists including (+) pentazocine, (+) SKF-10,047 and DTG have antidepressant properties (Urani *et al.*, 2001), as well as σ-1R antagonists, including progesterone, rimcazole and BD1047, reversing the effects of venlafaxine (a 5-HT and noradrenaline transporter inhibitor (Redrobe *et al.*, 1998, Dhir and Kulkarni, 2007).

Dipentylammonium

Simple ammonium salts have been tested for behavioural effects before, low doses of the primary ammonium salt, pentylammonium resulted in motor stimulatory effects (Widy-Tyszkiewicz and Czlonkowski, 1983, Widy-Tyszkiewicz and Sourkes, 1980), and treatment of rabbit platelet cells with pentylammonium resulted in 5-HT production (May *et al.*, 1967). Dipentylammonium is a high affinity σ-1R ligand with nanomolar affinity (1,000,000 times higher affinity than pentylammonium), therefore its behavioural effects were assessed using the forced swim test (Porsolt *et al.*, 1977) (one of the most used animal models for screening antidepressants (Petit-Demouliere *et al.*, 2005)) (Figure 3.28), which assesses despair behaviour and the tail suspension test which relies on similar despair behaviour. The following behavioural studies (Figures 3.28 to Figure 3.31) were carried out on my behalf, at The University Institute of Pharmaceutical Science, Panjab University, Chandigarh, India, under the direction of Professor Kulkarni.
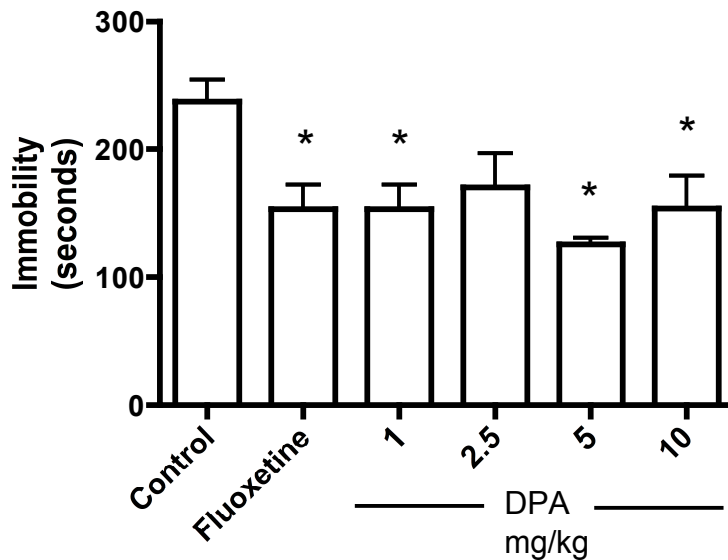
Figure 3.28: The effect of dipentylammonium (DPA) on despair behaviour in mice subjected to the forced swim test. The control consisted of 10ml/kg saline, fluoxetine (SSRI) 10mg/kg was used as a positive control (ANOVA *P* value 0.014). * Dunnett's multiple comparison post test vs control *P* < 0.05. 6 to 8 mice were used for each data point, error bars represent SEM.

When submitted to the forced swim test the control (10 ml/kg saline) mice exhibited despair behaviour, remaining still in the water (only making movements to keep their head above the water) for 238 ± 17 seconds out of a total of 6 minutes in the water. The SSRI, fluoxetine at 10mg/kg, significantly reduced the time spent immobile in the water to 152 ± 19 seconds (ANOVA post test, Dunnett's multiple comparison *P*<0.05). Similarly, dipentylammonium (1mg/kg, 5mg/kg and 10mg/kg) significantly reduced the time spent immobile in the water (all having ANOVA post test, Dunnett's multiple comparison *P*<0.05).

In order to assess whether dipentylammonium is reducing time spent immobile in the water through a σ-1R mediated mechanism, dipentylammonium was reassessed in the forced swim test in the presence and absence of the σ-1R antagonist BD1047 (Figure 3.29).
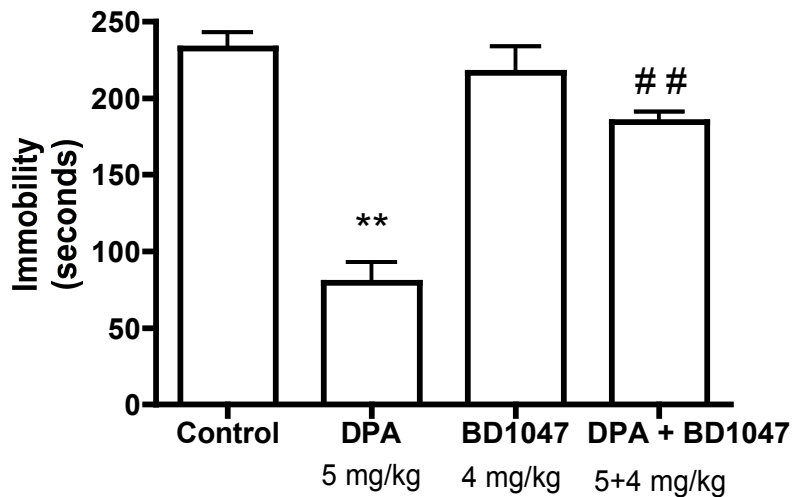
Figure 3.29: The effect of dipentylammonium (DPA) and σ-1R antagonist BD1047 on despair behaviour in mice subjected to the forced swim test. 6 to 8 mice were used for each data point, error bars represent SEM. (ANOVA *P* value, 0.0001). (**ANOVA post test, Tukey's multiple comparison, control vs DPA *P*< 0.01, ##ANOVA post test, Tukey's multiple comparison, DPA vs DPA+ BD1047 p<0.01)

Control mice (10ml/kg saline) subjected to the forced swim test remained immobile for 232 ± 10 out of the 6 minute test. Again a 5 mg/kg dose of dipentylammonium resulted in a significant decrease in time spent immobile, 80 ± 13 (**ANOVA post test, Tukey's multiple comparison, control vs DPA *P*< 0.01), whereas the σ-1R antagonist BD1047 alone at 4mg/kg had no significant effect on time spent immobile in the water. However, when a 4 mg/kg dose of the σ-1R antagonist BD1047 was injected along with a 5mg/kg dose of dipentylammonium, the effect of the dipentylammonium was reversed (##ANOVA post test, Tukey's multiple comparison, DPA vs DPA+ BD1047 p<0.01).

Dipentylammonium was also tested in another behavioural test, which also tests despair behaviour, the tail suspension test (Figure 3.30). The mouse is suspended by its tail 58 cm above the table top (such that the mouse cannot sense the table) for a period of 6 minutes. Despair behaviour is interpreted as time spent completely immobile (not struggling to escape).
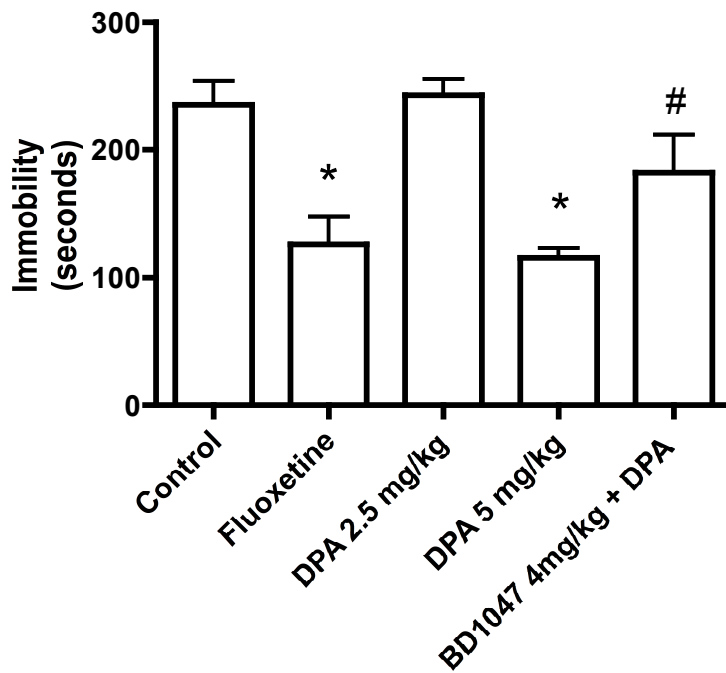
Figure 3.30: The effect of DPA and σ-1R antagonist BD1047 on despair behaviour in mice subjected to the tail suspension test. The control consisted of an injection of 10ml/kg saline, fluoxetine was used as a positive control at 10mg/kg. 6 to 8 mice were used for each data point, error bars represent SEM. (ANOVA *P* value <0.0001). * ANOVA post test, Tukey's multiple comparison, vs. control 5mg/kg *P*<0.05, # ANOVA post test Tukey's multiple comparison vs. fluoxetine *P*<0.05.

Control mice (10ml/kg saline) subjected to the tail suspension test exhibited despair behaviour remaining immobile for 235 ± 12seconds, as with the forced swim test the SSRI, fluoxetine (10mg/kg), resulted in a significant decrease in time spent immobile, 126 ± 22 seconds (ANOVA post test, Tukey's multiple comparison, Control vs Fluoxetine p< 0.05). Dipentylammonium at 2.5 mg/kg did not have a significant effect on immobility time in the tail suspension test, however dipentylammonium at 5mg/kg resulted in a significant decrease in time spent immobile in the tail suspension test 115 ± 7 seconds (ANOVA post test, Tukey's multiple comparison, Control vs DPA 5mg/kg p<0.05). Injecting the σ-1R antagonist BD1047 (4mg/kg) along with the 5mg/kg dipentylammonium reverses the effect of the dipentylammonium on the immobility time of the mice, resulting in an immobility time of 182± 30 seconds (ANOVA post test, Tukey's multiple comparison, DPA vs BD1047 4mg/kg + DPA 5mg/kg p<0.05). DPA alone or in combination with BD1047 had no effect on locomotion (Table 3.3).

Treatment	Dose (mg/kg)	Total Locomotive activity (Ambulations and rearing /15mins)
Vehicle Control	10 ml/kg	140 ± 15
DPA	5	128 ± 19
DPA + BD1047	5 + 4	114 ± 14

Table 3.3 Effect of σ-1R agonists on locomotive activity. Locomotive activity measured using an actophotometer (*n*=6 to 8).

Tripentylammonium

Tripentylammonium is a high affinity σ-1R ligand with nanomolar affinity, which is comparable with dipentylammonium. Tripentylammonium was therefore tested for antidepressant activity in the forced swim test (Figure 3.31).
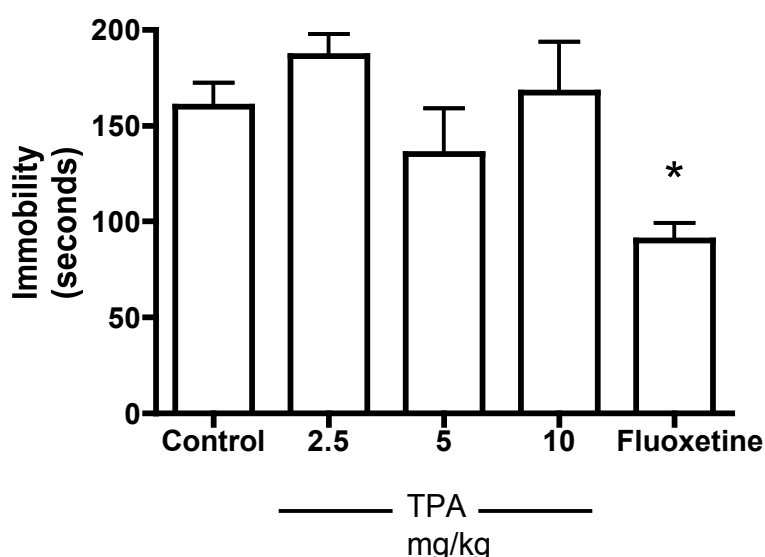
Figure 3.31: The effect of tripentylammonium (TPA) on despair behaviour in mice subjected to the forced swim test. The control consisted of 10ml/kg saline, 6 to 8 animals were used for each data point and the error bars represent SEM (*ANOVA Dunnett's post test P <0.05).

Tripentylammonium did not have any significant effect on the despair like behaviour of the mice, as measured by the immobility time in the forced swim test, at any of the doses tested (ANOVA Dunnett's post test P value >0.05).

3.13 Straight-chain ammonium salts discussion

Twenty two straight simple chain amines were tested for σ-1R affinity, all of which had never been tested for σ-1 affinity previously, and differ greatly from all previously know σ-1 ligands in their simplicity.

Primary ammonium salts

The simplest of ammonium salts tested were the primary ammonium salts, pentylammonium and hexylammonium have been shown previously to have antidepressant like activity in mouse models when administered at low doses (3mg/kg) and a depressant like affect at higher doses (100mg/Kg) (Widy-Tyszkiewicz and Czlonkowski, 1983, Widy-Tyszkiewicz and Sourkes, 1980). Widy-Tysziewiez et $al.$ (1980) suggests that the amines cause their behavioural effects through the 5-HT and dopamine receptors, however Widy-Tyszkiewicz et $al.$ (1980) had shown that the amines do not displace [³H] spiperone (a 5-HT$_{1A}$, 5-HT$_{2A}$, 5-HT$_7$, and D$_2$ receptor antagonist). Of the primary amines tested pentylammonium and hexylammonium had the highest affinity for the σ-1R. The affinity of hexylammonium for the σ-1R is 6mM, which is in the range the doses used by Widy-Tyszkiewiez et $al.,$ in the behavioural experiments suggesting that the amines might be causing their effect via the σ-1R. The affinity of these primary ammonium salts, for the σ-1R is low. However, there have been recent publications suggesting endogenous σ-1R ligands that have σ-1R activity despite their low affinity (Burchett and Hicks, 2006, Su et $al.$, 2009).

Secondary ammonium salts

Six secondary amines were tested in the [³H] (+) pentazocine competition assay, from the dimethylammonium with a 2 single carbon chains, to dihexylammonium with 2 six carbon long chains. Dimethylammonium, which has previously been shown to have anti tumour properties (Guest and Varma, 1991), and be present in human urine (Asatoor and Simenhoff, 1965, Zhang et $al.$, 1995), has an affinity for the σ-1R below 10mM and therefore it is unlikely that the anti tumour effects of dimethylammonium described by Guest and Varma (1991) are caused by an interaction with the σ-1R. However with each addition of a carbon to the chain there was an increased affinity for the σ-1R up until the five carbon long chain dipentylammonium (one way ANOVA P value 0.016), after which the affinity does not increase significantly for dihexylammonium. Dipentylammonium has a pK$_i$ of 7.37 ± 0.48, which is significantly higher than that of the well known σ-1R ligand,

rimcazole which as a pK_i ($\pm$ SEM) 6.22 $\pm$ 0.23 and at the same time it has a significantly lower affinity for the mAChR with a pK_i ($\pm$ SEM) 3.42 $\pm$ 0.24 compared to rimcazole with a pK_i ($\pm$ SEM) for the mAChR of 4.49 $\pm$ 0.10. Dipentylammonium is 7940 times more selective for the σ-1R then the mAChR, whereas σ-1R ligands such as (+) pentazocine are 162 times more selective, haloperidol 100 times more selective and rimcazole only 53 times more selective.

Dipentylammonium also has a lower affinity for the mAChR than another well known σ-1R ligand IPAG pK_i 4.3 (IPAG was not tested more than once in the QNB competition assay). Dipentylammonium has a 10 times lower affinity for the σ-1R than (+) pentazocine (the radioligand of choice in σ-1R binding assays), and haloperidol but has a 1000 times lower affinity for the mAChR than both (+) pentazocine and haloperidol. Dipentylammonium did have an effect on the calcium response induced by histamine, although dipentylammonium did not affect the EC_{50}, it did reduce the maximal response, however the dose required to cause this was 1mM, 1000 times that of dipentylammonium's affinity for the σ-1R. This shows that dipentylammonium is not binding to histamine receptor at the orthosteric site; rather it is either acting allosterically, or behaving as a functional antagonist, lowering calcium through another mechanism. Since the σ-1R agonists have been previously shown to cause σ-1 inhibition of calcium channels (Brent *et al.*, 1996b, Katnik *et al.*, 2006, Monnet *et al.*, 2003) this could be the explanation for the reduction in histamine-induced increase in cytoplasmic Ca^{2+}, and if so would be further suggest that dipentylammonium is a σ-1R agonist, either causing the movement of σ-1Rs to the cell surface (Hayashi and Su, 2001, Mavlyutov and Ruoho, 2007, Morin-Surun *et al.*, 1999) where they can prevent Ca^{2+} influx via interaction with ion channels (Monnet *et al.*, 2003) or preventing release of calcium from intracellular stores.

Dipentylammonium (100µM) alone did not raise cellular cAMP, nor did it inhibit the increase in cAMP caused by dopamine (100µM) or isoprenaline (100nM), which shows that it does not have affinity for the dopaminergic D_1 or D_5 receptors or the adrenergic β_2 receptors, which are coupled through G_s. Since dipentylammonium did not cause a decrease in dopamine-induced cAMP production it is possible to also rule out the D_2, D_3, and D_4 receptors, which are coupled through G_i. Dipentylammonium had no effect on the metabolism of the σ-1R negative HEK 293 cells, even when added at a dose 100 times its affinity for the σ-1R, indicating that it is non-toxic at these concentrations.

Our *in vitro* results suggest that these ligands are potential antidepressants. To determine whether they can be effective *in vivo*, we were able to have them tested in two animal models. Mice when subjected to the forced swim test exhibited despair behaviour, which was reduced significantly by dipentylammonium at 1, 5 and 10 mg/kg, having much the same effect on the despair behaviour as the SSRI antidepressant fluoxetine. There does not appear to be a dose dependent decrease in despair behaviour, however this maybe due to the lowest dose tested giving a maximal response. This suggests that dipentylammonium exhibits antidepressant activity equal to that of the SSRI fluoxetine. Furthermore when the σ-1R antagonist BD1047 (which has no affect on behaviour alone) was administered with the dipentylammonium, the antidepressant effect seen by dipentylammonium alone was reversed. The same antidepressant effect was seen in the tail suspension test, which is similar to the forced swim test in that it measures the despair behaviour exhibited by the mice suspended by their tail. The time where the mice remained immobile, not struggling to escape was decreased by a 5mg/kg dose of dipentylammonium to the same extent as the mice treated with the SSRI fluoxetine (10mg/kg). The effect of dipentylammonium on the immobility time of the mice in the tail suspension test was reversed when it was added in conjunction with the σ-1R antagonists BD1047, which further adds to the evidence that dipentylammonium is acting as a σ-1R agonist, and causing an antidepressant effect in the mice. Neither dipentylammonium *per se* nor in combination with BD1047 had an effect on locomotion suggesting that neither have psychostimulant or psychoinhibitory effects, providing strong evidence for dipentylammonium having antidepressant activity causing its antidepressant effects through a σ-1R mediated mechanism.

Tertiary ammonium salts

Eight tertiary ammonium salts were tested in the [^{3}H] (+) pentazocine competition assay, of these the two highest σ-1R affinity simple straight-chain amines were identified, tripentylammonium and trihexylammonium, with affinies of (pK$_i$ ± SEM) 7.83 ± 0.16 and 8.05 ± 0.40 respectively, both of which having higher affinities for the σ-1R than rimcazole, and both have no effect on the calcium response induced by histamine. Tripentylammonium also has an affinity for the mAChR (pK$_i$ ± SEM) 4.33 ± 0.38 that is statistically not different to that of rimcazole, however it is 2000 times more selective for the σ-1R over the mAChR where as rimcazole is only 53 times more selective, therefore tripentylammonium is a σ-1R ligand with a higher affinity for the σ-1R than rimcazole, and is more selective for the σ-1R over the mAChR than rimcazole .

Tripentylammonium (100μM) alone did not raise cellular cAMP, nor did it inhibit the increase in cAMP caused by dopamine (100μM) or isoprenaline (100nM), which shows that it does not have affinity for the dopaminergic D_1 or D_5 receptors or the adrenergic β_2 receptors, which are coupled through G_s. Since tripentylammonium did not cause a decrease in dopamine-induced cAMP production it is possible to also rule out the D_2, D_3, and D_4 receptors, which are coupled through G_i. Furthermore the cAMP assay provides evidence that the σ-1R itself is not coupling through G_s or G_i G-proteins since neither the σ-1R agonist (+) pentazocine or the antagonist IPAG raised cAMP levels alone, nor did they affect on the cAMP increase caused by dopamine or isoprenaline, there is also no suggestion of functional antagonism as the responses to dopamine and isoprenaline remained the same.

Neither dipentylammonium nor tripentylammonium had an effect on the growth of HEK 293 cells (σ-1R negative), measured using the MTS assay, at doses 100 times their affinity for the σ-1R, indicating that it is non-toxic at these concentrations.

Tripentylammonium despite having an affinity similar to that of dipentylammonium for the σ-1R failed to reduce despair behaviour in mice subjected to the forced swim test, this could be due to tripentylammonium not crossing the blood brain barrier, rapid metabolism or excretion and therefore not being accessible to the brain. It could equally be due to tripentylammonium having no activity at the σ-1R despite its high affinity for the σ-1R and its structural similarity to dipentylammonium, since tripentylammonium also did not have an effect on the histamine-induced calcium response, whereas dipentylammonium did. It has been shown previously that many antidepressant drugs including the tricyclic antidepressant imipramine and the SSRI citalopram (both of which have σ-1R affinity) along with other antidepressants that don't have reported σ-1R affinity (although that isn't to say they have no σ-1R affinity) maprotiline, amitripyline and clomipramine are able to inhibit L-type calcium channels (Zahradnik *et al.*, 2008). This modulation of ion channels is a possible mechanism for the antidepressant effects. Stimulation of neuron growth, which has previously been reported for the SSRI fluoxetine (which has σ-1R affinity) (Wang *et al.*, 2008) could be controlled by ion channel modulation by the σ-1R which would explain the shorter delay in effect of antidepressants such as chronic treatment with venlafaxine (Mitchell and Redfern, 2005), which has σ-1R affinity (Dhir and Kulkarni, 2007).

Quaternary ammonium salts

Four quaternary, positively charged ammonium salts were tested in the [³H] (+) pentazocine competition assay, all of which had low affinities for the σ-1R, with pK$_i$ values between 2 and 3, with the exception of tetramethylammonium, which had no affinity with in the range tested (maximum dose 10mM). From the quaternary ammonium salt binding data it is possible to conclude that a positively charged nitrogen results in a reduction in the affinity of a ligand for the σ-1R.

None of the simple straight-chain ammonium salts were able to cause a calcium response in Fura-2-AM loaded MDA-MB-468 cells when added at 100 times their affinity for the σ-1R, which means the straight-chain amines are unlikely to act as σ-1R antagonists. Tripentylammonium also has no effect on cell metabolism of the MDA-MB-468 cells, another indication that the simple straight-chain amines are not acting as σ-1R antagonists and are in fact σ-1R agonists.

Summary

To summarise and conclude this chapter, the straight-chain simple primary, secondary and tertiary ammonium salts have σ-1R affinity (the positively charged quaternary ammonium salts showed little affinity), which increases as the carbon chain length is increased between 2 carbons and 6 carbons. Beyond this the affinity for the σ-1R falls away. The high affinity straight-chain amines appear to be non toxic at doses 100 times their affinity for the σ-1R in σ-1R negative HEK 293 cells although none were able to induce a calcium response in the σ-1R expressing MDA-MB-468 cell line. Dipentylammonium (one of the ammonium salts with the highest affinity for the σ-1R), whilst being more selective for the σ-1R than the σ-1R ligands (+) pentazocine, IPAG, rimcazole and haloperidol, however was the only ammonium salt to reduce the maximal response to histamine. Furthermore dipentylammonium reduced the immobility time of mice in both the forced swim test and the tail suspension test whereas the structurally similar tripentylammonium did not, suggesting that dipentylammonium has antidepressant effects, which are reversed on addition of the σ-1R antagonist BD1047.

In summary, I have identified a non-toxic, high affinity σ-1R ligand, dipentylammonium that possesses potent antidepressant activity in animal *in vivo* assays. Further development of this molecule should be carried out to determine whether this compound can proceed into clinical trials, as an antidepressant, or a neuroprotective agent.

Chapter 4

4 Simple branched-chain ammonium salts - antagonists at the σ-1 receptor

4.1 Background

In Chapter 3 I have identified 3 high affinity σ-1R ligands, dipentylammonium, tripentylammonium and trihexylammonium, all of which show better or equal selectivity for the σ-1R over the mACh compared to rimcazole, haloperidol, and pentazocine. Furthermore, dipentylammonium showed antidepressant properties in the animal models. Their affinity for the σ-1R was higher than that of rimcazole. However, their affinity for the σ-1R is lower than that of pentazocine and haloperidol. Therefore, in order to try and find some higher affinity ligands for the σ-1R, or alter the activity at the σ-1R, and also try and keep the higher selectivity, whilst keeping to the original scope of the investigation with the simple single nitrogen ammonium salts, I moved on to investigate branched-chain ammonium salts. The branched-chain ammonium salts remain simple ammonium salts, and are the simplest variation on the theme that could alter the affinity for the σ-1R whilst staying within the original remit of the investigation.

4.2 Primary branched-chain ammonium salt affinity for the σ-1 receptor

Despite the straight-chain primary ammonium salts having low affinity for the σ-1R, the branched-chain primary ammonium salts described in this chapter were investigated, as they resemble part of IPAG, a known σ-1R antagonist.
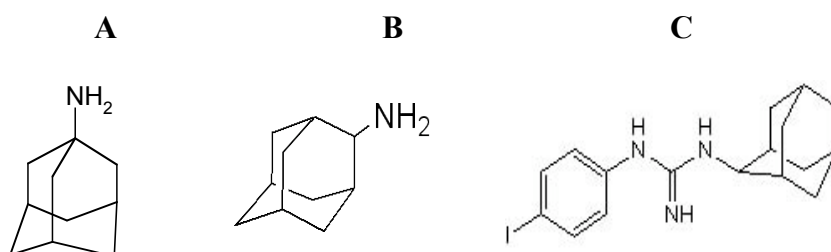
Figure 4.1: Structures of primary branched amines and IPAG
A 1-adamantylammonium, **B** 2-adamantylammonium, **C** IPAG.

The affinities of 1-adamantylammonium and 2-adamantylammonium (Figure 4.1a and 4.1b) for the σ-1R were assessed using radioligand competition binding (Figure 4.2), and the data are normalised to % specific $[^3H]$ (+) pentazocine binding, the curve in Figure 4.2 is made up of 6 independent binding assays.
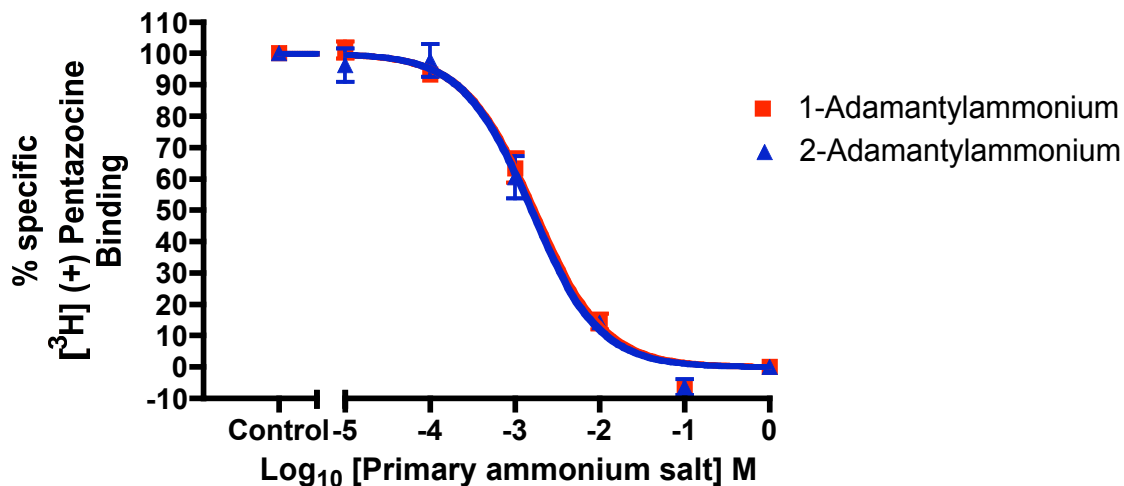
Figure 4.2: Binding of primary branched-chain ammonium salts to the σ-1R. Data represented as % Specific $[^3H]$ (+) pentazocine binding competing with 1-adamantylammonium and 2-adamantylammonium. Affinity (K_i 95% CI) for the σ-1R of 1-adamantylammonium is 0.73mM (0.48-1.11) and 2-adamantylammonium is 0.57mM (0.33-0.99). Error bars represent SEM from 4 independent radioligand competition assays.

In order to visualise the affinities for the σ-1R more clearly, K_i values obtained from the above competition binding curves were converted into pK_i values ($-log_{10}K_i$) shown in Figure 4.3 below.
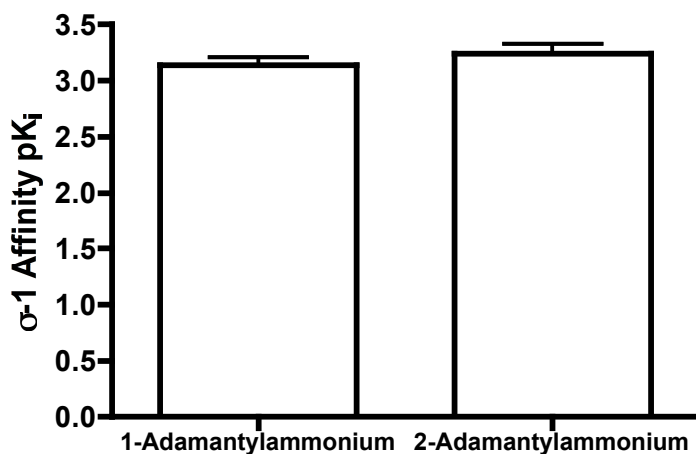
Figure 4.3: Summary of Branched-chain Primary ammonium salt binding to the σ-1R. pK_i (± SEM) for the primary ammonium salts 1-adamantylammonium and 2-adamantylammonium were pKi 3.13 (± 0.06) and 2-adamantylammonium was pKi 3.23 (± 0.09) respectively.

1-adamantylammonium and 2-adamantylammonium show similar binding properties with low affinities. The affinity of 1-adamantylammonium for the σ-1R was pK_i 3.13 (± 0.06) and 2-adamantylammonium was pK_i 3.23 (± 0.09). No other primary branched-chain ammonium salts were assessed for binding to the σ-1R.

4.3 Secondary branched ammonium salt affinity for the σ-1 receptor

In order to assess the structure activity relationship of the simple ammonium salts with the σ-1R, some simple branched-chain ammonium salts that were of similar chain length to the straight-chain ammonium salts with high affinity for the σ-1R, were tested for σ-1R affinity using $[^3H]$ (+) pentazocine in the radioligand competition assay. The binding data, normalised to % specific (+) pentazocine, are shown below in Figure 4.4.
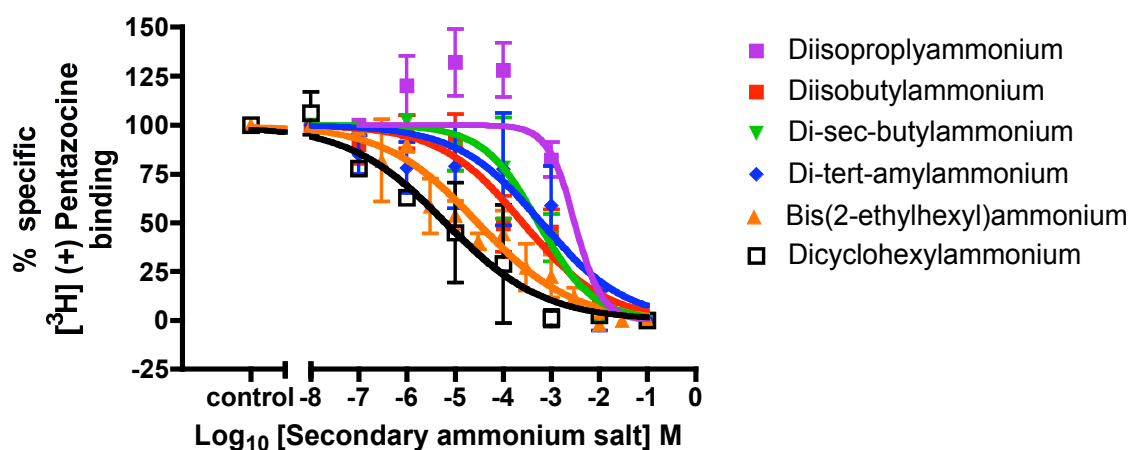
Figure 4.4: Binding of secondary branched-chain ammonium salts to the σ-1R. Binding of simple branched-chain secondary amines to the σ-1R, data represented as % specific binding of (+) pentazocine. Error bars represent SEM from 5 independent radioligand competition assays.

The Hill slope (nH) for the binding curves of diisobutylammonium and bis(2-ethylhexyl)ammonium differ significantly from -1 (one sample t-test *P* values 0.049 and <0.0001 respectively), therefore the binding of diisobutylammonium and bis(2-ethylhexyl)ammonium does not follow the law of mass action and the affinities can not be represented as K_i, instead the affinities are referred to as K_{50} values (the concentration of competing ligand that occupies 50% of the receptors). As for the other simple secondary branched-chain ammonium salts, diisopropylammonium (*P* value: 0.212), di-sec-butylammonium (*P* value: 0.359), di-tert-amylammonium (*P* value 0.106) and dicyclohexylammonium (*P* value 0.52), there was no significant deviation from the nH of -1. The nH values are represented in table 4.1 along with the comparison of binding models and F test values.

Ammonium salt	nH +/- SEM	Preferred binding model	F value and *P* value
Diisopropylammonium	-1.47 ± 0.33	One site	F=1.1 and *P* = 0.6
Diisobutylammonium	-0.51 ± 0.11	One site	F=2.2 and *P*=0.19
Di-sec-butylammonium	-0.75 ± 0.21	One site	F=0.4 and *P*=0.5
Bis(2-ethylhexyl)ammonium	-0.47 ± 0.07	Two site	F=4.0 and *P*=0.049
Dicyclohexylammonium	-0.43 ±0.18	One site	F=0.3 and *P*=0.5
Di-tert-amylammonium	-0.43 ± 0.18	One site	F=1.2 and *P*=0.2

Table 4.1: Hill coefficient and preferred binding model for branched-chain secondary ammonium salts at the σ-1R. *P* value refers to the chance of random error leading to accepting the alternative hypothesis (2 site model) rather than the null hypothesis (1 site model) (*n*=4).

In order to compare the affinities of the simple branched-chain ammonium salts that had nH values that differed significantly from -1 (diisobutylammonium and bis(2-(ethylhexyl)ammonium) the K_{50} values were converted to $-logK_{50}$ (pK_{50}) values. These values are represented in Figure 4.6.
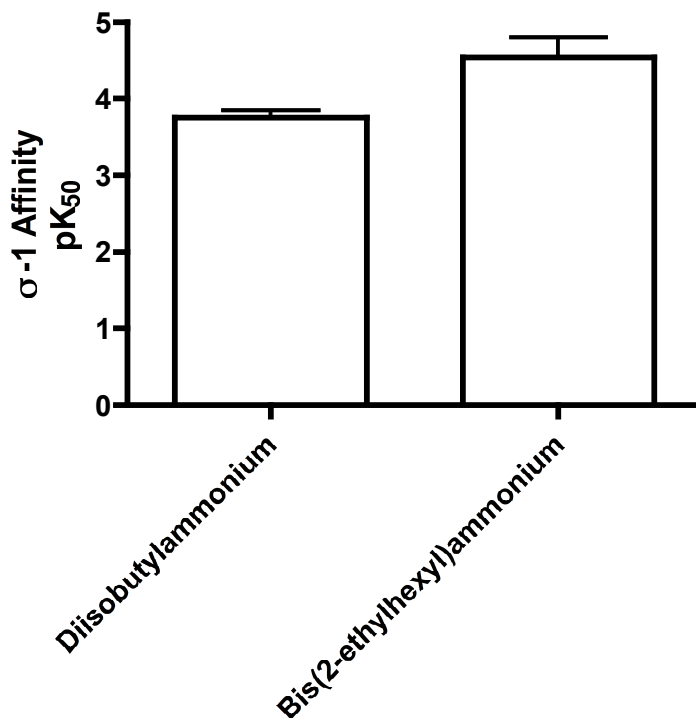
Figure 4.5: Summary of secondary branched-chain ammonium salts to the σ-1R
Summary of simple secondary branched-chain ammonium salts with nH values that differ significantly from -1, affinity for the σ-1R. The Mean pK_{50} ± SEM (*n*=4) for diisobutylammonium is 3.14 ± 0.02 and for bis(2-ethylhexyl)ammonium 4.54 ± 0.26.

In order to compare the affinities of the simple branched-chain ammonium salts, which have nH values that do not differ significantly from, -1 (and therefore the binding is assumed to follow the law of mass action) the K_i values were converted to pK_i values and represented in Figure 4.6.
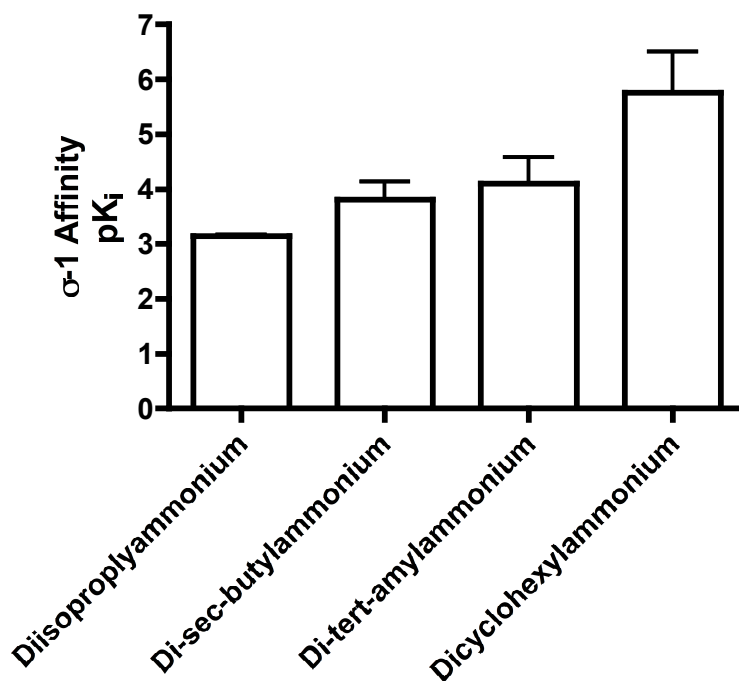
Figure 4.6: Summary of the binding of the simple branched-chain ammonium salts to the σ-1R. The affinity (pK$_i$ ± SEM) of the secondary branched-chain ammonium salts for the σ-1R are, diisopropylammonium 3.14 ± 0.02, di-sec-butylammonium 3.81 ± 0.33, di-tert-amylammonium 4.1 ± 0.5 and dicyclohexylammonium 5.76 ± 0.75. (*n*=4).

Bis(2-ethylhexyl)ammonium has the highest affinity for the σ-1R of the simple secondary branched-chain ammonium salts that have a statistically significant low nH value. Dicyclohexylammonium has the highest affinity for the σ-1R of the simple secondary branched-chain ammonium salts, which have an nH of 1. However, these affinities are much lower than the affinities of the straight-chain ammonium salts in the previous chapter, with the highest σ-1 affinity straight-chain secondary ammonium salt being tripentylammonium with a pK$_i$ of 7.34 ± 0.48 compared to the branched-chain ammonium salt bis(2-ethylhexyl)ammonium with a pK$_{50}$ of 4.54 ± 0.26 and dicyclohexylammonium with a pK$_i$ of 5.78 ± 0.74.

4.4 Tertiary branched-chain ammonium salt affinity for the σ-1 receptor

The simple straight-chain tertiary ammonium salts with carbon chain length between five and six carbons had the highest affinity for the σ-1R, therefore triisopentylammonium was tested for σ-1R affinity (being the longest simple branched-chain ammonium salt commercially available at the time along with N,N diisopropylethylammonium, which consists of two branched-chains and one straight-chain. The binding curves are represented in Figure 4.7.
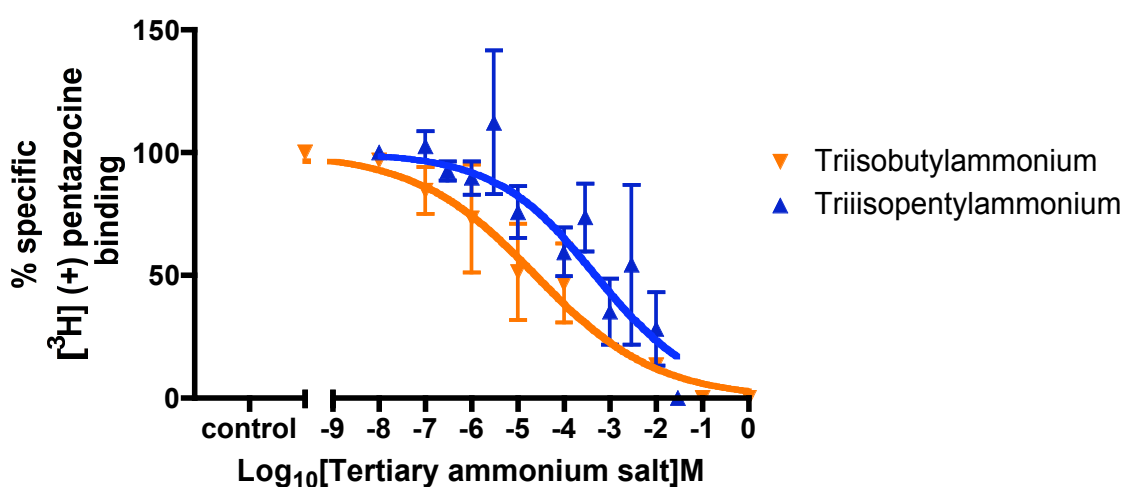
Figure 4.7: Tertiary branched-chain ammonium salt competition with [³H] (+) pentazocine in permeabilised MDA-MB-468 cells. Binding of simple branched-chain tertiary amines to the σ-1R, represented as % specific (+) pentazocine binding. Error bars represent SEM from 6 independent radioligand competition assays.

Once again the nH values for the binding curves of triisobutylammonium and triisopentylammonium differ significantly from -1 (nH values represented in Figure 4.8) (one sample t-test P values, 0.0011 and 0.0002 respectively), meaning that the binding of these two ammonium salts does not follow the law of mass action, and therefore the affinities are represented as K_{50} values. Triisobutylammonium has a K_{50} (95% CI) of 9.7 μM (6.9 to 80.1) and triisopentylammonium has a K_{50} (95% CI) of 196 μM (62 to 624). N,N-diisopropylethylammonium did not have affinity for the σ-1R within the range tested (highest dose 10mM).

Ammonium slat	nH +/- SEM	Preferred binding model	F value and *P* value
Triisobutylammonium	-0.33 ± 0.10	One site	F=0.3 and P=0.58
Triisopentylammonium	-0.36 ± 0.07	Two site	F=4.22 and P=0.047

Table 4.2: Hill coefficient and preferred binding model for branched-chain tertiary ammonium salts at the σ-1R. (*n*=6).

In order to compare the affinities of the branched-chain amines with nH values that were shallower than -1, the K_{50} values were converted to pK_{50} values, represented in Figure 4.9.
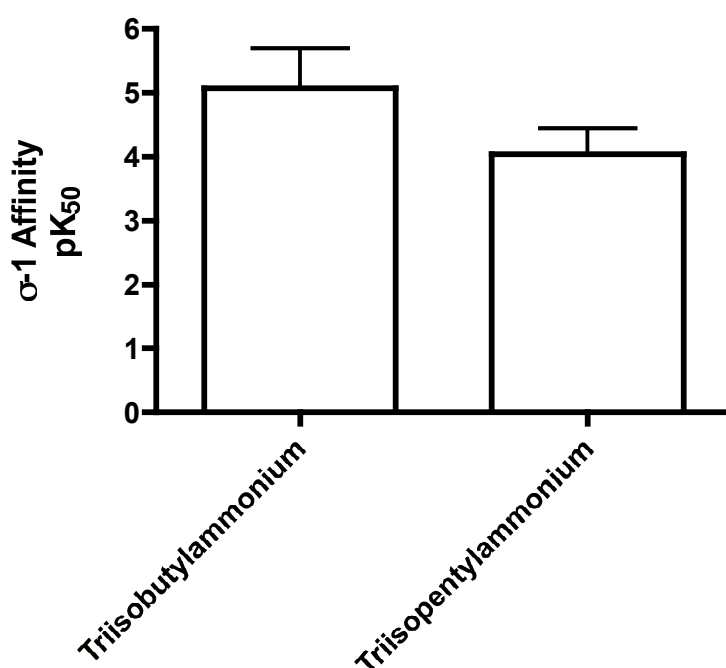
Figure 4.9: Summary of the simple tertiary branched-chain ammonium salts with nH values shallower than -1, binding to the σ-1R. The pK_{50} (± SEM) values are, triisobutylammonium 5.1 ± 0.6 and triisopentylammonium 4.1 ± 0.4. (*n*=6).

The shallow nH is a potential indication of G-protein coupling with the σ-1R (Connick *et al.*, 1992, Itzhak, 1989) and is discussed in detail with relation to σ-1R antagonists in chapter 5.

4.5   Calcium response to branched-chain ammonium salts

The branched-chain ammonium salts with the statistically significant shallow nHs were tested for σ-1 activity using the calcium response assay with Fura-2 loaded MDA-MB-468 cells. The calcium influx into the cytoplasm in response to the branched-chain ammonium salts at doses ten times the affinity for the σ-1R are represented in Figure 4.10.
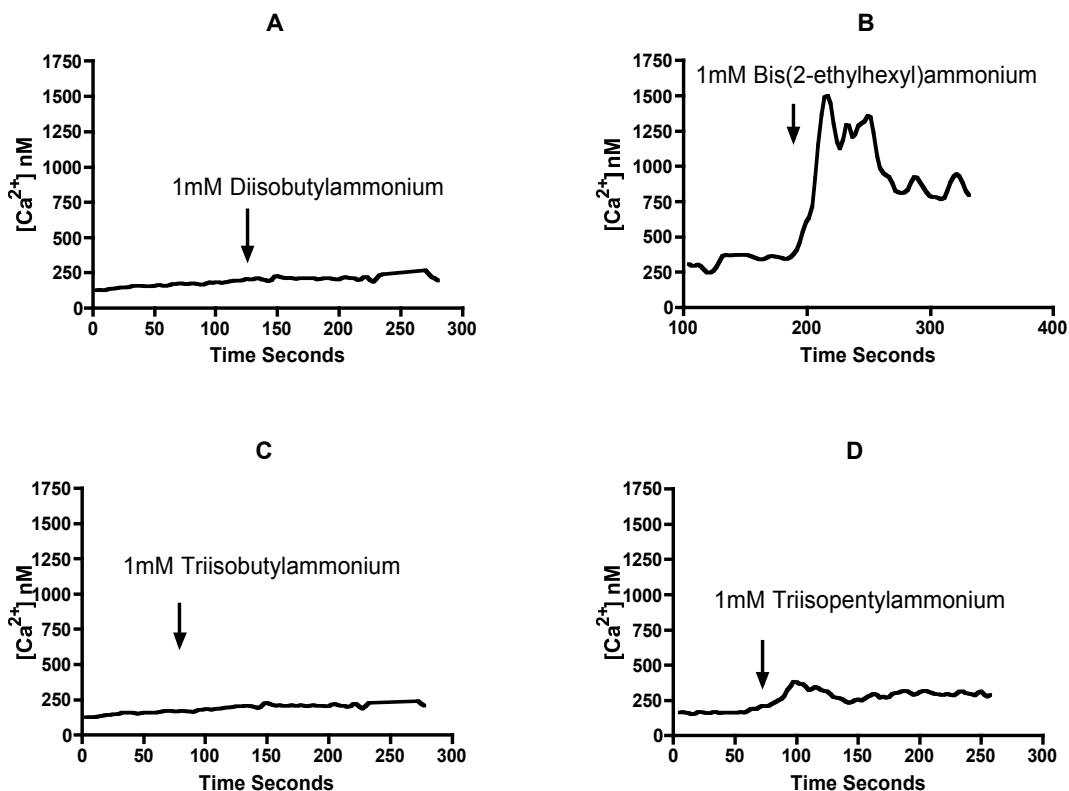
Figure 4.10: Calcium response to branched-chain ammonium salts.
A: 1mM Diisobutylammonium was added to a stirred suspension of Fura-2-AM loaded MDA-MB-468 cells, no increase in cytosolic free $[Ca^{2+}]$ was observed. **B:** 1mM bis(2-ethylhexyl)ammonium was added to the stirred suspension of Fura-2-AM loaded MDA-MB-468 cells which resulted in a large increase in cytosolic free $[Ca^{2+}]$. **C:** 1mM Triisobutylammonium was added to the stirred suspension of Fura-2-AM loaded MDA-MB-468 cells and no increase in cytosolic free $[Ca^{2+}]$ was observed. **D:** 1mM Triisopentylammonium was added to the stirred suspension of Fura-2-AM loaded MDA-MB-468 cells and a small increase in cytosolic free $[Ca^{2+}]$ was observed.

Bis(2-ethylhexyl)ammonium gave the largest calcium response after the addition of branched-chain ammonium salt at approximately ten times the affinity for the σ-1R and triisopentylammonium gave a small calcium response, whereas triisobutylammonium and diisobutylammonium (which did not have the 2 site model as the preferred model) did not give a response at all with the doses tested.

Since bis(2-ethylhexyl)ammonium gave the highest calcium influx on addition of 1mM, a full dose response was carried out. The dose response curve for calcium influx in response to bis(2-ethylhexyl)ammonium is shown in Figure 4.11.
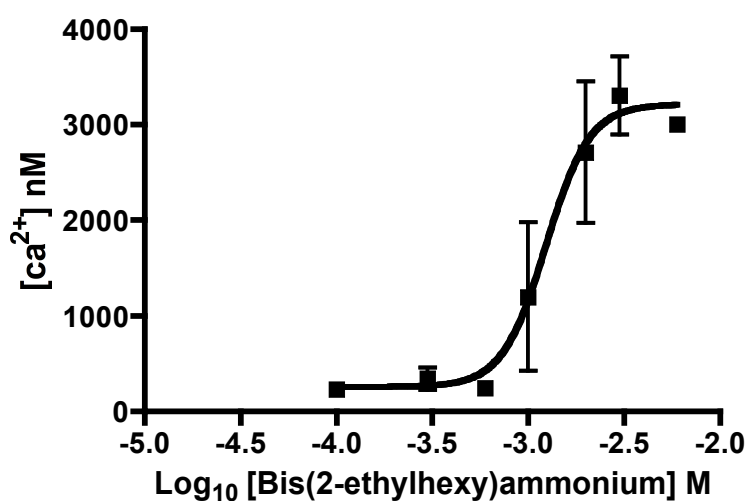
Figure 4.11: Cytosolic $[Ca^{2+}]$ increase dose response to bis(2-ethylhexyl)ammonium.
Bis(2-ethylhexyl)ammonium dose response in a suspension of MDA-MB-468 cells loaded with Fura-2-AM at 37°C. The pEC_{50} for bis(2-ethylhexyl)ammonium was 2.9 ± 0.1, with an nH value of 4 ± 3. Error bars represent SEM from 6 independent Fura-2 calcium assays.

Bis(2-ethylhexyl)ammonium dose-dependently caused an increase in calcium response, with a pEC_{50} value of 2.9 ± 0.1 which is over a 10 times higher dose than its affinity for the σ-1R pK_i 4.54 ± 0.26.

4.6   Branched-chain ammonium salts effect on cell metabolism

σ-1R antagonists cause cell death in σ-1R expressing cancer and tumour cell lines (Brent *et al.*, 1996a, Brent and Pang, 1995, Spruce *et al.*, 2004, Vilner *et al.*, 1995a). The branched-chain amines that induced a calcium response in the MDA-MB-468 (bis(2-ethylhexyl)ammonium and triisopentylammonium) were tested for their effects on cell metabolism in the MDA-MB-468 cell line using the MTS assay, the dose response curves are shown in Figures 4.12 and 4.13.
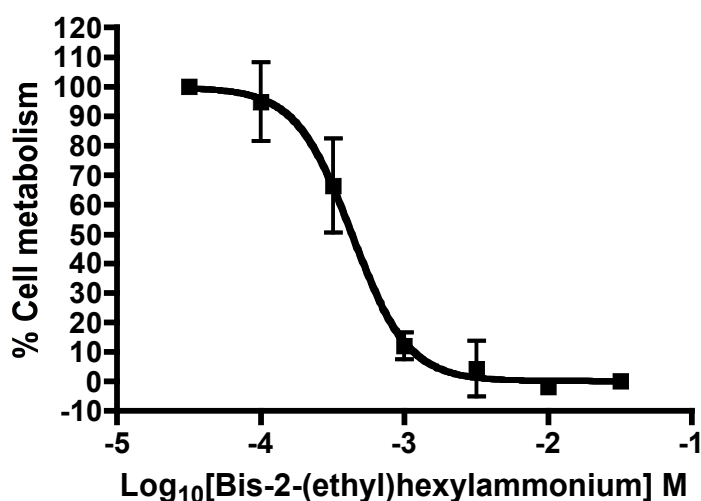
Figure 4.12: MTS assay dose response to bis(2-ethylhexyl)ammonium. The effect of bis(2-ethylhexyl)ammonium MDA-MB-468 cell metabolism, measured using the MTS assay kit, error bars represent SEM from 4 independent MTS assays. The pIC_{50} (±SEM) for bis(2-ethylhexyl)ammonium was 3.3 ± 0.1.

Bis(2-ethylhexyl)ammonium dose-dependently reduced cell metabolism in MDA-MB-468 cells, the pIC_{50} (±SEM) 3.3 ± 0.1 is over ten times higher than the affinity of bis(2-ethylhexyl)ammonium for the σ-1R (pK_{50} 4.54 ± 0.26).
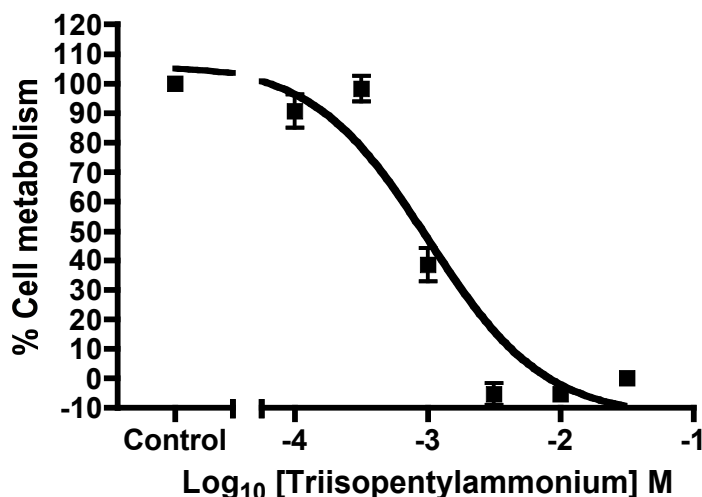
Figure 4.13: Triisopentylammonium dose response MTS assay. The effect on triisopentylammonium on MDA-MB-468 cell metabolism, measured using the MTS assay kit, error bars represent the SEM from 4 independent MTS assays. The $pIC_{50} \pm$ SEM, for triisopentylammonium was 2.96 ± 0.06.

Triisopentylammonium dose dependently reduced cell metabolism in MDA-MB-468 cells, with a pIC_{50} of 2.96 ± 0.06. The affinity of triisopentylammonium for the σ-1R is is pK_i ($\pm$SEM) 3.86 ± 0.41, almost ten times lower than the does needed to cause a 50% drop in cell metabolism.

4.7   σ-1 receptor knock-down: Are the branched-chain ammonium salts causing their effect through the σ-1 Receptor?

Bis(2-ethylhexyl)ammonium dose dependently increased the response seen in the calcium response assay in the Fura-2-AM loaded MDA-MB-468 cells, and dose dependently caused a decrease in cell metabolism in the MDA-MB-468. Triisopentylammonium also dose-dependently caused a decrease in cell metabolism in the MDA-MB-468 cells, and induced a small response in the Fura-2-AM loaded MDA-MB-468 cells. However the EC_{50} for the bis(2-ethylhexyl)ammonium calcium response assay and the IC_{50}s for the effects of both triisopentylammonium and bis(2-ethylhexyl)ammonium around a ten times higher dose than the affinities established from the [^{3}H] (+) pentazocine binding competition assays. It is possible that this discrepancy could be accounted for by the presence of HEPES in the DMEM in the MTS assay (as HEPES has σ-1R affinity), however in the calcium assay there is no HEPES in the buffer. Therefore in order to see if the branched-chain ammonium salts were having their effect thought the σ-1R, the σ-1R expression was

knocked down using a σ-1R siRNA. The expression of the σ-1R was measured using the specific binding of 30nM (+) pentazocine (Figure 4.14).
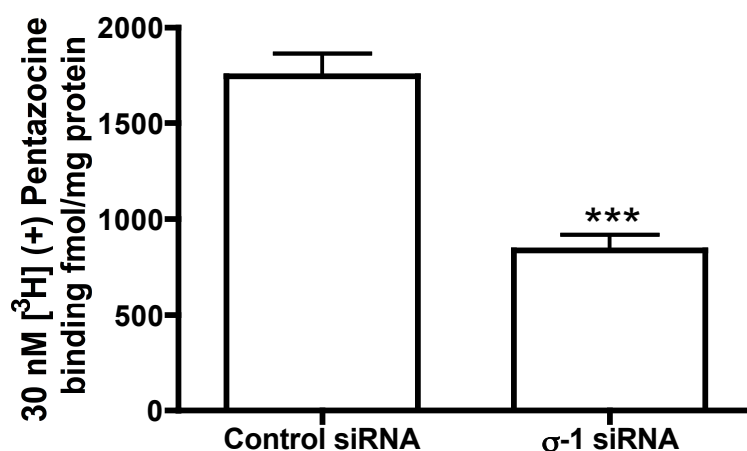
Figure 4.14: σ-1R knock-down with σ-1 siRNA compared to the non-targeting control siRNA. σ-1R expression in permeabilised MDA-MB-468 cells measured using 30nM [^{3}H] (+) pentazocine. The mean (fmol/mg $\pm$ SEM) for the binding of [^{3}H] (+) pentazocine in the MDA-MB-468 cells treated with the non-targeting control was 1749 $\pm$ 115 and for the MDA-MB-468 cells treated with the σ-1 siRNA 838 $\pm$ 200. The mean difference in binding from 8 independent experiments was 911 $\pm$ 151 fmol/mg *** t-test *P* value < 0.0001.

The σ-1 siRNA treatment of the MDA-MB-468 cells routinely resulted in an approximate 50% knock-down of the σ-1R, and caused no noticeable cell death, in the non targeting control or the σ-1 siRNA treated cells. Once the extent of the knock-down was established, the effect of the branched-chain amines on cell metabolism, in the siRNA treated MDA-MB-468 cells could be tested using the MTS assay. The dose-response curves to the branched-chain ammonium salts in the presence of the σ-1 siRNA or the non-targeting siRNA are show in Figure 4.15.
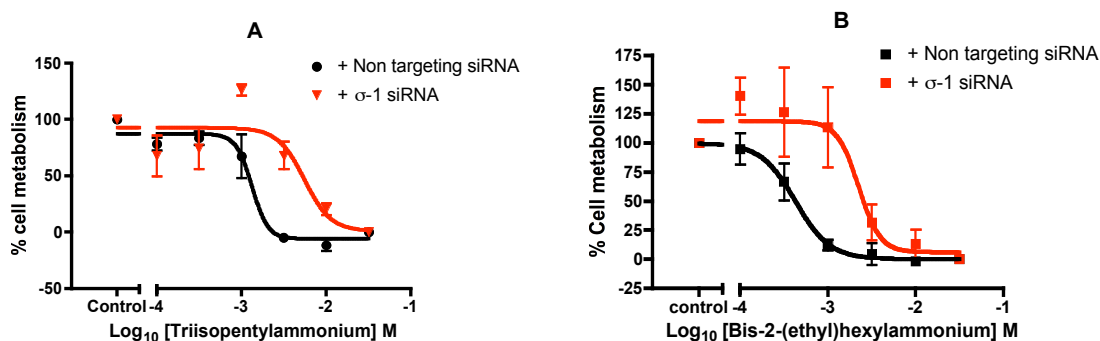
Figure 4.15: The effect σ-1R knock-down on the reduction in cell metabolism caused by σ-1R ligands. A The effect of triisopentylammonium on cellular metabolism in MDA-MB-468 cells in the presence of the σ-1 siRNA or the non-targeting siRNA. The pIC_{50} in the presence of the non-targeting siRNA for triisopentylammonium is 2.87 ± 0.17 and in the presence of the σ-1 siRNA 2.26 ± 0.21. **B** The effect of bis(2-ethylhexyl)ammonium in MDA-MB-468 cells in the presence of the σ-1 siRNA or the non-targeting siRNA. The pIC_{50} of bis(2-ethylhexyl)ammonium in the presence of the non-targeting siRNA is 3.19 ± 0.20 and in the presence of the σ-1 siRNA is 2.64 ± 0.19.

The addition of the σ-1 siRNA resulted in an increase in the concentration of the branched-chain ammonium salt required to cause a 50% drop in cell metabolism, whilst the non-targeting control had little effect on the cells. A comparison of the siRNA treated and control pIC_{50} for bis(2-ethylhexyl)ammonium can be seen in Figure 4.16, and triisopentylammonium in Figure 4.17.
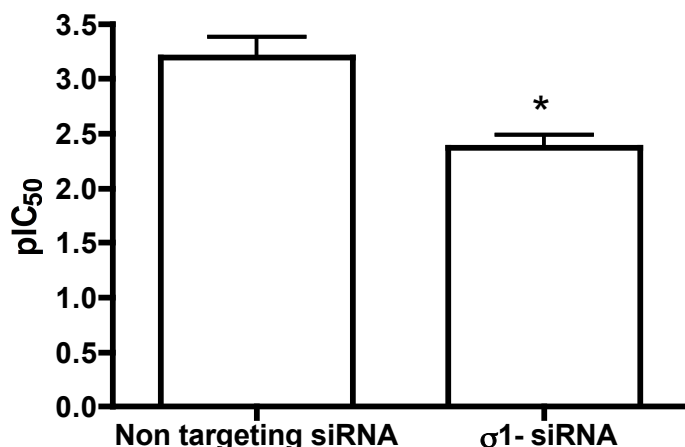
Figure 4.16: Summary of pIC$_{50}$ values for the effect of bis(2-ethylhexyl)ammonium on MDA-MB-468 cell growth. The effect of knocking down the σ-1R on the pIC$_{50}$ of cell metabolism when treated with bis(2-ethylhexyl)ammonium. The σ-1 siRNA treated MDA-MB-468 cells have a pIC$_{50}$ (2.64 ± 0.19) significantly lower than that of the MDA-MB-468 cells treated with the non targeting siRNA (3.19 ±0.20). Error Bars represent SEM from 3 independent experiments. * t-test P value 0.038.
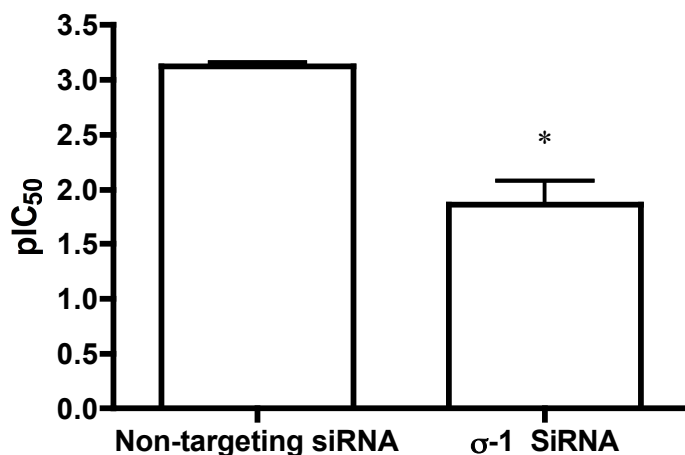
Figure 4.17: Summary of pIC$_{50}$ values for the effect of triisopentylammonium on MDA-MB-468 cell metabolism. The effect of knocking down the σ-1R on the pIC$_{50}$ of cell metabolism when treated with triisopentylammonium. The σ-1 siRNA treated MDA-MB-468 cells have a pIC$_{50}$ (2.26 ± 0.21) significantly lower than that of the MDA-MB468 cells treated with the non targeting siRNA (2.87 ± 0.17). Error bars represent SEM from 4 independent experiments. * t-test P value 0.018.

With an approximate 50% knock-down of the σ-1R, the effect of the branched-chain ammonium salts on MDA-MB-468 cell metabolism is reduced by approximately 10 times the concentration required to cause a 50% reduction in cell metabolism for both triisopentylammonium and bis(2-ethylhexyl)ammonium, which suggests there is no receptor reserve.

4.8 Alternative binding model for bis(2-ethylhexyl)ammonium

The single binding site model is not the only binding model that can be fitted to the data. A possible explanation for a shallow nH is that there are multiple sites to which the ligand is competing for, which have different affinities. A model for two affinity sites is fitted to the bis(2-ethylhexyl)ammonium data in Figure 4.18 below.
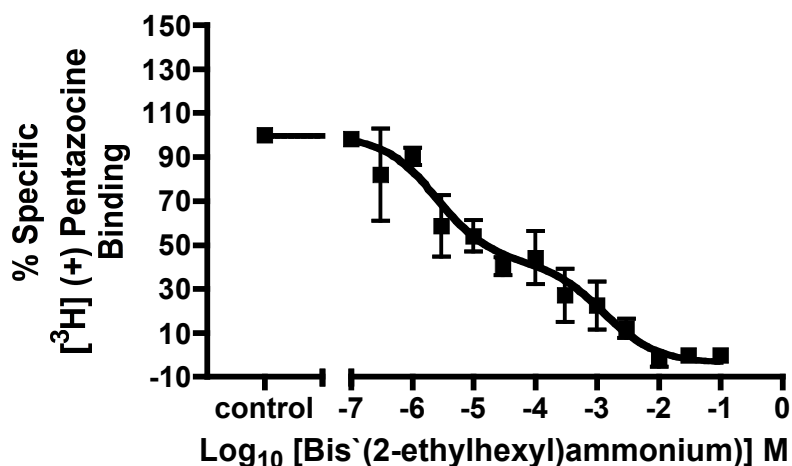
Figure 4.18: Multiple affinity sites for the binding of bis-2-(ethyl)ammonium to the σ-1R. Two-site fit to the bis(2-ethylhexyl)ammonium competition with [^{3}H] (+) pentazocine, with high affinity $pIC_{50} \pm$ SEM, 5.59 ± 2.26 (55.4 % of total binding) and low affinity $pIC_{50} \pm$ SEM, 2.91 ± 0.33 (44.6% of total binding) binding. (*n*=5).

Using the extra sum of squares F test the 2-site model was preferred with an F value of 4.01 and *P* value 0.049. The two site binding model was applied to the binding data for all the branched-chain ammonium salts, the data are shown in table 4.1 for the secondary ammonium salts and table 4.2 for the tertiary ammonium salts.

4.9 Branched-chain ammonium salt specificity for the σ-1 receptor: Muscarinic receptors

As described with the straight-chain ammonium salts in chapter 3 σ-1R ligands (+) pentazocine, BD737 and haloperidol have been shown to have μM affinity for the mAChR (Hong and Werling, 2002). In order to assess whether the branched-chain ammonium salts had affinity for the mAChR, they were put into the [³H] QNB competition assay, an example curve (triisopentylammonium) can be seen below in Figure 4.19, and the full list of branched-chain ammonium salts tested, their affinity for the mAChR, and the σ-1R can be seen in table 4.3
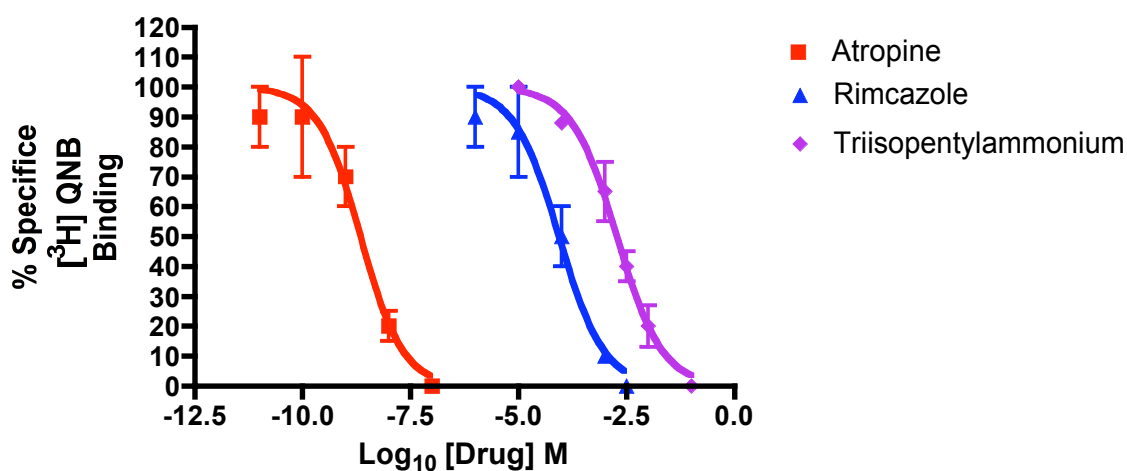
Figure 4.19: Example of branched-chain ammonium salts QNB displacement. The affinity of triisopentylammonium for the mAChR is (pK$_i$ ± SEM) 3.60 ± 0.11. Error bars represent SEM from between 4 and 7 independent radioligand competition assays.

Compound name	Type of compound	σ-1R affinity pK$_i$ ± SE	mAChR Affinity pK$_i$ ± SE	mACh K$_i$/σ-1 K$_i$	Number of assays (*n*)
Atropine	mACh antagonist	4.51 ± 0.42	9.40 ± 0.34	0.000012	4
Rimcazole	σ-1R ligand	6.22 ± 0.23	4.49 ± 0.10	53	7
Bis(2-ethylhexyl)ammonium	Secondary branched-chain ammonium salt	4.54 ± 0.26	3.92 ± 0.23	4.2	6
Triisopentylammonium	Tertiary branched-chain ammonium salt	6.03 ± 0.19	3.60 ± 0.11	269	5
2-adamantylammonium	Primary branched-chain ammonium salt	3.23 ± 0.09	3.37 ± 0.05	0.72	7
1-adamantylammonium	Primary Branched-chain ammonium salt	3.13 ± 0.06	3.22 ± 0.10	0.81	5

Table 4.3: Affinities of branched-chain ammonium salts for the σ-1R and mAChR, along with atropine a mAChR antagonist and rimcazole a σ-1R antagonist.

All of the branched-chain ammonium salts tested in the [³H] QNB competition assay had a lower affinity for the mAChR than the σ-1R antagonists rimcazole and haloperidol, and the σ-1R agonists (+) pentazocine and BD737.

4.10 Branched-chain ammonium salt specificity for the σ-1 receptor: dopaminergic and adrenergic receptors

As described in chapter 3 many σ-1R ligands have affinities with the dopaminergic receptors (Gundlach *et al*., 1986, Quirion *et al*., 1987). Therefore the branched-chain ammonium slats were tested for dopaminergic activity using the cAMP assay, and since MDA-MB-468 cells express both dopaminergic (Lang *et al.*, 2004) and adrenergic receptors (Drell *et al.*, 2003), which also couple through G_s G-protein activation of AC, the branched-chain ammonium salts (100μM) were tested for adrenergic receptor and dopaminergic receptor activity by measuring cAMP production in response to the ligands in MDA-MB-468 cells. Mean cAMP concentrations in response to ligands is shown in table 4.4. The dose response to dopamine and isoprenaline can be seen in chapter 3, (figure 3.27).

Drug	cAMP fmol/mg	Number of assays
Control (no drug)	8.7 ± 1.4	8
Dopamine	17.63 ± 2.5	8
Isoprenaline	22 ± 2.9	8
IPAG	8.9 ± 1.9	7
(+) Pentazocine	11.7 ± 2.0	3
Bis(2-ethylhexyl)ammonium	6.8 ± 2.0	6
Triisopentylammonium	7.8 ± 1.3	5
Dopamine + bis(2-ethylhexyl)ammonium	16.5 ± 7.2	4
Dopamine + triisopentylammonium	16.0 ± 2.0	6
Isoprenaline + bis(2-ethylhexyl)ammonium	20.1 ± 5.0	6
Isoprenaline + triisopentylammonium	30.3 ± 5.3	6

Table 4.4: cAMP concentration in response to dopamine, isoprenaline and branched-chain ammonium salts.

None of the branched-chain ammonium salts alone altered in cAMP levels in MDA-MB-468 cells, nor did they interfere with dopamine (100μM) cAMP production or isoprenaline (100nM) cAMP production, one way ANOVA *P* value 0.95.

4.11 Effects of branched-chain ammonium at the cell membrane

The σ-1R has been found to associate with membrane microdomains containing sphingolipids and rich in cholesterol, known as lipid rafts (Hayashi and Su, 2001, Hayashi and Su, 2003b, Hayashi and Su, 2003a, Hayashi and Su, 2004, Hayashi and Su, 2005b, Palmer *et al.*, 2007, Takebayashi *et al.*, 2004). The ganglioside G_{M1} is found in membrane microdomains enriched with cholesterol and sphingolipids, and it is this that the non toxic cholera toxin subunit B binds to, therefore fluorescent labelled cholera toxin B was used to highlight lipid raft formation, in response to σ-1R ligands (Figures 4.20-4.22).
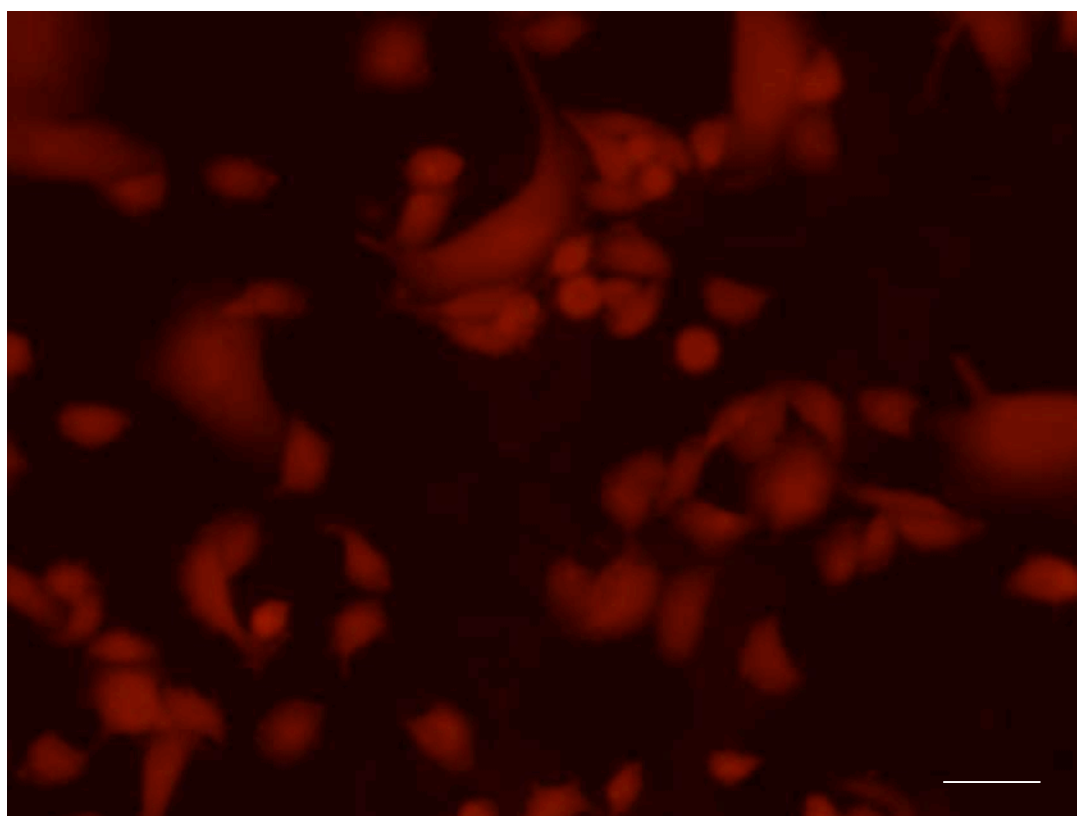
Figure 4.20: Control MDA-MB-468 cells stained with fluorescent cholera toxin B. Scale bar 50μm. Representative figure of 3 independent experiments.
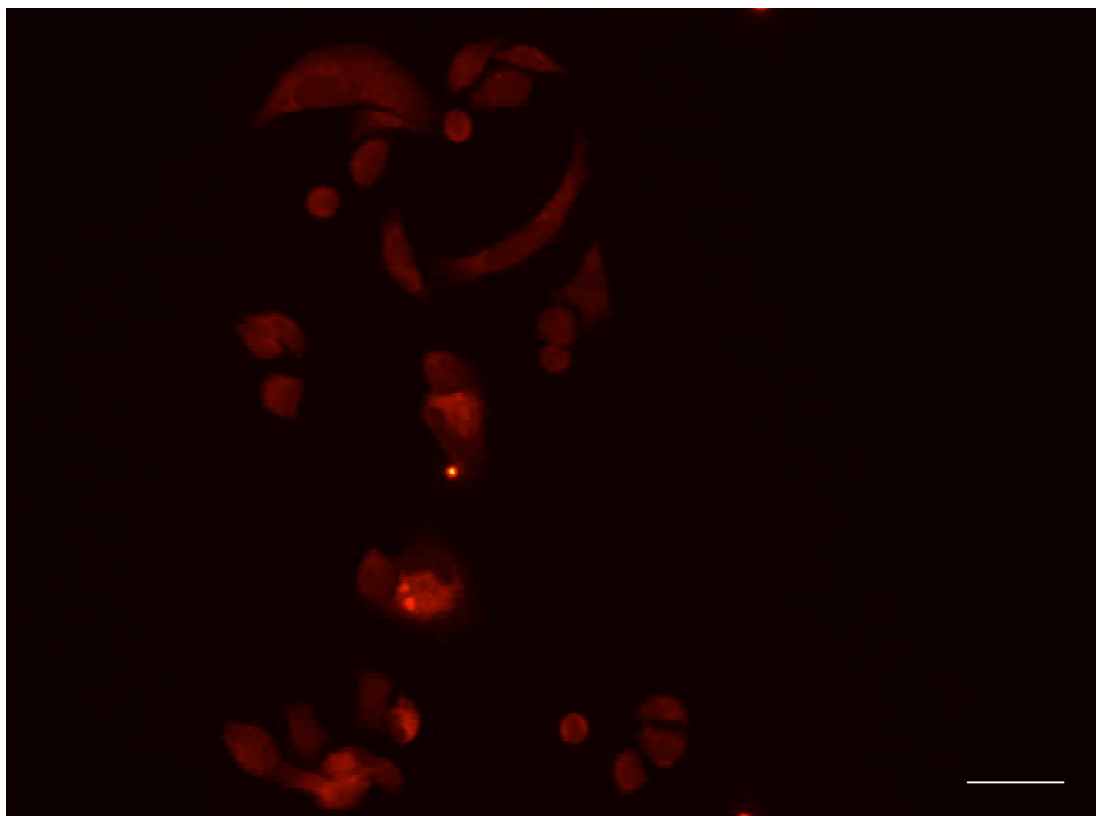
Figure 4.21: MDA-MB-468 cells treated with 1mM bis(2-ethylhexyl)ammonium, stained with fluorescent cholera toxin B. Scale bar 50µm Representative figure of 3 independent experiments..
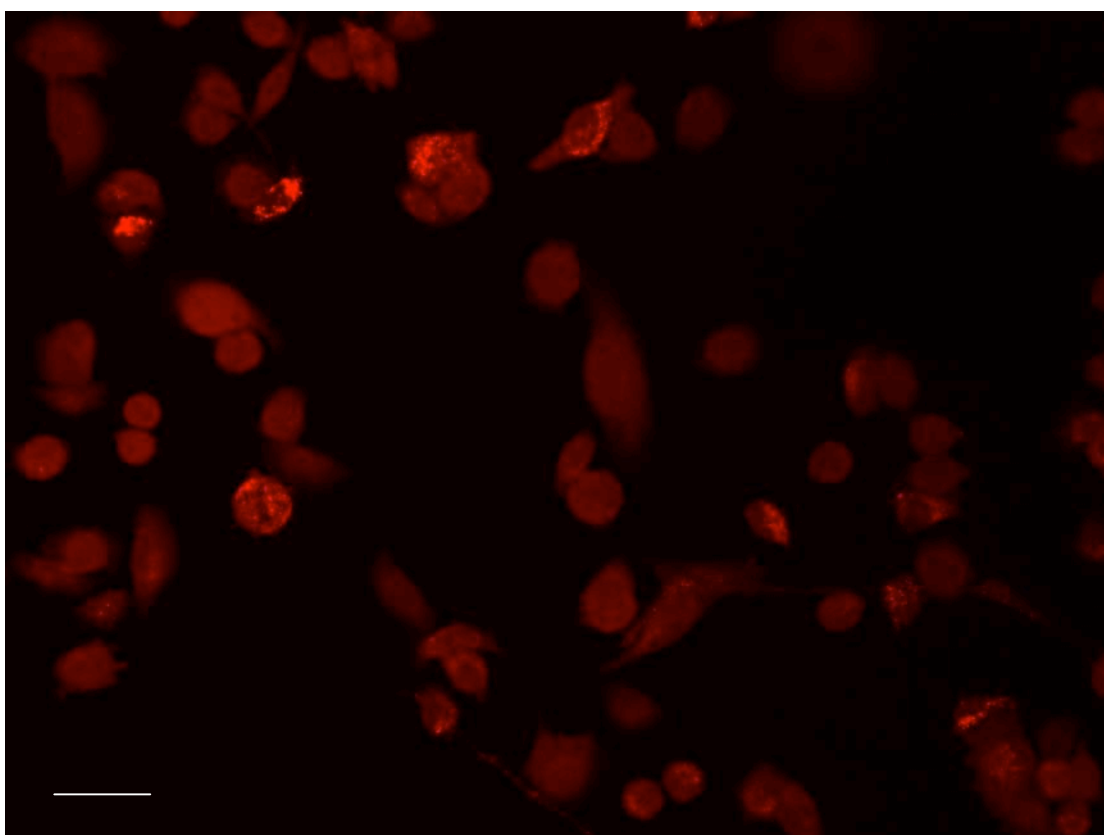
Figure 4.22: MDA-MB-468 cells treated with 10µM IPAG stained with fluorescent cholera toxin B. Scale bar 50µm. Representative figure of 3 independent experiments.

A 30 minute incubation of the MDA-MB-468 cells with bis(2-ethylhexyl)ammonium resulted in an increase in ganglioside G_{M1} patch formation (Figure 4.21), visualised with the florescent labelled cholera toxin B under a florescent microscope, compared to the control (Figure 4.20) which was incubated for 30 mins with PBS. IPAG (a σ-1R antagonist) was used as a positive control to show ganglioside G_{M1}, lipid raft patch formation (Figure 4.22).

4.12 *In vivo* effects of branched-chain ammonium salts

In order to assay the branched-chain ammonium salts that had σ-1R antagonist properties (bis(2-ethylhexyl)ammonium and triisopentylammonium) *in vivo* for anti-tumour activity, the cell line to be used in the assay needed to express the σ-1R. The Mac 13 cells were assayed for σ-1 receptor expression using radioligand binding ([^{3}H] (+) pentazocine saturation) (Figure 4.23).
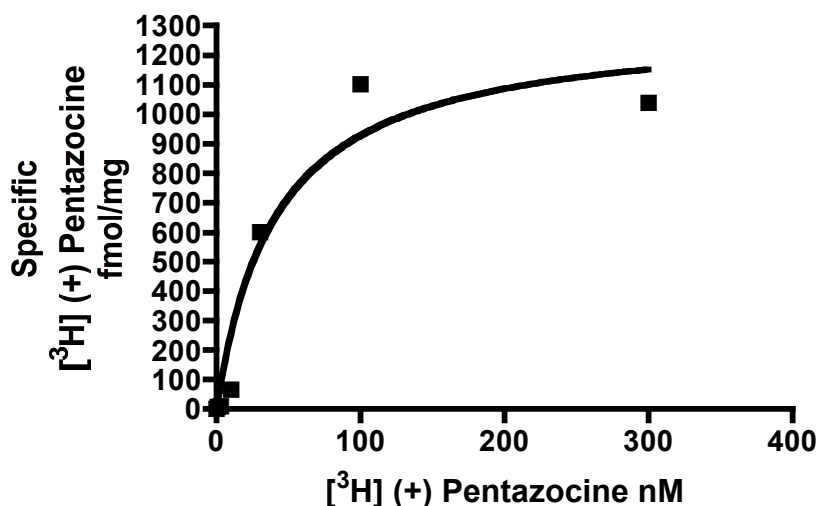
Figure 4.23 [^{3}H] (+) pentazocine saturation binding in Mac 13 cells. Non specific binding was determined in the presence of 1mM rimcazole. This is a representative figure of 3 independent experiments.

The mean ± SEM B_{max} for [^{3}H] (+) pentazocine saturation in the Mac 13 cell line, was 1310 ± 141 fmol/mg, and the mean ± SEM pK_d was 7.4 ± 0.1. Having established that Mac 13 cells express the σ-1R, the ammonium salts were again tested to see if they were able to affect cell growth using the MTS assay (Figure 4.24).
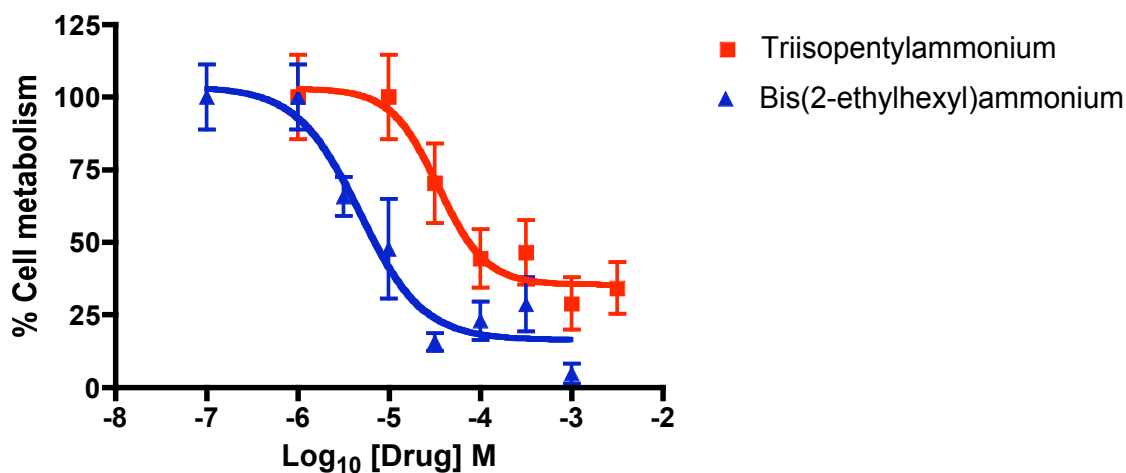
Figure 4.25: Effect of triisopentylammonium and bis(2-ethylhexyl)ammonium on cell metabolism of Mac 13 cells. Cultured Mac 13 cells treated with bis(2-ethylhexyl)ammonium and triisopentylammonium, cell metabolism measured using the MTS assay. Error bars represent SEM from 6 independent replicates.

Triisopentylammonium and bis(2-ethylhexyl)ammonium both cause a reduction in Mac 13 cell metabolism *in vitro* with mean ± SEM pIC$_{50}$ (*n*=6) values of 4.4 ± 0.2 and 5.3 ± 0.2 respectively, this is higher than the pIC$_{50}$ values observed for MDA-MB-468 cells (2.96 ± 0.06 and 3.3 ± 0.1 respectively).

Once the effects of the ammonium salts were established in the Mac 13 cells *in vitro* the ammonium salts were tested *in vivo* by Dr Steve Russell at Aston University. Mac 13 tumours were established in the mice 12 days before treatment with the ammonium salts began. Figure 4.26 shows the growth of the tumours for the ammonium salt treated mice compared to the control mice.
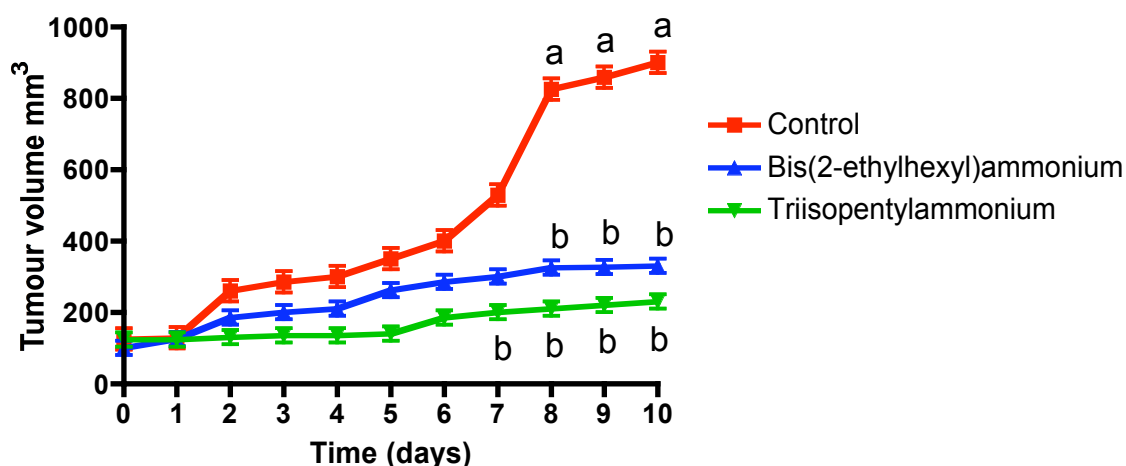
Figure 4.26: Effect of 10mg/kg bis(2-ethylhexyl)ammonium and triisopentylammonium on Mac13 tumour growth in mice. Bis(2-ethylhexyl)ammonium and triisopentylammonium treatment of mice carrying implanted Mac 13 tumours result in an inhibition of tumour growth compared to the control. Error bars represent SEM from 3 mice. ANOVA Dunnett's post test **a** $P<0.001$ from Day 0, **b** $P<0.001$ from control.

Daily treatment with 10mg/kg of bis(2-ethylhexyl)ammonium and triisopentylammonium resulted in a statistically significant reduction in tumour growth (ANOVA $P<0.001$), suggesting that the two σ-1R antagonist ammonium salts exhibit anti-tumour properties similar to that seen with the σ-1R antagonists IPAG and rimcazole (Spruce *et al.*, 2004).

4.13 Branched-chain ammonium salts discussion

Twelve branched-chain ammonium salts were tested for σ-1R affinity, all of which had never been assessed for σ-1R activity previously, and differ from all known σ-1R ligands in their simplicity, and differ from the ammonium salts tested in the previous chapter in being ever so slightly more complex in that the carbon chains are now branched.

The primary ammonium salts 1-adamantylammonium and 2-adamantylammonium are more complex than the other branched-chain ammonium salts tested, and resemble part of the well-known σ-1R antagonist IPAG. However, these two primary ammonium salts only had low affinity for the σ-1R, over 100,000 times lower affinity than IPAG for the σ-1R. Therefore it is clear that just the adamantyl group alone is not enough to make a high affinity σ-1R ligand. The adamantyl group may be responsible for the affinity of IPAG for the mACh receptor, since other previous studies have shown the adamantyl group to increase affinity for the mAChR (Gabrielevitz *et al.*, 1980) as well as 1-

adamantylammonium and 2-adamantylammonium both were more selective for the mAChR than the σ-1R (table 4.3).

The secondary and tertiary ammonium salts tested bear much more resemblance to the straight-chain ammonium salts tested in the previous chapter, with long carbon chains, only differing in that these chains are branched not straight. By adding these side branches to the chains of the simple ammonium salts dramatically altered their affinity for the σ-1R, and changed its activity at the σ-1R. The most dramatic example in change of affinity and change in activity at the σ-1R is bis(2-ethylhexyl)ammonium, by adding an ethyl group (C_2H_5) to the 2nd carbon along each of the carbon chains of dihexylammonium changed the binding properties of the ammonium salt giving a binding curve with a low nH value, and resulted in a 100 times loss of affinity, however in doing so it was now able to induce an increase in cytoplasmic calcium in the Fura-2-AM loaded MDA-MB-468 cells. The nH value for the cytoplasmic calcium influx into the cytoplasm in response to bis(2-ethylhexyl)ammonium (pseudo Hill slope since we are not looking at a simple 1 step event) of 4 ± 3 is very steep, this could be due to the fact that we are looking at cytoplasmic calcium influx which is further down stream of the ligand binding, meaning that the cytoplasmic calcium increase may not be proportional to receptor occupancy due to amplification of the signal. There are other potential explanations for the high nH value one of which could be allosteric regulation of the receptor.

A similar pattern was seen with the tertiary branched-chain ammonium salts, with triisopentylammonium, in adding a methyl (CH_3) group to the 4th carbon of each of the carbon chains in tripentylammonium, changed the shape of the binding curve resulting in a curve with a shallow nH and a reduction in affinity of almost 100 times. However this lower σ-1R affinity ammonium salt is able to induce an increase in cytoplasmic calcium in Fura-2-AM loaded MDA-MB-468 cells. The addition of the branches on the longer chain ammonium salts appears to have changed the activity at the σ-1R of the ammonium salt from agonists to antagonists, capable of inducing a calcium response, and causing a decrease in cellular metabolism, measured using the MTS assay. Moreover this reduction of cellular metabolism appears to be being mediated through the σ-1R, by knocking the σ-1R down by approximately 50% there is a 10 times reduction in cellular metabolism in response to bis(2-ethylhexyl)ammonium and triisopentylammonium. However, the dose required to induce a 50% reduction in cell metabolism, or 50% maximal calcium response was around ten times that of the affinity of bis(2-ethylhexyl)ammonium for the σ-1R. In

the case of the MTS assay there is 25mM HEPES in the buffer, which could account for any small discrepancy, although HEPES has an affinity for the σ-1R of 10mM so it is unlikely that HEPES could cause the 10 times discrepancy between IC_{50} and the affinity of bis(2-ethylhexyl)ammonium for the σ-1R. Moreover there is no HEPES in the calcium buffer, and the difference is the same. This difference can however be accounted for by there being two affinity states of the σ-1R for bis(2-ethylhexyl)ammonium. By fitting a different model to the bis(2-ethylhexyl)ammonium binding data, two affinities of bis(2-ethylhexyl)ammonium can be identified for the σ-1R. Giving a high affinity site of (pIC_{50} ± SEM) 5.59 ± 2.26 and a low affinity site of (pIC_{50} ± SEM) 2.91 ± 0.33, it is this low affinity site which corresponds to the doses at which bis(2-ethylhexyl)ammonium has its effects (Cytoplasmic $[Ca^{2+}]$ increase pEC_{50} 2.9 ± 0.1 and cell metabolism inhibition pIC_{50} 3.3 ± 0.1).

Further evidence that bis(2-ethylhexyl)ammonium is acting as a σ-1R antagonist is shown by its effects at the cell membrane on the formation of lipid rafts. A 1mM dose of bis(2-ethylhexyl)ammonium (the same as the dose required for 50% maximal calcium influx and a 50% reduction in cell metabolism) resulted in an increase in ganglioside G_{M1} patch formation, visualised with florescent cholera toxin B, in the same way as a 10μM dose of IPAG (a σ-1R antagonist). The formation of lipid rafts on the plasma membrane in response to σ-1R ligands could be the trigger of the calcium influx into the cytoplasm, since many types of ion channel (including voltage-gated calcium channels, voltage-gated potassium channel and calcium-activated potassium channels) are found localized within lipid rafts (Balijepalli *et al.*, 2006, Barfod *et al.*, 2007, Davies *et al.*, 2006, Martens *et al.*, 2001, Xia *et al.*, 2007) along with many regulators of ion channels which control calcium signalling (Isshiki and Anderson, 1999). The σ-1R has been shown to inhibit ion channels in the absence of ligands (Aydar *et al.*, 2002) and interact with lipid rafts possibly controlling the cholesterol content on the plasma membrane (Hayashi and Su, 2003b, Hayashi and Su, 2004, Hayashi and Su, 2005b, Mavlyutov and Ruoho, 2007, Palmer *et al.*, 2007, Takebayashi *et al.*, 2004).

Other secondary and tertiary branched-chain ammonium had low nH values, and lower affinities than the straight-chain ammonium salts, however they failed to induce a increase in cytoplasmic calcium when added at the same dose as bis(2-ethylhexyl)ammonium or triisopentylammonium (1mM). Triisopentylammonium and bis-2(ethyl)hexylammonium were the only two ammonium salts to have a preferred two site binding model, and were

also the only ammonium salts that were able to induce cytoplasmic calcium increase. In the case of diisobutylammonium which has a low nH value but did not induce a calcium response in Fura-2-AM loaded MDA-MB-468 cells, could be due to the fact that it has a much lower affinity for the σ-1R compared to bis(2-ethylhexyl)ammonium and triisopentylammonium, and therefore possibly requires a much higher dose to induce a calcium response. Another explanation for the lack of a calcium response to the other branched-chain ammonium salts, could be that they are partial agonists of the σ-1 receptor with low efficacy (note in the case of the σ-1R ligand nomenclature these are the σ-1R antagonists).

The radioligand binding data, with the low nH values, and preferred two site binding model, suggested that the secondary branched-chain ammonium salt bis(2-ethylhexyl)ammonium and the tertiary branched-chain ammonium salt triisopentylammonium are σ-1R antagonists. Further investigation into the effects of theses ammonium salts on membrane organisation, cytoplasmic calcium and cell growth revealed that both these ammonium salts had the same effects on the cell membrane, cytoplasmic calcium and cell growth as the previously characterised σ-1R antagonists IPAG, rimcazole, (Spruce *et al*., 2004), and haloperidol (Brent *et al*., 1996a). With this strong evidence suggesting that these branched-chain ammonium salts are σ-1R antagonists their *in vivo* effects in mice with transplanted σ-1R expressing Mac 13 tumours was assessed.

The Mac 13 cells were first tested for σ-1Rs using the MTS assay, the pIC_{50} values for bis(2-ethylhexyl)ammonium and triisopentylammonium were 4.4 ± 0.2 and 5.3 ± 0.2 respectively. These pIC_{50} values are considerably higher than those in the MDA-MB-468 cells (2.96 ± 0.06 and 3.3 ± 0.1 respectively), this could be explained by the lower expression of the σ-1R in these cells resulting in an easier release from the anti-apoptotic drive the σ-1R has over the cells, or it is a possibility that these cells express a higher level of mACh receptors compared to the MDA-MB-468 cells. Most colon cancer cell lines overexpress the m3 subtype of mAChR (Cheng *et al*., 2008) and antagonising mAChRs has been shown to result in apoptosis (Cheng *et al*., 2008, Song *et al*., 2003a, Song *et al*., 2003b). Both triisopentylammonium and bis(2-ethylhexyl)ammonium had affinity for the mAChR (table 4.3) (pK_i 3.6 ± 0.11 and 3.92 ± 0.23 respectively) meaning it is possible to speculate that the additional apoptotic effect seen in the Mac 13 cells is related to the mAChR affinity.

Mice with implanted Mac 13 tumours treated with the branched-chain ammonium salts (bis(2-ethylhexyl)ammonium and triisopentylammonium) showed a statistically significant inhibition of tumour growth compared to the control. These results suggest that bis(2-ethylhexyl)ammonium and triisopentylammonium are effective *in vivo* anti-tumour agents, most likely to be acting through a σ-1R mechanism, possibly involving calcium influx and plasma membrane reorganisation to form lipid rafts, to bring together signals that lead to apoptosis.

Summary

To sum up this chapter, I have shown that branched-chain ammonium salts have lower affinity for the σ-1R than the straight-chain ammonium salts from chapter 3. However, the binding studies revealed low nH values which suggested that they may be σ-1R antagonists. Two branched-chain ammonium salts in particular stood out, with statistically preferred 2 site binding models. These ammonium salts were bis(2-ethylhexyl)ammonium and triisopentylammonium, they were both capable of increasing cytoplasmic calcium in the same fashion as other well known σ-1R antagonists such as IPAG. Furthermore, bis(2-ethylhexyl)ammonium had the same effects on plasma membrane organisation into lipid rafts as the σ-1R antagonist IPAG. Both of these ammonium salts showed *in vitro* anti-cell growth in both human and mouse cell lines (MDA-MB-468 and Mac 13), and when tested *in vivo* they were both effective at inhibiting tumour growth in mice. Further investigation is required to ascertain whether these branched-chain ammonium salts can be developed as anti-tumour agents targeting the σ-1R.

Chapter 5

5 σ-1 receptor antagonists and G-protein coupling

5.1 Background

IPAG is a 'potent' σ-1R antagonist with a published affinity of 2.8nM (Whittemore *et al.*, 1997, Wilson *et al.*, 1991). When IPAG is added to the highly σ-1 expressing MDA-MB-468 cells it induces calcium influx into the cytoplasm. In order to assess the biological activity of the simple ammonium salts, the intention was to identify the EC_{50} for IPAG giving a suitable dose of IPAG to see if the simple ammonium salts affected the calcium influx into the cytoplasm. IPAG was chosen instead of the commonly used σ-1 antagonist rimcazole as preliminary experiments showed that rimcazole fluoresced at 510nm when excited between 280 and 360 nm (Figure 5.1).
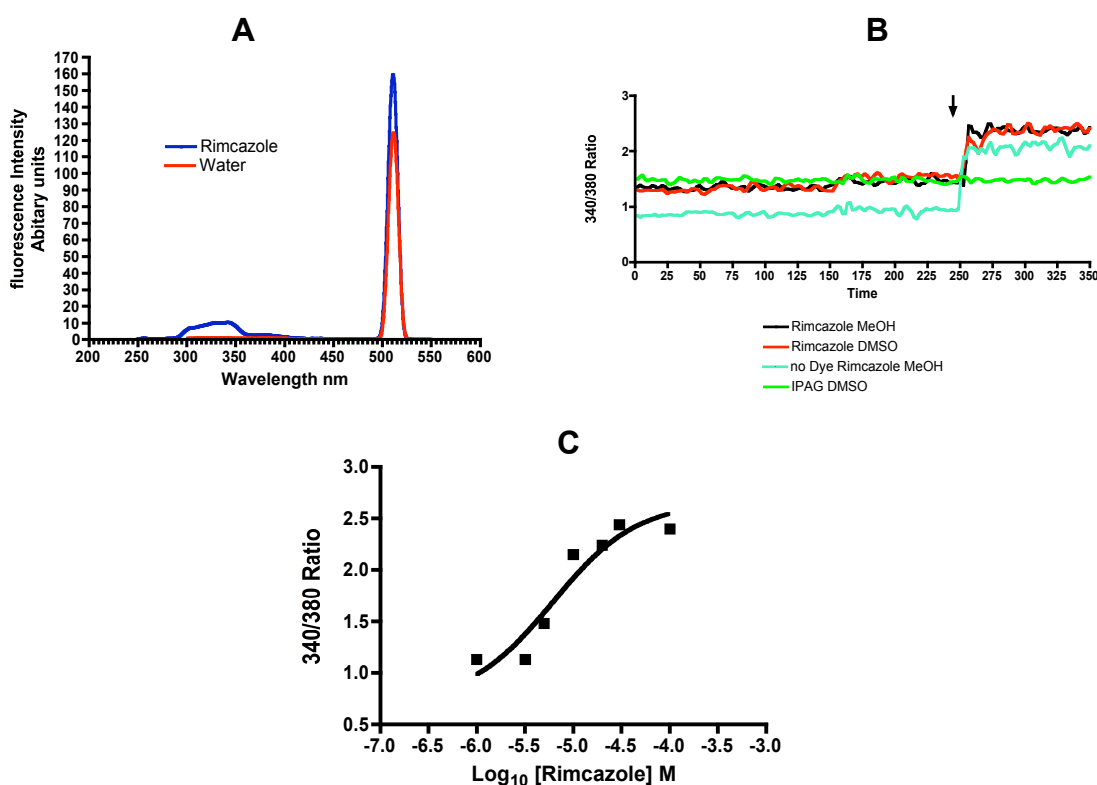
Figure 5.1: Rimcazole fluorescence. A: Rimcazole (100µM) wavelength scan showing an increase in emissions at 510nm when excited between 290 and 360nm, compared to water alone. **B:** Rimcazole dissolved in two different solvents (methanol (MeOH) or DMSO) added to a calcium free buffer not containing cells, with or with out Fura-2 shows an increase in 340/380 ratio, whereas IPAG does not. **C:** Rimcazole dose-response in the absence of Fura-2-AM loaded cells.

The intrinsic fluorescence of rimcazole leads to an apparent EC_{50} of 10μM in the absence of Fura-2-AM loaded cells, this brings into question the validity of previously published data studying the effects of rimcazole on intracellular calcium levels using a ratiometric Fura-2 system, therefore data such as that found in Aydar *et al.* (2006), Brent *et al.*, (1996b), Church and Fletcher, (1995), Spruce *et al.*, (2004) should be reviewed and re-interpreted.

Rimcazole therefore could not be used in the Fura-2 calcium assay and IPAG was selected instead, a dose-response curve was generated using increasing doses of IPAG added to stirred Fura-2-AM loaded MDA-MB-468 cells (Figure 5.2). The EC_{50} and 95% CI for IPAG in the calcium influx assay was 124 (96 – 160) μM.
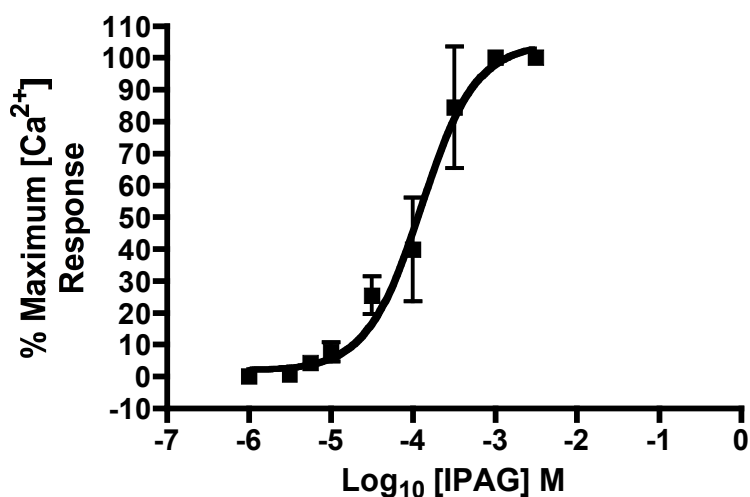
Figure 5.2: Cytosolic [Ca^{2+}] increase in response to IPAG, dose response. Data represented % maximum cytosolic calcium increase in response to IPAG in Fura-2-AM loaded MDA-MB-468 cells. The EC_{50} (95% CI) for IPAG was 124 (96 – 160) μM. Error bars represent SEM from 6 independent Fura-2 calcium assays.

IPAG also dose dependently leads to a reduction in cell metabolism in the σ-1R expressing MDA-MB-468 cells, this was measured using the MTS assay. A dose response was carried out in order to identify the IC_{50} for IPAG in the cell proliferation assay (Figure 5.3). The IC_{50} and 95% CI for IPAG's effect on cell proliferation was 30 (11.7 - 48.2) μM
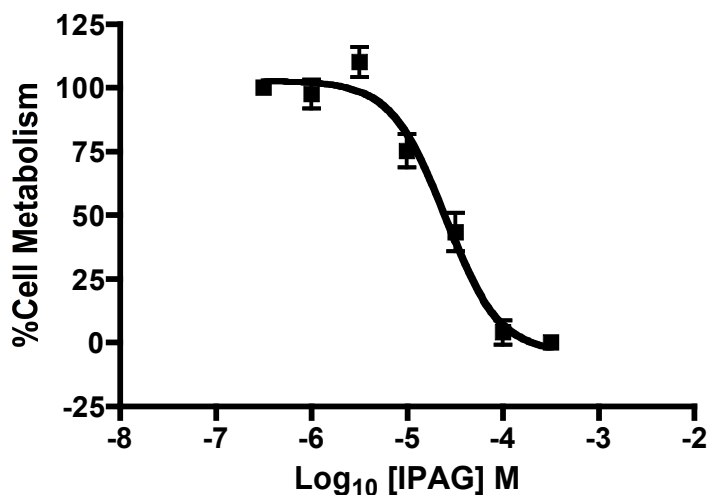
Figure 5.3: IPAG MTS assay dose response. Data represented as % cellular metabolic activity of MDA-MB-468 cells in response to IPAG, the IC_{50} (95% CI) for this assay was 30 (11.7 - 48.2) µM. Error bars represent SEM from 3 independent MTS assays.

The EC_{50} for IPAG in the Fura-2 calcium assay and the IC_{50} in the MTS assay are over 10,000 times higher than the published affinity for IPAG (Whittemore *et al.*, 1997, Wilson *et al.*, 1991). In order to assess whether IPAG was indeed causing its effects though the σ-1R, as there was a large discrepancy between the observed EC_{50} and IC_{50} values and the published affinity for the σ-1R, the σ-1 siRNA was used to knock-down the σ-1R in the MDA-MB-468 cell line and the calcium response to IPAG measured (Figure 5.4).
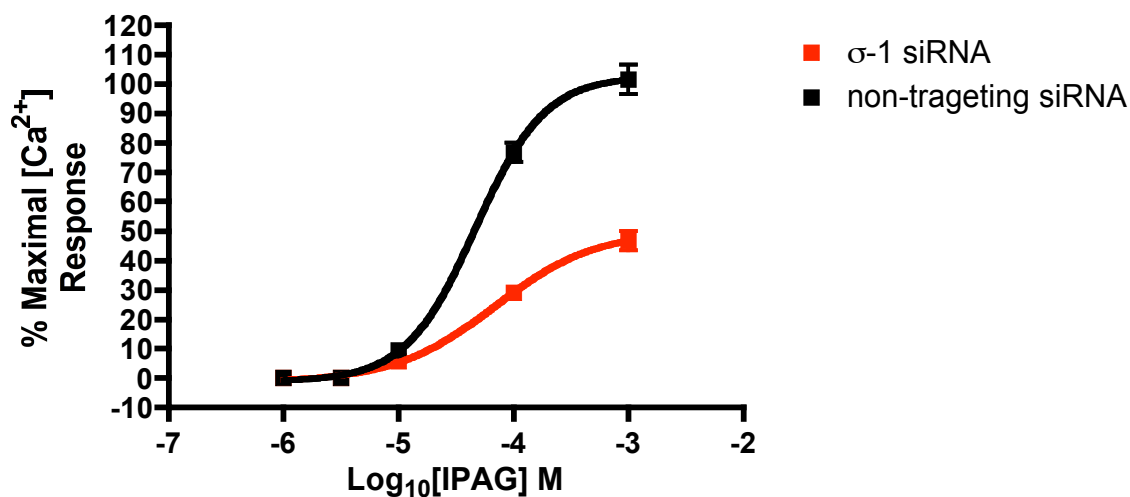
Figure 5.4: Effect of knocking down the σ-1R on cytoplasmic [Ca^{2+}]. Data represented % maximum cytosolic calcium increase in response to IPAG in Fura-2-AM loaded MDA-MB-468 cells treated with either the σ-1R siRNA or the non-targeting control. Error bars represent SEM from 3 independent Fura-2 calcium assays.

Knocking down the σ-1R by approximately 50% resulted in a decrease in maximal response by 50%, but did not affect the EC_{50}. This suggested that the σ-1R is involved in the effects of IPAG and therefore IPAG's affinity for the σ-1R was reassessed in the MDA-MB-468 cells. It also suggests that there is no receptor reserve for calcium signalling since reducing the receptor number by approximately 50% the maximal response is reduced by 50%.

5.2 IPAG affinity for the σ-1 receptor

To investigate the discrepancy between the published affinity of 2.8nM for IPAG (in guinea pig brain membranes) and the EC_{50} value observed in the calcium influx assay of 125μM and the IC_{50} of 30 μM in the MTS cell proliferation assay (using MDA-MB-468 cells), IPAG's affinity for the σ-1R in MDA-MB-468 cells was checked using [^{3}H] (+) pentazocine competition binding (Figure 5.5).
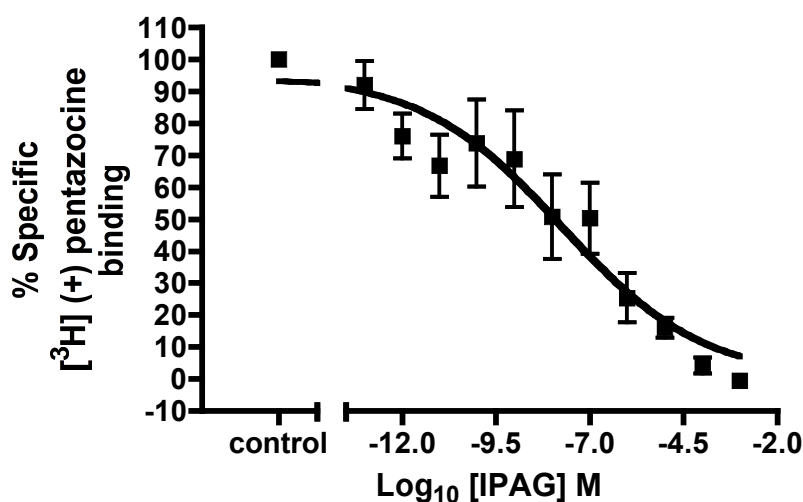
Figure 5.5: Single site fit for IPAG binding to the σ-1R. IPAG competition assay with 30nM [^{3}H] (+) pentazocine. A single site binding model gives a pK_{50} 7.82 ± 0.49 with an nH of -0.206. Error bars represent SEM from 9 independent radioligand competition assays.

The radioligand binding assay did indeed give an affinity for IPAG for the σ-1R in the low nanomolar range (15.1 nM compared to the published affinity of 2.8nM). However the single site binding model had a very low nH of -0.206, and the data did not appear to fit this model well. The 2 site binding model fits the data better (Figure 5.6).
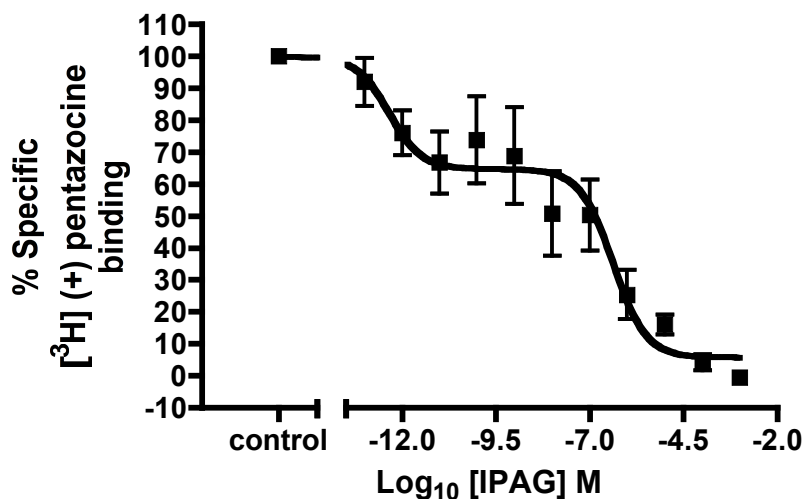
Figure 5.6: Multiple site fit for IPAG binding to the σ-1R. IPAG competition assay with 30nM [³H] (+) pentazocine. The 2 site binding model fits the binding data better giving $pK_{i\ high}$ (±SEM) 12.8 ± 0.6 (37% of total binding) and $pK_{i\ low}$ 6.3 ± 0.2 (63% total binding). Error bars represent SEM from 9 independent radioligand competition assays.

Using the extra sum of squares F test the 2-site model was preferred with an F value of 31.1 and *P* value less than 0.0001.

5.3 Effects of GTP on IPAG binding to the σ-1 receptor

The low nH value and two site binding fit can be an indication of G-protein coupling (Connick *et al.*, 1992, Itzhak, 1989). There are, however, other explanations for a multiple site curve, including pentazocine binding other receptors, such as the σ-2R. This can however be ruled out as pentazocine is 200 times more selective for the σ-1R than the σ-2R (Akunne *et al.*, 1997). In order to test for σ-1 interaction with a G-protein the [³H] (+) pentazocine / IPAG competition binding assay was carried out in the presence and absence of 1mM GTP (10 times the normal physiological concentration of GTP (Reinhardt *et al.*, 2002)). A saturating dose of GTP will encourage the spontaneous GDP/GTP exchange in the alpha sub unit of a heterotrimeric G-protein and therefore force the G-protein to remain active effectively uncoupling the G-protein from the receptor. If a G-protein is coupled with the σ-1R its activation and uncoupling will result in the loss of the 2 site binding curve.

Firstly, to see if GTP had any effect on the affinity of [³H] (+) pentazocine for the σ-1R saturation binding in the presence and absence of GTP was carried out (Figure 5.7).
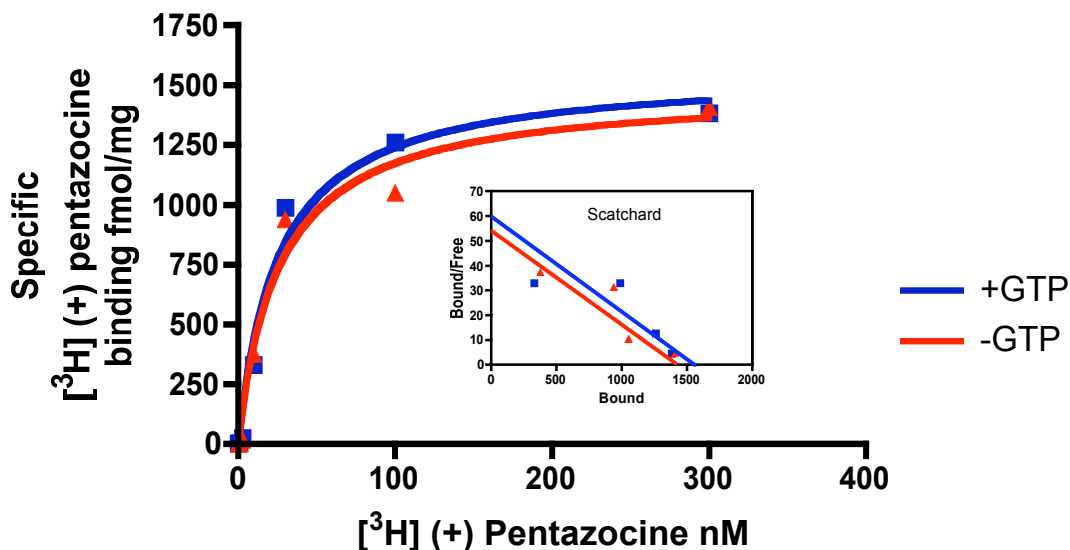
Figure 5.7: Saturation binding of [³H] (+) pentazocine in permeabilised MDA-MB-468 cells in the presence and absence of GTP. Representative figure of 3 independent radioligand saturation experiments. + GTP K_d 25.8 nM –GTP 26.4 nM.

1mM GTP has no noticeable effect on the binding of [³H] (+) pentazocine to the σ-1R in the permeabilised MDA-MB-468 cells, therefore the competition assay with IPAG was repeated in the presence of 1mM GTP (Figure 5.8).
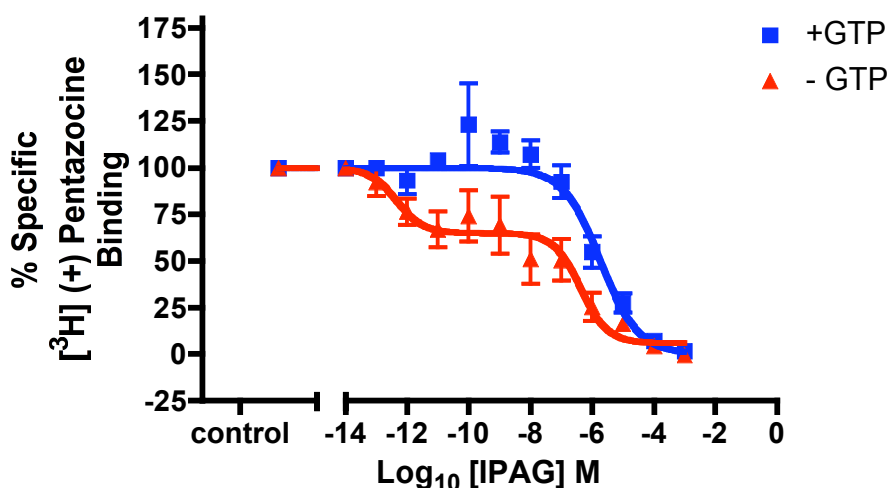
Figure 5.8: IPAG binding to the σ-1R in MDA-MB-468 cells. IPAG competitive binding assay using permeabilised MDA-MB-468 cells that had been washed with TBS to remove any endogenous GTP. With 30nM [³H] (+) pentazocine in the presence and absence of 1mM GTP. Error bars represent SEM from 9 independent radioligand competition assays.

The addition of 1mM GTP dramatically changes the shape of the binding curve; there is a dramatic increase in the nH (compared to the single site fit is used in the absence of GTP) (Figure 5.9). The affinity of IPAG for the σ-1R also shifts to the low affinity site ($pK_i \pm$ SEM 6.3 ± 0.2) in the presence of 1mM GTP, which has no significant difference from the low affinity site seen in the 2 site fit in the absence of GTP ($pK_i \pm$ SEM 6.8 ± 0.3) (t-test *P* value 0.183).
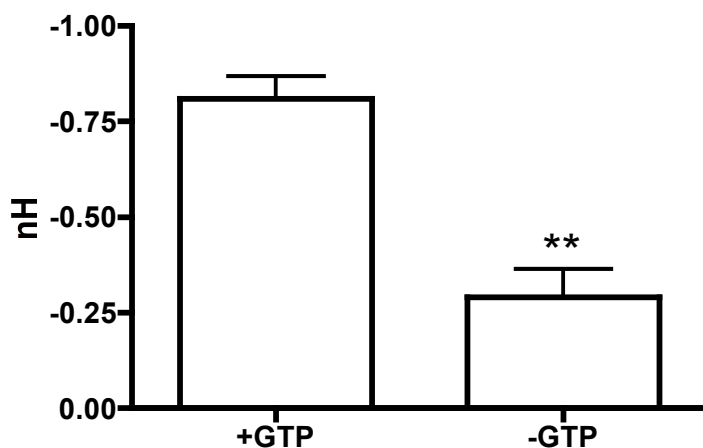
Figure 5.9: Hill coefficients for IPAG ± GTP: Hill coefficients for IPAG competition with ^{3}H (+) pentazocine binding in MDA-MB-468 cells. The mean nH for + GTP was -0.81 ± 0.05, and –GTP was -0.29 ± 0.07. Error bars represent SEM from 9 independent assays. ** *P* value 0.0015.

5.4 Effects of GTP on rimcazole binding to the σ-1 receptor

Rimcazole is a σ-1R antagonist, which has an affinity for the σ-1R of 1μM (Gilmore *et al.*, 2004, Husbands *et al.*, 1999) and has been previously shown to cause apoptosis in cancer cells through a σ-1R dependent pathway (Spruce *et al.*, 2004). Rimcazole could not be used in the calcium assay as it interfered with the wavelengths at which Fura-2 is read. However rimcazole did not interfere with the reading of the MTS assay, Figure 5.9 below shows the effect of the metabolic activity of MDA-MB-468 cells treated with rimcazole.
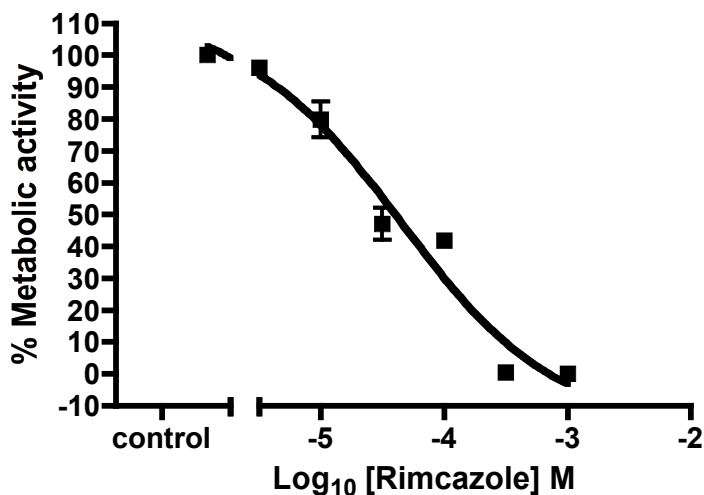
Figure 5.10: Rimcazole MTS assay dose response. % Cellular metabolism of MDA-MB-468 cells in response to rimcazole, with a pIC_{50} of 4.35 ± 0.20. Error bars represent SEM from 3 independent MTS assays.

Rimcazole dose dependently caused a reduction in MDA-MB-468 cell metabolic activity, with and IC_{50} of 45μM (95% CI 15-130μM) which is over 10 times higher than the published affinity for the σ-1R (0.9μM) (Gilmore *et al.*, 2004). The affinity of rimcazole was therefore assessed, and the effect of GTP on rimcazole binding measured in Figure 5.11.
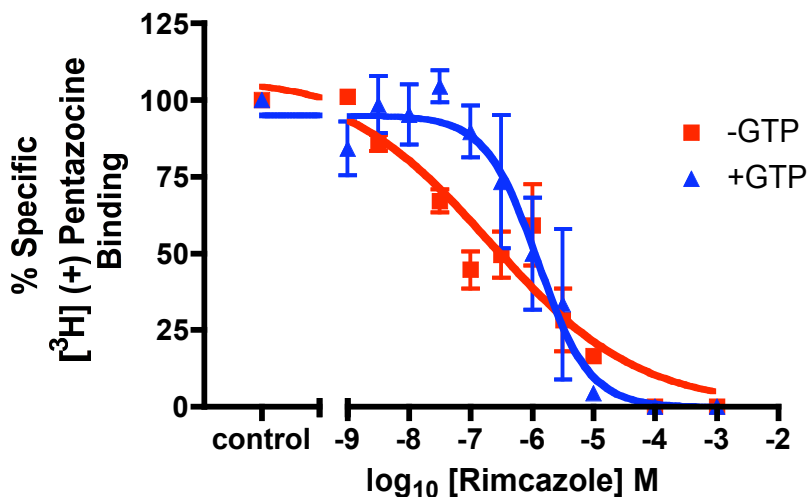
Figure 5.11: Effect of GTP on rimcazole binding. Rimcazole competitive binding assay using permeabilised MDA-MB-468 cells that had been washed with TBS to remove any endogenous GTP. Assays were performed using 30nM [^{3}H] (+) pentazocine in the presence and absence of 1mM GTP. Error bars represent SEM from 5 independent radioligand competition assays.

The binding of rimcazole to MDA-MB-468 cells that have had the GTP washed out shows, in the single site binding model, a low nH value (-0.4 ± 0.1, mean ± SEM n=5) with a pK$_{50}$ 6.9 ± 0.5 (mean ± SEM), with the addition of GTP there is a statistically significant increase in the Hill slope (-1.0 ± 0.4, mean ± SEM) with a P value of 0.025. Furthermore, the preferred model for binding of rimcazole in the absence of GTP is the 2-site binding model, using the extra sum of squares F test gave an F value of 3.54 and a p value of 0.028. The affinities for the σ-1R are pK$_{high}$ 8.3 ± 0.4 (mean ± SEM) pK$_{low}$ 5.23 ± 2.8 (mean ± SEM) with the pK$_{high}$ occupying 47% of the curve.

5.5   GTP metabolism in response to σ-1 receptor ligands

As shown above in Figures 5.8 to 5.11, GTP has a dramatic effect on the binding of IPAG and rimcazole to the σ-1R in permeabilised MDA-MB-468 cells. In order to assess the effect of σ-1R ligands on GTP metabolism to GDP and therefore the activity of G-proteins in response to the σ-1R ligands in the MDA-MB-468 cells, the GTP and GDP concentrations in the MDA-MB-468 cells was measured after a 30 minute treatment with the σ-1R ligands using HPLC. Some example dose response curves are shown below in Figure 5.12.
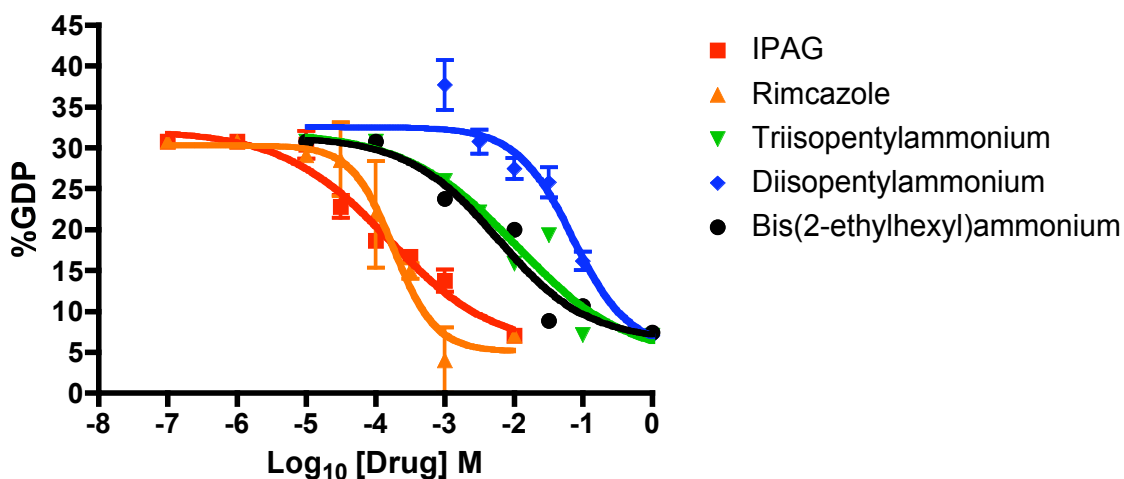
Figure 5.12: GTP metabolism to GDP in response to σ-1R ligands. σ-1R ligand inhibition of GTP metabolism to GDP measured using HPLC (GDP represented as a % of total GTP added at the start), after 30min treatment with the σ-1R ligand. Error bars represent SEM from between 4 and 5 GTP/GDP assays.

The two σ-1R ligands, IPAG and rimcazole, and the branched-chain ammonium salts resulted in a dose dependent reduction of GTP metabolism to GDP, whereas the straight-chain ammonium salts did not have a positive or negative effect on GTP metabolism to GDP. The full list of σ-1R ligands effects on GTP metabolism can be seen in table 5.1

Drug	$pIC_{50} \pm$ SEM	σ-1 Affinity pK_i or pK_{low}	N
IPAG	3.6 ± 0.1	6.3 ± 0.2	4
Rimcazole	3.8 ± 0.2	5.2 ± 2.8	4
Triisopentylammonium	2.1 ± 0.1	3.5 ± 0.5	3
Diisopentylammonium	1.3 ± 0.13	2.5 ± 0.3	3
Bis-(2ethyl hexyl)ammonium	2.6 ± 0.14	2.9 ± 0.3	3
Tripentylammonium	No curve	7.8 ± 0.2	3
Dipentylammonium	No curve	7.4 ± 0.5	3

Table 5.1: Inhibition of metabolism of GTP to GDP. Represented as $pIC_{50} \pm$ SEM; measured using HPLC.

The σ-1R antagonists IPAG and rimcazole and the branched-chain ammonium salts triisopentylammonium, diisopentylammonium, and bis(2-ethylhexyl)ammonium all dose dependently inhibited the metabolism of GTP to GDP, whereas the high σ-1R affinity straight-chain ammonium salts tripentylammonium and dipentylammonium did not increase or decrease GTP metabolism to GDP.

5.6 The effect of cholera toxin on IPAG-induced calcium influx

In order to assess which G-protein may be coupled to the σ-1R the MDA-MB-468 cells were treated with various G-protein inhibitors, one of which being cholera toxin (Figure 5.13). The α subunit of the cholera toxin is responsible for permanently ribosylating the G_s α subunit of the heterotrimeric G-protein, leading to permanent activation and uncoupling from receptors.
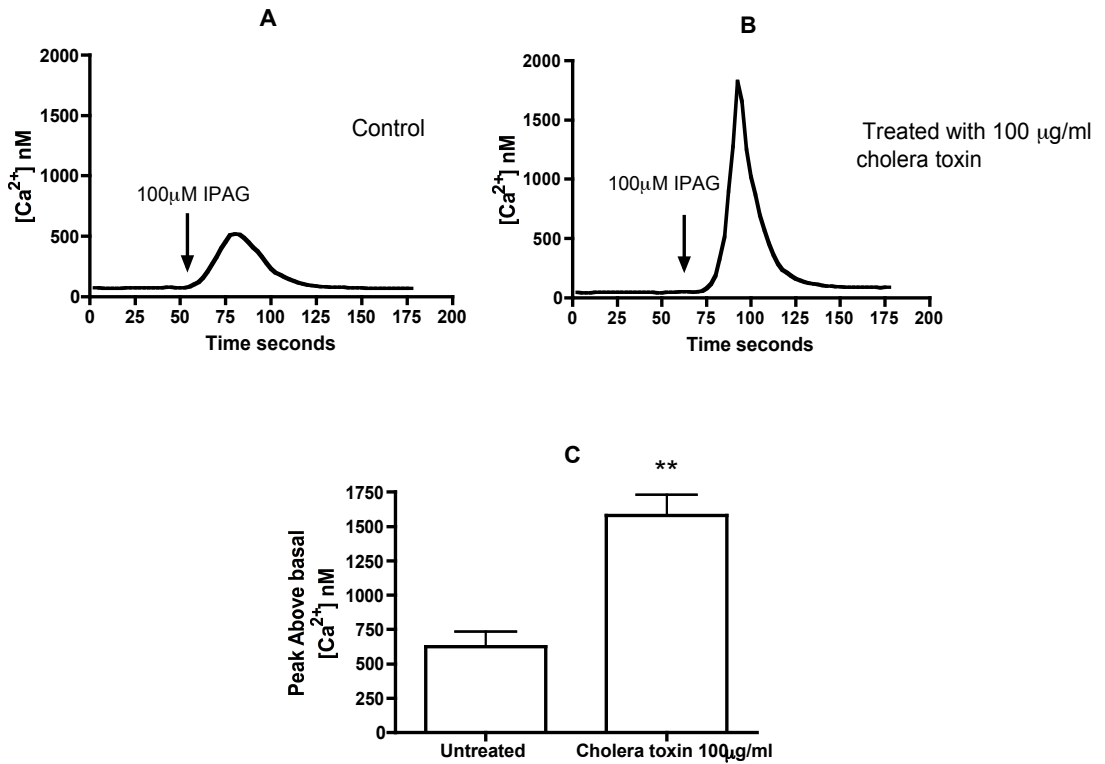
Figure 5.13: Effect of cholera toxin on IPAG-induced increase in cytosolic [Ca^{2+}]. A: Peak intracellular calcium above basal, in Fura-2 loaded MDA-MB-468 cells in response to 100μM IPAG. **B:** Peak intracellular calcium above basal, in Fura-2 loaded MDA-MB-468 cells in response to 100μM IPAG in cells treated overnight with 100μg/ml cholera toxin compared to untreated cells measured ratio of emissions at 510nm when excited at 340/380nm, ratio then converted to [Ca^{2+}]. **C:** Mean ± SEM calcium increase in response to IPAG from 3 independent Fura-2 calcium assays. ** P-value 0.0067.

The mean calcium response of the untreated MDA-MB-468 cells in response to 100μM IPAG was 600 ± 100 nM, whereas in cells treated with 100μg/ml cholera toxin had almost a three times greater response to 100μM IPAG with a mean calcium influx of 1600 ± 200 nM.

135

5.7   The effect of suramin on σ-1 ligand binding

Suramin is a synthetic polysulphonated naphthylamine benzamide-derivative that has been used for many years to treat African sleeping disease and river blindness. It however is also a G-protein inhibitor (Chung and Kermode, 2005); in the micromolar range it suppresses the release of GDP from the α subunit (Freissmuth *et al.*, 1996), which is the rate limiting step in G-protein activation. At low micromolar concentrations suramin inhibits the G_s α subunit (Hohenegger *et al.*, 1998), and at over 30 times higher concentrations will inhibit G_i and G_q (Beindl *et al.*, 1996). Suramin had no effect on pentazocine binding, therefore suramin was added to the radioligand competition assay with IPAG, in order to see if it had any effect on IPAG binding to the σ-1R in the permeabilised MDA-MB-468 cells (Figure 5.14).
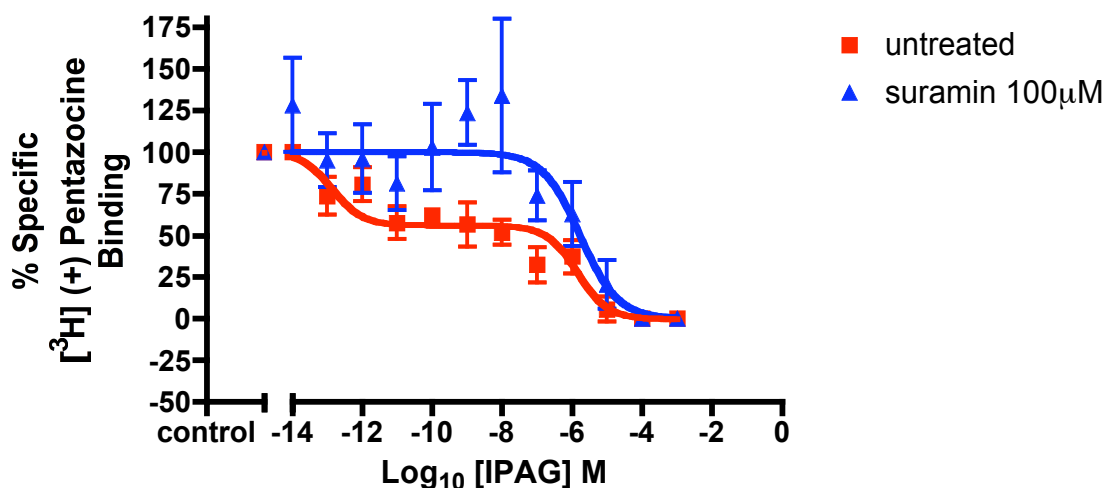
Figure 5.14: IPAG binding to the σ-1R ± suramin. IPAG competitive binding assay using permeabilised MDA-MB-468 cells that had been washed with TBS to remove any endogenous GTP. Assays were performed using 30nM [^{3}H] (+) pentazocine in the presence and absence of 100μM suramin. Error bars represent SEM from 5 independent radioligand competition assays.

The addition of 100μM suramin to the radioligand competition assay with IPAG resulted in a dramatic change in the nH (of the one site fit) shown in Figure 5.15 below.
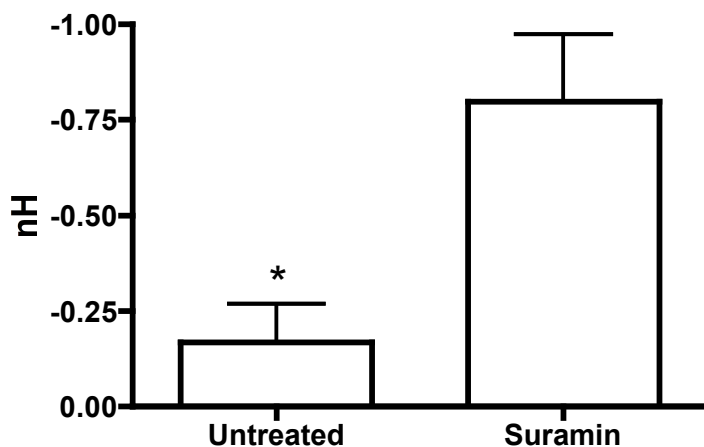
Figure 5.15: Hill coefficient (nH) for IPAG competition ± suramin. nH for IPAG competition with [^{3}H] (+) pentazocine binding in MDA-MB-468 cells. The mean nH value for untreated was -0.2 ± 0.1 and in the presence of 100μM Suramin -0.8 ± 0.2. * t-test *P* value 0.0342.

5.8 σ-1 receptor ligand efficacy

The activity of a drug at a receptor is not an all or nothing event where the drugs activity is simply a measure of its affinity for the receptors and the response is linearly proportional to the number of receptors occupied. Rather a drug may occupy just a small fraction of the available receptors and produce the maximal response whereas another drug may need to occupy a larger proportion of available receptors in order to produce the same response (Stephenson, 1956). The ability of a drug to cause a response is referred to as the drugs efficacy, and is different from a drugs affinity, which is a measure of the ability of a drug to bind to its target, and EC_{50}, which is a measure of potency (and is proportional to both affinity and efficacy). The 2-state receptor model (Figure 5.16) can be used to explain drug efficacy (although a very simple model).
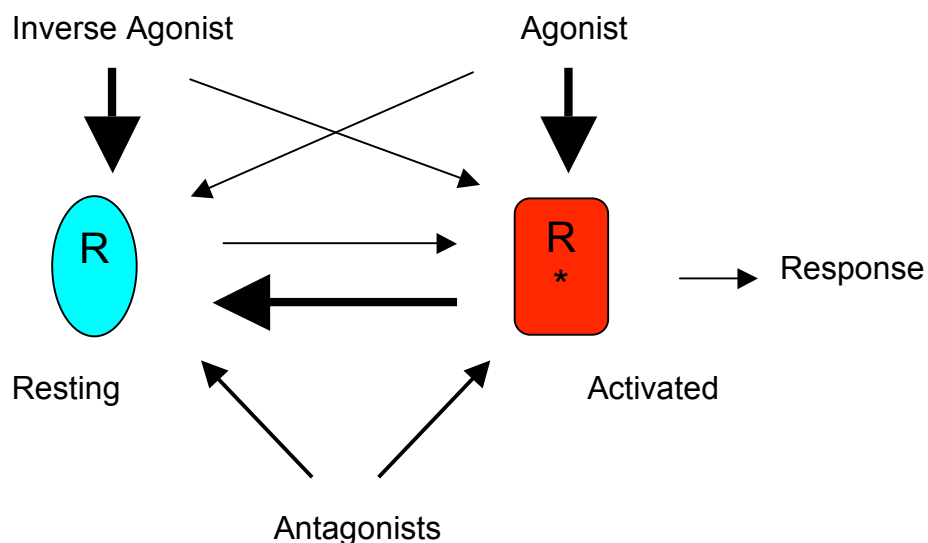
Figure 5.16: The 2-state model. The receptor has 2 conformational states R (resting) and R* (active), and exist in equilibrium. In the absence of ligand the equilibrium usually resides to the left (resting state). The addition of an agonist which has higher affinity for R* causes the shift of the equilibrium to the right, whereas the addition of an inverse agonist, which has higher affinity for R results in a shift of the equilibrium to the left. An antagonist has no preference for R or R* and does not affect the conformational equilibrium rather reduces the available sites for other ligands by competition.

The activated receptor R* and resting receptor R exist in an equilibrium which can be shifted on the addition of a drug, if this drug prefers R* over R (i.e. has higher affinity for R* than R) more of the receptor to which the drug is bound will adopt the R* formation and cause a response (these drugs are known as agonists) if there is a very large difference in the drugs affinity for R over R* nearly all the receptors will adopt the R* formation (a full agonist) if the difference in affinity is not so large less of the occupied receptors will adopt the R* formation (a partial agonist) therefore a greater proportion of receptors will need to be occupied in order to achieve the same amount of R*.

Should the drug prefer the R formation to R* then the equilibrium will be shifted to the inactive state (these types of drugs are known as inverse agonists). Antagonists are drugs that have no preference for R or R* and do not shift the equilibrium in either direction and do not invoke a response. It is thought there are relatively few full agonists, more likely they are partial agonists with very high efficacy, and the same for antagonists, which are more likely to be agonists or inverse agonists with very low efficacy.

Therefore the ratio of affinity of a drug for R to R* can be used to describe a drugs efficacy. The σ-1R ligands that showed a preference for the 2 site binding model in the radioligand binding assays are shown below in table 5.2, along with their affinities for the high affinity site (usually associated with the activated receptor state), low affinity site (usually associated with the resting receptor state) and the ratio of the low affinity to the high affinity giving an estimate measure of efficacy for the σ-1R ligand.

σ-1R ligand	K_{low} μM	K_{high} μM	K_{low}/K_{high}
IPAG	0.16	0.00000017	941176.5
Rimcazole	2.33	0.0021	1109.5
Triisopentylammonium	3800	5.7	666.6
Bis(2-ethylhexyl)ammonium	621.7	1.3	489.5

Table 5.2: σ-1R ligand affinities for the 2 site fit to σ-1Rs.

IPAG has the highest difference between the low affinity state and the high affinity state and there for should be the most efficacious, followed by rimcazole, bis(2-ethylhexyl)ammonium and triisopentylammonium.

5.9   σ-1 receptors and ion channels

The σ-1R has been previously shown to interact with a number of ion channels including N-, L, P/Q- and R-type calcium channels (Zhang and Cuevas, 2002), and voltage-gated potassium channels (Aydar *et al*., 2002, Soriani *et al.*, 1999, Soriani *et al.*, 1998). Aydar *et al.* (2002) showed using co-expression of the σ-1R and Kv ion channels in *Xenopus* oocytes, that the σ-1R could inhibit voltage-gated potassium channels in the presence or absence of σ-1R drugs, which suggests that the σ-1R is involved in a multi protein complex. Soriani *et al.* (1998) showed that σ-1R agonists could down-regulate potassium currents, and that this down-regulation is sensitive to cholera toxin, suggesting that this involves G_s dependent mechanism.

In order to ascertain whether the σ-1R antagonist IPAG causes its effects through modulation of voltage-gated potassium channels (in the MDA-MB-468 cell line) the cells were pre-treated with 1mM 4-aminopyridine (4-AP) which blocks voltage-gated potassium channels (Yuan *et al.*, 1995) before a 10μM dose of IPAG (Figure 5.16). The L-type

calcium channel blocker diltiazem (Tokuyama and Ho, 1996) was also used to assess the involvement of L-type calcium channels in IPAG-induced cytoplasmic calcium increase (Figure 5.17).
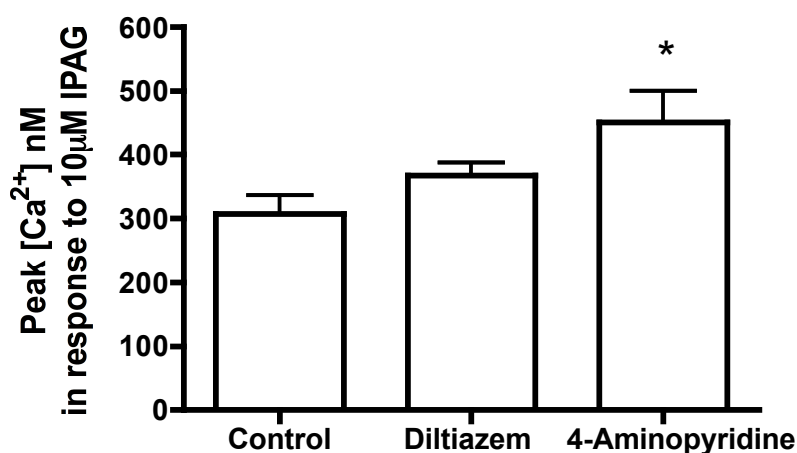
Figure 5.17: Peak cytosolic [Ca^{2+}] in response to 10µM IPAG. Fura-2 loaded MDA-MB-468 cells were pre-treated with TBS for the control, 10µM diltiazem or 1mM 4-AP, and the peak response above basal to IPAG measured taking the ratio of emission at 510nm when excited at 340/380nm, ratio then converted to [Ca^{2+}]. n=3. * *P* value 0.045

Diltiazem had no statistically significant effect on the increase cytoplasmic [Ca^{2+}] in response to 10µM IPAG (t-test *P* value 0.28). However 4-AP did cause a small but statistically significant increase in cytosolic calcium (t-test *P* value 0.045).

5.10 σ-1 receptor mutagenesis

Using site directed mutagenesis a series of σ-1R mutants, at sites within the extra-cellular loop or in the potential cholesterol binding site, were created and cloned into an expression vector containing a GFP tag, which allowed the expression of the σ-1R and mutants in HEK 293 cells to be visualised under a fluorescence microscope (Figure 5.18).
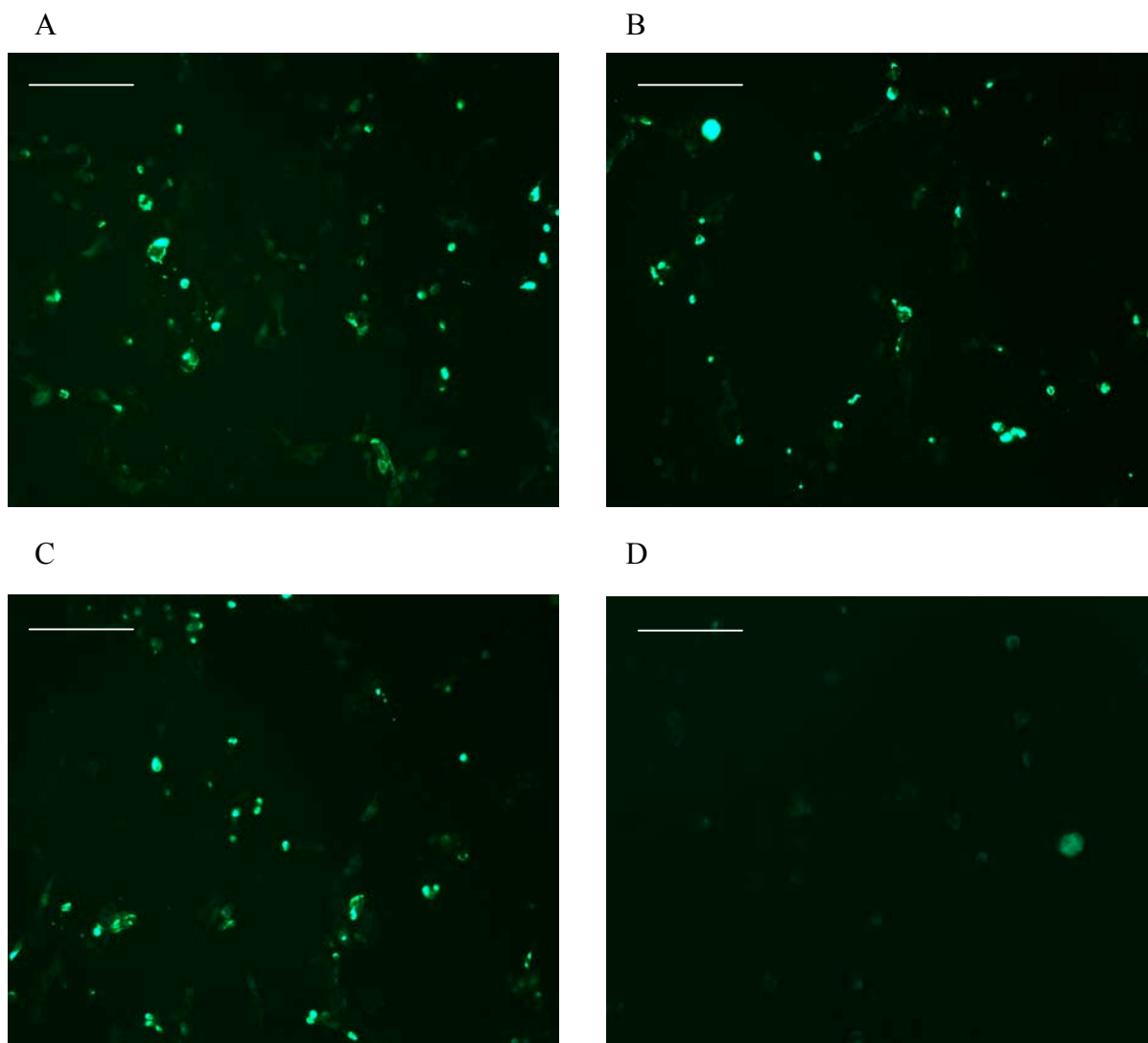
Figure 5.18: HEK 293 cells expressing σ-1R mutants viewed using a florescence microscope A: σ-1 GFP expressing HEK 293 cells, **B:** σ-1 E172G GFP expressing HEK 293 cells, **C:** σ-1 DHE53/55GHG GFP expressing HEK 293 cells, **D:** σ-1 EE41-42GG GFP expressing HEK 293 cells. Scale bar 50μm.

The affinity of the σ-1R mutants for (+) pentazocine was assessed using saturation binding assays, the saturation binding curves for σ-1 GFP and the untransfected cells can be seen in Figures 5.19 and 5.20 respectively. The other mutants' affinities are shown in table 5.3.
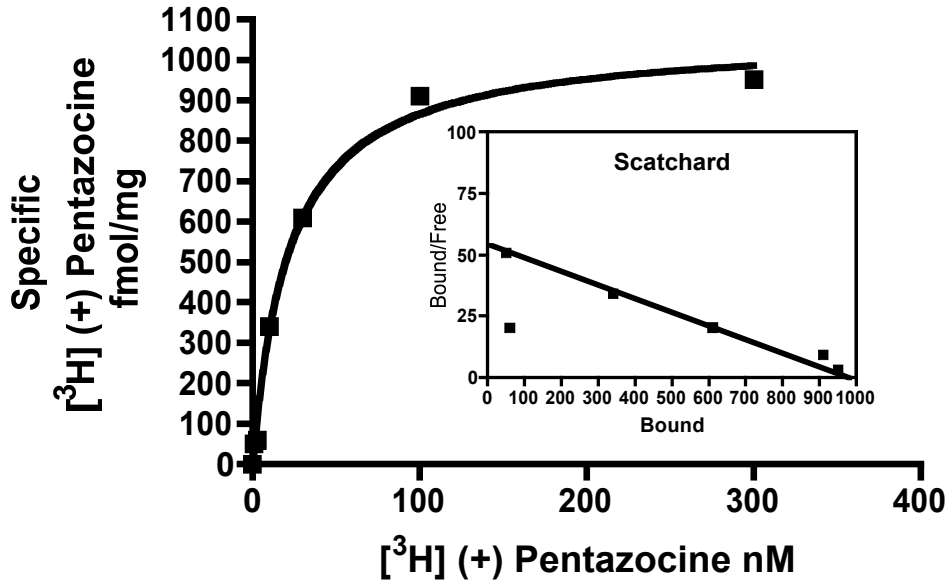
Figure 5.19: [³H] (+) pentazocine saturation binding in σ-1R transfected HEK-293 cells. Representative Figure of 6 independent [³H] (+) pentazocine saturation assays, Scatchard shown for visualization purposes as K_d and B_{max} were calculated using non-linear regression.

The B_{max} for pentazocine binding to the σ-1 GFP expressed in the HEK 293 cells is 1057 ± 47 fmol/mg that is approximately half of the expression seen in MDA-MB-468 cells (2300 ± 200 fmol/mg).
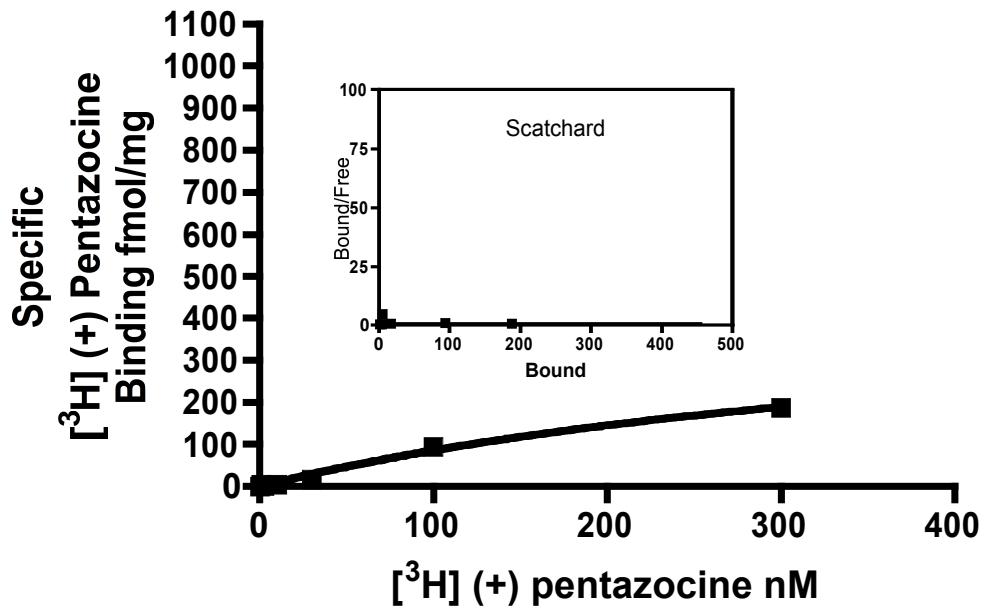
Figure 5.20: [³H] (+) pentazocine saturation binding in untransfected HEK-293 cells. Representative figure of 3; Scatchard shown for visualization purposes as K_d and B_{max} were calculated using non-linear regression.

σ-1R Mutant	pK$_d$ ± SEM	B$_{max}$ fmol/mg	Number of assays
σ-1 GFP	7.8 ± 0.1	1057±47	6
σ-1 E172G GFP	6.8 ± 0.1	1651±120	3
σ-1 DHE 53/55 GHG GFP	7.38 ± 0.05	1129±173	3
σ-1 EE 41-42 GG GFP	6.4 ± 0.1	745±165	2
Control (untransfected HEK293 cells)	6.2 ± 0.2	352±200	3

Table 5.3: Affinity (pK$_d$ ± SEM) of pentazocine for σ-1R mutants

Mutants D126G, E102G and E64G appeared not to express, as after several attempts at transfecting the HEK-293 cells with different clones of the mutant there was no visible GFP signal when viewed under the fluorescence microscope.

Mutants E172G and EE41-42GG showed a statistically significant reduction in affinity for [^{3}H] (+) pentazocine, compared to the σ-1 GFP (ANOVA P Value <0.001 and < 0.001 respectively) whilst expression remained at a similar level. The mutation in σ-1 E172G GFP is located in the putative cholesterol binding site described by Palmer *et al*., 2007 and the mutation in EE41-42GG GFP is located in the putative extracellular loop proposed by Aydar *et al.* 2006.

σ-1R knock-down results in restriction of growth and cell death in human lens cells (Wang and Duncan, 2006), therefore the σ-1 GFP construct and its mutants were expressed in HEK 293 cells which show little to no σ-1 expression to see if would increase cell growth (Figure 5.21).
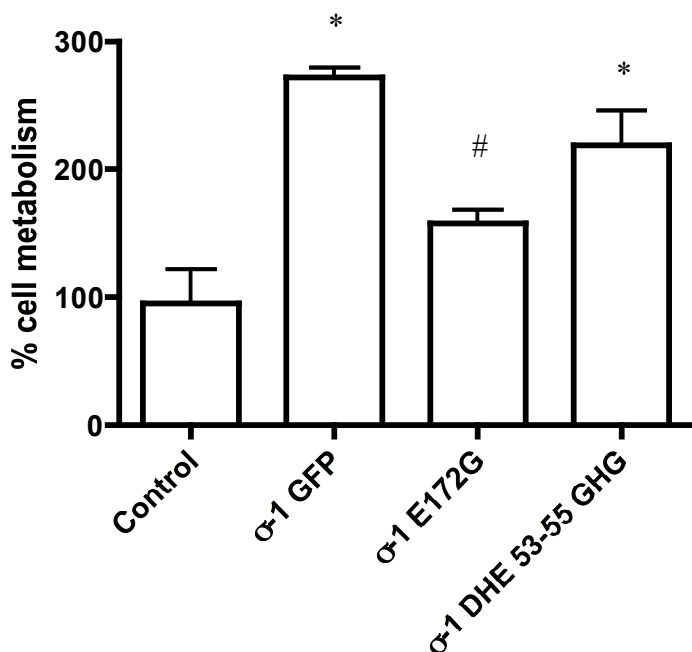
Figure 5.21: Increase in cell metabolism of HEK 293 cells transfected with σ-1 GFP and its mutants. Measured with the MTS assay, the control consisted of HEK 293 cells treated with transfection agent without DNA. Error bars represent SEM from 2 independent MTS assays. *ANOVA Tukey's post test vs control $P<0.01$, # ANOVA Tukey's post test vs σ-1 GFP $P< 0.05$.

Expressing the σ-1 GFP receptor more than doubled the growth of the HEK 293 cells compared to the control (*ANOVA Tukey's post test $P<0.01$) as did the σ-1 DHE 53-55 GHG GFP mutant (with the mutation in the extracellular loop) (*ANOVA Tukey's post test p<0.01), whereas the σ-1 E172G GFP, with the mutation in the putative cholesterol binding site (Palmer *et al.*, 2007) receptor did not showed a significant increase in cell growth (#ANOVA Tukey's post test p<0.05).

5.11 σ-1 receptor antagonists and G-proteins discussion

σ-1R ligands such as IPAG and rimcazole are thought of as antagonists, yet they are responsible for the cytoplasmic calcium increase in the cell that leads to PLC activation and PKB inhibition, whereas σ-1R ligands such a (+) SKF-10,047 and (+) pentazocine are thought of as agonists (due to the original effects seen in animals), yet they block the effects of the antagonists (Spruce *et al.*, 2004). All the studies that have looked at σ-1R coupling through G-proteins have focused of the σ-1R agonists, whereas the antagonists have been ignored. Considering the effects the σ-1R antagonists have on the cell, if there is G-protein coupling with σ-1R, the antagonists are possible the more likely tools to highlight it. In this chapter I focused on the σ-1R antagonists IPAG and rimcazole.

There is a large discrepancy between the IC_{50}/EC_{50} ($30\mu M/124\mu M$) values observed for the response to IPAG in the MTS and calcium assay compared to its published affinity (2.8nM) (Wilson *et al.*, 1991). This 10,000 times difference between the published affinity and the effective dose prompted a suspicion that either the published affinity was wrong or IPAG was having its effects through another receptor. Knocking down the σ-1R with the σ-1R specific siRNA resulted in a reduction in the maximal response to IPAG in the calcium assay. This taken with data from Spruce *et al.* (2004) which shows σ-1R agonists blocking the effects of IPAG (although a 30 minute pre-incubation is required), indicates that IPAG does indeed act through the σ-1 R. The attention turned therefore to the affinity of IPAG for the σ-1R. Wilson *et el.,* (1991) identified IPAG as a high affinity σ-1R ligand, although they do not present the competitive binding isotherm in the paper. The affinity of IPAG for the σ-1R was therefore reassessed using [³H] (+) pentazocine and permeabilised MDA-MB-468 cells. The competitive binding data revealed that when fitted with a single site model the affinity was 15nM, not far from the affinity given in Wilson *et al.* (1991), however the nH value for the single site model was very low (-0.21). Another study in which a similar compound to IPAG, 1-(4-iodophenyl)-3-(1-adamantyl)guanidine (PIPAG) was shown to have an nH value of 1 (Kimes *et al.*, 1992), however, the highest dose they use is 10nM, so it is likely that they have not gone high enough to see the low affinity binding site.

If the unlabelled drug (in this case IPAG) is competing for a single class of receptor the curve should descend from 90% specific binding to 10% specific binding over an 81 fold increase in concentration, resulting in an nH of -1. There are a number of explanations for

the low nH value, including negative cooperativity where the binding at one site lowers the affinity of other sites for the ligand, heterogeneous receptor population, where the receptors do not all bind the ligand with the same affinity and G-protein coupling where the interaction with a G-protein changes the affinity of the ligand for the receptor.

The heterogeneous population of σ receptors is not a satisfactory explanation, since for this to result in a shallow binding curve the radiolabelled drug has to have the same affinity at both sites, (+) pentazocine is reportedly highly selective for the σ-1R, 500 times more selective for the σ-1R over the σ-2R, 1000 times more selective for the σ-1R than the PCP site (Whittemore *et al.*, 1997), and 150 times more selective for the σ-1R over the mAChR (Hong and Werling, 2002). The negative cooperativity explanation is also unlikely as the σ-1R is only a small protein with a single binding site for (+) pentazocine potentially with in the a membrane spanning section of the receptor (Yamamoto *et al.*, 1999).

The binding data for IPAG and rimcazole in this chapter, and the binding data for bis(2-ethylhexyl)ammonium in the previous chapter, all have low nH values with the single site model and when compared to the two site model, using the difference in sum of squares F test, they all have high F values and significant *P* values, therefore the preferred binding model for these σ-1R 'antagonists' is the 2 site model. Figure 5.22 shows a simple model of how G-protein coupling results in two affinity states for a receptor.
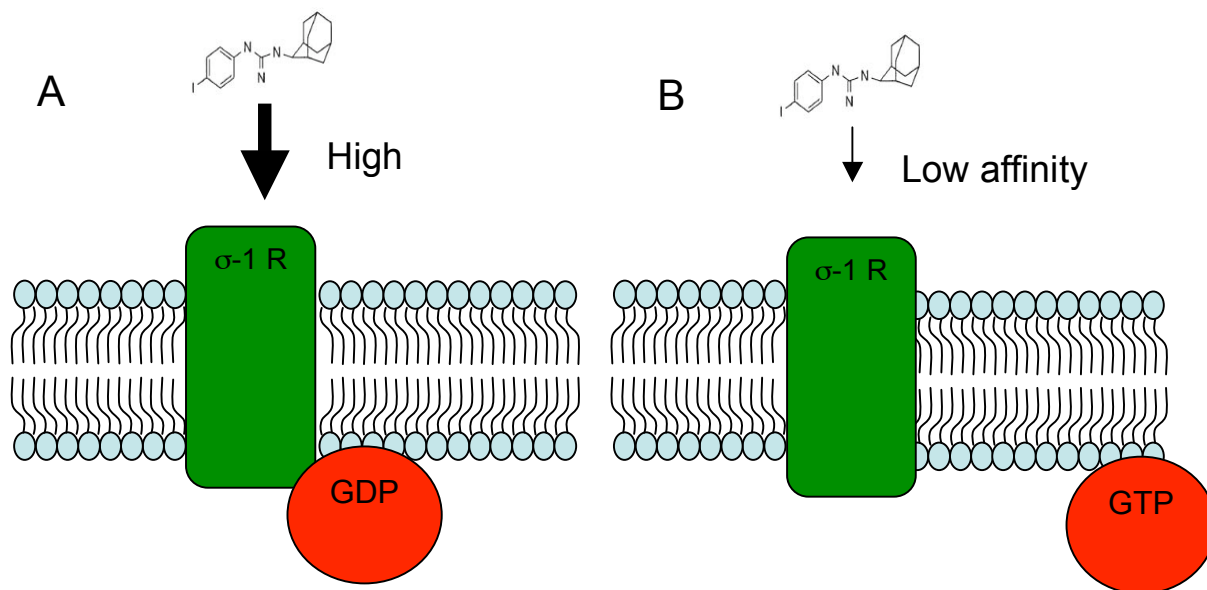
Figure 5.22: G-protein coupling affecting the affinity of the σ-1R for IPAG. A: The G-protein is bound to GDP and is inactive, coupled to the receptor causing the receptor to have high affinity for IPAG. **B:** The G-protein is bound to GTP and is activated and dissociated from the receptor causing the receptor to have low affinity for IPAG.

Addition of GTP (promoting G-protein activation) to the binding assay resulted in the nH value approaching -1 and the affinity of IPAG and rimcazole for the σ-1R shifting to the low affinity state (which coincides with EC_{50} and IC_{50} doses for the calcium and MTS assay), suggesting G-protein coupling. Furthermore, when suramin (which inhibits G_s (Hohenegger *et al.*, 1998), G_i and G_q (Beindl *et al.*, 1996)) is added to the IPAG binding assay, the binding curve is again shifted to the low affinity state with a nH value of -1, providing yet more evidence that the σ-1R is coupled in some way to a G-protein.

Further evidence that the σ-1R is coupled to a G-protein comes from the HPLC measurement of GTP metabolism to GDP in response to the σ-1R antagonists. The σ-1R antagonists rimcazole and IPAG, along with the ammonium salts triisopentylammonium diisopentylammonium and bis(2-ethylhexyl)ammonium, all dose-dependently reduced the formation of GDP suggesting that the σ-1R antagonists are preventing G-protein activation, or coupling with the receptor. This may go somewhat to explain the fact that the σ-1R antagonists are unusual in that they are causing their effects through the low affinity state of the σ-1R (G-protein uncoupled), although it should be noted that the model fitted to the binding data and described in Figure 5.19 above is a very simple view of G-protein coupling since it allows for the two affinity states (R and RG) but does not allow for the conversion between R and RG, and therefore the K_i values obtained should be treated with

care, Figure 5.23 shows more complex models that can be applied to G-protein receptor coupling.

L+R + G   ⇄   LR+G

Simple model

L+RG   ⇄   LRG

L+R + G   ⇄   LR+G
↓↑   ↓↑
Ternary Complex model
L+RG   ⇄   LRG

L+R+G   ⇄   LR+G
↓↑   ↓↑
L+R*+G   ⇄   LR*+G   **Extended Ternary complex model**
↓↑   ↓↑
L+R*G   ⇄   LR*G
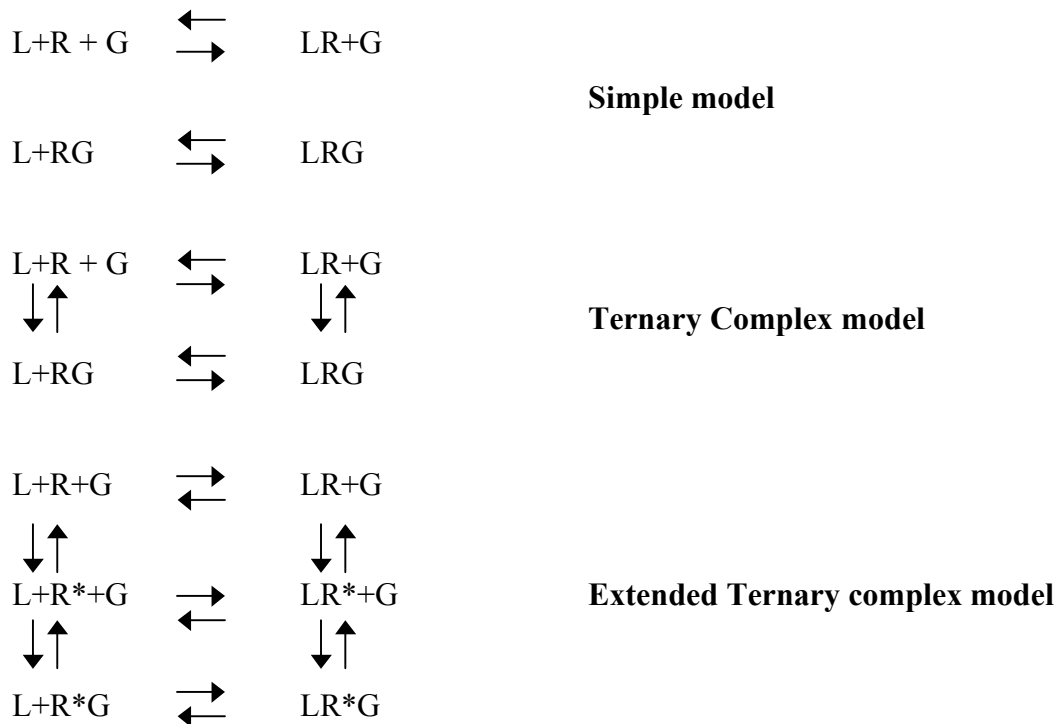
Figure 5.23 Ligand, Receptor and G-protein interactions
L- Ligand, R- Receptor, G- G-protein

These observations showing that the σ-1R is interacting with a G-protein, and that the σ-1R antagonists are reducing G-protein activity and causing their effects at doses that coincide with the low affinity state could possibly help explain the function of the σ-1R within the cell.

The σ-1R is not directly causing its effects via G-protein activation; rather the G-proteins are changing the σ-1Rs interactions with ion channels. With the G-protein uncoupled σ-1Rs are able to cause the influx of calcium in to the cytoplasm (or unable to prevent the influx of calcium into the cytoplasm). This is shown in the cholera toxin treated MDA-MB-468 cells, where there was a 3 times higher calcium response in the cells that had been G-protein uncoupled with cholera toxin compared to the control cells. Below are possible explanations for how this could be happening.
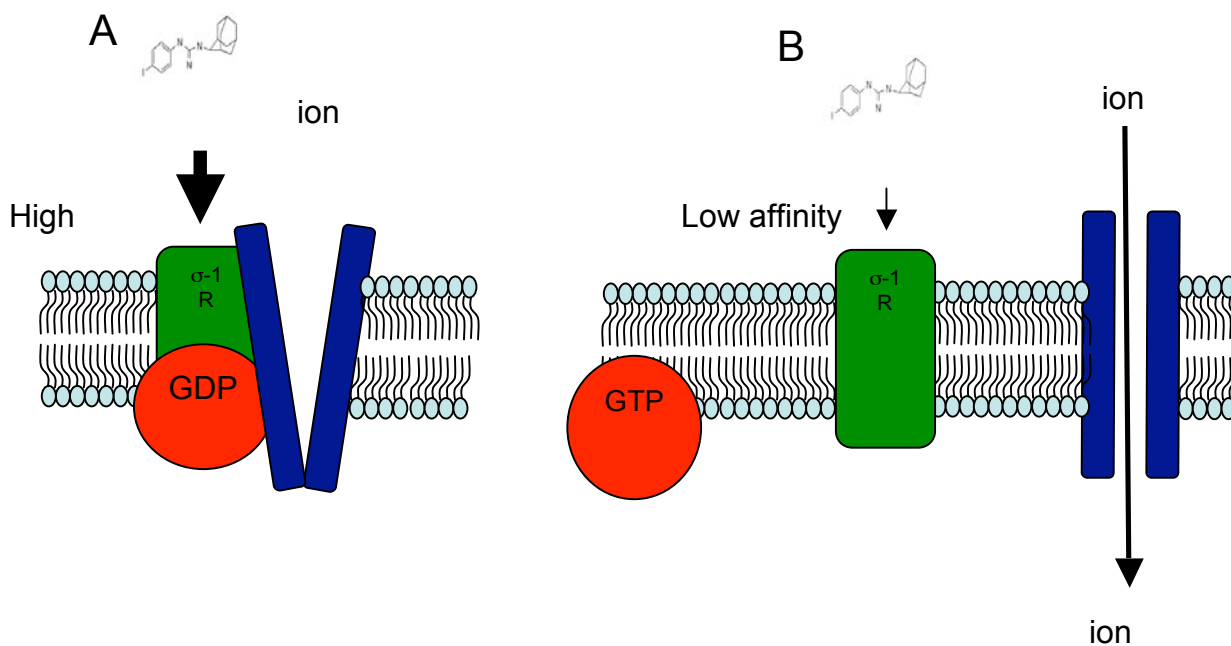
Figure 5.24: Possible multi-protein interaction A: Inactive G-protein coupled to the σ-1R and the ion channel preventing influx of ions into the cytoplasm. **B:** σ-1R, G-protein and ion channel complex dissociates allowing ions into the cytoplasm.

The σ-1R has been shown to interact with a wide range of ion channels (Aydar *et al.*, 2004, Soriani *et al.*, 1999, Soriani *et al.*, 1998, Tchedre *et al.*, 2008, Zhang and Cuevas, 2002), and it is possible that it may interact with whichever ion channel is available depending on the cell type (Campbell *et al.*, 1989). Soriani *et al.* (1999) showed that the σ-1R could inhibit potassium currents and that this interaction was cholera toxin sensitive, this is similar to the data I have presented in Figure 5.13, showing an larger increase in cytoplasmic calcium in the cholera toxin cells in response to IPAG. Both Lupardus *et al.* (2000) and Aydar *et al.* (2002) show the σ-1R inhibiting potassium currents, although they suggest no interaction with a G-protein. However both studies only look at agonist interactions with the σ-1R and both studies use ectopically overexpressed ion channels and receptors in oocytes, whereas the work by Soriani *et al* (1998), and the data I have presented in Figure 5.13 makes use of endogenous ion channels and receptors. Figure 5.24 shows how the σ-1R and G-proteins may interact with various ion channels.

Another possible explanation for the greater calcium response to IPAG seen in the cholera toxin treated MDA-MB-468 cells, could be that K_v channel activation is able to block (at least in part) calcium signalling (Chakraborti *et al.*, 2009). The K_v channel can be activated by G_s (Michaelevski *et al.*, 2002), such that activation of the σ-1R causes calcium channel

opening and the activation of G_s which causes K_v channel opening and inhibition of the calcium channel (Figure 5.25). Therefore when the G_s is uncoupled using cholera toxin there is no K_v channel opening resulting in no inhibition of the calcium channel resulting in a larger calcium response, as seen in Figure 5.13.
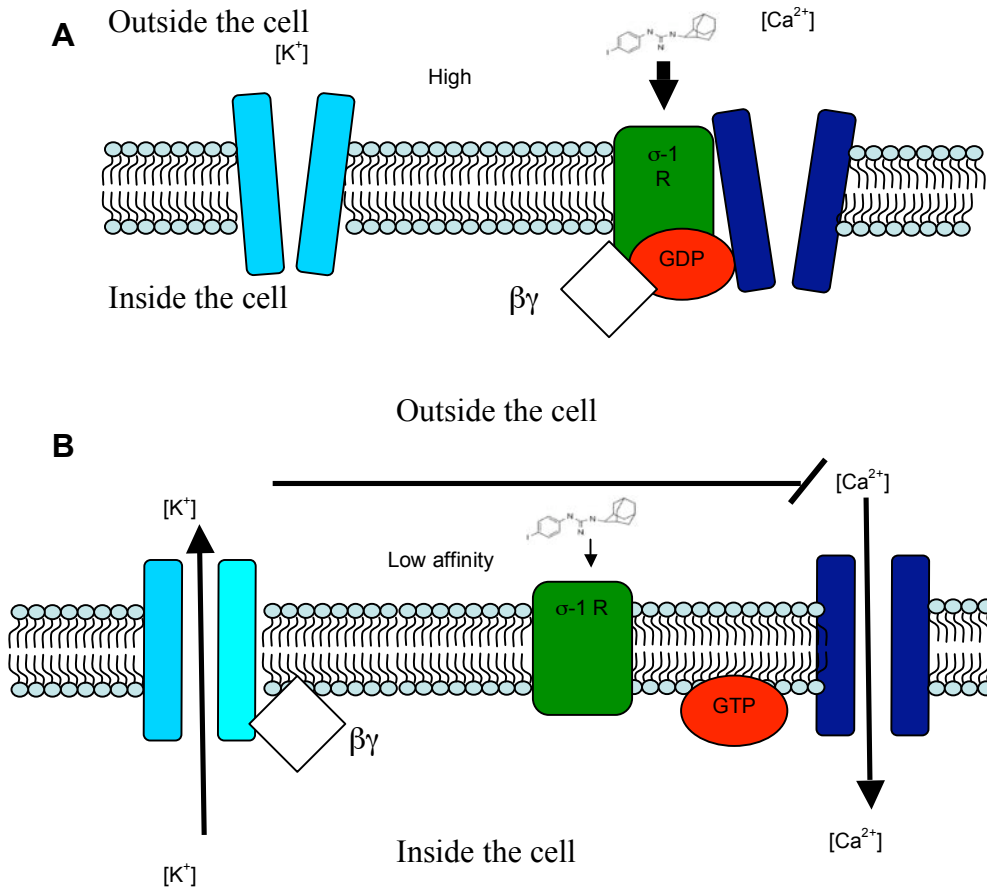
Figure 5.25: Possible G-protein activation of K_v channels resulting in decreased calcium influx. A: σ-1R G-protein and calcium channel form a complex preventing calcium entry, the G-protein inactive, and the K_v channel is closed. **B:** σ-1R activation causes the dissociation of the receptor from the calcium channel causing calcium influx and from the G-protein which activates the K_v channel allowing potassium into the extra-cellular space causing the inhibition of the calcium channel.

This model is supported at least in part by the data in Figures 5.13 and 5.16 however there are some problems. Firstly there is no evidence of cAMP production in response to σ-1R antagonists (table 3.2), which you would expect if you were activating G_s. Furthermore, the σ-1R antagonists result in a dose dependent reduction of GTP metabolism to GDP, which is the reverse of what you would expect if there were G-protein activation. There is also the problem that the increase in cytosolic calcium is smaller with the K_v channel blocker than when the G-protein is uncoupled using cholera toxin, although it may be possible that the G-protein has a larger role in reducing the calcium influx then just

activating the K_v channel, possibly by helping form the complex between the σ-1R and the calcium channel which prevents calcium influx.

The main problem with the explanations above for the effects of G_s on σ-1R-induced cytoplasmic calcium increases (which is itself the explanation put forward to explain the effects of GTP on antagonist binding to the σ-1R) is that there is a dose dependent reduction in GTPase activity in response to σ-1R antagonists, and that there is no evidence of cAMP production in response to σ-1R antagonists. These observations could be explained by the G-protein not being activated by the σ-1R but rather acting as part of the complex causing the inhibition of ion channels and dissociation of the G-protein from the σ-1R and ion channel is not caused by the G-protein being activated but rather some other factor. This other factor could be lipid raft formation, causing the separation of the σ-1R, G-protein and ion channel complex (Figure 5.26).
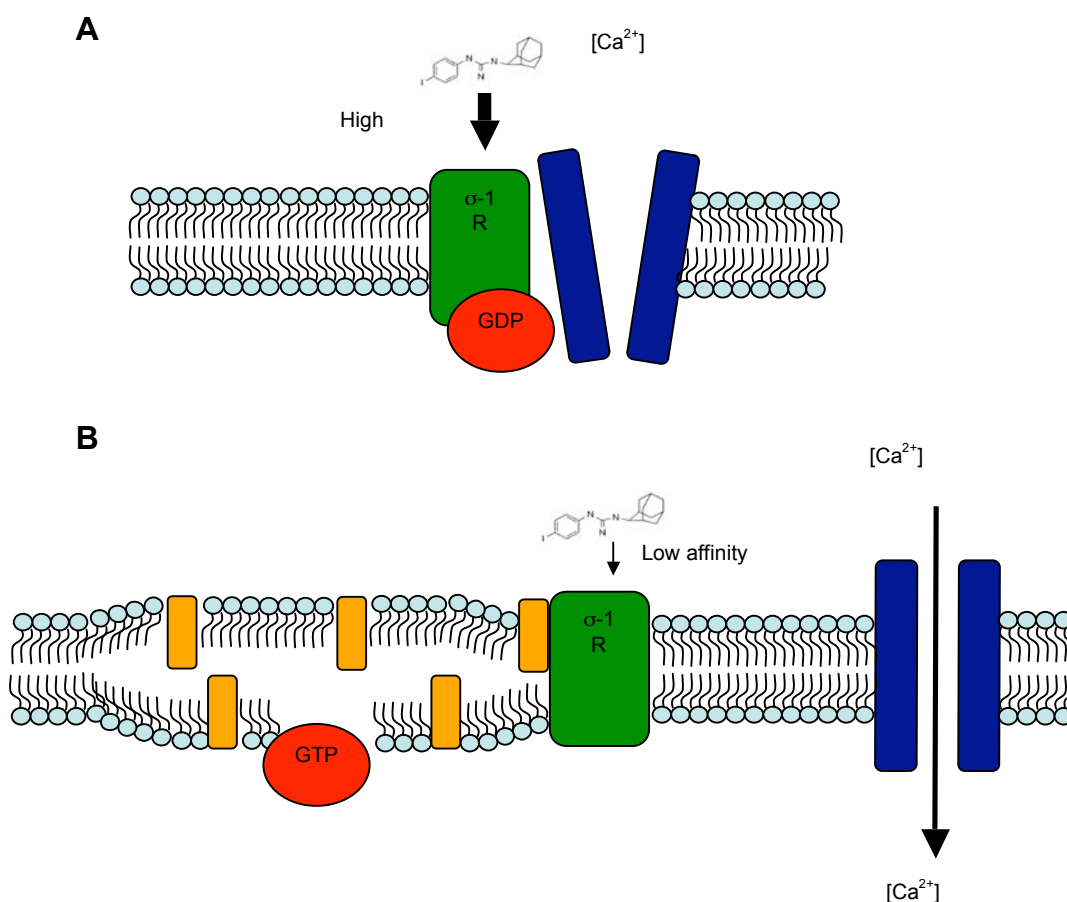
Figure 5.26: Lipid rafts and σ-1Rs. A: The σ-1R forms a complex with the G-protein and ion channel preventing channel opening. **B:** σ-1R interaction with σ-1R antagonists leads to lipid raft formation and the G-protein is partitioned away from the ion channel causing the σ-1R to dissociate from the ion channel allowing channel opening.

There are many examples of the σ-1R interacting with lipid rafts (Hayashi and Su, 2003b, Hayashi and Su, 2003a, Hayashi and Su, 2004, Hayashi and Su, 2005b, Palmer *et al.*, 2007, Takebayashi *et al.*, 2004), and in Chapter 4 I have shown that the σ-1R antagonists cause lipid raft formation (Figures 4.20 to 4.22). There are several lines of evidence that lipid rafts are able interact with G-proteins and modulate their activity (Miura *et al.*, 2001, Morris *et al.*, 2008, Pontier *et al.*, 2008, Quinton *et al.*, 2005, Stuven *et al.*, 2003). Work by Mirura *et al.* (2001) and by Pontier *et al.* (2008) showed, by measuring cAMP production, that G_s signalling is increased after disruption of lipid rafts by depleting cholesterol, suggesting that lipid rafts are capable of partitioning G_s preventing it from interacting with other proteins. The cholera toxin calcium data in Figure 5.13, the σ-1R antagonist induce lipid rafts in Figures 4.21 and 4.22, and the GTPase activity shown in Figure 5.12 all support this hypothesis that lipid rafts being created in response to σ-1R antagonists, and that this results in the G-protein being partitioned away from the ion channel (and preventing the G-protein being activated reducing GTPase activity) which allows the ion channel to open. The cAMP data however do not appear to support this hypothesis, as σ-1R antagonists did not cause a statistically significant reduction in cAMP production in response to isoprenaline (adrenergic β1 and β2 agonist) and dopamine which couple through G_s, although the decrease may only be a small one depending on the abundance of G_s in the MDA-MB-468 cells, and in order to see the effect a pre-incubation with σ-1R antagonist may be required for lipid rafts to form before the addition of isoprenaline or dopamine.

In this chapter I set out to determine whether the σ-1R couples though a G-protein, using σ-1R antagonists rather than agonists as previously used in most other studies of this aspect of the σ-1R. The binding studies using the σ-1R antagonists IPAG and rimcazole revealed low nH values (characteristic of multiple binding sites) and 2 site binding model was statistically preferred over the single site model. Addition of GTP to the assay completely abolished the high affinity site and returned the nH value to 1, which strongly indicates that there is some form of G-protein interaction with the σ-1R. However, this interaction is far from conventional since when GTP metabolism to GDP is measured in response to well known σ-1R antagonists and the branched-chain ammonium salts from chapter 4, the GTP metabolism goes down dose dependently. It is tempting at this point to try to redefine the σ-1R antagonists IPAG, rimcazole and bis(2-ethylhexyl)ammonium as inverse agonists, as they dose dependently reduce G-protein activity and dose dependently cause apoptosis. However, the GTP shift is in the wrong direction as an inverse agonist

(according to the 2 site model Figure 5.16) should have a higher affinity for the free (not interacting with G-protein) receptor. If the σ-1R was being activated by the antagonists, which in turn activated a G-protein, the GTP metabolism to GDP should have gone up. Further evidence suggests an interaction the σ-1R with G-proteins, since suramin, which uncouples G_s alone or with G_i depending on the concentrations used also abolished the high affinity binding site. Furthermore, cholera toxin treatment of MDA-MB-468 cells resulted in an enhanced calcium response to IPAG. Despite the interaction being unconventional it seems clear that there is an interaction between the σ-1R and a G-protein or G-proteins. I have suggested a number of possible mechanisms for the σ-1Rs interaction with a G-protein, using the evidence gathered within this chapter, however, further investigation of the σ-1R is required to either build on or improve the explanations I have put forward.

In this chapter I also investigated the molecular biology of the σ-1R and looked into the effects of σ-1R mutants on ligand binding and on cell growth of cells containing the mutant receptors. The σ-1R mutant (σ-1 E172G GFP) with the mutation in the putative cholesterol binding site (Palmer *et al.*, 2007) had a significantly reduced affinity for the σ-1R, furthermore when transfected into (σ-1R negative) HEK 293 cells it was unable to increase cell growth (measured with the MTS assay) compared to the control HEK cells, whereas the wild type σ-1R transfected into the HEK 293 cells resulted in approximately 3 times more cell growth (measured using the MTS assay). As previously discussed the σ-1R is potentially important in the transport of cholesterol from the endoplasmic reticulum to the plasma membrane, and this evidence suggests that preventing the σ-1R from interacting with cholesterol reduces its ability to protect the cell from apoptosis, and possibly drive cell growth and division.

Chapter 6

6 General discussion and conclusions

6.1 Summary: What is the σ-1R really doing, and how is it doing it?

The σ-1R's ability to bind to a wide range of compounds, and interact with an equally wide range of intracellular effectors such as G-proteins, ion channels and other receptors as well as appearing to modulate the plasma membrane, has led to confusion about what the σ-1R does, and how it does it. A major example of this is the σ-1R ligand nomenclature, with the σ-1R antagonists causing an increase in cytoplasmic calcium, and the σ-1R agonists blocking these effects. This is the reverse of a normal receptor agonist: antagonist relationship; it came about as discussed in the introduction, through the observations seen in animal experiments with σ-1R agonists, and agents that blocked these effects were designated antagonists. It was only later identified that the σ-1R antagonists have a biochemical effect, causing an increase in cytoplasmic calcium and activating apoptotic mechanisms. Although it should be noted that not all σ-1R antagonists have a biochemical effect and as such may be true σ-1R antagonists in the pharmacological sense of the word. For example progesterone is designated as a σ-1R antagonist, yet does not induce the aforementioned effects, it could also be a partial agonist (partial antagonist as far as σ-1R terminology is concerned) with low efficacy. A full review of σ-1R ligands is required to sort out what biological effects each ligand has and whether it should be designated as an agonist, antagonist or inverse agonist. However, without properly defining what the σ-1R does and how it does it this would be a pointless exercise, as without knowing what the activated σ-1R does it is impossible to assign the label agonist to a ligand.

As it stands it has been shown that the σ-1R expression is involved in cell survival (Aydar *et al.*, 2004, Bem *et al.*, 1991, Wang and Duncan, 2006, Zhu *et al.*, 2003), and controlling its actions with σ-1R agonists led to increased cell survival, whereas σ-1R antagonists have the opposite effect, activating apoptotic pathways leading to cell death (Spruce *et al.*, 2004, Wang *et al.*, 2005). The evidence from previous reports suggests that treatment with σ-1R agonists led to the translocation of the σ-1R to the plasma membrane (Hayashi and Su, 2003a, Morin-Surun *et al.*, 1999) where it can interact with ion channels, preventing apoptotic signals (Cantarella *et al.*, 2007), overexpressing the σ-1R has the same effect and this is seen in tumour cell lines expressing the σ-1R this suggests that the current nomenclature regarding agonists may in fact be the correct one. It is possible that the σ-1R

agonist treatment results in an increased receptor reserve by sending more σ-1Rs to the plasma membrane, which would explain why a pre-incubation period was required to reduce the effects of the σ-1R antagonists seen in work by Spruce *et al.* (2004).

The ability to control cell survival is at the root of the σ-1Rs activities, 'activating' the receptor with σ-1R agonists potentially leads to greater expression of the σ-1R at the plasma membrane, and causes increased cell growth (or prevents cell death). This process has potentially evolved to protect cells during ischemic conditions and a number of studies have looked into the potential for σ-1R agonists as protective agents during ischemic conditions (Goyagi *et al.*, 2003, Goyagi *et al.*, 2001, Katnik *et al.*, 2006, Maurice and Lockhart, 1997). The anti-apoptotic effect of the σ-1R is possibly responsible for the chronic effects of antidepressants; studies have shown increased neurogenesis with chronic treatment with fluoxetine (Marcussen *et al.*, 2008), since fluoxetine and many other clinically used antidepressants have σ-1R activity (Itzhak and Kassim, 1990, Narita *et al.*, 1996). Within this thesis, in chapter 3, I have identified a novel selective, high affinity σ-1R ligand, dipentylammonium, which has shown significant antidepressant activity in animal models of depression, and these antidepressant effects were reversed with a σ-1R antagonist, strongly suggesting that dipentylammonium exerts its antidepressant effect through a σ-1R mediated mechanism. Whether this mechanism involves the endoplasmic reticulum stress response (Itzhak and Kassim, 1990, Narita *et al.*, 1996), controlling cytoplasmic calcium, preventing apoptosis and driving cell division or by inducing increased neurotransmitter release (Bermack and Debonnel, 2001), has yet to be identified. There is the possibility of both of these mechanisms taking place, accounting for the acute and chronic effects seen with other antidepressants in animal models.

The flip side of the σ-1R coin are the σ-1R antagonists (as discussed previously these are possibly inverse agonists if we were going to stick to correct pharmacological terminology although as discussed in chapter 5 the GTP shift is in the wrong direction), which induce apoptosis in a dose dependent manner as seen in chapter 5 with IPAG and in chapter 4 with the branched-chain ammonium salts. Knocking down the σ-1R showed that the branched-chain ammonium salts were having their effect through the σ-1R as their effects were reduced (chapter 4). Furthermore, the calcium response to IPAG was reduced (chapter 5). Previous studies have shown that σ-1R antagonists (Brent and Pang, 1995, Palmer *et al.*, 2007, Spruce *et al.*, 2004, Wang *et al.*, 2005) and σ-1R silencing (Wang and Duncan, 2006) leads to cell death, and have suggested mechanisms through which this may occur.

Spruce *et al.* (2004) suggest the activation of caspases in response to calcium influx into the cytoplasm, whilst other studies also suggest lipid raft formation and cholesterol transport to the plasma membrane disruption as a trigger for apoptosis (Hayashi and Su, 2003b, Hayashi and Su, 2003a, Hayashi and Su, 2004, Hayashi and Su, 2005b, Palmer *et al.*, 2007, Takebayashi *et al.*, 2004). In chapter 4 I show that IPAG and the branched-chain ammonium salt, bis(2-ethylhexyl)ammonium, induce an increase in cytoplasmic calcium and lipid raft formation, as I discussed in chapter 5 these two processes could be linked and possibly explain the unconventional G-protein coupling. In chapter 4 I also show that the branched-chain ammonium salts bis(2-ethylhexyl)ammonium and triisopentylammonium are effective against tumour growth both *in vitro* and *in vivo*. The hypothesis that the σ-1R is a ligand operated endoplasmic reticulum chaperone protein, when activated helps mediate the endoplasmic reticulum stress response, appears to explain the two sides of the σ-1Rs actions, although the exact details still need to be identified. Activating the σ-1R protects the cell from apoptosis most likely by controlling plasma membrane ion channels and cholesterol content/transport from the endoplasmic reticulum. Disruption of the σ-1R leads to dysregulation of ion channels, and cholesterol content/transport from the ER and ultimately leading to apoptosis.

Within this thesis I have identified a structure activity relationship between the simple ammonium salts and the σ-1R. The straight-chain ammonium salts increase in affinity for the σ-1R between two and six carbon long chains, with the highest affinity ammonium salts being the five carbon long chain secondary and tertiary ammonium salts. Dipentylammonium was shown to have effective antidepressant like effects, which were σ-1R antagonist sensitive, when tested in the animal model.

Slightly changing the ammonium salts structure, resulting in branched-chain ammonium salts, dramatically changed their effect at the σ-1R, there was a marked reduction in affinity for the σ-1R and the nH values were low. When the branched-chain ammonium salts were tested in the calcium assay and in the MTS assay two showed responses, bis(2-ethylhexyl)ammonium and triisopentylammonium, these were also the two ammonium salts which had a preferred two site binding model. These two ammonium salts were tested *in vivo* where they were shown to inhibit tumour growth compared to the control.
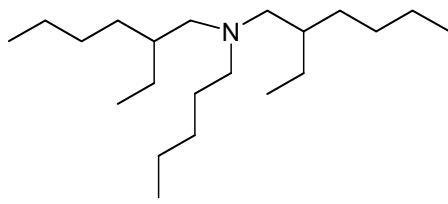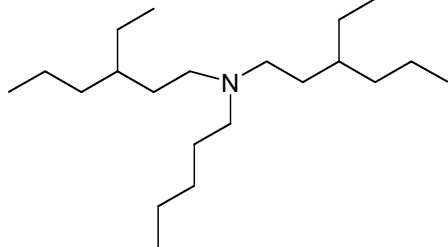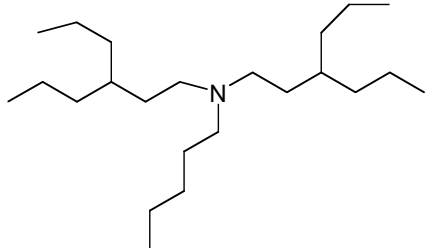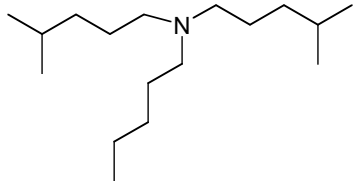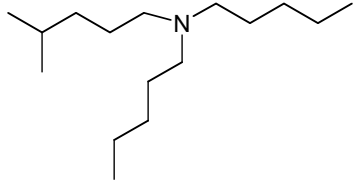
Also in this thesis I have investigated the coupling of the σ-1R with G-proteins. σ-1R antagonists show low nH values in the binding experiments, which suggests multiple

affinity binding sites. In addition to the low nH values in the binding experiments for IPAG, rimcazole, and the two branched-chain ammonium salts with σ-1R activity, I show that the presence of GTP is capable of returning the nH value to 1 and abolishing the high affinity binding site for IPAG and rimcazole. Furthermore, suramin treatment of the cells has the same effect as adding GTP to the binding assay (uncoupling G-proteins) resulting in the loss of the high affinity binding site. All this evidence suggests G-protein coupling, however, when the metabolism of GTP to GDP was measured using HPLC, the metabolism of GTP to GDP was reduced dose dependently in response to the σ-1R antagonists and branched-chain ammonium salts (not, however, the straight-chain ammonium salts), this suggested a reduction in G-protein activity in response to the σ-1R antagonists.

In summary with in this thesis I have shown the identification of a series of novel σ-1R ligands, three of which I have shown to have *in vivo* activity, two antagonists which were effective against tumour growth and one agonist which produced antidepressant like effects in the animal models.

6.2 Future directions and perspectives

The σ-1R agonists that I have identified had high affinity of the σ-1R. Modifying these to try to create σ-1R antagonists (two of which appeared to be effective), the affinity for the σ-1R was dramatically reduced. One way to try to increase the affinity whilst retaining the σ-1R antagonist activity would be to create a series of mixed ammonium salts (with both branched and straight carbon chains) as well as varying the length and position of the branches (table 6.1).

Ammonium salt	Structure
Pentyl bis(2-ethylhexyl)ammonium	
Pentyl bis-3-(ethyl)hexylammonium	
Pentyl bis-3-(propyl)hexylammonium	
Diisopentylpentylammonium	
dipentylisopentylammonium	

Table 6.1 A selection of possible ammonium salt structures that could increase σ-1R affinity whilst keeping the σ-1R antagonist activity.

Branched-chain ammonium salts with higher affinity for the σ-1R could yield more effective anti-proliferative drugs, and effective labels for tumour imaging. Anavex is investigating a compound (Anavex 1007) which is currently in preclinical trials as part of its Sigmaceptor™-C program, its reported action is to modulate σ-1Rs controlling ion channels as well as antagonising the subgroup of muscarinic receptors, mAChR$_3$, which also has an anticancer effect (Song *et al.*, 2007). Increasing mAChR$_3$ affinity along with σ-1R affinity of the branched-chain ammonium salts could yield an effective anticancer agent. Acetylcholine is synthesised and released from tumours as an autocrine growth

factor. Antagonising the mAChR leads to apoptosis (Cheng *et al.*, 2008, Song *et al.*, 2003b, Song *et al.*, 2003a). As discussed in chapter 4 this could be an explanation for the increased activity of bis(2-ethylhexyl)ammonium and triisopentylammonium in the mouse colon cancer cells compared to the human breast cancer cell line. The increase in affinity that the adamantyl group gives (Gabrielevitz *et al.*, 1980) could be used to try to create a higher affinity mixed σ-1R antagonist mAChR agonist by adding the adamantyl group to bis(2-ethylhexyl)ammonium, or to triisopentylammonium along with the other combinations suggested in table 6.1

In order to further assess the G-protein coupling of the σ-1R and the effects of agonists and antagonists, GTPγ[^{35}S] binding studies could be used to assess the effects of the σ-1R with σ-1R agonists and antagonists alone and on other G-protein coupled receptors. A similar study has already looked at the effects of σ-1R antagonists on μ opioid receptors (Kim *et al.*, 2010) The results of which appear to contradict the GTP metabolism data which I present in chapter 5. Their data suggest the σ-1R antagonist BD1047 has no effect on G-protein activity alone but increases G-protein activity when administered along with μ opioid agonists. The doses of σ-1R antagonist used in this study were quite low, since I have shown that σ-R antagonists show a multiple affinity binding states, with the lower affinity state appearing to be the state through which the antagonists have their effects. It is possible that they did not use a high enough dose to see the effect of the σ-1R antagonist alone. Further GTPγ[^{35}S] binding studies utilizing a wider range of σ-1R antagonists, and doses within the range used in chapter 5 could add to the evidence that the σ-1R interacts with G-proteins. Attempting co-immunoprecipitation of the σ-1R and its potentially coupled G-protein is another way of possibly identifying the G-protein that is coupling to the σ-1R. Looking for multiple bands in a polyacrylamide gel electrophoresis (PAGE) of the immunoprecipitated material before using mass spectrometry to identify the material isolated along with the σ-1R. This may prove difficult since the σ-1R has been shown to interact with a number of other receptors depending on the cells investigated and maintaining the G-protein coupling during the immunoprecipitation may not be possible, also the G-protein interaction may not be direct as discussed in chapter 5 with respect to lipid rafts.

It has been shown that σ-1R expression alone is not enough to show susceptibility to apoptosis in response to σ-1R antagonists (Spruce *et al.*, 2004) which is in part why the σ-1R antagonists make potentially attractive anticancer agents as they appear to only target

σ-1R-expressing tumours rather than other non cancer tissues. The selection of cancer tissue over normal tissues by the σ-1R antagonists is likely to be caused by different coupling of the receptor within different cell types. Repeating the experiments from chapter 5 with the antagonists in other systems such as brain tissue could yield different binding patterns with respect to the two site binding and GTP shift, different calcium responses and potentially reveal different coupling of the σ-1R.

The σ-2R, which I have largely ignored due to the fact little is known about it in comparison to the σ-1R, needs to be identified. As yet it has not been cloned although photolabelling suggests it has a lower molecular weight that the σ-1R (Hellewell and Bowen, 1990) and it is not clear whether it is a real protein or just a pharmacological artefact, possibly through alternative splicing of the σ-1R (Aydar *et al.*, 2004) although in the σ-1R knock-out mouse DTG (which is not specific to the σ-1R) binding appeared to be unaffected (Langa *et al.*, 2003). The σ-2R has been suggested as the major anti-apoptotic receptor of the sigma receptor "family" although it is not confirmed whether the σ-1R and σ-2R form a receptor family. They could be entirely distinct proteins that happen to have very similar binding properties. This made its identification through bioinformatics difficult as it may share little resemblance to the σ-1R at the DNA or protein level. Knowing the molecular weight of the protein should make it possible to isolate, using fractionation and/or two dimensional PAGE and then using mass spectrometry to try to identify the protease treated proteins within the fraction. With the identification of the σ-2R its coupling with and mechanism by which it can cause apoptosis may become clearer and the relation to the σ-1R may be identified.

Further investigation into the straight-chain ammonium salts, and σ-1R agonists in general could be carried out, to investigate the mechanism by which they cause their anti-depressant effect. σ-1R agonists may increase neurotransmitter release or the response to the neurotransmitter by interaction with the neurotransmitter receptor. Alternatively, σ-1R agonists may cause increased neurogenesis, which could lead to the antidepressant effects. The monoamine theory of depression fails to explain why chronic treatment with antidepressant drugs is required to see a clinical effect in patients. Since a large number of clinically effective antidepressant drugs have σ-1R affinity the σ-1R could be the explanation for many antidepressant effects. Anavex is currently investing a number of compounds in relation to neuroprotective agents, which act as σ-1R agonists. Further

investigation into dipentylammonium as a neuroprotective agent could lead to an effective agent combating not only depression but with potential against Alzheimer's disease, epilepsy, Parkinson's and other neurodegenerative diseases.

The extent of the σ-1Rs involvement in depression could be investigated further making use of the σ-1R knock-out mouse. By simply comparing the effects of antidepressants, which have known σ-1R affinity, in wild type and knock-out mice would indicate the σ-1Rs involvement in the antidepressant effects. If the σ-1R is not involved in the effects of drugs such as fluoxetine, the knock-out mice will respond equally well to the antidepressant as the wild type. This could also be carried out to assess the effects of the σ-1R agonists, which appear to have antidepressant activity, this could confirm beyond doubt that the σ-1R agonists cause their antidepressant effects through the σ-1R.

I have identified simple ligands can have high affinity for the σ-1R and they can be agonists and antagonists. Preliminary studies show these ligands show good selectivity and go against the dogma put forward by leading chemists (Ley and Baxendale, 2002). I have also shown that σ-1Rs are G-protein coupled; further work required in understanding this interaction as it does not fit the model derived from traditional (seven transmembrane) G-protein coupled receptors. It is unclear at this stage whether σ-R ligands have a role to play in modern medicine.

Appendices

7 Appendices

7.1 Abbreviations used

Abbreviation	Full name
(+) Pentazocine	(1S,9S,13S)-1,13-dimethyl-10-(3-methylbut-2-en-1-yl)-10-azatricyclotrideca-2,4,6-trien-4-ol
[^{3}H]	Tritium
[Ca^{2+}]	Calcium ion concentration
[K^+]	Potassium ion concentration
3PPP	(3-(3-hydroxyphenyl)-N-n- propylpiperidine)
4-AP	4-Aminopyridine
5-HT	5-hydroxytryptamine
AC	Adenylyl cyclase
ATCC	American Type Culture Collection
BD1047	N-[2-(3,4-Dichlorophenyl)ethyl]-N-methyl-2-(dimethylamino)ethylamine
BD737	1S,2R-(−)-cis-N-[2-(3,4-dichlorophenyl)ethyl]-N-methyl-2-(1-pyrrolidinyl)cyclohexylamine
B$_{max}$	Maximum binding of a ligand to a receptor
BSA	Bovine serum albumin
cAMP	Cyclic adenosine monophosphate
CI	Confidence intervals
CNS	Central nervous system
CO_2	Carbon Dioxide
cpm	Counts per minute
DHEAS	Dehydroepiandrosterone
DISC	Death inducing signalling complex
DMEM	Dulbecco Modified Eagle's minimum essential media
DMSO	Dimethyl sulfoxide
DPM	Disintegrations per minute
DTG	1,3-di-o-tolylguanidine
$E.\ coli$	$Escherichia\ coli$

EC_{50}	Effective concentration of a drug to cause 50% maximal response
ECACC	European Collection of Cell Cultures
EDTA	Ethylenediaminetetraacetic acid
EPB	Emopamil binding protein
FCS	Foetal Calf serum
$GDP\beta S$	Guanosine-5'-O-(2-thiodiphosphate)
GPI	Glycosylphosphatidylinositol
GppNHp	5'-Guanylyl imidodiphosphate
G-Protein	GTP-binding protein
GTP	guanosine triphosphate
$GTP\gamma S$	guanosine 5'-O-(gamma-thio)triphosphate
H_1R	Histamine 1 Receptor
H_2R	Histamine 2 Receptor
H_3R	Histamine 3 Receptor
H_4R	Histamine 4 Receptor
HCl	Hydrochloric acid
HCl•	Hydrochloride salt
HEK 293	Human Embryonic Kidney cell line
HPLC	High Performance Liquid Chromatography
IC_{50}	Concentration required to cause a 50% drop in maximal response.
IP_3	Inositol 1,4,5-trisphosphate
IP_5	Inositol 1,3,4,5,6 pentakisphosphate
IPAG	1-(4-Iodophenyl)-3-(2-adamantyl)guanidine
K_{50}	Equilibrium dissociation constant for binding that does not follow the laws of mass action
K_d	Equilibrium Dissociation Constant derived from saturation binding
K_i	Equilibrium Dissociation Constant derived from competitive radioligand binding
MAC 13	Mouse Colon Cancer Cell line
MAC 16	Mouse Colon Cancer Cell line
mAChR	Muscarinic acetylcholine Receptor
MDA-MB-468	Human Breast adenocarcinoma cell line
MTS	3-(4,5-dimethylthiazol-2-yl)-5-(3-carboxymethoxyphenyl)-2-(4-sulfophenyl)-2H-tetrazolium
nH	The Hill coefficient (slope factor) of competitive binding curves

NMDA	N-methyl-D-aspartic acid
PAGE	Polyacrylamide gel electrophoresis
PBS	Phosphate Buffered saline
PCP	1-(1-phenylcyclohexyl)piperidine
pEC_{50}	Negative logarithm of the dose required to generate 50% of the maximal response.
pH	The negative logarithm of the concentration of Hydrogen ions in a solution in moles per litre
pIC_{50}	Negative logarithm of the dose required to reduce a response by half.
PIPAG	1-(4-Iodophenyl)-3-(1-adamantyl)guanidine
pK_{50}	Negative logarithm of the concentration of ligand required to occupy 50% of receptors when the binding does not follow the laws of mass action
PKB	Protein Kinase B
pK_d	Negative logarithm of the equilibrium dissociation constant that is derived from saturation binding assays
pK_i	Negative logarithm of the equilibrium dissociation constant that is derived from competitive binding assays
PLC	Phospholipase C
PMS	Phenazine methosulphate
QNB	L-quinuclidinyl [phenyl-4-^{3}H] benzilate
R	Resting state receptor
R*	Activated state receptor
Rimcazole	9-(3-((3R,5S)-3,5-dimethylpiperazin-1-yl)propyl)-9H-carbazole
RPMI	Roswell Park Memorial Institute
SD	Standard deviation
SEM	Standard Error of the mean (SD/√n)
siRNA	Short Interfering Ribonucleic Acid
SKF-10,047	N-allylnormetazocine
SSRI	Selective Serotonin Reuptake Inhibitor
TBS	Tris(hydroxymethyl)aminomethane buffered saline
Tris	Tris(hydroxymethyl)aminomethane
σ-1R	Sigma-1 receptor

7.2 σ-1 receptor coding gene sequence

```
atgcagtggg ccgtgggccg gcggtgggcg tgggccgcgc tgctcctggc
tgtcgcagcg gtgctgaccc aggtcgtctg gctctggctg ggtacgcaga
gcttcgtctt ccagcgcgaa gagatagcgc agttggcgcg gcagtacgct
gggctggacc acgagctggc cttctctcgt ctgatcgtgg agctgcggcg
gctgcaccca ggccacgtgc tgcccgacga ggagctgcag tgggtgttcg
tgaatgcggg tggctggatg ggcgccatgt gccttctgca cgcctcgctg
tccgagtatg tgctgctctt cggcaccgcc ttgggctccc gcggccactc
ggggcgctac tgggctgaga tctcggatac catcatctct ggcaccttcc
accagtggag agagggcacc accaaaagtg aggtcttcta cccagggggag
acggtagtac acgggcctgg tgaggcaaca gctgtggagt gggggccaaa
cacatggatg gtggagtacg gccggggcgt catcccatcc accctggcct
tcgcgctggc cgacactgtc ttcagcaccc aggacttcct caccctcttc
tatactcttc gctcctatgc tcggggcctc cggcttgagc tcaccaccta
cctctttggc caggaccctt ga
```

7.3 σ-1 Receptor protein sequence

```
mqwavg rr wa waalllavaa vltqvvwlwl gtqsfvfqre eiaqlarqya
gldhelafsr livelrrlhp ghvlpdeelq wvfvnaggwm gamcllhasl
seyvllfgta lgsrghsgry waeisdtiis gtfhqwregt tksevfypge
tvvhgpgeat avewgpntwm veygrgvips tlafaladtv fstqdfltlf
ytlrsyargl rlelttylfg qdp
```

rr — Endoplasmic localisation signal

References

8   References

ABLORDEPPEY, S., FISCHER, J. & GLENNON, R. (2000) Is a nitrogen atom an important pharmacophoric element in sigma ligand binding? *Bioorg Med Chem,* 8**,** 2105-11.

AYDAR, E., ONGANER, P., PERRETT, R., DJAMGOZ, M. B. & PALMER, C. P. (2006) The expression and functional characterization of sigma σ1 receptors in breast cancer cell lines. *Cancer Lett,* 242**,** 245-57.

AYDAR, E., PALMER, C. P. & DJAMGOZ, M. B. (2004) Sigma receptors and cancer: possible involvement of ion channels. *Cancer Res,* 64**,** 5029-35.

AYDAR, E., PALMER, C. P., KLYACHKO, V. A. & JACKSON, M. B. (2002) The sigma receptor as a ligand-regulated auxiliary potassium channel subunit. *Neuron,* 34**,** 399-410.

BEINDL, W., MITTERAUER, T., HOHENEGGER, M., IJZERMAN, A. P., NANOFF, C. & FREISSMUTH, M. (1996) Inhibition of receptor/G protein coupling by suramin analogues. *Mol Pharmacol,* 50**,** 415-23.

BERGERON, R., DE MONTIGNY, C. & DEBONNEL, G. (1999) Pregnancy reduces brain sigma receptor function. *Br J Pharmacol,* 127**,** 1769-76.

BERMACK, J. E. & DEBONNEL, G. (2005) The role of sigma receptors in depression. *J Pharmacol Sci,* 97**,** 317-36.

BIBBY, M. C., DOUBLE, J. A., ALI, S. A., FEARON, K. C., BRENNAN, R. A. & TISDALE, M. J. (1987) Characterization of a transplantable adenocarcinoma of the mouse colon producing cachexia in recipient animals. *J Natl Cancer Inst,* 78**,** 539-46.

BOX, G. E. P. (1953) Non-Normality and Tests on Variences. *Biometrika,* 40**,** 318-335.

BRACQUART, D., COUSIN, C., CONTREPAS, A. & NGUYEN, G. (2009) The prorenin receptor. *J Soc Biol,* 203**,** 303-10.

BRENT, P. J., PANG, G., LITTLE, G., DOSEN, P. J. & VAN HELDEN, D. F. (1996a) The sigma receptor ligand, reduced haloperidol, induces apoptosis and increases intracellular-free calcium levels $[Ca^{2+}]_i$ in colon and mammary adenocarcinoma cells. *Biochem Biophys Res Commun,* 219**,** 219-26.

BRENT, P. J., SAUNDERS, H. & DUNKLEY, P. R. (1996b) Intrasynaptosomal free calcium levels in rat forebrain synaptosomes: modulation by sigma (σ) receptor ligands. *Neurosci Lett,* 211**,** 138-42.

BURCHETT, S. A. & HICKS, T. P. (2006) The mysterious trace amines: protean neuromodulators of synaptic transmission in mammalian brain. *Prog Neurobiol,* 79**,** 223-46.

CAMPBELL, B. G., SCHERZ, M. W., KEANA, J. F. & WEBER, E. (1989) Sigma receptors regulate contractions of the guinea pig ileum longitudinal muscle/myenteric plexus preparation elicited by both electrical stimulation and exogenous serotonin. *J Neurosci,* 9**,** 3380-91.

CENDAN, C. M., PUJALTE, J. M., PORTILLO-SALIDO, E., MONTOLIU, L. & BAEYENS, J. M. (2005) Formalin-induced pain is reduced in $\sigma(1)$ receptor knockout mice. *Eur J Pharmacol,* 511**,** 73-4.

CHAMBERLAIN, L. H., BURGOYNE, R. D. & GOULD, G. W. (2001) SNARE proteins are highly enriched in lipid rafts in PC12 cells: implications for the spatial control of exocytosis. *Proc Natl Acad Sci U S A,* 98**,** 5619-24.

CHARNEY, D. S. & MANJI, H. K. (2004) Life stress, genes, and depression: multiple pathways lead to increased risk and new opportunities for intervention. *Sci STKE,* 2004**,** re5.

CHENG, Y. & PRUSOFF, W. H. (1973) Relationship between the inhibition constant (K_i) and the concentration of inhibitor which causes 50 per cent inhibition (I_{50}) of an enzymatic reaction. *Biochem Pharmacol,* 22**,** 3099-108.

CHU, E. C. & TARNAWSKI, A. S. (2004) PTEN regulatory functions in tumor suppression and cell biology. *Med Sci Monit,* 10**,** RA235-41.

CIZZA, G., RAVN, P., CHROUSOS, G. P. & GOLD, P. W. (2001) Depression: a major, unrecognized risk factor for osteoporosis? *Trends Endocrinol Metab,* 12**,** 198-203.

CONNICK, J. H., HANLON, G., ROBERTS, J., FRANCE, L., FOX, P. K. & NICHOLSON, C. D. (1992) Multiple sigma binding sites in guinea-pig and rat brain membranes: G-protein interactions. *Br J Pharmacol,* 107**,** 726-31.

COZZI, N. V., GOPALAKRISHNAN, A., ANDERSON, L. L., FEIH, J. T., SHULGIN, A. T., DALEY, P. F. & RUOHO, A. E. (2009) Dimethyltryptamine and other hallucinogenic tryptamines exhibit substrate behavior at the serotonin uptake transporter and the vesicle monoamine transporter. *J Neural Transm.*

DANAEI, G., VANDER HOORN, S., LOPEZ, A. D., MURRAY, C. J. & EZZATI, M. (2005) Causes of cancer in the world: comparative risk assessment of nine behavioural and environmental risk factors. *Lancet,* 366**,** 1784-93.

DHIR, A. & KULKARNI, S. K. (2007) Involvement of sigma-1 receptor modulation in the antidepressant action of venlafaxine. *Neurosci Lett,* 420**,** 204-8.

DUNCAN, R. E., EL-SOHEMY, A. & ARCHER, M. C. (2004) Mevalonate promotes the growth of tumors derived from human cancer cells in vivo and stimulates proliferation in vitro with enhanced cyclin-dependent kinase-2 activity. *J Biol Chem,* 279**,** 33079-84.

EDIDIN, M. (2001) Shrinking patches and slippery rafts: scales of domains in the plasma membrane. *Trends Cell Biol,* 11**,** 492-6.

FERRIS, R. M., HARFENIST, M., MCKENZIE, G. M., COOPER, B., SOROKO, F. E. & MAXWELL, R. A. (1982) BW 234U, (cis-9-[3-(3,5-dimethyl-1-piperazinyl)propyl]carbazole dihydrochloride): a novel antipsychotic agent. *J Pharm Pharmacol,* 34**,** 388-90.

FREISSMUTH, M., BOEHM, S., BEINDL, W., NICKEL, P., IJZERMAN, A. P., HOHENEGGER, M. & NANOFF, C. (1996) Suramin analogues as subtype-selective G protein inhibitors. *Mol Pharmacol,* 49**,** 602-11.

FROGER, A. & HALL, J. E. (2007) Transformation of plasmid DNA into *E. coli* using the heat shock method. *J Vis Exp***,** 253.

FUKUSHIMA, T., HIRASAKI, A., JONES, K. A. & WARNER, D. O. (1996) Halothane and potassium channels in airway smooth muscle. *Br J Anaesth,* 76**,** 847-53.

GABRIELEVITZ, A., KLOOG, Y., KALIR, A., BALDERMAN, D. & SOKOLOVSKY, M. (1980) Interaction of phencyclidine and its new adamantyl derivatives with muscarinic receptors. *Life Sci,* 26**,** 89-95.

GILMORE, D. L., LIU, Y. & MATSUMOTO, R. R. (2004) Review of the pharmacological and clinical profile of rimcazole. *CNS Drug Rev,* 10**,** 1-22.

GLENNON, R. A., YOUSIF, M. Y., ISMAIEL, A. M., EL-ASHMAWY, M. B., HERNDON, J. L., FISCHER, J. B., SERVER, A. C. & HOWIE, K. J. (1991) Novel 1-phenylpiperazine and 4-phenylpiperidine derivatives as high-affinity sigma ligands. *J Med Chem,* 34**,** 3360-5.

GRYNKIEWICZ, G., POENIE, M. & TSIEN, R. Y. (1985) A new generation of Ca2+ indicators with greatly improved fluorescence properties. *J Biol Chem,* 260**,** 3440-50.

GUEST, I. & VARMA, D. R. (1991) Developmental toxicity of methylamines in mice. *J Toxicol Environ Health,* 32**,** 319-30.

HAYASHI, T. & SU, T. (2005) The sigma receptor: evolution of the concept in neuropsychopharmacology. *Curr Neuropharmacol,* 3**,** 267-80.

HAYASHI, T. & SU, T. P. (2001) Regulating ankyrin dynamics: Roles of sigma-1 receptors. *Proc Natl Acad Sci U S A,* 98**,** 491-6.

HAYASHI, T. & SU, T. P. (2003) Sigma-1 receptors (sigma(1) binding sites) form raft-like microdomains and target lipid droplets on the endoplasmic reticulum: roles in endoplasmic reticulum lipid compartmentalization and export. *J Pharmacol Exp Ther,* 306**,** 718-25.

HELLEWELL, S. B. & BOWEN, W. D. (1990) A sigma-like binding site in rat pheochromocytoma (PC12) cells: decreased affinity for (+)-benzomorphans and lower molecular weight suggest a different sigma receptor form from that of guinea pig brain. *Brain Res,* 527**,** 244-53.

HOLLSTEIN, M., SIDRANSKY, D., VOGELSTEIN, B. & HARRIS, C. C. (1991) p53 mutations in human cancers. *Science,* 253**,** 49-53.

HONG, W. & WERLING, L. L. (2000) Evidence that the σ(1) receptor is not directly coupled to G proteins. *Eur J Pharmacol,* 408**,** 117-25.

HONG, W. & WERLING, L. L. (2002) Binding of sigma receptor ligands and their effects on muscarine-induced Ca^{2+} changes in SH-SY5Y cells. *Eur J Pharmacol,* 436**,** 35-45.

HOOPER, N. M. (1999) Detergent-insoluble glycosphingolipid/cholesterol-rich membrane domains, lipid rafts and caveolae (review). *Mol Membr Biol,* 16**,** 145-56.

HUTCHISON, C. A., 3RD, PHILLIPS, S., EDGELL, M. H., GILLAM, S., JAHNKE, P. & SMITH, M. (1978) Mutagenesis at a specific position in a DNA sequence. *J Biol Chem,* 253**,** 6551-60.

HYMAN, S. E. & NESTLER, E. J. (1996) Initiation and adaptation: a paradigm for understanding psychotropic drug action. *Am J Psychiatry,* 153**,** 151-62.

ISSHIKI, M. & ANDERSON, R. G. (1999) Calcium signal transduction from caveolae. *Cell Calcium,* 26**,** 201-8.

ITZHAK, Y. (1989) Multiple affinity binding states of the sigma receptor: effect of GTP-binding protein-modifying agents. *Mol Pharmacol,* 36**,** 512-7.

ITZHAK, Y., RUHLAND, M. & KRAHLING, H. (1990) Binding of umespirone to the sigma receptor: evidence for multiple affinity states. *Neuropharmacology,* 29**,** 181-4.

JELACIC, T. M., SIMS, S. M. & CLAPHAM, D. E. (1999) Functional expression and characterization of G-protein-gated inwardly rectifying K+ channels containing GIRK3. *J Membr Biol,* 169**,** 123-9.

KATO, K., HAYAKO, H., ISHIHARA, Y., MARUI, S., IWANE, M. & MIYAMOTO, M. (1999) TAK-147, an acetylcholinesterase inhibitor, increases choline acetyltransferase activity in cultured rat septal cholinergic neurons. *Neurosci Lett,* 260**,** 5-8.

KENAKIN, T. P. (1984) The classification of drugs and drug receptors in isolated tissues. *Pharmacol Rev,* 36**,** 165-222.

KIM, F. J., KOVALYSHYN, I., BURGMAN, M., NEILAN, C., CHIEN, C. C. & PASTERNAK, G. W. (2010) {sigma}1 Receptor Modulation of G-Protein-Coupled Receptor Signaling: Potentiation of Opioid Transduction Independent from Receptor Binding. *Mol Pharmacol,* 77**,** 695-703.

KIMES, A. S., WILSON, A. A., SCHEFFEL, U., CAMPBELL, B. G. & LONDON, E. D. (1992) Radiosynthesis, cerebral distribution, and binding of [125I]-1-(p-iodophenyl)-3-(1-adamantyl)guanidine, a ligand for sigma binding sites. *J Med Chem,* 35**,** 4683-9.

KNUDSON, A. G., JR. (1971) Mutation and cancer: statistical study of retinoblastoma. *Proc Natl Acad Sci U S A,* 68**,** 820-3.

KOLANJIAPPAN, K., RAMACHANDRAN, C. R. & MANOHARAN, S. (2003) Biochemical changes in tumor tissues of oral cancer patients. *Clin Biochem,* 36**,** 61-5.

LEGEMBRE, P., DABURON, S., MOREAU, P., MOREAU, J. F. & TAUPIN, J. L. (2006) Modulation of Fas-mediated apoptosis by lipid rafts in T lymphocytes. *J Immunol,* 176**,** 716-20.

LEY, S. V. & BAXENDALE, I. R. (2002) New tools and concepts for modern organic synthesis. *Nat Rev Drug Discov,* 1**,** 573-86.

LURJE, G. & LENZ, H. J. (2009) EGFR signaling and drug discovery. *Oncology,* 77**,** 400-10.

MARKOWITZ, S. D. & BERTAGNOLLI, M. M. (2009) Molecular origins of cancer: Molecular basis of colorectal cancer. *N Engl J Med,* 361**,** 2449-60.

MARTIN, W. R., EADES, C. G., THOMPSON, J. A., HUPPLER, R. E. & GILBERT, P. E. (1976) The effects of morphine- and nalorphine- like drugs in the nondependent and morphine-dependent chronic spinal dog. *J Pharmacol Exp Ther,* 197**,** 517-32.

MATSUNO, K., SENDA, T., KOBAYASHI, T., OKAMOTO, K., NAKATA, K. & MITA, S. (1997) SA4503, a novel cognitive enhancer, with sigma 1 receptor agonistic properties. *Behav Brain Res,* 83**,** 221-4.

MATTSON, M. P. & CHAN, S. L. (2003) Calcium orchestrates apoptosis. *Nat Cell Biol,* 5**,** 1041-3.

MAURICE, T., HIRAMATSU, M., KAMEYAMA, T., HASEGAWA, T. & NABESHIMA, T. (1994) Behavioral evidence for a modulating role of sigma

ligands in memory processes. II. Reversion of carbon monoxide-induced amnesia. *Brain Res,* 647**,** 57-64.

MAURICE, T. & LOCKHART, B. P. (1997) Neuroprotective and anti-amnesic potentials of sigma (σ) receptor ligands. *Prog Neuropsychopharmacol Biol Psychiatry,* 21**,** 69-102.

MAURICE, T. & SU, T. P. (2009) The pharmacology of sigma-1 receptors. *Pharmacol Ther,* 124**,** 195-206.

MAY, B., MENKENS, I. & WESTERMANN, E. (1967) Differential release of serotonin and histamine from blood platelets of the rabbit by aliphatic and aromatic amines. *Life Sci,* 6**,** 2079-85.

MERRITT, E. A., SIXMA, T. K., KALK, K. H., VAN ZANTEN, B. A. & HOL, W. G. (1994) Galactose-binding site in Escherichia coli heat-labile enterotoxin (LT) and cholera toxin (CT). *Mol Microbiol,* 13**,** 745-53.

MICHAELEVSKI, I., CHIKVASHVILI, D., TSUK, S., FILI, O., LOHSE, M. J., SINGER-LAHAT, D. & LOTAN, I. (2002) Modulation of a brain voltage-gated K+ channel by syntaxin 1A requires the physical interaction of Gbetagamma with the channel. *J Biol Chem,* 277**,** 34909-17.

MITCHELL, P. J. & REDFERN, P. H. (2005) Animal models of depressive illness: the importance of chronic drug treatment. *Curr Pharm Des,* 11**,** 171-203.

MOEBIUS, F. F., BERMOSER, K., REITER, R. J., HANNER, M. & GLOSSMANN, H. (1996) Yeast sterol C8-C7 isomerase: identification and characterization of a high-affinity binding site for enzyme inhibitors. *Biochemistry,* 35**,** 16871-8.

MOEBIUS, F. F., STRIESSNIG, J. & GLOSSMANN, H. (1997) The mysteries of sigma receptors: new family members reveal a role in cholesterol synthesis. *Trends Pharmacol Sci,* 18**,** 67-70.

NARITA, N., HASHIMOTO, K., IYO, M., MINABE, Y. & YAMAZAKI, K. (1995) Lack of neuroprotective effect of sigma receptor ligands in the neurotoxicity of p-chloroamphetamine in rat brain. *Eur J Pharmacol,* 293**,** 277-80.

NARITA, N., HASHIMOTO, K., TOMITAKA, S. & MINABE, Y. (1996) Interactions of selective serotonin reuptake inhibitors with subtypes of sigma receptors in rat brain. *Eur J Pharmacol,* 307**,** 117-9.

NESTLER, E. J., BARROT, M., DILEONE, R. J., EISCH, A. J., GOLD, S. J. & MONTEGGIA, L. M. (2002) Neurobiology of depression. *Neuron,* 34**,** 13-25.

ODAGAKI, Y., TOYOSHIMA, R. & YAMAUCHI, T. (2005) Lack of G protein-coupled sigma receptors in rat brain membranes: receptor-mediated high-affinity GTPase activity and [^{35}S]GTPγS binding studies. *J Neural Transm,* 112**,** 873-83.

PALMER, C. P., MAHEN, R., SCHNELL, E., DJAMGOZ, M. B. & AYDAR, E. (2007) Sigma-1 receptors bind cholesterol and remodel lipid rafts in breast cancer cell lines. *Cancer Res,* 67**,** 11166-75.

PETIT-DEMOULIERE, B., CHENU, F. & BOURIN, M. (2005) Forced swimming test in mice: a review of antidepressant activity. *Psychopharmacology (Berl),* 177**,** 245-55.

PORSOLT, R. D., BERTIN, A. & JALFRE, M. (1977) Behavioral despair in mice: a primary screening test for antidepressants. *Arch Int Pharmacodyn Ther,* 229**,** 327-36.

QUIRION, R., BOWEN, W. D., ITZHAK, Y., JUNIEN, J. L., MUSACCHIO, J. M., ROTHMAN, R. B., SU, T. P., TAM, S. W. & TAYLOR, D. P. (1992) A proposal for the classification of sigma binding sites. *Trends Pharmacol Sci,* 13**,** 85-6.

REDROBE, J. P., BOURIN, M., COLOMBEL, M. C. & BAKER, G. B. (1998) Dose-dependent noradrenergic and serotonergic properties of venlafaxine in animal models indicative of antidepressant activity. *Psychopharmacology (Berl),* 138**,** 1-8.

RESH, M. D. (1999) Fatty acylation of proteins: new insights into membrane targeting of myristoylated and palmitoylated proteins. *Biochim Biophys Acta,* 1451**,** 1-16.

ROE, M. W., LEMASTERS, J. J. & HERMAN, B. (1990) Assessment of Fura-2 for measurements of cytosolic free calcium. *Cell Calcium,* 11**,** 63-73.

ROMAN, F. J., PASCAUD, X., MARTIN, B., VAUCHE, D. & JUNIEN, J. L. (1990) JO 1784, a potent and selective ligand for rat and mouse brain sigma-sites. *J Pharm Pharmacol,* 42**,** 439-40.

RUGGERO, D. (2009) The role of Myc-induced protein synthesis in cancer. *Cancer Res,* 69**,** 8839-43.

SCHILDKRAUT, J. J., GORDON, E. K. & DURELL, J. (1965) Catecholamine metabolism in affective disorders. I. Normetanephrine and VMA excretion in depressed patients treated with imipramine. *J Psychiatr Res,* 3**,** 213-28.

SCHWARZ, S., POHL, P. & ZHOU, G. Z. (1989) Steroid binding at sigma-"opioid" receptors. *Science,* 246**,** 1635-8.

SHARKEY, J., GLEN, K. A., WOLFE, S. & KUHAR, M. J. (1988) Cocaine binding at sigma receptors. *Eur J Pharmacol,* 149**,** 171-4.

SHIRAYAMA, Y., NISHIKAWA, T., UMINO, A. & TAKAHASHI, K. (1993) p-chlorophenylalanine-reversible reduction of sigma binding sites by chronic imipramine treatment in rat brain. *Eur J Pharmacol,* 237**,** 117-26.

SILVIUS, J. R. (2003) Role of cholesterol in lipid raft formation: lessons from lipid model systems. *Biochim Biophys Acta,* 1610**,** 174-83.

SIMONY-LAFONTAINE, J., ESSLIMANI, M., BRIBES, E., GOURGOU, S., LEQUEUX, N., LAVAIL, R., GRENIER, J., KRAMAR, A. & CASELLAS, P. (2000) Immunocytochemical assessment of sigma-1 receptor and human sterol

isomerase in breast cancer and their relationship with a series of prognostic factors. *Br J Cancer,* 82**,** 1958-66.

SINGER, S. J. & NICOLSON, G. L. (1972) The fluid mosaic model of the structure of cell membranes. *Science,* 175**,** 720-31.

SKEBERDIS, V. A., JUREVICIUS, J. & FISCHMEISTER, R. (1997) Beta-2 adrenergic activation of L-type Ca^{++} current in cardiac myocytes. *J Pharmacol Exp Ther,* 283**,** 452-61.

STAHL, S. M. (2005) Antidepressant treatment of psychotic major depression: potential role of the sigma receptor. *CNS Spectr,* 10**,** 319-23.

STEPHENSON, R. P. (1956) A modification of receptor theory. 1956. *Br J Pharmacol,* 120**,** 106-20; discussion 103-5.

SU, T. P. (1982) Evidence for sigma opioid receptor: binding of [^{3}H]SKF-10047 to etorphine-inaccessible sites in guinea-pig brain. *J Pharmacol Exp Ther,* 223**,** 284-90.

SU, T. P. (1993) Delineating biochemical and functional properties of sigma receptors: emerging concepts. *Crit Rev Neurobiol,* 7**,** 187-203.

SU, T. P., HAYASHI, T. & VAUPEL, D. B. (2009) When the endogenous hallucinogenic trace amine N,N-dimethyltryptamine meets the sigma-1 receptor. *Sci Signal,* 2**,** pe12.

SU, T. P., LONDON, E. D. & JAFFE, J. H. (1988) Steroid binding at sigma receptors suggests a link between endocrine, nervous, and immune systems. *Science,* 240**,** 219-21.

SUZUKI, T. (2002) Lipid rafts at postsynaptic sites: distribution, function and linkage to postsynaptic density. *Neurosci Res,* 44**,** 1-9.

TOKUYAMA, S., HIRATA, K., IDE, A. & UEDA, H. (1997) Sigma ligands stimulate GTPase activity in mouse prefrontal membranes: evidence for the existence of metabotropic sigma receptor. *Neurosci Lett,* 233**,** 141-4.

TOKUYAMA, S. & HO, I. K. (1996) Inhibitory effects of diltiazem, an L-type Ca^{2+} channel blocker, on naloxone-increased glutamate levels in the locus coeruleus of opioid-dependent rats. *Brain Res,* 722**,** 212-6.

UKAI, M., MAEDA, H., NANYA, Y., KAMEYAMA, T. & MATSUNO, K. (1998) Beneficial effects of acute and repeated administrations of sigma receptor agonists on behavioral despair in mice exposed to tail suspension. *Pharmacol Biochem Behav,* 61**,** 247-52.

URANI, A., ROMAN, F. J., PHAN, V. L., SU, T. P. & MAURICE, T. (2001) The antidepressant-like effect induced by sigma(1)-receptor agonists and neuroactive steroids in mice submitted to the forced swimming test. *J Pharmacol Exp Ther,* 298**,** 1269-79.

VAUPEL, D. B. (1983) Naltrexone fails to antagonize the sigma effects of PCP and SKF 10,047 in the dog. *Eur J Pharmacol,* 92**,** 269-74.

VILNER, B. J., DE COSTA, B. R. & BOWEN, W. D. (1995a) Cytotoxic effects of sigma ligands: sigma receptor-mediated alterations in cellular morphology and viability. *J Neurosci,* 15**,** 117-34.

VILNER, B. J., JOHN, C. S. & BOWEN, W. D. (1995b) Sigma-1 and sigma-2 receptors are expressed in a wide variety of human and rodent tumor cell lines. *Cancer Res,* 55**,** 408-13.

VOGT, P. K. (1993) Cancer genes. *West J Med,* 158**,** 273-8.

VOLZ, H. P. & STOLL, K. D. (2004) Clinical trials with sigma ligands. *Pharmacopsychiatry,* 37 Suppl 3**,** S214-20.

WANG, J. W., DAVID, D. J., MONCKTON, J. E., BATTAGLIA, F. & HEN, R. (2008) Chronic fluoxetine stimulates maturation and synaptic plasticity of adult-born hippocampal granule cells. *J Neurosci,* 28**,** 1374-84.

WANG, L. & DUNCAN, G. (2006) Silencing of sigma-1 receptor induces cell death in human lens cells. *Exp Cell Res,* 312**,** 1439-46.

WHITTEMORE, E. R., ILYIN, V. I. & WOODWARD, R. M. (1997) Antagonism of N-methyl-D-aspartate receptors by sigma site ligands: potency, subtype-selectivity and mechanisms of inhibition. *J Pharmacol Exp Ther,* 282**,** 326-38.

WILSON, A. A., DANNALS, R. F., RAVERT, H. T., SONDERS, M. S., WEBER, E. & WAGNER, H. N., JR. (1991) Radiosynthesis of sigma receptor ligands for positron emission tomography: ^{11}C- and ^{18}F-labeled guanidines. *J Med Chem,* 34**,** 1867-70.

YAMAMOTO, H., MIURA, R., YAMAMOTO, T., SHINOHARA, K., WATANABE, M., OKUYAMA, S., NAKAZATO, A. & NUKADA, T. (1999) Amino acid residues in the transmembrane domain of the type 1 sigma receptor critical for ligand binding. *FEBS Lett,* 445**,** 19-22.

YOSHIDA, H. (2007) ER stress and diseases. *FEBS J,* 274**,** 630-58.

YUAN, X. J., TOD, M. L., RUBIN, L. J. & BLAUSTEIN, M. P. (1995) Hypoxic and metabolic regulation of voltage-gated K^+ channels in rat pulmonary artery smooth muscle cells. *Exp Physiol,* 80**,** 803-13.

ZAHRADNIK, I., MINAROVIC, I. & ZAHRADNIKOVA, A. (2008) Inhibition of the cardiac L-type calcium channel current by antidepressant drugs. *J Pharmacol Exp Ther,* 324**,** 977-84.

ZILFOU, J. T. & LOWE, S. W. (2009) Tumor Suppressive Functions of p53. *Cold Spring Harb Perspect Biol,* 1**,** a001883.